Universitat de Girona

PREDICTION OF POSTPRANDIAL BLOOD GLUCOSE UNDER INTRA-PATIENT VARIABILITY AND UNCERTAINTY AND ITS USE IN THE DESIGN OF INSULIN DOSING STRATEGIES FOR TYPE 1 DIABETIC PATIENTS

Maira Alejandra GARCÍA JARAMILLO

Dipòsit legal: GI-1542-2011
http://hdl.handle.net/1xxxxxx

DOCTORAL THESIS

Prediction of postprandial blood glucose under intra-patient variability and uncertainty and its use in the design of insulin dosing strategies for type 1 diabetic patients

by

Maira Alejandra García Jaramillo

2011

Doctoral Programme in Technology

Advisors:
Dr. Josep Vehí and Dra. Remei Calm

Thesis submitted in partial fulfillment of the requirements for the degree of Doctor of Philosophy (Major subject: Computer Science) at the University of Girona.

Universitat de Girona

Departament d'Enginyeria Elèctrica, Electrònica i Automàtica

Prediction of postprandial blood glucose under intra-patient variability and uncertainty and its use in the design of insulin dosing strategies for type 1 diabetic patients

By

Maira Alejandra García Jaramillo

A dissertation presented to the University of Girona
in partial fulfillment of the requirements of the degree of
DOCTOR OF PHILOSOPHY

Advisors

Dr Josep Vehí

Dra Remei Calm

Girona, Spain
June, 2011

Con todo mi amor y devoción para mi madre.
Ella ha sido el motor que me ha impulsado
durante todos estos años
para lograr mis sueños y metas.

Mami este es el fruto de tu sacrificio,
amor, entrega, apoyo y dedicación
para formarme personal y profesionalmente.

Disculpame por tantos años de ausencia física
pero mi amor, mente, alma y corazón,
todo lo que soy y lo que seré
siempre han estado y estarán contigo.

Universitat de Girona
Departament d'Enginyeria Elèctrica, Electrònica i Automàtica

Abstract

Diabetes is a metabolic disease characterized by elevated plasma glucose levels, corresponding to acute or chronic hyperglycaemia, which can lead to long-term micro- or macrovascular complications. This is so due to the lack of insulin secretion by the *beta*-cells in the islets of Langerhans in the pancreas (type 1 diabetes) or a combination of resistance to insulin action and an inadequate compensatory insulin secretory response (type 2 diabetes). Diabetes is one of the most serious diseases that must be regulated artificially. According to the latest data from the International Diabetes Federation, it is estimated that the number of diabetics worldwide will increase from 284.6 million in 2010 to 438.4 million in 2030, equivalent to 6.6% and 7.8%, respectively, of the world's adult population aged between 20 and 79 years.

The conventional diabetes therapy is usually based on subcutaneous insulin injections. Because of the difficulty inherent in selecting the correct insulin dose and the risk of hyper- and hypoglycaemic episodes in patients with type 1 diabetes, dosage-aid systems are very useful for these patients. Calculating a risk index requires the evaluation of the impacts of bolus insulin and food intake on postprandial glucose levels, to predict short-term postprandial glycaemia sufficiently accurately. The use of dynamic models provides valuable information about postprandial glucose excursions. However, one of the main challenges to be considered is the large intra-individual variability among patients. The different sources of uncertainty, such as the uncertainty in the food intake, are other challenges to be considered because it is not possible to measure precisely the carbohydrate content and meal composition of a mixed meal in real-life situations. These factors make it necessary to develop prediction tools that can accommodate different sources of uncertainty (inputs, parameters, and initial states).

In this study, I propose a novel method to estimate the dose and injection-to-meal time for low-risk intensive insulin therapy. This dosage-aid system uses an optimization algorithm to determine the insulin dose and injection-to-meal time that minimizes the risk of postprandial hyper- and hypoglycaemia in type 1 diabetic patients. To this end, the algorithm applies a methodology that quantifies the risk of experiencing different grades of hypo- or hyperglycaemia in the postprandial state induced by insulin therapy according to an individual patient's parameters. This methodology is based on modal interval analysis (MIA), a mathematical theory developed by researchers at the University of Barcelona and the University of Girona. Applying MIA, the postprandial glucose level is predicted with consideration of intra-patient variability and other sources of uncertainty. A worst-case approach is then used to calculate the risk index. In this way, a safer prediction of possible hyper- and hypoglycaemic episodes induced by the insulin therapy tested can be calculated in terms of these uncertainties. A study of the behaviour of three postprandial insulin action and glucose kinetics models in the context of intra-patient variability and uncertainty about food intake also revealed that, with such variability, simple glucose–insulin models may be sufficient to describe the patient dynamics in most situations.

Universitat de Girona
Departament d'Enginyeria Elèctrica, Electrònica i Automàtica

Resumen

La diabetes es una enfermedad metabólica caracterizada por niveles elevados de glucosa en plasma (hiperglucemia), que puede conducir a largo plazo a complicaciones micro y macrovasculares. Esta enfermedad se debe a la falta de secreción de insulina por parte de las células *beta* de los islotes de Langerhans en el páncreas (diabetes tipo 1) o a una resistencia celular a la acción de la insulina combinada con una deficiente secreción de insulina del páncreas (diabetes tipo 2). La diabetes es una de las enfermedades más graves que deben ser reguladas artificialmente. Según los últimos datos de la International Diabetes Federation, se estima que el número de diabéticos en todo el mundo pasará de 284,6 millones en 2010 hasta 438,4 millones en 2030, lo que equivale a 6,6 % y el 7,8%, respectivamente, de la población adulta del mundo en edades comprendidas entre 20 y 79 años.

La terapia convencional de la diabetes generalmente se basa en inyecciones subcutáneas de insulina. Debido a la inherente dificultad en la selección de una correcta dosis de insulina y el riesgo de episodios de hiper e hipoglucemia en pacientes con diabetes tipo 1, los sistemas de ayuda a la dosificación de insulina son muy útiles para mejorar la calidad de vida de estos pacientes. El cálculo de un índice de riesgo que permita predecir de forma segura la glucemia postprandial a corto plazo, requiere la evaluación de los efectos del bolo de insulina y la ingesta de alimentos en la glucosa postprandial. El uso de modelos dinámicos proporciona información valiosa acerca de excursiones de la glucosa postprandial. Sin embargo, uno de los principales retos a considerar es la gran variabilidad intraindividual entre los pacientes. Diferentes fuentes de incertidumbre tal como la incertidumbre en los alimentos ingeridos, son otros retos que deben ser considerados ya que no es posible medir con precisión la cantidad y el contenido de carbohidratos de una comida mixta en situaciones de la vida real. Estos factores hacen necesario el desarrollo de herramientas de predicción que tengan en cuenta diferentes fuentes de incertidumbre (entradas, parámetros y condiciones iniciales).

En esta tesis, se propone un nuevo método para estimar la dosis y el instante de inyección que genere el menor riesgo para una terapia intensiva de insulina. Este sistema de ayuda a la dosificación utiliza un algoritmo de optimización para determinar la dosis de insulina y el instante de inyección que reduzcan al máximo el riesgo de hiperglucemia e hipoglucemia posprandial en pacientes diabéticos tipo 1. Para ello, el algoritmo aplica una metodología que cuantifica el riesgo de sufrir diferentes grados de hipoglucemia e hiperglucemia en estado postprandial inducida por la terapia de insulina de acuerdo a los parámetros de cada paciente. Esta metodología se basa en el análisis intervalar modal (MIA), una teoría matemática desarrollada por investigadores de la Universidad de Barcelona y la Universidad de Girona. Aplicando MIA se predice el nivel de glucosa postprandial considerando la variabilidad intrapaciente y otras fuentes de incertidumbre. Para calcular el índice de riesgo se utiliza un planteamiento del peor caso. De esta manera se calcula una predicción más segura de posibles episodios de hiperglucemia e hipoglucemia inducida por la terapia de insulina en términos de dichas incertidumbres. Considerando la variabilidad intrapaciene y la incertidumbre presente en la ingesta de alimentos, fue realizado un estudio del comportamiento de tres modelos de acción de insulina y cinética de la glucosa posprandial con-

cluyendo que con dicha variabilidad un modelo de glucosa-insulina de baja complejidad puede ser suficiente para describir la dinámica de los pacientes en la mayoría de las situaciones.

Universitat de Girona
Departament d'Enginyeria Elèctrica, Electrònica i Automàtica

Resum

La diabetis és una malaltia metabòlica caracteritzada per nivells elevats de glucosa en plasma (hiperglucèmia), que a llarg termini pot conduir a complicacions micro i macrovasculars. Aquesta malaltia es deu a la manca de secreció d'insulina per part de les cèl·lules beta en els illots de Langerhans del pàncrees (diabetis tipus 1) o una resistència cel·lular a l'acció de la insulina combinada amb una deficient secreció d'insulina del pàncrees (diabetis tipus 2). La diabetis és una de les malalties més greus que han de ser regulades artificialment. Segons les últimes dades de la International Diabetes Federation, s'estima que el nombre de diabètics a tot el món passarà de 284,6 milions el 2010 fins 438,4 milions el 2030, el que equival a 6,6 % i a 7,8% , respectivament, de la població adulta del món d'edats compreses entre 20 i 79 anys.

La teràpia convencional de la diabetis generalment es basa en injeccions subcutànies d'insulina. A causa de la dificultat inherent en la selecció de la dosi correcta d'insulina i el risc d'episodis d'hiper i hipoglucèmia en pacients amb diabetis tipus 1, els sistemes d'ajuda a la dosificació d'insulina són molt útils per millorar la qualitat de vida d'aquests pacients. El càlcul d'un índex de risc que permeti predir de manera segura la glucèmia postprandial a curt termini, requereix l'avaluació dels efectes del bol d'insulina i de la ingesta d'aliments durant la glucosa postprandial. L'ús de models dinàmics proporciona informació valuosa sobre les excursions de la glucosa postprandial. No obstant això, un dels reptes principals a considerar és la gran variabilitat intraindividual entre els pacients. Diverses fonts d'incertesa, tals com la incertesa en la ingesta d'aliments, s'han considerar, ja que no és possible mesurar amb precisió la quantitat i composició de carbohidrats d'un menjar mixt en situacions de la vida real. Aquests factors fan necessari el desenvolupament d'eines de predicció que tinguin en compte diverses fonts d'incertesa (entrades, paràmetres i condicions inicials).

En aquesta tesi, es proposa un nou mètode per estimar la dosi i l'instant d'injecció que generi el menor risc per a una teràpia intensiva d'insulina. Aquest sistema d'ajuda a la dosificació utilitza un algorisme d'optimització per a determinar la dosi d'insulina i l'instant d'injecció que redueixin al màxim el risc d'hiperglucèmia i hipoglucèmia postprandial en pacients diabètics tipus 1. Per això, l'algorisme aplica una metodologia que quantifica el risc de patir diferents graus d'hipoglucèmia i hiperglucèmia en estat postprandial induïda per la teràpia d'insulina d'acord amb els paràmetres de cada pacient. Aquesta metodologia es basa en l'anàlisi intervalar modal (MIA), una teoria matemàtica desenvolupada per investigadors de la Universitat de Barcelona i la Universitat de Girona. Aplicant MIA es prediu el nivell de glucosa postprandial considerant la variabilitat intrapacient i altres fonts d'incertesa. Per calcular l'índex de risc s'utilitza un plantejament del pitjor cas. D'aquesta manera es calcula una predicció més segura de possibles episodis d'hiperglucèmia i hipoglucèmia induïda per la teràpia d'insulina en termes de les incerteses. Considerant la variabilitat intrapaciene i la incertesa present en la ingesta d'aliments, es va realitzat un estudi del comportament de tres models d'acció d'insulina i cinètica de la glucosa postprandial concloent que amb aquesta variabilitat, un model de glucosa-insulina de baixa complexitat pot ser suficient per descriure la dinàmica dels pacients en la majoria de les situacions.

Acknowledgements

I wish to express my sincere thanks to all those people who directly or indirectly contributed to and supported the development of this thesis. It is very difficult to mention them all, but I want everyone to know that I am deeply grateful.

I would like to express my gratitude and thanks to my supervisors Prof Josep Vehí and Dr Remei Calm. I thank Josep for his academic and financial support, patience, confidence, and guidance through this long process. To Remei, thanks for your academic support, encouragement, dedication, patience, and advice, and for being my adoptive mother in Girona.

I would also like to thank to Dr Jorge Bondia for his clever advice throughout these years, which contributed greatly to the success of my research. I also thank Dr Cristina Tarín and Dr Paolo Rossetti for their suggestions concerning my research.

Particular thanks go to all the members of the MICELab research group for their friendship and support during my time there and to all the members of the INSULAID project for their valuable contributions and support.

I thank the University of Girona for economic support through the research scholarship "Beca de Recerca UdG BR04/23" (three years and five months). This work was also partially funded by the Spanish Ministry of Science and Innovation through the coordinated research projects DPI2004-07167-C02, DPI2006-15476-C02-02, DPI-2007-66728, and DPI-2010-20764-C02, and by the government of Catalonia through grant SGR00296.

I have been fortunate to make many good friends throughout my life, and to them also my heartfelt thanks. To Jairo, Eduard, Monica, and Mauricio A, because I have always had their support and friendship, despite the distance. And remember guys, my achievements are your achievements! To Yenny and Mauricio Z for their invaluable friendship, personal support, and encouragement during the last five years. I also want to thank Yenny for her sisterly affection and Mauricio Z for his advice on writing this dissertation. I also thank the families of Mujica Ruiz and Ruiz Alvarez for their friendship, and for receiving me into their family.

I offer my regards and blessings to the family of Montenegro Martinez, to my sister Adriana and my nieces Sofia and Mariana, and to my grandparents Ligia, Gregorio, and Socorro, who have supported me in every sense during my life.

The last and longest paragraphs are dedicated to the great loves of my life, without whose constant efforts it would not have been possible to achieve my goals. I owe my deepest gratitude to my mother for her sacrifice, dedication, devotion, and love; she has taught me to fight for my dreams, and encouraged me to learn about other cultures and to overcome professional and personal problems. Excuse me Mum, for so many years of physical absence, but my heart, my soul, and everything I am have always been and will always be with you.

I am deeply grateful to Augustin and Alcides, who gave me the unconditional support and love of parents, and thank them for being my accomplices in my antics as a child and for their advice, patience, dedication, and commitment to my education. Despite not having my father with me, God has allowed me these two extraordinary parents.

During my doctoral studies, I was lucky enough to meet a wonderful person who changed my life with his unconditional love. I thank Fabian for his patience, support, encouragement, and dedication during the most difficult phase of my research and for giving me important suggestions about it. To Fabian, thanks also for giving me the best gift, our kitty Nino, who puts a smile on my face every day.

Finally, I wish to thank my family and all the people who care about me and about whom I care.

Thank you all!

Maira A. García Jaramillo
Girona, Spain
June 2011

Nomenclature

The following acronyms, abbreviations and variables are used in this thesis.

Acronyms and abbreviations

AP	Artificial Pancreas
ADA	American Diabetes Association
CGM	Continuous Glucose Monitor
CHO	Carbohydrates
CSII	Continuous subcutaneous insulin infusion
DCCT	Diabetes Control and Complications Trial
DM	Diabetes Mellitus
EGP	Endogenous Glucose Production
FDA	Food and Drug Administration
HbA1c	Glycosylated Haemoglobin
ICU	Intensive Care Unit
ID	Insulin pharmacodynamics
IDF	International Diabetes Federation
IU	Insulin Unit
IP	Insulin pharmacokinetics
IvalDb	Interval Value Double
IVGTT	Intravenous Glucose Tolerance Test
JDRF	Juvenile Diabetes Research Foundation
MCS	Monte Carlo Simulation
MDI	Multiple Daily Injection
MI	Monomeric Insulin
MIA	Modal Interval Analysis
NIH	National Institutes of Health
NPH	Neutral Protamine Hagedorn
OGTT	Oral Glucose Tolerance Test
PD	Pharmacodynamics
PK	Pharmacokinetics
RI	Risk Index
SAAM	Simulation Analysis and Modeling
SC	Subcutaneous
SD	Standard Deviation
T1DM	Type 1 diabetes mellitus
UVa	University of Virginia

Variables

αh_m	Weight of relative importance of mild hypoglycaemia
αH_m	Weight of relative importance of mild hyperglycaemia
αh_s	Weight of relative importance of severe hypoglycaemia
αH_s	Weight of relative importance of severe hyperglycaemia
BW	Body weight (kg)

D	Amount of carbohydrates ingested (mg)
d_i	Insulin dose (mU)
Δt	Integration step
$\gamma(t)$	Weighting function for the time occurrence of hyperglycaemia
G_b	Plasma glucose concentration in basal state (mg)
GC	Preprandial glucose measurement (mg/dL)
G_{max}	Upper bound of the predicted manifold glucose trajectories (mg/dL)
G_{min}	Lower bound of the predicted manifold glucose trajectories (mg/dL)
h_m	Glucose range of mild hypoglycaemia (mg/dL)
H_m	Glucose range of mild hyperglycaemia (mg/dL)
h_s	Glucose range of severe hypoglycaemia (mg/dL)
H_s	Glucose range of severe hyperglycaemia (mg/dL)
I	Insulin concentration (mU L^{-1})
I_b	Basal value of insulin concentration (mU dL^{-1})
II	Initial bolus insulin dose (mU min^{-1})
IM	Initial injection-to-meal time (min)
J	Cost function that represent the risk index
J_{hm}	Risk of mild hypoglycaemia
J_{Hm}	Risk of mild hyperglycaemia
J_{hs}	Risk of severe hypoglycaemia
J_{Hs}	Risk of severe hyperglycaemia
R_a	Glucose absorption rate (mg min^{-1})
S	Appearance rate of insulin in plasma (mU min^{-1})
t_{im}	Relative time between insulin injection and meal ingestion (min)
u	Insulin input (mU min^{-1})
V_g	Glucose distribution space (dL)
V_i	Insulin distribution volume (L kg^{-1})

Contents

List of Figures

List of Tables

Chapter 1

Introduction

This introductory chapter presents an overview of the thesis, beginning with the general considerations that motivated this research. The main problems and challenges, the objectives, and the methodology used in this study are briefly explained. Finally, a description of the structure and content of the thesis is presented.

1.1 Motivation

Diabetes mellitus (DM) is a metabolic disease characterized by elevated plasma glucose levels, corresponding to acute or chronic hyperglycaemia, which can lead to long-term micro- or macrovascular complications. Because of these complications, diabetes is a major cause of death in most countries. According to the International Diabetes Federation (IDF), cardiovascular diseases resulting from damage to the large blood vessels cause the death of 50% or more of people with diabetes, depending on the population examined. In a study of 216 countries and territories for the years 2010 and 2030, the IDF concluded that close to four million deaths in the 20–79 years age group can be attributed to diabetes in 2010, accounting for 6.8% of global all-cause mortality in this age group (Shaw et al., 2010)
.

Diabetes is rapidly emerging as a global health-care problem, which threatens to reach pandemic levels by 2030. One of the main reasons for this increase in the disease is the changes in lifestyle that have led to low levels of physical activity and increasing obesity. Most people in whom diabetes is diagnosed in childhood or adolescence have type 1 diabetes. It is estimated that some 76,000 children aged under 15 years develop type 1 diabetes annually worldwide, and this number is increasing at an alarming rate.

In the 1990s, the Diabetes Control and Complications Trial (DCCT) (DCCT, 1993) showed that any improvement in glucose control, as measured by the level of glycated haemoglobin (HbA1c), reduces the risk of the chronic complications associated with diabetes. HbA1c is a form of haemoglobin used primarily to identify the average plasma glucose concentration over prolonged periods of time. Based on these results, euglycaemia has been established as the control objective for patients with type 1 diabetes, unless contraindications exist. However, no universal, efficient, and safe system for normalizing the glucose levels of DM patients is yet available.

In type 1 diabetes, the insulin-producing cells of the pancreas are destroyed, which can ultimately lead to a total loss of insulin production. Therefore, exogenous insulin administration

is required to replace its physiological secretion. Different dosage regimens are used, such as multiple daily injection (MDI) therapy, continuous subcutaneous insulin infusion (CSII) with an external pump, or conventional treatment. MDI therapy is based on multiple insulin injections using a combination of short- and long-acting insulin analogues. Treatment with CSII combines continuous baseline insulin release by administering additional short-acting insulin before meals and in response to high glycaemic values. Insulin is administered from a small infuser subcutaneously via a catheter.

Typically, before each meal, the patient measures his/her preprandial blood glucose level and calculates the adjusted insulin dose in relation to the planned carbohydrate intake, according to rules prescribed in the therapy plan by the physician. This therapy involves a risk of severe hypoglycaemia, with all its consequences, if the dose is too high. Although several rules exist for the calculation of the bolus insulin dose, and these have even been recently incorporated into the automatic calculations of some insulin pumps, trial-and-error adjustments of the therapy must be made. The therapeutic goal in type 1 diabetes is to minimize the number of hypoglycaemic episodes and maximize the patient's glucose control. For this reason, the automatic control of insulin infusion, called the closed-loop insulin delivery or "artificial pancreas" has been presented as the ideal technological solution (Hoshino et al., 2009; Kumareswaran et al., 2009; Bondia et al., 2010).

The closed-loop insulin delivery requires a continuous glucose monitors (CGMs) to measure glucose concentration, an algorithm to determine the insulin delivery rate and an insulin pump delivering computed insulin doses. Closed-loop systems can be divided into "fully closed-loop" and "semi-closed-loop". The former do not require any information provided by the patient while the latter require that the patient introduces the time and size of the meal. Currently, there is a large international effort to develop an artificial pancreas. So far, a few prototypes have been developed and testing has been limited to clinical settings.

The United States Food and Drug Administration (US FDA) has established a multidisciplinary group of scientists and clinicians, in partnership with the National Institutes of Health (NIH), to address the clinical, scientific, and regulatory challenges related to this unique medical product. Further evidence supporting its utility is the almost simultaneous open call for an artificial pancreas by the NIH in the USA. The European Commission and the Juvenile Diabetes Research Foundation (JDRF) have also been principal players in the development of an artificial pancreas.

Despite the extensive work that has already been done to develop the artificial pancreas, many challenges are still to be faced, such as the accuracy and reliability of current CGMs, and the safety of insulin pumps. The lack of accuracy and reliability of CGM systems has been a technological bottleneck for the automation of insulin delivery. Different CGMs have reported relative errors greater than 20%. This is challenging for a closed-loop controller, especially when the temporal pattern of this error presents in the form of a bias. Similarly, reliability is one of the main requirements for CGMs. To improve their reliability, self-monitoring capacity should be embedded in CGMs, and should include the detection of abrupt faults and malfunctions (Mazze et al., 2009). In relation to the insulin pumps, although these are highly developed to be integrated into an artificial pancreas, is still necessary to improve their reliability. Most infusion system failures involve the infusion set components and the subcutaneous infusion site, e.g. obstruction of infusion set, infection of infusion site, leakage from the infusion site or leakage at the infusion set connection (Guilhem et al., 2006).

Current insulin pumps are "open-loop" systems. Although the user can measure blood glucose levels and alter the insulin dose accordingly, pumps do not automatically respond to changes in blood glucose level. Considering the inherent difficulty in selecting the insulin dose and the risk of hyper- and hypoglycaemic episodes, dosage-aid systems would be extremely useful for patients with type 1 diabetes.

An insulin dosage tool relies on sufficiently accurate predictions of glycaemia. However, there exists great intra- and inter-individual variability in patient behaviour. Intra-patient variability is related to the changes that occur within a patient during the day, such as the diurnal changes in insulin sensitivity. The factors that affect inter-patient variability include sex, age, weight, hormonal changes, stress, illness, and activity levels. Different sources of uncertainty are also important in the prediction of glycaemia. An important source of uncertainty is the patient's food intake, because it is difficult to estimate this precisely for a mixed meal. Therefore, the development of prediction tools that can accommodate different sources of uncertainty (input, parameters, and initial states) is required.

Many systems have been developed to educate and support the patient in the process of establishing the correct dose of insulin (Lehmann and Deutsch, 1995). Most of these systems are intended for educational purposes (Levy et al., 1989; Lehmann and Deutsch, 1992a; Hejlesen et al., 2000; Agar et al., 2005; Hedbrant et al., 2007), and only a few decision-support systems have been developed (Hejlesen et al., 1997; Mougiakakou and Nikita, 2000; Campos-Delgado et al., 2003; Cook et al., 2005). Insulin dosage advisory systems have also been incorporated into insulin pumps (Takahashi et al., 2008; Zisser et al., 2008), based on proportionality rules that consider the insulin/carbohydrate ratio, insulin sensitivity, and the insulin remaining from previous injections "insulin on board". Nevertheless, none of them addresses the problem of different sources of uncertainty, as mentioned previously. This study was specifically directed to overcoming this problem.

This research presents a novel method for estimating the dose and injection time relative to meal times required for low-risk intensive insulin therapy. The algorithm is based on the interval simulation of an individual patient's glucoregulatory model. The interval simulation is performed using modal interval analysis (MIA) (Gardeñes et al., 2001), which allows the overestimation of interval computations to be avoided or minimized under some conditions. MIA has been successfully applied to different fields, such as fault detection (Sainz et al., 2002; Calderón-Espinoza et al., 2007), control (SIGLA/X Group, 1999; Herrero, 2006b), computer graphics (Flórez-Díaz, 2008), and global optimization (Sainz et al., 2008), among others.

Several mathematical models that include subcutaneous insulin absorption, carbohydrate digestion and absorption, insulin pharmacokinetics and pharmacodynamics, and glucose metabolism are studied here using MIA to allow the computation of the tight enclosure of the envelope that includes all possible behaviours of the system. These models can be combined to represent a glucoregulatory model. Therefore, a library of interval models of the physiological subsystems of glucose regulation was developed. Some of these models have been used for the prediction of plasma glucose (considering uncertainty) (Calm et al., 2007a,b; Bondia et al., 2007; García-Jaramillo et al., 2009a; Bondia et al., 2009; García-Jaramillo et al., 2011a; Calm et al., 2011; Revert et al., 2011).

The interval glucose prediction is used to develop a method to quantify the risk of suffering

different grades of hypo- and hyperglycaemia. The risk index (RI) is calculated based on a suitable cost function, and the dosage-aid system then calculates the optimum insulin dosage and injection-to-meal time with the lowest risk according to the model.

The method developed here can be used by patients and physicians to evaluate the risk of hypoglycaemia or hyperglycaemia within the framework of a dosage-aid system.

1.2 Problems and Challenges

A list of the main problems in the development of insulin dosage tools is outlined below.

- **Inter- and intra-patient variability**: A dosage-aid system must be patient-specific because of the large inter-subject variability in glucose regulation. For instance, two children of the same age and weight often require quite different amounts of insulin. The insulin dosage tools must also cope with intra-patient variability. The tool must take into account the variations in insulin sensitivity that arise from circadian rhythms, changes in insulin absorption, etc.
- **Sources of uncertainty**: Food intake is an important source of uncertainty because accurate estimates are difficult to make for a mixed meal. In this regard, it is well known that diabetic patients tend to consistently underestimate the carbohydrate content of their meals (Graff et al., 2000). The input, parameters, and the initial state of the model may also include uncertainty. The disturbances affecting the system, such as stress and exercise, are other sources of uncertainty.
- **Model identification**: Model identification in diabetes is a complex process because simple models cannot represent all the glucose dynamics, and complex models are difficult or impossible to identify (Galvanin et al., 2009).
- **Long physiological delays in the subcutaneous route**: In healthy people, insulin is delivered from the β-cells in the pancreas to the portal circulation. The delay in insulin action in this case is about 30 min (Hovorka, 2006). When the subcutaneous route is used for the delivery of insulin, the delay in insulin action is about 80 min from the time of infusion, even when rapid-acting insulin analogues are used. More delay is attributable to the glucose sensing in the subcutaneous route, because the transport of glucose from blood to the interstitial fluid.
- **Risks of intensive therapy**: The counteraction of intensive insulin therapy required to achieve glucose control objectives is an increase in the risk of severe hypoglycaemia, with all its consequences. One fact that illustrates the difficulties of achieving an optimal metabolic control is that, even in the DCCT study, which had a significant infrastructure, less than 5% of patients with intensified treatment achieved optimal HbA1c levels (<6.5%), and they did so at the expense of suffering more frequent severe hypoglycaemia (DCCT, 1993). Non-achievement of the control goals is frequently a source of frustration for the patients and their physicians as well, since it is well known that poorly controlled diabetes leads to chronic complications with significant morbidity and mortality.

1.3 Objectives

The general objective of this research was to include intra-patient variability and different sources of uncertainty in the design of strategies for insulin dosage adjustment.

To achieve this objective, the study addressed the following specific aims:

1. To consider the different sources of uncertainty and the large inter- and intra-patient variability, in order to obtain an optimal interval simulation that includes all possible behaviours of the glucose–insulin system. For this purpose, interval analysis has been shown to be a potential tool, because uncertainty can be naturally described as intervals, not only in the patient model parameters, but also in the initial states and inputs (for instance, the rough estimation of carbohydrate intake). MIA is used to reduce the impact of multiple instances of the same variable in the expression to be evaluated, leading to an overestimation of the result. By applying MIA, different models of the glucose–insulin system can be examined to achieve the optimal calculation. A library of glucoregulatory interval models can then be constructed.

2. To quantify hypo- and hyperglycaemia risk indices based on interval predictions of the patient's postprandial glucose. In this way, a risk prediction system can be established to quantify the risk of different grades of hypo- and hyperglycaemic episodes in the postprandial state for a given insulin therapy. By considering inter- and intra-patient variability and other sources of uncertainty, we can more safely predict the possible hyper- and hypoglycaemic episodes induced by the insulin therapy tested.

3. To develop an insulin dosage-aid system based on worst case analysis and risk prediction to estimate the bolus insulin dose and injection times. The information contained in the risk index is integrated into an optimization algorithm to calculate the insulin dose and injection-to-meal time that minimize the risk of postprandial hyper- or hypoglycaemia in type 1 diabetic patients.

1.4 Thesis Structure

This thesis is organized into three parts, as shown in Figure 1.1. Part I is related to the background of type 1 diabetes, and the state-of-the-art of the plasma glucose and insulin modelling are presented. Part II focuses on the methodology used in developing a library of interval models of the physiological subsystems of glucose regulation. Finally, the insulin dosage-aid system is presented in Part III.

Here, a more detailed overview of all the chapters of the dissertation is described:

- **Chapter 1** outlines the motivation for this research, the problems and challenges involved, and the research objectives.

- **Chapter 2** starts with an overview of diabetes, in which the complications and health-care costs for diabetic patients are described. Next, different types of insulin and the major advances in insulin therapy for type 1 diabetic patients are presented. The variability in blood glucose prediction is also explained. The state-of-the-art of the different mathematical models that describe the processes of insulin pharmacokinetics and pharmacodynamics, carbohydrate absorption, and glucose transport and elimination are presented.

- **Chapter 3** addresses the techniques used to solve the problem of simulating uncertain systems, with a particular emphasis on the concepts and results of MIA.

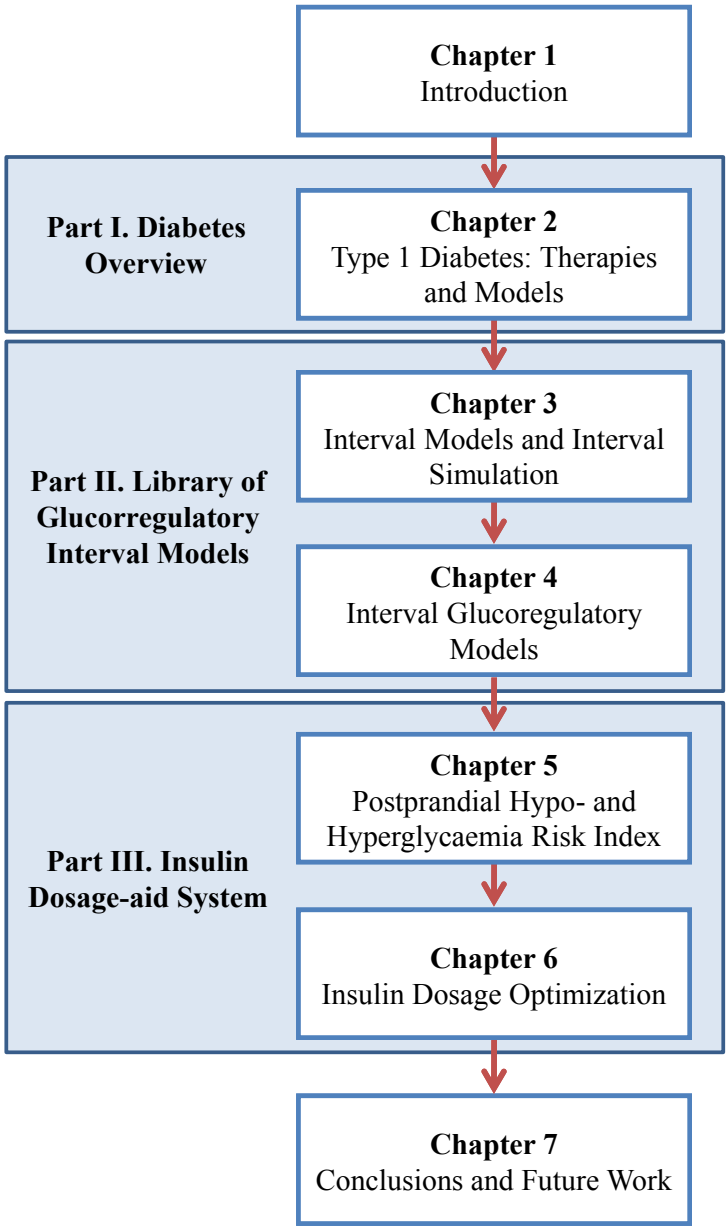

Figure 1.1: Thesis outline.

- **Chapter 4** presents the prediction of plasma glucose using MIA. This prediction is performed while considering different sources of uncertainty. Therefore, a selection of the models presented in Chapter 2 is studied to produce the optimal calculation. Next, the results obtained with MIA are compared with those obtained with Monte Carlo simulation (MCS) with a uniform probability distribution. Finally, three plasma glucose interval models are compared.

  Publications related to this chapter:

  [**Calm2007a**] Calm, R., García-Jaramillo, M., Vehí, J., Bondia, J., Tarín, C., and García-Gabín, W. (2007). Prediction of glucose excursions under uncertain parameters and

food intake in intensive insulin therapy for type 1 diabetes mellitus. In *29th Annual International Conference of the IEEE Engineering in Medicine and Biology Society*, pages 1770-1773, 22-26 August, Lyon, France.

[**Calm2007b**] Calm, R., García-Jaramillo, M., Vehí, J., Bondia, J., Tarín, C., and García-Gabín, W. (2007). Simulación intervalar del metabolismo de la glucosa en pacientes con diabetes mellitus tipo 1. In *IX Jornadas de ARCA*. Sistemas Cualitativos y Diagnosis, Lloret de Mar, Spain.

[**Bondia2007**] Bondia, J., Calm, R., García-Jaramillo, M., Vehí, J., Tarín, C., and García-Gabín, W. (2007). Predicción de glucemia en pacientes con diabetes tipo 1 ante incertidumbre. In *I Simposio de Modelado y Simulación de sistemas dinámicos (SIMOSI)*, Congreso Español de Informática (CEDI), Zaragoza, Spain.

[**Calm2011**] Calm, R., García-Jaramillo, M., Bondia, J., Sainz, M., and Vehí, J. (2011). Comparison of interval and monte carlo simulation for the prediction of postprandial glucose under uncertainty in type 1 diabetes mellitus. *Computer Methods and Program in Biomedicine*, In press.

[**Garcia-Jaramillo2011b**] García-Jaramillo, M., Calm, R., Bondia, J., and Vehí, J. (2011b). Interval simulation of glucose prediction models in presence of intra-individual variability and uncertain food intake. In *Workshop on Control, Dynamics, Monitoring and Applications*, Caldes de Montbui, Spain.

[**Garcia-Jaramillo2011c**] García-Jaramillo, M., Calm, R., Bondia, J., and Vehí, J. (2011c). Prediction of postprandial blood glucose under uncertainty and intra-patient variability in type 1 diabetes: a comparative study of three interval models. *Computer Methods and Programs in Biomedicine*, *Submitted*.

- **Chapter 5** describes computing the risk of postprandial hypo- and hyperglycaemia in type 1 diabetic patients while considering intra-patient variability and other sources of uncertainty. First, a brief summary of the principal methods used to analyse the risk of suffering hypo- and hyperglycaemic events is presented. A method of quantifying the risk of suffering different grades of hypo- or hyperglycaemia, using interval prediction, is then proposed. Finally, a model-based prediction of worst-case glucose excursions is made by considering intra-patient variability and uncertain initial states and food intake.

  Publications related to this chapter:

  [**Garcia-Jaramillo2009a**] García-Jaramillo, M., Calm, R., Bondia, J., Tarín, C., and Vehí, J. (2009). Computing the risk of postprandial hypo- and hyperglycemia in type 1 diabetes mellitus considering intrapatient variability and other sources of uncertainty. *Journal of Diabetes Science and Technology*, 3(4):895-902.

  [**Garcia-Jaramillo2009b**] García-Jaramillo, M., Calm, R., Bondia, J., Tarín, C., and Vehí, J. (2009). Prediction of postprandial hypo- and hyperglycemia events by means of interval models with uncertain parameters and food intake. Poster, In *2nd International Conference on Advanced Technologies & Treatments For Diabetes*, Athens, Greece.

- **Chapter 6** describes the dosage-aid system. First, a chronological summary is given of the different methods used to support the patient in the insulin dosage process for different purposes. Next, the methodology and algorithm used to calculate the optimum insulin

dose and injection-to-meal time based on a worst-case approach are described. Finally, to demonstrate the feasibility of the proposed methodology, three different scenarios for a virtual patient with nominal parameters are considered to calculate the insulin doses and injection-to-meal times with the lowest risk.

Publications related to this chapter:

[**Calm2009**] Calm, R., García-Jaramillo, M., Bondia, J., and Vehí, J. (2009). Insulin dosage based on risk index of postprandial hypo- and hyperglycemia in type 1 diabetes mellitus with uncertain parameters and food intake. In *Small Workshop on Interval Methods (SWIM)*, Lausanne, Switzerland.

[**Garcia-Jaramillo2011a**] García-Jaramillo, M., Calm, R., Bondia, J., Tarín, C., and Vehí, J. (2011a). Insulin dosage optimization based on prediction of postprandial glucose excursions under uncertain parameters and food intake. *Computer Methods and Programs in Biomedicine*, In press.

- **Chapter 7** discusses the conclusions and contributions of this research, and future work.

Chapter 2

Type 1 Diabetes: Therapies and Models

2.1 Glucose–Insulin System

The normal regulation of the blood glucose level is achieved by the glucose–insulin system. A healthy person normally has a fasting sugar level in the range of 70–110 mg/dL. After 1 g/kg of glucose intake, the glucose level increases to 120–140 mg/dL, returning to baseline after 2 h. Exogenous factors that affect the blood glucose concentration include food intake, rate of digestion, exercise, and reproductive state. A simple description of the glucose–insulin system is shown in Figure 2.1. When a person eats a meal, his/her glucose level rises (the blood glucose level moves to the red area) and the pancreas responds by secreting insulin, which signals to the liver to stop making glucose. The medical term for high blood glucose is "hyperglycaemia".

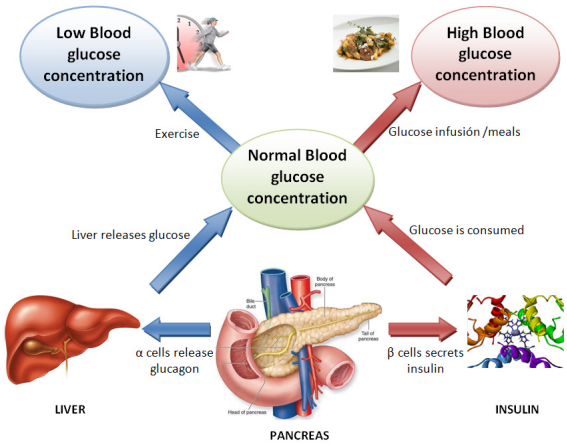

Figure 2.1: The blood glucose–insulin system (adapted from Makroglou et al. (2006)).

Insulin is a hormone produced by the β-cells of the islets of Langerhans in the pancreas (see Figure 2.2). The main action of insulin is to regulate the glucose levels in the blood, allowing the body's cells to absorb glucose from the bloodstream, which brings the blood glucose to the green area.

When there is too much insulin in the bloodstream and too little food has been eaten, the

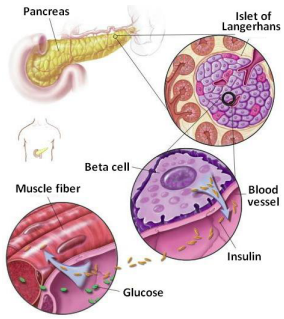

Figure 2.2: Insulin production in the human pancreas (taken from National Institutes of Health (2006)).

glucose level decreases. The same situation occurs when exercise has been undertaken without extra food intake. These situations correspond to the blue area in Figure 2.1. The medical term for low blood glucose is "hypoglycaemia". When a person has hypoglycaemia, the α-cells react by releasing glucagon, which acts on the liver cells, causing them to release glucose into the blood until the person is back in the green area again (Makroglou et al., 2006). In a healthy person, the production of glucagon declines when the blood glucose and insulin concentrations rise after a meal. Glucagon and insulin are part of a feedback system that maintains the blood glucose at the correct level.

2.2 Diabetes Overview

Diabetes mellitus (DM) is a metabolic disease characterized by elevated plasma glucose levels. The metabolic control objective is to normalize the blood sugar and prevent or delay the onset of long-term complications. Unlike a healthy person, when a diabetic patient ingests 1 g/kg glucose, his/her blood glucose levels become high, and only return to baseline after 4–6 h. This is shown in Figure 2.3, where the oral glucose tolerance test (OGTT) is represented schematically.

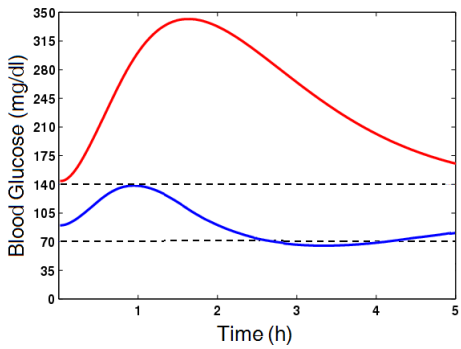

Figure 2.3: Oral glucose tolerance test. The blue line corresponds to a healthy person and the red line to a diabetic patient.

DM is one of the most serious diseases that must be regulated artificially. According to the latest data from the *International Diabetes Federation* (IDF), it is estimated that the number

of diabetics worldwide will increase from 284.6 million in 2010 to 438.4 million in 2030, equivalent to 6.6% and 7.8%, respectively, of the world's adult population aged between 20 and 79 years (see Figure 2.4). Between 2010 and 2030, there will be a 69% increase in the number of adults with diabetes in developing countries and a 20% increase in developed countries (Shaw et al., 2010). These statistics are probably an underestimate of the future prevalence of diabetes in this pandemic. The worldwide increase in people with diabetes is attributable to an aging population, the growth in population size, urbanization, and the high prevalence of obesity and sedentary lifestyles.

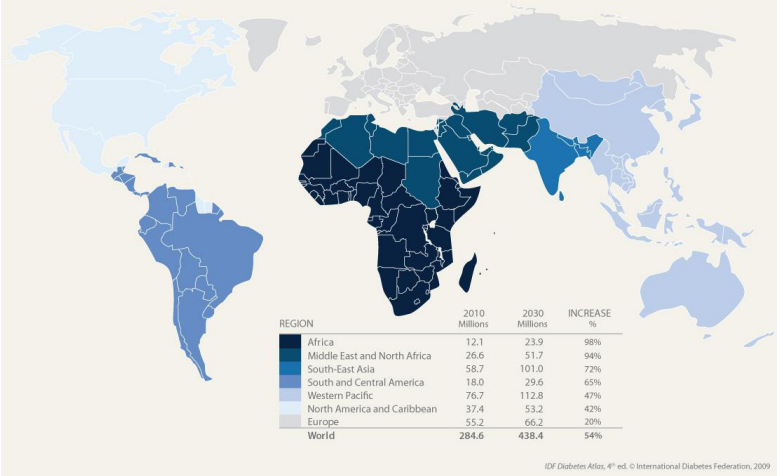

Figure 2.4: IDF regions and global projections for the number of people with diabetes (20–79 years), 2010–2030. (Taken from International Diabetes Federation (2009)).

The health-care costs of diabetic people are double the costs incurred by people without diabetes. In Europe, health spending by diabetics is estimated to be between USD 3000 and USD 6500 annually. This range is exceeded in the United States. Health-care expenditure on diabetes will account for 12% of the total health-care expenditure in the world in 2010. The total annual global health expenditure for diabetes in 2010 was estimated to fall between USD 376 billion (R=2) and USD 672 billion (R=3), where R is the ratio of diabetic to non-diabetic medical care expenses (Zhang et al., 2010). Figure 2.5 shows the estimated expenditure for diabetes by IDF region for 2010 and 2030, assuming R=2. For the reasons discussed above, there are clear economic and social benefits in identifying effective therapies for diabetes.

Clinically, glycaemic control is assessed by the measurement of glycosylated haemoglobin (HbA1c). It is based on the fact that red blood cells live for approximately 120 days and reflect the average measurement of blood glucose over the past 6–12 weeks. This test, in conjunction with home glucose monitoring, is used as the basis for treatment adjustments.

The normal range for the HbA1c test is 4–6% for people without diabetes. The Diabetes Association recommends that the ideal range of HbA1c for adults and adolescents with diabetes is generally less than 7% and that physicians should re-evaluate and, in most cases, significantly change the treatment regimen in patients with HbA1C consistently above this level (American Diabetes Association, 2004).

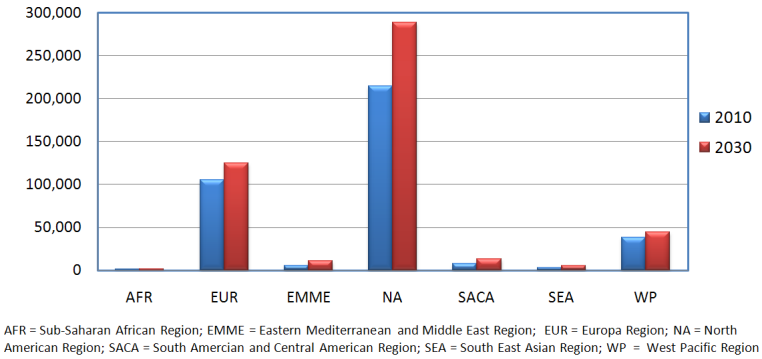

Figure 2.5: Health expenditures (USD) for diabetes in 2010 and 2030 by region (International Diabetes Federation, 2009).

2.2.1 Types of diabetes

Diabetes mellitus is usually referred to simply as "diabetes", which means "flowing through", while "mellitus" means "sweet as honey". Diabetes is also described as either insulin dependent (IDDM) or non-insulin dependent (NIDDM), or, more recently, as type 1 diabetes and type 2 diabetes, respectively.

In the past, diabetes was diagnosed by tasting the urine. The only treatment was alcohol, which lowers the blood sugar level. Before insulin was discovered, type 1 diabetes always resulted in death, usually quite quickly. Insulin has been medically available since 1921.

An updated etiological classification of diabetes mellitus was made by the American Diabetes Association (ADA) (American Diabetes Association, 2010).

Type 1 diabetes

Type 1 diabetes mellitus (T1DM, previously known as insulin-dependent or childhood-onset diabetes) is an autoimmune disease characterized by elevated plasma glucose levels, corresponding to acute or chronic hyperglycaemia. This results from the destruction by cells of the immune system of the insulin-producing β-cells in the islets of Langerhans in the pancreas, ultimately leading to the total loss of insulin production. Without insulin, glucose remains in the bloodstream, so blood glucose levels increase, especially after meals are consumed (Hanas, 2004). The glucose is then passed out of the body in the urine.

The symptoms of type 1 diabetes are tiredness, hunger, polyuria, polydipsia, and weight loss. Untreated hyperglycaemia can lead to serious long-term complications, including cardiovascular diseases, kidney failure, blindness, and stroke.

In the 1990s, the Diabetes Control and Complications Trial (DCCT) (DCCT, 1993) showed that any improvement in glucose control, as measured by the level of HbA1c, reduces the risk of the chronic complications associated with diabetes. For this reason, euglycaemia has been established as the control objective for patients with type 1 diabetes, except when some contraindication exists. The treatment required to achieve this glucose control objective involves the injection of insulin into the body, exercise, and a healthy diet. A type 1 diabetic patient is

dependent on insulin injections because insulin is not secreted by the pancreas. However, this therapy has a counteraction which is it increases the risk of severe hypoglycaemia, with all its consequences. When hypoglycaemia is untreated, it will worsen and cause confusion, clumsiness, or fainting. Severe hypoglycaemia can lead to seizures, coma, and even death.

Type 2 diabetes

Type 2 diabetes involves a reduction in the efficiency of insulin in promoting the transport of plasma glucose into cells due to a resistance to insulin, resulting in the eventual loss of insulin production. Initially, oral drugs, such as metformin, are required to increase the body's sensitivity to insulin, or to increase the release of insulin from the pancreas. Over time, the number of β-cells starts to decline, and then the type 2 diabetic patient must be treated with insulin injections like the type 1 diabetic to maintain his/her blood sugar at normal levels. Approximately 90–95% of diabetic patients have type 2 diabetes.

A degree of hyperglycaemia sufficient to increase the risk of macrovascular and microvascular complications, but without clinical symptoms, may be present for a long time before type 2 diabetes is detected.

2.2.2 Complications

Diabetes mellitus is a disease with a great socio-sanitary impact because of its high frequency and, more importantly, the consequences of its chronic complications. Insulin deficiency causes elevated plasma glucose concentrations, and if these are not controlled well, they may precipitate short-term and long-term complications.

Short-term complications

Hypoglycaemia and hyperglycaemia are considered short-term complications of diabetes. The symptoms of hypoglycaemia include: weakness or shakiness, sweating, dizziness, hunger, nervousness, and confusion. If hypoglycaemia is not treated, headache, irritability, poor circulation, poor co-ordination, and numbness in the mouth and tongue may occur. Serious hypoglycaemia can result in altered consciousness, seizures, coma, and even death.

The symptoms of hyperglycaemia include excessive thirst and hunger, frequent urination, nausea, vomiting, and lack of energy. Prolonged hyperglycaemia can lead to a condition called "ketoacidosis". Ketoacidosis is caused by high levels of ketones in the blood and urine, and can lead to acidosis, a condition in which the blood is too acidic. When this happens, the condition is known as "diabetic ketoacidosis" (DKA). Unless treated promptly, DKA may induce a diabetic coma.

Long-term complications

High blood sugar levels over the long term increase the risk of a series of medical problems. Long-term complications may cause small and large blood vessel disease (see Figure 2.6). Small blood vessel disease (microvascular disease) can damage the kidneys, eyes, or nerves, and large blood vessel disease (macrovascular disease) can cause heart disease, stroke, or peripheral vascular disease. In Table 2.1, the long-term complications of diabetes are described (Beers and Jones, 2004).

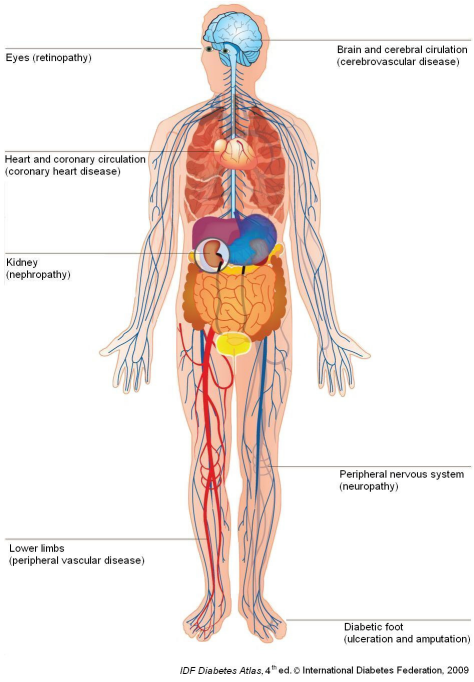

Figure 2.6: The major complications of diabetes (Taken from International Diabetes Federation (2009)).

Diabetic complications can often be prevented if the doctor's orders are followed and the patient's blood sugar levels are controlled.

2.2.3 Type 1 diabetes therapy

The real cure for diabetes would be a pancreatic or Langerhans islet transplantation. However, for immunological reasons, this transplantation is not always successful and the procedure poses serious risks. Islet cell transplantation requires the use of immune-suppressing medications, and the body often destroys the transplanted islet cells, just as it destroyed its own natural islet cells, making the medication-free period short-lived. Furthermore, an insufficient supply of islet cells is an obstacle to the wider use of this treatment. Transplantation is usually reserved for those with very difficult-to-control diabetes. Approaches that simulate β-cell replenishment by neogenesis or the replication of stem cells are still in the research stage (Efrat, 2003). Until now, the most widely used therapy has been the subcutaneous injection of insulin.

One of the main problems in the field of biomedical engineering is the control of blood glucose. This is because patients are extremely diverse in their physiological dynamics, and their characteristics also vary with time. Because there is no outer control loop replacing the partially or totally deficient system of blood glucose control in the human body, patients must regulate their glucose levels manually. They must decide the appropriate insulin dose to be injected based on their measured glucose levels. Good nutrition and regular physical activity are also important components of diabetes treatment and the prevention of long-term complications.

Tissue or Organ affected	Disease	What happens	Complications
Eyes	Glaucoma and retinopathy	Pressure builds up inside the eye, which can decrease blood flow to the retina and optic nerve and damage them. The small blood vessels of the retina become damaged; fluid leaks into the black of the eyes, and abnormally weak blood vessels grow and can burst	Loss of vision and ultimately, blindness
Kidneys	Nephropathy	The changes in the very small blood vessels of the kidneys produce damage to the filtering ability of these	Poor kidney function; kidney failure and the need for dialysis or kidney transplantation
Nervous system	Neuropathy	The small blood vessels that feed nerves in the hands and feet and nerves that control unconscious functions, such as blood pressure, digestive processes and sexual functioning, become damaged. The function abnormally or stop functioning overall	Numbness and tingling especially the feet and legs, sensitivity to touch or muscle weakness, chronic pain, numbness and muscle wasting, sores and ulcers; dizziness or faintness due to a drop in blood pressure after standing or sitting up
Heart	Coronary heart	Fat (plaque) and blood blots build up in the large blood vessels and stick to the vessels walls. This provoke blockage of the blood vessels supplying blood to the heart	Heart attack
Brain	Cerebrovascular	The artery that supplies blood to the brain tissue is blocked, or a ruptured artery causes bleeding into the brain	Aphasia, dizziness, loss of balance or coordination; sudden blurred, double or decreased vision in one or both eyes; stroke
Peripheral arteries	Peripheral Vascular	Build-up of plaque in the arteries that are located of the body reducing the flow of blood to the legs	Foot ulcers, infections, and even loss of a toe, foot, or lower leg

Table 2.1: The long-term complications of diabetes.

Insulin therapy

The intensive insulin therapy required to achieve the glucose control objective in T1DM patients is based on the administration of basal and bolus insulin to replace its physiological secretion. This insulin is released by the pancreas in a healthy person after a meal (see Figure 2.7), between meals, and during the night. Therefore, in a T1DM patient, the bolus insulin emulates the secretion of insulin after a meal, while the basal insulin emulates the insulin secretion between meals and during the night.

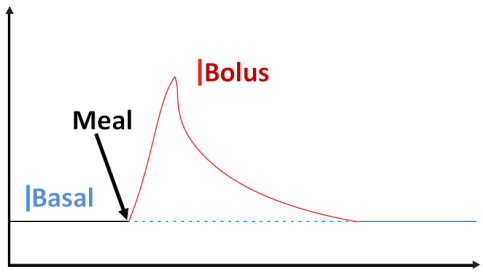

Figure 2.7: Endogenous insulin release in a healthy person to a food intake.

Before the eighties, insulin was extracted from bovine or pig pancreas. Since 1980, insulin with the same structure as human insulin has been synthesized, and insulin analogues have been

developed using genetic manipulation. Currently, the available insulin analogues are classified according to their duration of action as rapid-acting (e.g., Lispro, Aspart), short-acting (e.g., regular Actrapid), intermediate-acting (e.g., NPH, Lente), and very-long-acting insulins (e.g., Glargine, Detemir). Regular short-acting and rapid-acting insulins are given as a bolus injection before meals. Rapid-acting insulin analogues have a much more rapid action than short-acting insulins, as can be seen in Table 2.2. Intermediate-acting and very-long-acting insulins are used as basal insulin, and are injected once or twice daily, according to the dosage regimen. A review of insulin analogues and a representation of the insulin profiles achieved with different dosage regimens has been published by Gossain (2003).

Insulin	Onset of action	Peak effect	Duration
Lispro	5-15 minutes	30-90 minutes	3-5 hours
Aspart	10-20 minutes	1-3 hours	3-5 hours
Regular insulin	30-60 minutes	1-5 hours	6-10 hours
Buffered regular insulin	30-60 minutes	1-3 hours	8 hours
Lente	1-3 hours	6-14 hours	16-24 hours
NPH	1-2 hours	6-14 hours	16-24+ hours
Glargine	1.1 hours	None	$\sim$24 hours
Ultralente	4-6 hours	8-20 hours	>24 hours

Table 2.2: Pharmacokinetics of available insulin products.

A combination of basal and bolus insulin can be used to achieve normal glucose levels. Different dosage regimens are used, such as multiple daily injections (MDI) regimens, continuous subcutaneous insulin infusion (CSII), or conventional treatment. A common treatment for type 1 patients involves injecting a combination of short- and intermediate-acting insulins twice daily, before breakfast and before the evening meal. Intensified regimens can improve the control of blood glucose, and involve multiple daily injections of short-acting insulins with meals and a long-acting insulin at night, or CSII with a short-acting insulin delivered through a pump. The effects of CSII on glycaemic control were compared with those of MDI injections by Jeitler et al. (2008). This meta-analysis showed that CSII gives a greater reduction of HbA1c than MDI both in adults and adolescents with type 1 diabetes.

The frequency and quantity of the insulin dose depend on each individual patient's weight, physical activity, carbohydrates consumed, insulin sensitivity, disease history, etc. Before each meal, patients normally measure their preprandial blood glucose level and then calculate the adjusted insulin dose in relation to the planned carbohydrate intake, according to rules prescribed by the physician involved in the therapy plan. If the dose is too high, there is a risk of severe hypoglycaemia, with all its consequences.

Because the use of an external closed-loop system that can replace a partially or totally deficient system of blood glucose control in the human body is still in the research stage, patients must regulate their glucose levels themselves. They must decide the appropriate insulin dose to be injected based on glucose measurements and meal intakes.

The concept of glycaemic control in a "closed loop" is an attractive idea that has arisen from the weaknesses inherent in injection therapies or traditional therapies based on insulin

pumps. These therapies are likely to produce abnormal glucose levels, and present difficult and inappropriate tasks for the patient. For these reasons, a substitute for the healthy beta cell of the pancreas, which simulates its endocrine function, called the "artificial pancreas" (AP), can be established to provide fully automated glycaemic control, or a closed loop (Kumareswaran et al., 2009). This AP consists of continuous glucose monitoring coupled to an insulin-delivery device, and a closed-loop algorithm which provides the correct dose of insulin at the right time without human intervention (Harvey et al., 2010).

In recent years, significant progress has been made in the development of an AP. Improvements in continuous glucose monitors have meant considerable progress in this direction. Today, the problem lies in the demands of "closing the loop", because this advance requires better-performing sensors (more reliable and accurate) and control algorithms that take into account the drawbacks of subcutaneously use and telemedicine support. The main actors in the development of the AP, in addition to the European Commission, have been the Juvenile Diabetes Research Foundation (JDRF) and the National Institute of Health (NIH) in the USA. Globally, the most important advances in the field of AP development have been made through the "Artificial Pancreas Project" (Kowalski and Lum, 2009), launched by the JDRF in 2006 to validate the effectiveness of new technologies in continuous glucose monitoring and to promote the development of simulators that will allow us to "close the loop" by linking continuous glucose monitors with insulin pumps.

Diet and physical activity

Several studies have clearly demonstrated the benefits of a healthy diet, regular exercise, and weight loss for individuals already diagnosed with diabetes (Fowler, 2007). Obese people have a higher incidence of hypertension and hyperlipidaemia than non-obese people, which may further increase their risk of the microvascular and macrovascular complications of diabetes (Mokdad et al., 2003).

Therefore, an important part of treating people with type 1 diabetes is good nutrition, careful monitoring of carbohydrate and fat intake, regular physical activity, maintenance of a healthy weight, and not smoking. Diabetic patients should eat at about the same times each day and try to be consistent with the types of food eaten. In this way, glucose levels that are too high or too low can be prevented. To this end, it is recommended that diabetic patients create a meal plan that accommodates their health goals, food preferences, and lifestyles. The American Diabetes Association and the American Dietetic Association have information for planning healthy, balanced meals.

The patient with type 1 diabetes must learn to count or at least closely estimate the amount of carbohydrate that is consumed to help regulate their blood glucose levels and to adjust their insulin dose. Failure to do so can lead to dangerous hyperglycaemia or hypoglycaemia. Patients adjust their doses of insulin according to the amount of carbohydrate consumed and their insulin therapy. For therapies involving multiple daily injections or CSII, the patient must calculate the dose based on his/her carbohydrate intake. However, when fixed doses of rapid- or short-acting insulin are administered, the diabetic patient must keep the amount of carbohydrate relatively constant from meal to meal (Rabasa-Lhoret et al., 1999).

Exercise is also an essential part of treatment because regular exercise helps control blood glucose. It also helps to burn excess calories and fat, to achieve a healthy weight. However,

physical activity lowers blood glucose, often long after the patient has finished exercising. Therefore, it is necessary to monitor blood glucose before and after physical activity, and to be wary of hypoglycaemia, which can develop during or even several hours after exercise. The diabetic patient should also have carbohydrate sources available and consume them as necessary to avoid hypoglycaemia.

Exercise affects the insulin dose required. When a diabetic patient exercises, he/she needs less insulin because exercise allows glucose to enter the muscle cells for immediate use. Therefore, the diabetic patient must determine the effect of exercise on his/her blood glucose, adjusting the insulin dose by self-monitoring.

2.2.4 Variability on blood glucose prediction

Great inter- and intra-patient variability is a major challenge in developing an AP. The factors that affect inter-patient variability include sex, age, weight, hormonal changes, stress, illness, and activity levels. Other factors that may cause fluctuations in glucose metabolism include variations in meal absorption, insulin sensitivity, and subcutaneous absorption.

Intra-patient variability is related to the changes that occur within a patient during the day, such as the diurnal changes in insulin sensitivity. The significant variability that occurs in the relevant parameters between patients and within a given patient during the course of the day or week has been documented in the literature (Simon et al., 1987; Bremer and Gough, 1999; Acikgoz and Diwekar, 2010). Various errors can also influence inter- and intra-patient variability, including errors in counting the carbohydrates in meals, sensor measurements, and the accuracy of blood glucose meters (Chassin et al., 2004; Kildegaard et al., 2007; Kirchsteiger et al., 2009).

Different studies of this variability can be found in the literature. For example, the variability in subcutaneous absorption has been widely studied by Heinemann (2002); Barnett (2003); Heise et al. (2004); Guerci and Sauvanet (2005); Scholtz et al. (2005); Goykhman et al. (2009). Uncertainty in the amount of meal and the times of meals have also been examined (Graff et al., 2000; Chassin et al., 2004; Kildegaard et al., 2007; Kirchsteiger et al., 2009).

Inter- and intra-patient variability can create difficulties in continuous glucose control, and it may be virtually impossible to apply the same controller to different patients, or even to the same patient, who may show large variations on different days. Therefore, different diabetes simulators have been developed to accommodate this variability in virtual patients (Wilinska and Hovorka, 2008). In a model based control, the success of an optimal control method depends on the accuracy of the model and how well this variability is taken into account.

2.3 Plasma Glucose and Insulin Modelling

To perform a model-based *in silico* simulation and for clinical diabetes decision support, a pharmacodynamic model of the interaction between glucose and insulin is required. This mathematical model describes the processes of insulin pharmacokinetics (PK) and pharmacodynamics (PD), carbohydrate absorption, and glucose transport and elimination (see Figure 2.8). Many models of glucose regulation have been proposed in recent decades, using experimental data to measure glucose production, glucose utilization, and insulin and meal absorption. A review of glucose–insulin dynamics has been presented by Nucci and Cobelli (2000), Mari (2002),

Makroglou et al. (2006) and Wilinska and Hovorka (2008).

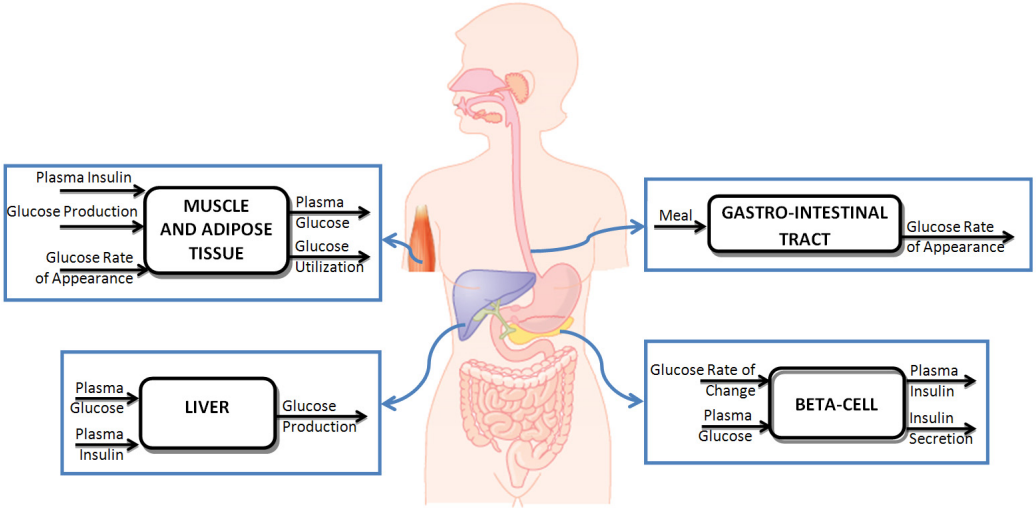

Figure 2.8: Unit processes in glucose and insulin subsystems.

Mathematical models of diabetes are used for a variety of applications: to estimate insulin sensitivity, for educational purposes, and as advisory systems. According to Chee and Fernando (2007), these models range from simple expressions that relate glucose and insulin in linear models (e.g., Ackerman et al. (1964); Cerasi et al. (1974); Salzsieder et al. (1985)), to simple non-linear models (e.g., Bergman et al. (1981); Candas and Radziuk (1994); De Gaetano and Arino (2000)), to more comprehensive mathematical models (e.g., Sorensen (1985); Cobelli et al. (1986); Parker et al. (1999); Hovorka et al. (2004); Dalla Man et al. (2007b)). Compartment models have been used by some of these authors in the development of their models. This allows them to describe the processes that occur in the inaccessible portions of the system, because they are not directly measurable. The inaccessible portion of a system is represented by a number of interconnected compartments.

Models that describe the glucose–insulin system allow the estimation of the plasma glucose concentration, which is difficult to measure in a clinical environment. Based on this estimation, it might be possible to optimize an insulin therapy.

Different models of subcutaneous insulin absorption, gastric emptying, digestion and absorption, insulin kinetics, and glucose metabolism are described in this section.

2.3.1 Subcutaneous insulin absorption

As discussed in Section 2.2.3, people with type 1 diabetes must inject themselves with insulin one or more times daily. After a subcutaneous injection, the insulin is gradually absorbed by the body, and once inside the individual, the insulin concentration is time dependent.

When a specific amount of insulin is injected subcutaneously into a patient, it diffuses throughout the adipose tissue, where it undergoes a series of molecular transformations, to be absorbed into the bloodstream through the capillary wall. This process is known as the

absorption of insulin (see Figure 2.9).

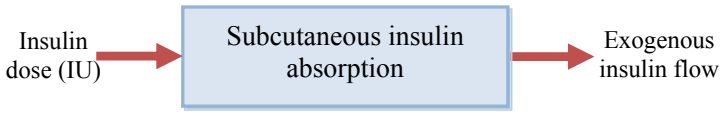

Figure 2.9: Diagram of the insulin absorption model.

A comparison of six models that represent the insulin via the subcutaneous absorption was presented by Nucci and Cobelli (2000). Four of these are compartment models as shown Figure 2.10 (Kobayashi et al., 1983; Kraegen and Chisholm, 1984; Puckett and Lightfoot, 1995; Shimoda et al., 1997), one based on a logistic equation (Berger and Rodbard, 1989) and one complex conceptual model (Trajanoski et al., 1993).

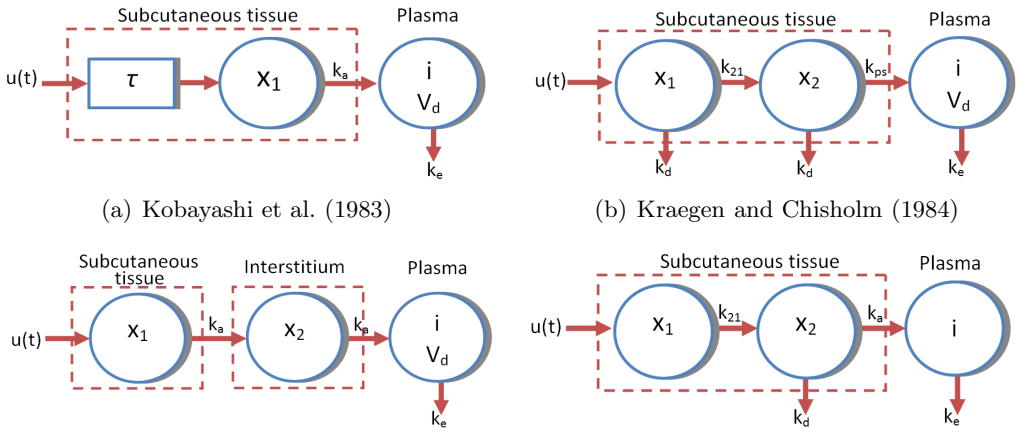

(a) Kobayashi et al. (1983)

(b) Kraegen and Chisholm (1984)

(c) Puckett and Lightfoot (1995)

(d) Shimoda et al. (1997))

Figure 2.10: Compartment models of insulin absorption.

Several models have been proposed for various insulin preparations, most of which are compartmental models. For example, a single compartment with first-order kinetics and a pure delay was proposed by Kobayashi et al. (1983) to describe the subcutaneous absorption of regular insulin (RI). The term "regular insulin" is taken to mean regular human insulin. As seen in Figure 2.10(a), in this model the input $u(t)$ (Umin^{-1}) is the rate of insulin administration, τ (min) is the time lag, k_a and k_e (min^{-1}) are the rate constants for absorption and elimination respectively and the compartment x_1 (μU) represents the amount of insulin in the subcutaneous depot. Later, Kraegen and Chisholm (1984) presented a two-compartment description of subcutaneous insulin kinetics for regular insulin with five parameters, including the insulin degradation rate in the subcutaneous tissue k_d. The input $u(t)$ and the parameters V_d and k_e (see Figure 2.10(b)) have the same meanings as in the previous model.

The model of Kraegen and Chisholm (1984) was refined with a more minimal approach by Puckett and Lightfoot (1995), who modelled the long-acting ultralente insulin in addition to regular insulin. The difference between this and the previous model is in the removal of insulin degradation, k_d, (see Figure 2.10(c)) from the subcutaneous distribution pools and the imple-

mentation of an effectiveness parameter at the injection site. The parameter k_a represents the rate constant from the subcutaneous depot to the interstitial fluids and from the interstitial fluids to the blood.

Two insulin preparations, regular insulin and a monomeric insulin (MI) analogue, were modelled by Shimoda et al. (1997) with a two-compartment model. It was fitted to clinical data from 10 type 1 diabetes patients, although the model was not identifiable a priori. The rate constants k_d and k_e are the degradation constants in the subcutaneous tissue and plasma, respectively. Compartment x_1 represents the subcutaneous insulin mass where the injection takes place and compartment x_2 the subcutaneous insulin mass proximal to the plasma (see Figure 2.10(d)).

More dynamics of insulin analogues (regular, NPH, lente, and ultralente) were incorporated by Berger and Rodbard (1989) in a non-compartmental model. This model has been adopted by the Automated Insulin Dosage Advisor (AIDA) decision-support system Lehmann and Deutsch (1992a). The subcutaneous insulin plasma rate of appearance is described with a three-parameter logistic equation with linear dose dependence. The model accounts for the inverse dynamics between absorption and the insulin dose, which are more important when a bolus injection is considered. The same relationship between dose and absorption time is taken into account by Trajanoski et al. (1993), who simplified the model of subcutaneous insulin absorption proposed by Mosekilde et al. (1989) to describe MI absorption.

Subsequently, based on the work of Trajanoski et al. (1993), a novel, comprehensive, generic subcutaneous insulin absorption model that included the insulin glargine was proposed by Tarín et al. (2005), using partial differential equations. This model allows the exogenous insulin flow into the bloodstream of each insulin preparation/class to be computed over time, depending on the injected insulin dose. In contrast to Trajanoski et al. (1993), who considered only two different association states for insulin, the hexameric and dimeric, a bound insulin state was adopted. This allows the consideration of reduced insulin solubility at physiological pH and the precipitation or crystallization of very-long-acting insulin analogues, such as insulin glargine, which delay absorption.

The Tarín et al. model of subcutaneous insulin absorption allows the simulation of rapidly acting insulin analogues, short-acting (regular) insulin preparations, intermediate-acting insulins (both semilente and NPH types), and very-long-acting insulin analogues. Figure 2.11 shows the resulting exogenous insulin flow profiles using the Tarín et al. (2005) model after the injection of 10 IU of the different insulin formulations modelled. This model has been incorporated into the AIDA v4 Diabetes Simulator (Lehmann et al., 2009).

Later, Wilinska et al. (2005) evaluated 11 compartment-based models that simulate the CSII. According to his evaluation, the best model was the 10th model, which was a four-compartment model of MI absorption with fast/slow absorption channels and local insulin degradation.

More recently, non-linear compartment models of subcutaneous absorption have been developed. A model formed by the two compartments S_1 and S_2, which represents the absorption of subcutaneously administered short-acting insulin (e.g., lispro), was developed by Hovorka et al. (2004). Later, Dalla Man et al. (2007a) presented a model with two compartments that represented polymeric (I_{sc1}) and monomeric (I_{sc2}) insulin in the subcutaneous tissue.

The main features of the models mentioned in this subsection are shown in chronological

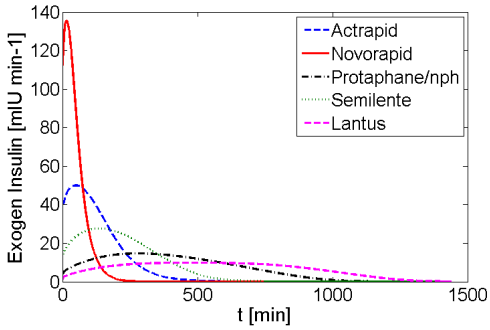

Figure 2.11: Exogenous insulin flow corresponding to 10 IU of different insulin formulations.

order in Table 2.2.

Model	Model type	Insulin type
Kobayashi et al. (1983)	Single compartment	RI
Kraegen and Chisholm (1984)	Dual compartment	RI
Berger and Rodbard (1989)	Noncompartmental	RI, NPH, lente, and ultralente
Mosekilde et al. (1989)	Noncompartmental	RI
Trajanoski et al. (1993)	Noncompartmental	MI
Puckett and Lightfoot (1995)	Dual compartment	RI and ultralente
Shimoda et al. (1997)	Dual compartment	RI and MI
Tarín et al. (2005)	Comprehensive	RI, NPH, lente, ultralente and Glargine
Wilinska et al. (2005)	Four compartment	MI
Hovorka et al. (2004)	Dual compartment	RI
Dalla Man et al. (2007a)	Dual compartment	RI and MI

Table 2.3: Summary of the subcutaneous absorption models.

In summary, the kinetics of most insulin analogues are best represented with non-compartmental models, whereas compartmental models have mainly been used to represent the kinetics of regular insulin. Similarly, most existing models describe only one type of insulin, or a limited number of types.

The models proposed by Hovorka et al. (2004), Wilinska et al. (2005), and Dalla Man et al. (2007a) have been incorporated into the library of interval glucoregulatory models proposed in Chapter 4 of this work. The Tarín et al. (2005) model has been used to represent subcutaneous insulin absorption in different examples presented in this thesis.

2.3.2 Gastric emptying, digestion, and absorption

Digestion is the process in which food is converted into simple compounds by chemical processes to be absorbed and assimilated by the body. Digestion can occur at many levels in the body. Generally, it refers to the breakdown of macromolecules or the matrices of cells or tissues into

smaller molecules and component parts.

The process of meal glucose rate of appearance can be divided into several main processes, including digestion in the stomach and gut, gastric emptying into the gut, absorption from the gut, and subsequent transport into the plasma. Figure 2.12 is a diagram of the gastric emptying, digestion, and absorption model.

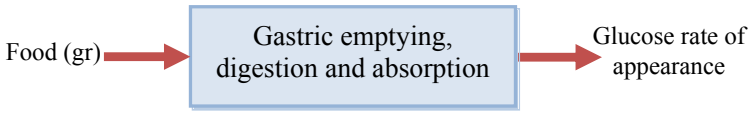

Figure 2.12: Diagram of gastric emptying, digestion, and absorption model.

The input into this model corresponds, in the simplest cases, to the carbohydrate intake. In more elaborate models, the carbohydrates, monosaccharides, oligosaccharides, and polysaccharides can be distinguished in the portions, and are also measured in grams. In even more sophisticated models, the input may introduce carbohydrates (and their types), proteins, and lipids to emulate more complex intake.

The kinetics of meal glucose appearance in the plasma is the least commonly studied area when the glucose–insulin system is modelled. This is attributable to the different factors that affect the dynamic model. For example, the rate of absorption of a mixed meal depends on its fat, protein and fiber content and the time of day at which the meal is consumed, which affect the absorption dynamics. Therefore, the meal carbohydrate content and type and the meal time are the main factors affecting meal glucose appearance in the plasma.

Most models reported in the literature typically focus on the gut absorption of glucose, and mixed meals have been considered only recently. Compartment and non-compartment models have been used to represent these dynamics.

One of the most popular models to describe the kinetics of meal glucose appearance in the plasma was presented by Lehmann and Deutsch (1992b). This model uses two compartments: the first regulates the glucose flux from the stomach to the small intestine with a triangular or trapezoidal function, and the second regulates the glucose entering the portal vein with a first-order linear function. Previously, a one-compartment model was used to describe the absorption model with a linear function, as described by Lehmann and Deutsch (1992b), whereas implementing a power exponential for the process of gastric emptying was developed by Elashoff et al. (1982). A similar approach was taken by Fisher (1991).

Later, Worthington (1997) also used a one-compartment model, but included a time delay to represent the glucose absorption from the gut. This time delay had the smallest fitting error that was obtained with a model fitted to plasma glucose, so it is dependent on the model of glucose kinetics used.

A two-compartment chain with identical fractional transfer rates was proposed by Hovorka et al. (2004) to describe the catabolism of carbohydrates to monosaccharides (mostly glucose) that takes place during meal digestion, as well as intestinal absorption. The model includes two

parameters: carbohydrate bioavailability and the time to the peak appearance of glucose from the gut. The glucose flux from the gut is assumed to be a saturable process.

Other models take into account the type of meal content, such as those listed below. Arleth et al. (2000) classified gut absorption according to the class of carbohydrates, based on their different absorption rates: sugars, rapidly absorbed starches, and slowly absorbed starches. The ingestion of the only liquid meal was represented as a square pulse by Fabietti et al. (2001), who described the appearance of glucose in the peripheral circulation with a third-order glucose transfer function. Later, a mixed-meal model was developed by Roy and Parker (2006) to include the absorption of carbohydrates, protein, and free fatty acids, based on Lehmann and Deutsch (1992b).

The physiological model of intestinal glucose absorption proposed by Dalla Man et al. (2006) consists of two stomach compartments and one intestinal-tract compartment, after they had evaluated the Elashoff et al. (1982) and Lehmann and Deutsch (1992b) models. The process of the gastrointestinal subsystem is as follows: the meal is digested in the stomach with a grinding coefficient; then, the chyme (partially digested food) enters the intestine with a fractional coefficient of transfer; finally, the glucose is absorbed and enters the bloodstream. The non-linear gastric emptying rate is described by a hyperbolic tangent function of the proportion of the consumed carbohydrates remaining in the stomach. There is no saturation term for gastric emptying or gut absorption for large meals.

The models formulated by Hovorka et al. (2004) and Dalla Man et al. (2006) have been incorporated into the library of interval glucoregulatory models proposed in Chapter 4 of this work.

2.3.3 Insulin action and glucose kinetics

When insulin acts on the bloodstream, it influences the blood glucose level, producing effects in various tissues. The insulin is degraded and removed. This process is called "insulin action" and typically includes a remote compartment to represent the delay in its action. Modelling the glucose distribution incorporates: the introduction of glucose into the system from the gut; the insulin-dependent and -independent glucose utilizations; the removal of glucose by the kidneys; and the buffering of glucose by the liver. Finally, the glucose dynamics include the interactions of blood glucose with all the systems in the patient's body. The conceptual paradigm for models that represent the kinetics of glucose and insulin action is illustrated in Figure 2.13.

As mentioned at the beginning of this section, models of glucose kinetics and insulin action can be classified as simple expressions that relate glucose and insulin to very complex mathematical models. One of the first linear models proposed in the literature was formulated by Ackerman et al. (1964). This model consists of a system of equations in which the parameters have been lumped into two dependent variables and four rate constants. Salzsieder et al. (1985) also presented a linear model that was intended to be individually identifiable and physiologically relevant. It was based on a combination of black-box model identification from normal dog experimental data and state–space model identification from long-term diabetic dogs.

In the early 1980s, the minimal model was proposed by Bergman et al. (1981), and is composed of two parts: the minimal model for glucose disappearance and the minimal model for insulin kinetics. This model introduced the variable insulin action to account for the delay in

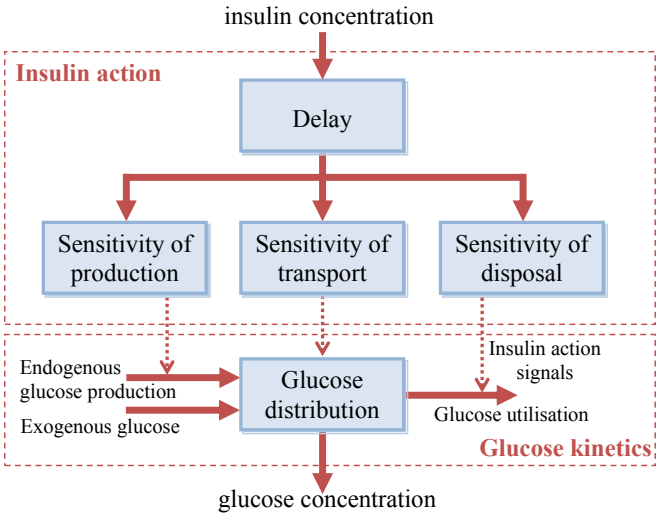

Figure 2.13: Representation of the glucose-insulin system (Wilinska and Hovorka, 2008).

insulin transport to the periphery, as well as the insulin sensitivity of the cells, thus combining transport kinetics and action dynamics. The minimal model was originally developed to estimate insulin sensitivity and glucose effectiveness from the intravenous glucose tolerance test (IVGTT), but it has also been widely used in the area of glucose control (Wilinska and Hovorka, 2008), and different modifications have been presented and validated (Fernandez et al., 2007).

Many variations of the minimal model have been proposed, and a more formal mathematical analysis of this model is given by De Gaetano and Arino (2000). The original minimal model is composed of two separate parts, but the glucose–insulin system is an integrated dynamic physiological system, which should be dealt with as a whole. Therefore, De Gaetano and Arino (2000) proposed a global dynamic model of the glucose–insulin system that incorporated a delay differential equation model. Later, based on this model, Mukhopadhyay et al. (2004) added a generic weight function to the delay integral kernel for the pancreatic response to glucose. Another variation of the minimal model was proposed by Derouich and Boutayeb (2002) to introduce parameters related to physical exercise.

Caumo and Cobelli (1993) formulated a new model to interpret labelled IVGTT data because the minimal model provided a non-physiological pattern of hepatic glucose production. In this model, the fast and medium compartments were combined and the losses from both compartments were made equal to allow their unique identifiability. However, this model requires the use of glucose tracers to be uniquely identifiable, and is therefore impractical for widespread clinical use. A two-compartment model was also developed by Vicini et al. (1997) based on the model of Caumo and Cobelli (1993), the objective of which was to provide indices of glucose effectiveness and insulin sensitivity.

Later, a glucose–insulin reference model was formulated by Vicini et al. (1999) to investigate the consequences of the single glucose compartment hypothesis embedded in the minimal model of glucose disposal. For this, they used the model by Caumo and Cobelli (1993) as the reference for glucose kinetics; to define the insulin subsystem, the C-peptide model published by Toffolo et al. (1995) was modified to describe the post-hepatic insulin delivery, i.e., after its extraction

by the liver; and the derivation of the peripheral uptake indices was based on the model of Vicini et al. (1997).

The two-compartment minimal model proposed by Vicini et al. (1997) can be seen as the immediate precursor of the model formulated by Hovorka et al. (2002). The model proposed by Hovorka et al. (2002) was built on experimental and modelling work, which used glucose tracers to determine the structure and parameter values for the glucose kinetics in normal subjects under basal conditions and during the IVGTT. The effects of insulin on glucose distribution/transport, glucose disposal, and endogenous glucose production are taken into account in this model. The model has been used for both simulation and control purposes in many different scenarios, from critical patients (Hovorka et al., 2007) to overnight experiments (Hovorka et al., 2004) with successful results, and recently it has been implemented in a mathematical patient simulator (Wilinska et al., 2010).

More recently, the minimal model has also been modified for intensive care unit (ICU) patients by Van Herpe et al. (2006). Other variations of the minimal model have been proposed by Dua et al. (2006) and Roy and Parker (2006). A good overview of the minimal model is presented by Bergman (1997).

One of the initial comprehensive models was formulated by Guyton et al. (1978). The glucoregulatory system was structured organ-by-organ to simulate the whole body physiologically, but it was unsuitable for parametrization in individual subjects (Palerm, 2003). This model was extended by Sorensen (1985), who divided the body into six physiological compartments, as can be seen in Figure 2.14, where the organ groups represent the central nervous system, lung and myocardial, gastrointestinal, hepatic, renal, and peripheral tissues. The model is composed of eight mass balance equations and 17 parameters for the glucose subsystem, seven mass balance equations and 18 parameters for the insulin subsystem, and a single mass balance equation and two parameters for the glucagon subsystem. To represent a subject with T1DM, insulin secretion is disabled in this model, and meal disturbances and the parameters for the uncertainty analysis are taken into account.

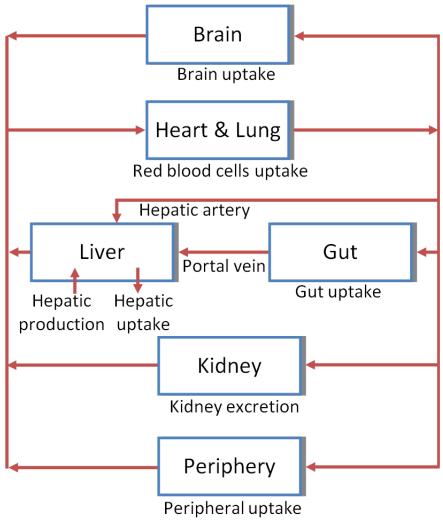

Figure 2.14: Flow diagram representing the Sorensen glucose model.

Guyton's model was also used by Lehmann and Deutsch (1992b) in combination with the PK model for insulin action designed by Berger and Rodbard (1989). Guyton incorporated the dynamics for the appearance of glucose from a carbohydrate meal. Lehmann and Deutsch (1992b) concluded that the model was not sufficiently refined for individual simulations, and therefore the model can only be used as a tool for education/teaching/demonstration of the glucose–insulin interaction in T1DM for patients and medical staff. For this reason, the model is used in a freeware educational simulator program, called AIDA, about the glucose–insulin interaction, insulin dosage, and dietary adjustments in diabetes mellitus (Lehmann, 2001). Based on this model, Parker et al. (1999) designed another extension of Sorensen's model with the objective of implementing the carbohydrate meal dynamics presented by Lehmann and Deutsch (1992b).

Finally, one of the most recent and most used models representing the glucose–insulin system was formulated by Dalla Man et al. (2007b). Dalla Man and colleagues introduced a minimal model assessment of insulin sensitivity on a multi-sample OGTT (seven samples over 2 h). To develop the model was used a database of 204 healthy persons, who received a triple racer, mixed meal. Because the model refers to a healthy person, a model that simulates the specific metabolic parameters of a T1DM patient was adapted from it by Magni et al. (2007). The main change was to replace the subsystem of the pancreatic β-cells with a unit that models the dynamics of a subcutaneous infusion of insulin.

The model of Dalla Man et al. was integrated into the UVa simulator (Kovatchev et al., 2009), which is an in silico model of type 1 diabetes accepted by the US FDA as a substitute for animal trials in the preclinical testing of closed-loop control strategies.

In general, the main advantage of the simple models is the minimal numbers of parameters required to allow the identification of the model, but with a low glucose prediction accuracy. Conversely, comprehensive models use a large number of parameters to describe the full system, taking into account all interactions. This allows better accuracy in the glucose prediction.

More information about the mathematical models that are used to control the glucose–insulin system can be found in the following reviews: Carson and Cobelli (2001); Palerm (2003); Boutayeb and Chetouani (2006); Makroglou et al. (2006); Chee and Fernando (2007); Wilinska and Hovorka (2008); Wong (2008); Cobelli et al. (2009).

The models proposed by Bergman et al. (1981), Hovorka et al. (2004), Dalla Man et al. (2007b), and Panunzi et al. (2007) are examined in detail in Chapter 4.

2.4 Summary

In this chapter, some medical background about diabetes and a brief overview of existing physiological models that describe the glucoregulatory system of healthy subjects and patients with diabetes have been presented. The different subsystems have been represented by compartment and non-compartment models, which can be classified as simple equations to very complex mathematical models. The classifications of the long-term complications of diabetes and the pharmacokinetics of the available insulin products were also presented.

Chapter 3

Interval Models and Interval Simulation

Dynamic models provide valuable information about the postprandial glucose excursion. However, one of the main challenges that must be considered is the large intra-individual variability among the patients. Another important source of uncertainty is food intake, because it is impossible to measure the carbohydrate content of a mixed meal precisely in real-life situations. These factors make it necessary to develop prediction tools that can accommodate different sources of uncertainty (inputs, parameters, and initial states).

These uncertainties can be unstructured (the equations that model the system are unknown) or structured (the equations are known but the values of their parameters are unknown). They cannot be represented with quantitative models, i.e., models in which the parameters are real numbers. If it is necessary to consider these uncertainties, other kinds of models are required to overcome this shortcoming of quantitative models. Some types of models that can represent the uncertainties of systems are qualitative, fuzzy, and interval models.

Uncertainty will be represented here by an interval model, i.e., a model in which the parameters, inputs, and/or initial states take interval values.

This chapter presents different techniques to solve the problem of simulating uncertain systems. The way to deal with this problem is with the theory of modal interval analysis (MIA), so a particular emphasis is given to the concepts and results of MIA.

3.1 Modal Interval Analysis

MIA is a logical and algebraic completion of classical interval analysis in which several of the semantic and algebraic shortcomings of classical interval analysis are overcome. The main concept is the modal interval, which incorporates in its definition a logical quantifier to give meaning to the interval computations. Some basic definitions and results of MIA are presented in this section. The reader is referred to Gardeñes et al. (2001) and Sainz et al. (2002) for a deeper coverage of this subject.

3.1.1 Definition

A modal interval is defined as a couple $X = (X', \forall)$ or $X = (X', \exists)$ where X' is its classic interval *domain*, $X' \in I(\mathbb{R})$, and the quantifiers $\forall$ and $\exists$ are a selection *modality*. The set of the modal intervals is represented by $I^*(\mathbb{R})$. Modal intervals of the type $X = (X', \exists)$ are called *proper intervals* or *existential intervals*, modal intervals of the type $A = (X', \forall)$ are called *improper intervals* or *universal intervals*. The canonical representation of a modal interval is:

- Proper interval: $X = [a, b] = ([a, b]', \exists)$ if $a \leq b$
- Improper interval: $X = [a, b] = ([b, a]', \forall)$ if $a \geq b$
- Point-wise interval: $X = [a, b] = ([a, b]', \{\exists, \forall\})$ if $a = b$

For example, the interval [4,6] corresponds to $([4, 6]', \exists)$ and the interval [7,5] corresponds to $([5, 7]', \forall)$. The bounds a and b are named as the *infimum*, $a = Inf([a, b])$ and the *supremum*, $b = Sup([a, b])$ of the interval. A *point-wise* interval $[a, a]$, also represented as $[a]$, can be considered as proper or improper and it is identifiable with the real number a. The set of n-dimensional modal interval vectors will be denoted by $I^*(\mathbb{R}^n) := \{([a_1, b_1], \ldots, [a_n, b_n])/[a_i, b_i] \in I^*(\mathbb{R})\ i = 1, \ldots, n\}$. Definitions and relationship in $I^*(\mathbb{R})$ are generalized in a natural way in $I^*(\mathbb{R}^n)$.

For an interval $A = [a_1, a_2]$ the operators $Prop$, $Impr$ and $Dual$ are defined as:

$$Prop([a_1, a_2]) := \begin{cases} [a_1, a_2] & \text{if } a_1 \leq a_2 \\ [a_2, a_1] & \text{if } a_1 > a_2. \end{cases}$$

$$Improp([a_1, a_2]) := \begin{cases} [a_2, a_1] & \text{if } a_1 \leq a_2 \\ [a_1, a_2] & \text{if } a_1 > a_2. \end{cases}$$

$$Dual([a_1, a_2)] := [a_2, a_1].$$

Example 3.1 Given a modal interval $A = [-3, 3]$ the operators $Prop$, $Impr$ and $Dual$ are:

$$Prop([3, -3]) = [-3, 3],$$
$$Impr([-3, 3]) = [3, -3],$$
$$Dual([-3, 3]) = [3, -3].$$

3.1.2 Modal interval relations and operations

The process of construction of modal intervals is completed with the concept of modal quantifier Q defined by:

$$Q(x, A)P(x) := \begin{cases} (\exists x \in A')P(x), & \text{if } A = (A', \exists) \\ (\forall x \in A')P(x), & \text{if } A = (A', \forall), \end{cases}$$

which allows to define the set of real predicates accepted by a modal interval A:

$$Pred(A) := \{P(\cdot) \in Pred(\mathbb{R})\ Q(x, A)P(x)\}.$$

With the identification of a modal interval with the set of those real predicates which it accepts: $A \leftrightarrow P(A)$ arises the inclusion of two intervals as the inclusion of the set of predicates that they accept, that is to say, if A, $B \in I^*(\mathbb{R})$

$$A \subseteq B :\Leftrightarrow Pred(A) \subseteq Pred(B).$$

Using their canonical coordinates $A = [a_1, a_2]$ and $B = [b_1, b_2]$, this inclusion maintains the traditional *modus operandi*; that is to say

$$[a_1, a_2] \subseteq [b_1, b_2] \Leftrightarrow (a_1 \geq b_1, a_2 \leq b_2).$$

Example 3.2 Given two modal intervals $A = ([-2, 2]', \exists) = [-2, 2]$ and $B = ([-2, 2]', \forall) = [2, -2]$, B is included in A because $[2, -2] \subseteq [-2, 2]$ is true, which means that the set of accepted predicates by B is included to the set accepted by A.

Geometrical representations of modal intervals and the inclusion and inequalities relations can be seen in Figure 3.1.

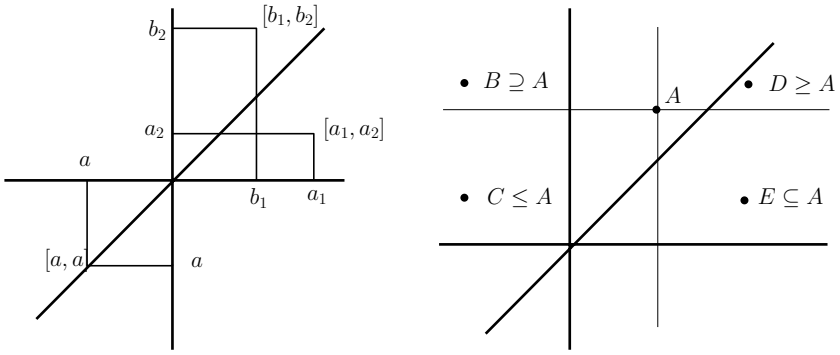

Figure 3.1: (a) Geometrical representation of modal intervals (b) Inclusions and inequalities.

The lattice operations meet ($\wedge$) and join ($\vee$) on $I^*(\mathbb{R})$ for a bounded family of modal intervals $A(I) := \{A(i) = [a_1(i), a_2(i)] \in I^*(\mathbb{R})\ i \in I\}$ (I is the index's domain) are defined as the $\subseteq$-maximum interval contained in all $A(i)$, for the meet, and the $\subseteq$-minimum interval which contains all $A(i)$, for the join, i.e.,

$$\bigwedge_{i \in I} A(i) = A \in I^*(\mathbb{R}) \text{ is such that } \forall i \in I\ X \subseteq A(i) \Leftrightarrow X \subseteq A,$$
$$\bigvee_{i \in I} A(i) = B \in I^*(\mathbb{R}) \text{ is such that } \forall i \in I\ X \supseteq A(i) \Leftrightarrow X \supseteq B,$$

denoted by $A \wedge B$ and $A \vee B$ for the corresponding two-operands case. The result, as a function of the interval bounds, is

$$\bigwedge_{i \in I} A(i) = [\max_{i \in I}\ a_1(i), \min_{i \in I}\ a_2(i)]$$

$$\bigvee_{i\in I} A(i) = [\min_{i\in I}\ a_1(i), \max_{i\in I}\ a_2(i)].$$

With these operations the set of modal intervals is a reticle for this $\subseteq$-relation, while the classic intervals are not, therefore, modal intervals are a reticular completion of the set of classic intervals. Both operators are isotonic, i.e., if $A_i \subseteq B_i$ for every $i \in I$, then

$$\bigwedge_{i\in I} A_i \subseteq \bigwedge_{i\in I} B_i \qquad \text{and} \qquad \bigvee_{i\in I} A_i \subseteq \bigvee_{i\in I} B_i,$$

and they also *associative* and *distributive* with respect to each other.

Example 3.3 Given two modal intervals $A = [-2, 2]$ and $B = [6, 4]$,

$$A \wedge B = [-2, 2] \wedge [6, 4] = [6, 2]$$

$$A \vee B = [-2, 2] \vee [6, 4] = [-2, 4]$$

In the set of the real numbers there are two relationships: $\leq$ and $\geq$ and the extension of these relationships to intervals is defined by:

$$[a_1, a_2] \leq [b_1, b_2] :\Leftrightarrow (a_1 \leq b_1, a_2 \leq b_2),$$

which leads to the lattice operators "Min" and "Max": for a bounded family of modal intervals $A(I) := \{A(i) \in I^*(\mathbb{R})|\ i \in I\}$

$$\begin{array}{l}\underset{i\in I}{\text{Min}}\ A(i) = A \in I^*(\mathbb{R}) \text{ is such that } (\forall i \in I)\ X \leq A(i) \Leftrightarrow X \leq A;\\ \underset{i\in I}{\text{Max}}\ A(i) = B \in I^*(\mathbb{R}) \text{ is such that } (\forall i \in I)\ X \geq A(i) \Leftrightarrow X \geq B\end{array}$$

and computationally

$$\underset{i\in I}{\text{Min}}\ A(i) = [\min_{i\in I} a_1(i), \min_{i\in I} a_2(i)],$$

$$\underset{i\in I}{\text{Max}}\ A(i) = [\max_{i\in I} a_1(i), \max_{i\in I} a_2(i)]$$

The set of the modal intervals is also a lattice for this $\leq$-relation. Figure 3.2(a) shows geometrical representation of the Meet, Join and figure 3.2(b) representation of Min and Max operators for two intervals.

3.1.3 Modal interval arithmetic

The modal interval arithmetic coincides with the so-called Kaucher complete interval arithmetic (Kaucher, 1980). However, MIA not only extends the classical interval arithmetic to include the whole interval lattice, but it gives logical meaning to the results, which is related to the modality of the involved intervals (e.g., proper or improper).

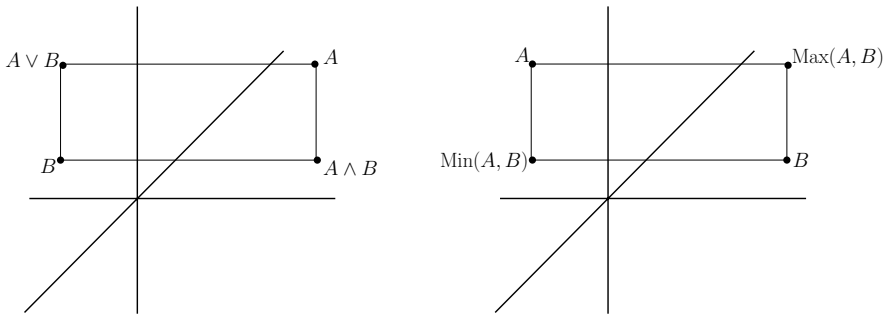

Figure 3.2: Lattice operators: (a) Meet, Join and (b) Max, Min.

The basic four operations are defined as:

$$Sum : A + B = [a_1 + b_1, a_2 + b_2]$$
$$Rest : A - B = [a_1 - b_2, a_2 - b_1]$$

$$\begin{aligned} Product : A * B = \quad & [a_1b_1, a_2b_2] \text{ if } a_1 \geq 0, a_2 \geq 0, b_1 \geq 0, b_2 \geq 0 \\ & [a_1b_1, a_1b_2] \text{ if } a_1 \geq 0, a_2 \geq 0, b_1 \geq 0, b_2 < 0 \\ & [a_2b_1, a_2b_2] \text{ if } a_1 \geq 0, a_2 \geq 0, b_1 < 0, b_2 \geq 0 \\ & [a_2b_1, a_1b_2] \text{ if } a_1 \geq 0, a_2 \geq 0, b_1 < 0, b_2 < 0 \\ & [a_1b_1, a_2b_1] \text{ if } a_1 \geq 0, a_2 < 0, b_1 \geq 0, b_2 \geq 0 \\ & [\max(a_1b_1, a_2b_2), \min(a_2b_1, a_1b_2)] \text{ if } a_1 \geq 0, a_2 < 0, b_1 \geq 0, b_2 < 0 \\ & [0, 0] \text{ if } a_1 \geq 0, a_2 < 0, b_1 < 0, b_2 \geq 0 \\ & [a_2b_2, a_1b_2] \text{ if } a_1 \geq 0, a_2 < 0, b_1 < 0, b_2 < 0 \\ & [a_1b_2, a_2b_2] \text{ if } a_1 < 0, a_2 \geq 0, b_1 \geq 0, b_2 \geq 0 \\ & [0, 0] \text{ if } a_1 < 0, a_2 \geq 0, b_1 \geq 0, b_2 < 0 \\ & [\min(a_1b_2, a_2b_1), \max(a_1b_1, a_2b_2)] \text{ if } a_1 < 0, a_2 \geq 0, b_1 < 0, b_2 \geq 0 \\ & [a_2b_1, a_1b_1] \text{ if } a_1 < 0, a_2 \geq 0, b_1 < 0, b_2 < 0 \\ & [a_1b_2, a_2b_1] \text{ if } a_1 < 0, a_2 < 0, b_1 \geq 0, b_2 \geq 0 \\ & [a_2b_2, a_2b_1] \text{ if } a_1 < 0, a_2 < 0, b_1 \geq 0, b_2 < 0 \\ & [a_1b_2, a_2b_2] \text{ if } a_1 < 0, a_2 < 0, b_1 < 0, b_2 \geq 0 \\ & [a_2b_2, a_1b_1] \text{ if } a_1 < 0, a_2 < 0, b_1 < 0, b_2 < 0 \end{aligned}$$

if $0 \notin [b_1, b_2]$

$$\begin{aligned} Division : A/B = \quad & [a_1/b_2, a_2/b_1] \text{ if } a_1 \geq 0, a_2 \geq 0, b_1 > 0, b_2 > 0 \\ & [a_2/b_2, a_1/b_1] \text{ if } a_1 \geq 0, a_2 \geq 0, b_1 < 0, b_2 < 0 \\ & [a_1/b_2, a_2/b_2] \text{ if } a_1 \geq 0, a_2 < 0, b_1 > 0, b_2 > 0 \\ & [a_2/b_1, a_1/b_1] \text{ if } a_1 \geq 0, a_2 < 0, b_1 < 0, b_2 < 0 \\ & [a_1/b_1, a_2/b_1] \text{ if } a_1 < 0, a_2 \geq 0, b_1 > 0, b_2 > 0 \\ & [a_2/b_2, a_1/b_2] \text{ if } a_1 < 0, a_2 \geq 0, b_1 < 0, b_2 < 0 \\ & [a_1/b_1, a_2/b_2] \text{ if } a_1 < 0, a_2 < 0, b_1 > 0, b_2 > 0 \\ & [a_2/b_1, a_1/b_2] \text{ if } a_1 < 0, a_2 < 0, b_1 < 0, b_2 < 0 \end{aligned}$$

The next equation can also used for the division

$$\frac{1}{B} = \left[\frac{1}{b_2}, \frac{1}{b_1}\right] \quad \text{and if } \; 0 \notin [b_1, b_2]$$
$$\frac{A}{B} = A * \frac{1}{B}$$

3.1.4 Semantic extensions

In the set-theoretical interval analysis, the semantic extension of an $\mathbb{R}^n$ to $\mathbb{R}$ continuous function $z = f(x_1, \ldots, x_n)$ is the *interval united extension* R_f of f which for the interval argument $X' = (X'_1, \ldots, X'_n) \in I(\mathbb{R}^n)$ is defined as the range of $f-$values on X'

$$\begin{aligned} R_f(X'_1, \ldots, X'_n) &:= \{f(x_1, \ldots, x_n) \mid x_1 \in X'_1, \ldots, x_n \in X'_n)\} \\ &= [\min\{f(x_1, \ldots, x_n) \mid x_1 \in X'_1, \ldots, x_n \in X'_n\}, \\ &\quad \max\{f(x_1, \ldots, x_n) \mid x_1 \in X'_1, \ldots, x_n \in X'_n\}]. \end{aligned}$$

Since the range of values of a general function is generally not computable, set-theoretical interval extensions $fR(X'_1, \ldots, X'_n)$ are defined like their corresponding real functions $f(x_1, \ldots, x_n)$, if only replacing their numerical arguments $x_1, \ldots, x_n$ by the interval arguments $X'_1, \ldots, X'_n$, and their "real" arithmetic operators w by their corresponding interval operations W which, in the common case of the truncated computations of any actual arithmetic, must be the outwards-directed ones W^R; indeed, $X'WY' \subseteq X'W^RY' := Out(X'WY')$. The relation between both extensions is

$$R_f(X'_1, \ldots, X'_n) \subseteq fR(X'_1, \ldots, X'_n),$$

where $fR(X'_1, \ldots, X'_n)$, computable from the bounds of the intervals $X'_1, \ldots, X'_n$, may usually represent an overestimation of $R_f(X'_1, \ldots, X'_n)$.

The critical basic fact is that the classic interval extensions of f obtain only one kind of interval predicate compatible with the outer rounding of $f(X')$: if $Z' = fR(X'_1, \ldots, X'_n)$, the only valid semantic statement will be

$$(\forall x_1 \in X'_1) \ldots (\forall x_n \in X'_n)\ (\exists z \in Z')\ z = f(x_1, \ldots, x_n).$$

In the context of the modal intervals, it may be expected, as a starting point, that as soon as the $\mathbb{R}$-predicate $P(x)$ results into the modal interval predicate $Q(x, X)P(x)$, the relation $z = f(x_1, \ldots, x_n)$ must become some kind of interval relation $Z = F(X_1, \ldots, X_n)$ guaranteeing some sort of $(n + 1)$- dimensional interval predicate of the form

$$Q_1(x_1, X_1) \ldots Q_n(x_n, X_n)\ Q_z(z, Z)\ z = f(x_1, \ldots, x_n),$$

where an ordering problem obviously arises since the quantifying prefixes are not generally commutative.

3.1.5 Semantic functions

The extension of a given function $f : \mathbb{R}^n \to \mathbb{R}$ to modal intervals will now be discussed. In MIA, the similar role to the "united extension" for the classical intervals (Moore, 1979) is played by the semantic $*$ and $**$-functions, denoted by f^* and f^{**}.

A key concept in MIA is the $*$-semantic extension f^* of a continuous function f to a modal interval vector $X \in \mathbb{R}^n$, which can be seen as the modal interval counterpart of the range (or interval united extension) of a continuous function in classic Interval Analysis. f^* is defined by:

$$\begin{aligned} f^*(X) &:= \bigvee_{x_p \in X'_p} \bigwedge_{x_i \in X'_i} [f(x_p, x_i), f(x_p, x_i)] \\ &= \left[\min_{x_p \in X'_p} \max_{x_i \in X'_i} f(x_p, x_i), \max_{x_p \in X'_p} \min_{x_i \in X'_i} f(x_p, x_i) \right] \end{aligned}$$

where $x = (x_p, x_i)$ is the component-splitting corresponding to the proper and improper components of $X = (X_p, X_i)$.

Another semantic extension defined in MIA is the $**$-semantic extension, which is the dual formulation of the $*$-semantic extension. It is defined by

$$\begin{aligned} f^{**}(X) &:= \bigwedge_{x_i \in X'_i} \bigvee_{x_p \in X'_p} [f(x_p, x_i), f(x_p, x_i)] \\ &= \left[\max_{x_i \in X'_i} \min_{x_p \in X'_p} f(x_p, x_i), \min_{x_i \in X'_i} \max_{x_p \in X'_p} f(x_p, x_i) \right] \end{aligned}$$

Remark 3.1 *If $X_i = \emptyset$, (allowing for the abuse of language), then*

$$\begin{aligned} f^*(X) = f^{**}(X) &= [\min\{f(x_1, \ldots, x_n) \mid x_1 \in X'_1, \ldots, x_n \in X'_n\}, \\ &= \max\{f(x_1, \ldots, x_n) \mid x_1 \in X'_1, \ldots, x_n \in X'_n\}], \end{aligned}$$

which corresponds to the interval united extension R_f of classical interval analysis.

If $X_p = \emptyset$, it results instead

$$\begin{aligned} f^*(X) = f^{**}(X) &= [\max\{f(x_1, \ldots, x_n) \mid x_1 \in X'_1, \ldots, x_n \in X'_n\}, \\ &= \min\{f(x_1, \ldots, x_n) \mid x_1 \in X'_1, \ldots, x_n \in X'_n\}], \end{aligned}$$

Example 3.4 For the continuous real function $f(x_1, x_2) = (x_1 + x_2)^2$ the computation of the *-semantic and the **-semantic functions for $X = ([-1, 1], [1, -1])$ yields the following results:

$$f^*([-1,1],[1,-1]) = \bigvee_{x_1\in[-1,1]'} \bigwedge_{x_2\in[-1,1]'} [(x_1+x_2)^2,(x_1+x_2)^2]$$
$$= \bigvee_{x_1\in[-1,1]'} [\text{if } x_1<0 \text{ then } (x_1-1)^2 \text{ else } (x_1+1)^2, 0] = [1,0]$$

$$f^{**}([-1,1],[1,-1]) = \bigwedge_{x_2\in[-1,1]'} \bigvee_{x_1\in[-1,1]'} [(x_1+x_2)^2,(x_1+x_2)^2]$$
$$= \bigwedge_{x_2\in[-1,1]'} [0, \text{if } x_2<0 \text{ then } (x_2-1)^2 \text{ else } (x_2+1)^2] = [0,1].$$

However, in general, f^* and f^{**} are not generally computable, except for simple functions like this example or arithmetic operators.

Remark 3.2 *From the duality between the lattice operators meet and join, $f^{**} = Dual(f^*(Dual(X)))$ and a double implementation to obtain both semantic extensions is not necessary. Interesting properties of the semantic extensions are the isotonicity*

$$X \subseteq Y \Rightarrow f^*(X) \subseteq f^*(Y) \text{ and } f^{**}(X) \subseteq f^{**}(Y)$$

and the inclusion

$$f^*(X) \subseteq f^{**}(X).$$

In the special case when $f^*(X) = f^{**}(X)$, f is said to be *JM-commutable* (Join-Meet commutable) for $X \in I^*(\mathbb{R}^n)$. Classic examples are the arithmetic operators, which according to the previous definitions, can be calculated by means of operations between the bounds of the intervals (SIGLA/X Group, 1999).

3.1.6 Semantic theorems

Two key results, named semantic theorems, give logical interpretation to these semantic extensions.

Theorem 3.1 *(*-semantic theorem) Given a continuous real function $f : \mathbb{R}^n \to \mathbb{R}$, a modal vector $X = (X_p, X_i) \in I^*(\mathbb{R}^n)$ and $Z \in I^*(\mathbb{R}^n)$, then*

$$f^*(X) \subseteq Z \Leftrightarrow (\forall x_p \in X_p')\ Q(z,Z)\ (\exists x_i \in X_i')\ z = f(x_p, x_i).$$

where $Q = \exists$ when Z is a proper interval and $Q = \forall$ when Z is an improper interval.

Example 3.5 For the continuous real function $f(x,y) = x + y$

$$f^*([x_1,x_2],[y_1,y_2]) = [x_1+y_1, x_2+y_2].$$

For $X = [1,2]$ and $Y = [2,3]$ and since the result is $Z = [3,5]$, we may write $[1,2] + [2,3] = [3,5]$, with the meaning

$$(\forall x \in [1,2]')\ (\forall y \in [2,3]')\ (\exists z \in [3,5]')\ x + y = z.$$

Similarly, for $X = [1, 2]$ and $Y = [4, 1]$ the result is $Z = [3, 5]$ and $[1, 2] + [4, 1] = [5, 3]$ means in this case

$$(\forall x \in [1, 2]')\ (\forall z \in [3, 5]')\ (\exists y \in [1, 4]')\ x + y = z.$$

And so on, for $X = [2, 1]$ and $Y = [1, 4]$ the result is $Z = [3, 5]$ and $[2, 1] + [1, 4] = [3, 5]$ means

$$(\forall y \in [1, 4]')\ (\exists x \in [1, 2]')\ (\exists z \in [3, 5]')\ x + y = z;$$

for $X = [2, 1]$ and $Y = [3, 2]$ the result is $Z = [5, 3]$ and $[2, 1] + [3, 2] = [5, 3]$ with the interpretation

$$(\forall z \in [3, 5]')\ (\exists x \in [1, 2]')\ (\exists y \in [2, 3]')\ x + y = z.$$

Theorem 3.2 *(**-semantic theorem) Given a continuous real function $f : \mathbb{R}^n \to \mathbb{R}$, a modal vector $X = (X_p, X_i) \in I^*(\mathbb{R}^n)$ and $Z \in I^*(\mathbb{R}^n)$, then*

$$f^{**}(X) \supseteq Z \ \Leftrightarrow (\forall x_i \in X_i')\ Q(z, Dual(Z))\ (\exists x_p \in X_p')\ z = f(x_p, x_i).$$

Example 3.6 For the function $f(x, y) = xy$ and $X = [-1, 2]$, $Y = [5, 3]$ the value of f^* and f^{**} is $f^*([-1, 2], [5, 3]) = f^{**}([-1, 2], [5, 3]) = [-3, 6]$. Then, in accordance with both semantic theorems,

$$(\forall x \in [-1, 2]')\ (\exists z \in [-3, 6]')\ (\exists y \in [3, 5]')\ z = xy,$$

$$(\forall y \in [3, 5]')\ (\forall z \in [-3, 6]')\ (\exists x \in [-1, 2]')\ z = xy.$$

Both semantic theorems are extremely important because they make equivalent any logical formula involving intervals, functional predicates, and the universal quantifiers preceding the existential ones to an interval inclusion.

3.1.7 Modal rational extensions

Semantic extensions f^* and f^{**} can be equal or not, but they are out of reach for any direct computation except for simple real functions. When the continuous function f is a rational function, there exist modal rational extensions that are obtained using a computing program defined by the syntax tree of the expression of the function in which the real arguments are transformed into interval arguments and the real operators are transformed into their $*$-semantic extensions. If f is a $\mathbb{R}^n$ to $\mathbb{R}$ rational function, its rational extension to the modal intervals $X_1, \ldots, X_n$, represented by $fR(X_1, \ldots, X_n)$, is the function fR from $I^*(\mathbb{R}^n)$ to $I^*(\mathbb{R})$ defined by the computational program indicated by the syntax tree of f when the real operators are transformed to their semantic extensions.

Example 3.7 For the continuous function $f(x,y) = \dfrac{x}{x+y}$, the modal ration extension to the intervals $X = [1,2]$, $Y = [3,4]$ is

$$fR_1([1,2],[3,4]) = \frac{[1,2]}{[1,2]+[3,4]} = \left[\frac{1}{6}, \frac{2}{4}\right]$$

$$fR_2([1,2],[3,4]) = \frac{1}{1+\dfrac{y}{x}} = \frac{1}{1+\dfrac{[3,4]}{[1,2]}} = \left[\frac{1}{5}, \frac{2}{5}\right]$$

Different values are obtained for fR, therefore, to these possible variations of a rational function of real variable, the criteria which characterize the functions that give the optimal solution is studied in the next subsection.

Important results about the interpretability and optimality of rational extensions are described in the next subsection.

3.1.8 Interpretability and optimality

The problem with the semantic extensions f^* and f^{**} is that are interpretable but not generally computable and rational extensions are computable but not generally interpretable. The interpretation problem for the modal syntactic functions fR, which are the core of numerical computing, consists in relating them to the corresponding semantic functions by means of inclusion relations which are interpretable in accordance with the Semantic Theorems. In this case, if for $X \in I^*(\mathbb{R}^n)$ one of the relations

$$f^*(X) \subseteq fR(X) \text{ or } f^{**}(X) \supseteq fR(X),$$

then the computation $fR(X)$ is called *interpretable*.

In the other hand, the lack of computability of f^* and f^{**} can be solved by means of modal syntactic computations which are inner or outer approximations, although in many cases it will involve a loss of information. To avoid it it will be necessary to find criteria such that, in an ideal arithmetic without rounding,

$$f^*(X) = fR(X) = f^{**}(X).$$

In this case $fR(X)$ is called *optimal*, i.e., fR is an optimal computation on X.

Definition 3.1 *(Optimality) A modal syntactic function fR is said to be optimal if for every $X \in I^*(\mathbb{R}^n)$, for which $fR(Prop(X))$ is defined, the conditions $f^* = f^{**}$ and $fR(X) = f^*(X)$ do hold.*

Similarly we can speak of optimality on a given interval-domain: If this property holds particularly for an $A \in I^*(\mathbb{R}^n)$, we will say that fR is optimal for A.

In case of only the equality $fR(X) = f^*(X)$ being meant, without any previous supposition about the equality of $f^*(X)$ and $f^{**}(X)$, we will speak of $*$-optimality; and similarly we would

speak of $**$-optimality for the case of $fR(X) = f^{**}(X)$.

MIA provides a collection of results about the inclusions or equalities that solve part of the double problem of the interpretability of modal rational extensions and the computability of semantic extensions. The next definitions are required for a correct understanding of the following results about the interpretability of rational extensions (for a detailed description of these theorems, see Gardeñes et al. (2001)).

Uni-incidence and multi-incidence

An important role in obtaining these relations of inclusion and equality is played by the incidence of the involved variables.

Definition 3.2 *(Uni-incidence and multi-incidence) A component x_i of x is "uni-incident" in a continuous real function f it occupies only one leaf of the syntactic tree of f. Otherwise x_i is "multi-incident" in $f(x)$. A vector x is "uni-incident" in $f(x)$, when each one of its components does hold this property.*

Example 3.8 In the function $f : \mathbb{R}^2 \to \mathbb{R}$ defined by

$$f(x_1, x_2) = x_2 + \frac{x_1^2}{x_2}$$

the variable x_1 is uni-incident and x_2 multi-incident.

Interpretability in the uni-incidence case

A first result will relate the modal semantic extension f^* with the outer rounding of the modal syntactic extension $Out(fR(X))$. For that, and considering a function as a composition of their operators, it is possible to consider a successive application of the semantic theorems.

Theorem 3.3 *(*-interpretability of modal syntactic functions) If the improper components of X are uni-incident in $fR(X)$ and $Out(fR(Prop(X)))$ does exist, then $Out(fR(X)) \supseteq f^*(X)$.*

This theorem states that if the continuity of the functions on the implied domains by $Out(fR(Prop(A)))$ is assured, and if for the digitalization of the data of A and all the elementary operations defining $fR(.)$ is used the external rounding, then the result $fR(A)$ is interpretable in the terms of the $*$-semantic theorem.

Example 3.9 For the continuous function $f(x, y) = \dfrac{xy}{y+1}$, the modal ration extension to the intervals $X = [1, 2]$, $Y = [3, 4]$ is

$$fR([1, 2], [3, 4]) = \frac{[1, 2] * [3, 4]}{[3, 4] + 1} = \left[\frac{3}{5}, 2\right].$$

As there are no improper arguments,

$$Out\left(\left[\frac{3}{5}, 2\right]\right) \supseteq f^*(X, Y),$$

which can be interpreted with the *-semantics

$$(\forall x \in [1,2]')\ (\forall y \in [3,4]')\left(\exists z \in Out\left(\left[\frac{3}{5},2\right]'\right)\right) z = \frac{xy}{y+1}.$$

The same applies for any superset of $Out([3/5,2])$.

Theorem 3.4 *(**-interpretability of modal syntactic functions) If the proper components of X are uni-incident in $fR(X)$, and $Inn(fR(Prop(X)))$ does exist, then*

$$Inn(fR(X)) \subseteq f^{**}(X),$$

where Inn represents the inner rounding of the interval $f(R)$.

$$Inn(fR(X)) = Dual(Out(fR(Dual(X)))) \subseteq Dual(f^{*}(Dual(X))) = f^{**}(X).$$

According with this theorem, if the domains implied in the definition of $f^{**}(A)$ and the definition and computation of $fR(Prop(A))$ are well defined, because they do not comprise any divide by 0, then the result of the computation $Inn(fR(A))$ is acceptable from the point of view of the $**$-semantic theorem and can be interpreted according to this same theorem.

Example 3.10 For the continuous function $f(x,y) = \dfrac{xy}{y+1}$, the modal rational extension to the intervals $X = [1,2]$, $Y = [4,3]$ is,

$$fR([1,2],[4,3]) = \frac{[1,2] * [4,3]}{[4,3]+1} = \left[1,\frac{6}{5}\right]$$

At is uni-incident in the proper parameters,

$$Inn\left(\left[1,\frac{6}{5}\right]\right) \subseteq f^{**}(X,Y),$$

which can be interpreted with the **-semantics

$$(\forall y \in [3,4]')\left(\forall z \in Inn\left(\left[1,\frac{6}{5}\right]'\right)\right)(\exists x \in [1,2]')\ z = \frac{xy}{y+1}.$$

The same conclusion can be stated for any subset of $Inn([1,6/5]')$.

Theorem 3.5 *(Interpretability of modal syntactic functions) If all the fR- variables are uni-incident, then with an ideal arithmetic*

$$f^{*}(X) \subseteq fR(X) \subseteq f^{**}(X)$$

or else

$$f^{*}(X) \subseteq Out(fR(X)) \text{ and } Inn(fR(X)) \subseteq f^{**}(X).$$

Optimality in the uni-incidence case

Now on we will find out criteria to characterize the all the fR-variables are uni-incident functions for which the program $fR(.)$, assuming an ideal computation (without rounding), is such that

$$f^*(X) = fR(X) = f^{**}(X).$$

Theorem 3.6 *(Optimality and uni-incidence) If in $fR(X)$ all arguments are uni-incident and f is globally JM-commutable, then*

$$f^*(X) = fR(X) = f^{**}(X).$$

Remark 3.3 *In particular, if all the X components are uni-incident and with the same modality, $f^*(X) = fR(X) = f^{**}(X)$.*

In what now follows we will construct the fundamental class of uni-incident optimal modal syntactic functions. The uni-incident hypothesis is assumed but usually not explicitly repeated.

Theorem 3.7 *(Left monotonous associativity) If g is a monotonous operator of one variable and $fR(X)$ is optimal, then $gR(fR(X))$ is also optimal.*

Remark 3.4 *A more precise and only a little more verbose statement of the previous theorem would be: if g is a one variable monotonous operator and if $fR(X)$ does exist,*

$$(g \circ f)^*(X) = g^*(f^*(X))$$

and in case $fR(X)$ is optimal

$$(g \circ f)^*(X) = (g \circ f)R(X) := gR(fR(X)).$$

Example 3.11 Let us consider the function $h(x, y) = e^{x+y}$ composed of the operators $f(x, y) = x + y$ and $g(z) = e^z$. As fR is optimal and g is one-variable and monotonous, then $h^*(X, Y) = hR(X, Y) = e^{X+Y}$. For $h(x, y) = (x + y)^2$, composed of $f(x, y) = x + y$ and $g(z) = z^2$, fR is optimal but g is one-variable and not monotonous, and the result is not applicable.

Theorem 3.8 *(Right monary associativity) If $g_1(x_1), \ldots, g_n(x_n)$ are continuous operators of one variable and $fR(X)$ is optimal, then $fR(g_1R(X_1), \ldots, g_nR(Xn))$ is also optimal.*

Example 3.12 For the right associativity, the right one-variable operators do not need monotony; on the contrary, the left one-variable operators do. Thus, $x^2 + y^2$ is optimal because it is composed of $g_1R(x) = x^2$, $g_2R(y) = y^2$, and

$$\left.\begin{array}{l} fR(g_1R(x), g_2R(y)) = g_1R(x) + g_2R(y) \\ g_1R \text{ is optimal (one-variable and continuous)} \\ g_2R \text{ is optimal (one-variable and continuous)} \end{array}\right\} \Rightarrow fR \text{ optimal}$$

Tree-optimality

The following concept leads to important results about the optimality when there are multi-incident variables.

Definition 3.3 *A syntactic tree of a continuous function f is tree-optimal on X if, for any of its non-uniformly monotonic operators (eg. $*, /$) it is followed downwards in the syntactic tree only by one-variable operators (eg. pow, exp, sin) and upwards by uniformly monotonic operators (eg. $+, -$).*

Example 3.13 The continuous function $f(x, y, z, u) = xy + zu$, which has a rational syntactic extension given by

$$fR(X, Y, Z, U) = X * Y + Z * U,$$

is tree-optimal in any $(X, Y, Z, U) \in I^*(\mathbb{R}^4)$ because the involved non-uniformly monotonic operator $*$ is followed downward by variables (see Figure 3.3(a)). However, the continuous function

$$g(x, y, z, u) = (x + y)(z + u),$$

which has rational syntactic extension given by

$$gR(X, Y, Z, U) = (X + Y) * (Z + U),$$

is not tree-optimal in all $I^*(\mathbb{R}^4)$ because the non-uniformly monotonic operator $*$ is followed downward by the binary operator $+$ (see Figure 3.3(b)). However, it can be optimal on a given X. For instance, if $\emptyset \notin X'$, fR is optimal.

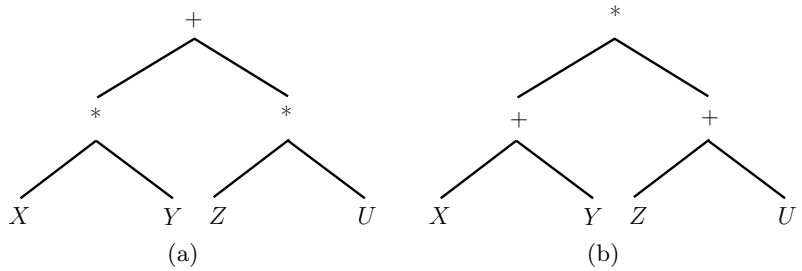

Figure 3.3: Syntactic tree of a rational function: (a) fR (b) gR

Theorem 3.9 *(Optimality of tree-optimal modal syntactic functions) If $fR(X)$ is tree-optimal and X is uni-incident in fR, then $fR(X)$ is optimal (that is, $f^*(X) = fR(X) = f^{**}(X)$ as far as X is uni-incident in fR).*

Example 3.14 The $\mathbb{R}^4$ to $\mathbb{R}$ continuous function defined by $f(x, y, z, u) = xy + zu$ is tree-optimal and therefore an optimal modal syntactic function for every $(X, Y, Z, U) \in I^*(\mathbb{R}^4)$.

The $\mathbb{R}^4$ to $\mathbb{R}$ continuous function defined by $g(x, y, z, u) = (x+y)(z+u)$ is neither tree-optimal nor optimal for some (X, Y, Z, U) for example:

$$\begin{aligned} g^*([-2,2],[-1,1],[-1,1],[2,-2]) &= [1.5,-1.5], \\ g^{**}([-2,2],[-1,1],[-1,1],[2,-2]) &= [-1.5,1.5], \\ gR([-2,2],[-1,1],[-1,1],[2,-2]) &= [0,0], \end{aligned}$$

But it is optimal in other domains, for example

$$\begin{aligned} g^*([1,3],[0,3],[4,2],[3,1]) &= [7,18], \\ g^{**}([1,3],[0,3],[4,2],[3,1]) &= [7,18], \\ gR([1,3],[0,3],[4,2],[3,1]) &= [7,18]. \end{aligned}$$

Interpretability in the multi-incidence case

The following theorems provide two important results in the case of multi-incident components.

Theorem 3.10 *(Coercion to *-interpretability) If in $fR(X)$ there are multi-incident improper components, and if Xt^* is obtained from X by substituting all the incidences of each multi-incident improper component into a point-wise interval defined for any point of its domain, then $f^*(X) \subseteq fR(Xt^*)$ (the existence requirements being presupposed).*

Example 3.15 For the continuous function $f(x,y) = y - xy$, its $*$-semantic extension to the intervals $X_1 = [2,3]$, $X_2 = [4,3]$ is

$$f^*([2,3],[4,3]) = \bigvee_{x \in [2,3]'} \bigwedge_{y \in [3,4]'} [y - xy, y - xy] = [-6,-4].$$

For the modal syntactic extensions $fR(Xt^*)$ we have

$$\begin{aligned} fR_1([2,3],[4,4]) &= [4,4] - [2,3] * [4,4] = [-8,-4] \\ fR_2([2,3],[3,3]) &= [3,3] - [2,3] * [3,3] = [-6,-3] \end{aligned}$$

and $f^*(X) \subseteq fR_1(Xt^*), f^*(X) \subseteq fR_2(Xt^*)$.

Theorem 3.11 *(Coercion to **-interpretability) If in $fR(X)$ there are multi-incident proper components, and if Xt^{**} is obtained from X by substituting all the incidences of each multi-incident proper component into a point-wise interval defined for any point of its domain, then $fR(Xt^{**}) \subseteq f^{**}(X)$ (the existence requirements being presupposed).*

Theorem 3.12 *(Interval coercion to *-interpretability) If $fR(X)$ is tree-optimal with multi-incident improper components, and if XT^* is obtained from X by transforming, for every multi-incident improper component, all incidences but one into their duals, then*

$$f^*(X) \subseteq fR(XT^*)$$

(the existence requirements being presupposed).

Theorem 3.13 *(Interval coercion to **-interpretability) If $fR(X)$ is tree-optimal with multi-incident proper components, and if XT^{**} is obtained from X by transforming, for every multi-incident proper component, all incidences but one into its dual, then*

$$fR(XT^{**}) \subseteq f^{**}(X)$$

(the existence requirements being presupposed).

Example 3.16 For $f(x,y) = y - xy$ and $X = ([2,3],[4,3])$ is

$$\begin{aligned} f^*(X) = & \bigvee_{x\in[2,3]'} \bigwedge_{y\in[3,4]'} [y-xy, y-xy] \\ = & \bigvee_{x\in[2,3]'} [3-3x, 4-4x] = [-6,-4], \end{aligned}$$

$$fR(XT^*) = \quad [4,3] - [2,3] * [3,4] = [-8,3],$$

or

$$fR(XT^*) = [3,4] - [2,3] * [4,3] = [-6,-4],$$

where, for both computations, the relation $f^*(X) \subseteq fR(XT^*)$ holds. For the same function and $X = ([1,3],[3,4])$

$$\begin{aligned} f^{**}(X) = & \quad f^*(X) = \bigvee_{y\in[3,4]'} \bigwedge_{x\in 1,3]'} [y-xy, y-xy], \\ = & \bigvee_{y\in[3,4]'} [y-3y, y-y] = [-8,0] \end{aligned}$$

$$fR(XT^{**}) = \quad [3,4] - [1,3] * [4,3] = [-6,0],$$

or

$$fR(XT^{**}) = [4,3] - [1,3] * [3,4] = [-8,0],$$

and $fR(XT^{**}) \subseteq f^{**}(X)$. (The reason for the coincidence, when such is the case, will be found later on).

Definition 3.4 *(Total monotony) A continuous real function f is x-totally monotonous for a multi-incident variable $x \in \mathbb{R}$ if it is uniformly monotonous for this variable and for each one of its incidences (considering each leaf of the syntactic tree as an independent variable). Any uni-incident uniformly monotonous variable is totally monotonous too.*

Theorem 3.14 *(Interval *-partially optimal coercion) Let X be an interval vector, and fR defined in the domain $Prop(X)$ and totally monotonous for a subset Z of multi-incident components. Let XDT^* be the enlarged vector of X, such that each incidence of every multi-incident component of the subset with total monotony is included in XDT^* as an independent component, but transformed into its dual if the corresponding incidence-point has a monotony-sense contrary to the global one of the corresponding Z-component; for the rest, every multi-incident improper component is transformed into its dual in every of its incidences except one. Then*

$$f^*(X) \subseteq fR(XDT^*).$$

Moreover if $fR(X)$ is tree-optimal,

$$fR(XDT^*) \subseteq fR(XT^*),$$

under the condition that the multi-incident components not belonging to Z suffer in XT^* the same transformation as in XDT^*.

Example 3.17 Let us consider the continuous function f from $\mathbb{R}^2$ to $\mathbb{R}$ defined by $f(x,y) = xy + \dfrac{1}{x+y}$ with $X = [10,5]$ and $Y = [2,-1]$. Ac- cording with theorem of coercion to the $*$-interpretability, there exist four possibilities for the computation of $fR(XT^*)$

$$\begin{aligned}
fR(XT_1^*) &= X * Y + \frac{1}{\mathrm{Dual}(X) + \mathrm{Dual}(Y)} \subseteq [20.0833, -9.75] \\
fR(XT_2^*) &= \mathrm{Dual}(X) * Y + \frac{1}{X + \mathrm{Dual}(Y)} \subseteq [10.1428, -4.8889] \\
fR(XT_3^*) &= \mathrm{Dual}(X) * \mathrm{Dual}(Y) + \frac{1}{X + Y} \subseteq [-9.75, 20.0834] \\
fR(XT_4^*) &= X * \mathrm{Dual}(Y) + \frac{1}{\mathrm{Dual}(X) + Y} \subseteq [-4.8888, 10.1429]
\end{aligned}$$

The derivatives prove that f is y-uniformly monotonous, isotonic for the first incidence and antitonic for the second one. As X is improper there exist two possibilities for the computation of $fR(XDT^*)$

$$\begin{aligned}
fR(XDT_1^*) &= X * Y + \frac{1}{\mathrm{Dual}(X) + \mathrm{Dual}(Y)} = fR(XT_1^*) \subseteq fR(XT_4^*) \\
fR(XDT_2^*) &= \mathrm{Dual}(X) * Y + \frac{1}{X + \mathrm{Dual}(Y)} = fR(XT_2^*) \subseteq fR(XT_3^*)
\end{aligned}$$

verifying the relations of inclusion due to the tree-optimality of fR.

Theorem 3.15 *(Interval **-partially optimal coercion) Let X be an interval vector, and fR defined in the domain $Prop(X)$ and totally monotonous for a subset Z of multi-incident components. Let XDT^{**} be the enlarged vector of X, such that each incidence of every multi-incident component of the subset with total monotony is included in XDT^* as an independent component, but transformed into its dual if the corresponding incidence-point has a monotony-sense contrary to the global one of the corresponding Z-component; for the rest, every multi-incident proper component is transformed into its dual in every of its incidences except one. Then*

$$fR(XDT^{**}) \subseteq f^{**}(X)$$

Moreover if $fR(X)$ is tree-optimal,

$$fR(XT^{**}) \subseteq fR(XDT^{**}).$$

under the condition that the multi-incident components not belonging to Z suffer in XT^{**} the same transformation as in XDT^{**}.

Theorem 3.16 *(Partially optimal coercion) Let X be an interval vector, and fR defined on the domain $Prop(X)$ and totally monotonous for all its multi-incident components. Let XD be the enlarged vector of X, such that each incidence of every multi-incident component is included in XD as an independent component, but transformed into its dual if the corresponding incidence-point has a monotony-sense contrary to the global one of the corresponding $X-$component. Then*

$$f^*(X) \subseteq fR(XD) \subseteq f^{**}(X).$$

Optimality in the multi-incidence case

Theorem 3.17 *(Coercion to optimality) Let X be an interval vector, $fR(X)$ defined and tree-optimal on the domain X' and f totally monotonous for all its multi-incident components. Let XD be defined as the enlarged vector of X, such that each incidence of every multi-incident component is included in XD as an independent component, but transformed into its dual if the corresponding incidence-point has a monotony-sense contrary to the global one of the corresponding X-component. Then,*

$$f^*(X) = fR(XD) = f^{**}(X).$$

This theorem is very useful when the function involved in the logical formula verifies the optimality conditions, because the rational computation $fR(XD)$ is the equal to $f^*(X)$, except for rounding. If the function is not totally monotonic for each multi-incident component, these theorems can be partially applied to reduce the complexity of the problem. All these computations are carried out by controlling the rounding of the operations and taking into account the multi-incident variables in the functions.

Example 3.18

1. for $f(x) = x - x$, is $fR(XD) = X - Dual(X)$ or $fR(XD) = Dual(X) - X$,
2. for $f(x) = \dfrac{x}{x}$, is $fR(XD) = \dfrac{X}{Dual(X)}$ or $fR(XD) = \dfrac{Dual(X)}{X}$, whenever $0 \notin X'$,
3. for $f(x) = \dfrac{1}{(1+x)} + \dfrac{1}{(1-x)}$ and $X = \left[\dfrac{1}{4}, \dfrac{1}{2}\right]$, is

$$fR(XD) = \frac{1}{(1 + Dual(X))} + \frac{1}{(1 - X)} = \frac{1}{\left(1 + \left[\frac{1}{2}, \frac{1}{4}\right]\right)} + \frac{1}{\left(1 - \left[\frac{1}{4}, \frac{1}{2}\right]\right)}$$

because the f-tree is optimal in this case for $X' \subseteq [0, 1)'$.

MIA provides a strong theoretical background for dealing with problems involving uncertainty and logical quantifiers. Different works involving the application of MIA have been proposed. More specifically, in his thesis, Vehí (Vehí, 1998) proposed a methodology for designing robust controllers. In (Armengol, 1999), Armengol proposed an original approach to deal with the problem of robust fault detection involving dynamic systems. Calm presented an MIA approach to tackle the problem of simulation and control (Calm, 2005). Herrero (Herrero, 2006b) proposed a new approximate methodology based on MIA for solving complex problems, such as quantified real constraint. MIA was used by Wan (Wan, 2007) for the computation of robust controllable sets for general constrained non-linear uncertain discrete-time systems. Another application of MIA was formulated by Flórez (Flórez-Díaz, 2008) to solve reliability problems in the intersection test for the ray tracing of implicit surfaces. Finally, based on the work presented by Armengol, Gelso (Gelso, 2009) proposed a methodology for fault detection, isolation, and identification based on interval models. Other studies that have used MIA can also be found in the literature (SIGLA/X Group, 1999; Sainz et al., 2002; Calderón-Espinoza et al., 2007; García et al., 2008; Sainz et al., 2008).

3.2 Interval Simulation

The simulation of a model with particular real values for the parameters, starting from any initial state, yields trajectories of the output variables across time. When the quantities involved in the simulation take values inside the intervals of variation, the set of trajectories determines a plane band bounded by an envelope, as depicted in Figure 3.4. At each time step of the simulation, the envelope, i.e., the possible maximum and minimum values of the variable, must be determined. This is a range computation problem. The function whose range must be determined is defined by the interval model of the system, and the parameter space is determined by the interval values of the parameters, the input, and the initial state. The simulation of an interval model provides intervals (ranges) that can be estimates of the envelopes. These envelopes can be obtained by numerical integration, qualitative reasoning, fuzzy logic, etc. (Calm, 2005). A way to compute these estimates is by interval arithmetic (Calm et al., 2007a).

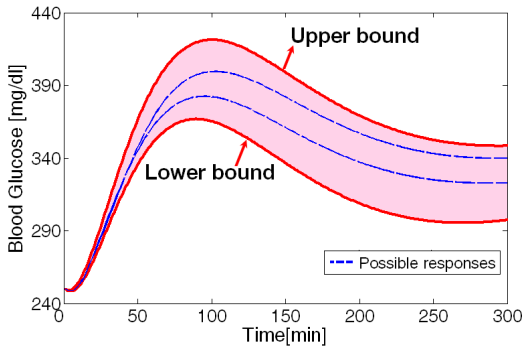

Figure 3.4: Output of an interval dynamic model: upper and lower bounds of the multiple possible system responses (shared area).

Interval arithmetic has been implemented in different arithmetic libraries. However, interval arithmetic applications have the limitations inherent to interval arithmetic. The main limitation of interval arithmetic is that it has not some of the properties of real number arithmetic, for instance the distributive property (Armengol, 1999). This means that the exact range of a function is not always computable. Therefore, the results are often very overbounded, and if tighter results are needed, high computational efforts are required. Some solvers based on interval arithmetic are presented in this section.

3.2.1 Programming tools

Different interval arithmetic libraries have been developed to perform classical or complex interval operations that handle different data types. They have been implemented in different platforms and programming languages, and some of the software has even been commercialized. A brief list of different software packages (Interval Computations, 2010) that permit the development of numerical applications using interval arithmetic is presented below.

- Boost (Brönnimann et al., 2003): Interval C++ library implemented within the popular BOOST C++ Libraries framework, which consists on a set of free peer-reviewed portable and standard C++ source libraries. The design of the library is unique in that uses policies to specify the variable behaviors: rounding, checking and comparisons.

- COSY (Makino and Berz, 2006): Can be used as stand-alone program or via C++ and Fortran 90/95 frontends. COSY is based on Taylor model and interval methods. It is intended for verified solution of such problems as ordinary differential equations, quadrature, range bounding, etc.
- FADBAD/TADIFF (Bendtsen and Stauning, 1996): Implemented in C++ code, implements the forward, backward and Taylor methods utilizing C++ templates and operator overloading. These AD-templates enable the user to differentiate functions that are implemented in arithmetic types, such as doubles and intervals. One of the major ideas in FADBAD++ is that the AD-template types also behave like arithmetic types.
- Gaol (Goualard, 2002): C++ interval arithmetic library that offers the relational interval operators used in interval constraint programming. Gaol provides support for the double-precision interval and only global rounding is available.
- HSolver (Ratschan and She, 2004): Allows analysis of hybrid systems with non-linear ODEs over an unbounded time horizon, uses intervals as its main work-horse.
- INTLAB (Rump, 1999): MATLAB toolbox for self-validating algorithms that include interval arithmetic for real and complex data, including vectors and matrices, interval arithmetic for real and complex sparse matrices, automatic differentiation, etc.
- MISO (Modal Interval Solver) (Herrero, 2006a): Software package developed using the wxWidgets framework, that containing a set of solvers based on MIA. The solver were implemented in C++ code. These solvers are:
  - FSTAR solver: Allows doing computations with Modal Intervals.
  - QRCS solver: Allows proving the satisfiability of a class of quantified real constraints.
  - MINIMAX solver: Allows solving constrained minimax optimization problems.
  - QSI solver: Allows obtaining inner and outer approximations of the solution set of a class of quantified real constrains.
  - SQUALTRACK solver: Allows detecting faults in dynamic systems.
- PROFIL/BIAS (Programmer's Runtime Optimized Fast Interval Library, Basic Interval Arithmetic Subroutines) (Knüppel, 1994): C++ class library provides a user-friendly environment for implementing interval algorithms. It is a public-domain software in continuous evolution that emphasizes the efficient use of hardware, portability, and the independence of a particular presentation of intervals.
- RealPaver (Granvilliers and Benhamou, 2006): Interval software implementing constraint satisfaction techniques for solving nonlinear systems.
- ValEncIA-IVP (Rauh et al., 2005): Software for the validation of state enclosures using interval arithmetic for initial value problems, which can be applied to the simulation of systems with both uncertain parameters and uncertain initial conditions. It was developed using PROFIL/BIAS 2.0.2, FADBAD++ 1.4, and gcc4.0.2 under SuSe Linux 10.0.
- VNODE-LP (Nedialkov, 2002): C++ package for computing bounds on solutions in IVPs for Ordinary Differential Equations (ODE).
- VSPODE (Validating Solver for Parametric ODEs) (Lin and Stadtherr, 2006): Based on VNODE, but uses Taylor models as the underlying validated data type. It helps to obtain validated solutions of IVPs for ODEs with interval-valued parameters and initial values.

In this work, the IvalDb (Interval Value Double) library was used (Herrero, 2006a). IvalDb is a module of the FSTAR solver that is incorporated in the Modal Interval Solver (MISO) package. The main feature of IvalDb is the set of modal interval arithmetic operators, like $+$, $-$, log, sin, etc., which take advantage of the C++ operator overloading concept. The IvalDb library was inspired by an existing single floating point precision modal interval library (García Reyero and Martínez, 1999), which controls numerical errors using floating point emulation. IvalDb doubles the floating point precision and uses a much simpler strategy to control numerical errors. The IvalDb library was developed by Pau Herrero in the MICELab group of the University of Girona.

3.2.2 f^* algorithm

As shown in the previous section, computing the *-semantic extension (f^*) of a continuous function f using any interpretable rational extension can cause an overestimation of the interval evaluation, attributable to possible multiple occurrences of a variable. For this reason, an algorithm based on MIA and branch-and-bound techniques, which allows the approximation of f^* by computing the inner and outer approximations, was proposed by (Herrero, 2006b) in his PhD thesis.

The f^* algorithm can be considered sound because it provides an inner approximation of the $*$-semantic extension, or expressed differently, all the points of the inner approximations belong to the solution. The f^* algorithm is complete because it also provides an outer approximation of the $*$-semantic extension, which guarantees that all the solution points are included in the approximation provided. This algorithm can be found online, incorporated in the MISO package (Herrero, 2006a).

A set of strategies was introduced to make the f^* algorithm suitable for practical applications. Basically, these strategies try to reduce, as far as possible, the number of bisections and to obtain better local approximations of the resulting partitions. Some of these improvements are simple algorithmic tricks, while others are based on important results of MIA.

The main problem of the f^* algorithm is its computational complexity, attributable to the branch-and-bound techniques used.

3.2.3 Simulators for uncertain models

A brief description of some simulators for uncertain models is given here. These are classified according to the information used for the simulation (see Figure 3.5). Simulators that can be used to deal with qualitative and semi-qualitative models focus on the generation of envelopes. A review on interval model simulators has been presented by Armengol et al. (2000).

Quantitative simulation

Quantitative simulation is used to make numerical predictions about the system states. This implies the prediction of the values of the variables at determined time points. Different methods based on quantitative simulation to simulate the behavior of interval models are:

- Superimposed thresholds (constant or variable): the envelope behavior is obtained by superimposing a tolerance to the nominal trajectory.

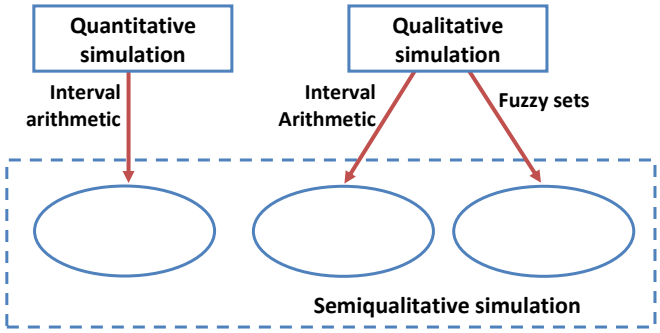

Figure 3.5: Classification of simulators.

- Quantitative model methods: the envelope is obtained by superimposing the trajectories obtained by means of a numeric simulation for all the sample models. The sample models can be chosen randomly (Monte Carlo) or systematically.

- Optimization: finding the limits of the envelope at a given time point is equivalent to finding the maximum and the minimum of a function into a parameter space, i.e. solving a global optimization problem.

Qualitative simulation

Qualitative simulation predicts qualitative states in which the system will be, by using qualitative information about the relations between the variables. Qualitative simulations can be classified into two types: non-constructive and constructive. Non constructive qualitative simulation consists of two phases (Coghill, 1996): TG (Transition Generation), in which the transitions are generated, and QA (Quantitative Analyisis), in which the states are filtered using the model to eliminate the ones that do not fulfil the constraints (constraint propagation). Most of the qualitative simulators of this type are not casual and do not hence consider time explicitly. Therefore, they predict the sequence of states that the system goes trough but do not provide information about their occurrence time point or their duration. Constructive qualitative simulators, however are casual and consider time.

Some qualitative simulators are, for example, QSIM (Qualitative Simulator) (Kuipers, 1994), PA (Predictive Algorithm) (Wiegand, 1991).

Semi-qualitative simulation

When some numerical knowledge is available, as in interval models, there are still notable deficiencies in the attempts that have been made to take advantage of it in qualitative simulators. Quantitative information can be added to enhance these qualitative methods. The resulting methods are called semiqualitative methods. Some qualitative simulators are, for example, Q2 (Kuipers and Berleant, 1988), Q3 (Berleant and Kuipers, 1993), SQSIM (Kay, 1996). Moreover, some semiqualitative simulators are based on fuzzy sets, or interval arithmetic, e.g. NIS (Numerical Interval Simulator) (Vescovi et al., 1995), NSIM (Numerical Simulator using Interval Methods) (Kay and Kuipers, 1992), Simulator of (Gasca et al., 2002).

3.3 Monte Carlo Simulation

The Monte Carlo method dates from the 1940s, when it was used by physicists working on nuclear weapons projects in the Los Alamos National Laboratory (Metropolis, 1987). Randomization methods based on Monte Carlo techniques are popular methods by which the effects of uncertainty are incorporated into numerical models. In these techniques, the parameters are randomly sampled from underlying probability distributions. Monte Carlo simulation (MCS) offers an alternative to analytical mathematics with which to understand a statistic's sampling distribution and to evaluate its behaviour in random samples.

MCS is mainly used when an exact result is unfeasible or impossible to compute with a deterministic algorithm. During MCS, values are sampled at random from the input probability distributions. Each set of samples is called an "iteration", and the resulting outcome from that sample is recorded. MCS does this hundreds or thousands of times, and the result is a probability distribution of the possible outcomes. In this way, MCS provides a much more comprehensive view of what may happen. A procedural problem that arises in virtually every MCS study concerns the number of independent trials (sample size) that must be performed to guarantee a specified bound or error (Fishman, 1996).

The analytical and computational steps that are needed for performing MCS are:

- Definition of the system.
- Generation of random numbers.
- Generation of random variables.
- Evaluation of the model N(number of iterations) times.
- Statistical analysis of the resulting behavior.
- Study of efficiency and convergence.

The definition of the system should include its boundaries, input parameters, output (or behaviour) measures, architecture, and the models that relate the input parameters and the architecture to the output parameters.

The chief advantage of MCS, compared with the other numerical methods that can solve the same problems, is that it is conceptually very simple. It does not require any specific knowledge of the form of the solution or its analytic properties. MCS is also relatively easy to implement on a computer. The main disadvantage of MCS is that it is slow. Many samples may be required (in the order of thousands or even millions) to obtain acceptable precision in the answer. In particular, because the probabilistic error bound decreases with the reciprocal square root of the number of iterations, to achieve one more decimal digit of precision in the answer requires $10^2 = 100$ times more iterations.

In this work, the interval parameters are represented in terms of normal and uniform probability distributions to generate MCSs.

The uniform distribution

A random variable with a uniform distribution, $\mathrm{U}(a, b)$, can take on any value in its range with equal probability, where the parameters a and b are the lower and upper bounds of this range (see Figure 3.6). The probability density function of the continuous uniform distribution is:

$$f(x) = \begin{cases} \dfrac{1}{b-a} & for\ a \leq x \leq b \\ 0 & otherwise. \end{cases}$$

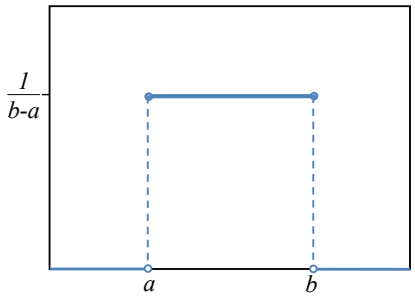

Figure 3.6: Probability density function of $\mathrm{U}(a, b)$.

In its standard form, $\mathrm{U}(0, 1)$, the uniform distribution is the building block of all MCS work because, in one way of another, the variables with all other distribution functions are derived from it. This is because the $\mathrm{U}(0, 1)$ distribution can be used to simulate a set of random probabilities, which are used to generate other distribution functions with inverse transformation and acceptance/rejection methods.

To simulate a uniform distribution, we must be able to generate a set of numbers that are equiprobable, independent, and reproducible. In this work, uncertainties in the MCS interval parameters are represented in terms of uniform probability distributions. A number of possible postprandial responses based on this distribution were obtained by applying MCS. However, MCS cannot guarantee that the actual response for a given model is within this group of responses, leading to missed hypo- and hyperglycaemic events. Moreover, a large computational effort might also be required when the number of uncertain parameters increases. The implementation of MCS is described in Chapter 4.

The normal distribution

The normal distribution is a symmetric bell-shaped curve characterized fully by its parameters: mean μ (where the peak of the density occurs) and variance σ^2 (which indicates the spread or girth of the bell curve), as shown in Figure 3.7. The normal distribution is often used to describe, at least approximately, any variable that tends to cluster around a mean. The distribution of a random variable X, for which the probability density function is f, is given by:

$$f(x) = \frac{1}{\sqrt{2\pi\sigma^2}} e^{\frac{(x-\mu)^2}{2\sigma^2}} \quad \text{for} \quad -\infty \leq x \leq \infty$$

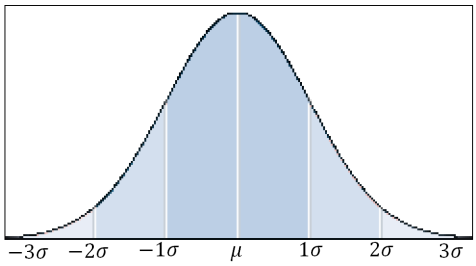

Figure 3.7: Probability distribution around the mean in a distribution $\mathrm{N}(\mu, \sigma)$.

In Chapter 5, a MCS study is carried out to represent the parameter uncertainty in terms of a normal probability distribution. The objective was to calculate the probability of the occurrence of hypo- and hyperglycaemic events.

3.4 Summary

In this chapter, a brief description has been presented of the interval arithmetic libraries and different simulator for uncertain models. The main concepts and results of MIA have been briefly introduced, with particular emphasis on the interpretability and optimality of the syntactic functions. With this result, the computation of semantic extensions of continuous functions is possible using an interval rational computation. MIA allows the efficient computation of these extensions and guarantees optimality in the case of total monotony. If the function is not totally monotonic for each multi-incident component, these theorems can be partially applied to reduce the complexity of the problem.

Chapter 4

Interval Glucoregulatory Models

In this chapter, modal interval analysis (MIA) (Gardeñes et al., 2001) has been applied to the prediction of plasma glucose in the context of uncertain food intake and uncertain patient parameters, such as insulin sensitivity. As result, the upper and lower bounds of all the possible glucose excursions experienced by the patient are predicted. One of the main problems of interval computations is the overestimation of the result, due to the existence of multiple instances of the same variable in the expression to be evaluated. MIA allows the impact of this problem to be reduced. Each interval function to be evaluated is automatically analysed and put, if possible, in its optimal form, yielding an exact computation of the range.

In the previous chapter, a summary of the principal results of MIA was presented. Some mathematical models of the glucose–insulin system referred to in Chapter 2 are examined here, with different sources of uncertainty. Each model is first described (Section 4.1) and then studied using MIA to achieve an optimal computation (Section 4.3). For each model, the results obtained with MIA are compared with those obtained with MCS, considering the uniform probability distribution. The superior performance of MIA is demonstrated, allowing to address the worst-case analysis in a mathematically guaranteed way, with little computational effort.

In Section 4.4, a comparison of three plasma glucose interval models is presented to demonstrate the dominance of intake in the postprandial phase when the different sources of uncertainty are considered.

4.1 Model of Glucose Regulation in T1DM

Mathematical models of glucose regulation have been studied over the past 40 years. Makroglou et al. (2006) has presented an overview of the glucose–insulin regulatory models available in the literature. More recently, the engineering effort in modelling the insulin–glucose system throughout the last 50 years has been presented by Cobelli et al. (2009), starting with the minimal model and including subsequent models. The most well-known model is the so-called "minimal model", which contains a minimal number of parameters (Bergman et al., 1981) and is widely used in physiological research to estimate glucose effectiveness and insulin sensitivity in the IVGTT.

In this section, different models of the glucose–insulin system are described in detail (see Figure 4.1). The models have been selected according to the needs of the research projects INSULAID (Bondia and Vehí, 2007) and INSULAID2 (Bondia and Vehí, 2010), in which the

study underlying this thesis has been involved.

Two carbohydrate digestion and absorption models are presented (Hovorka et al., 2004; Dalla Man et al., 2006). Three compartment models of subcutaneous insulin absorption have been described (Hovorka et al., 2004; Wilinska et al., 2005; Dalla Man et al., 2007a) for the bolus administration and the infusion of rapid-acting insulin. Finally, four insulin action and glucose kinetics models are described. These models were intended for different purposes: measurement of insulin sensitivity and control (Bergman et al., 1981), simulation and control (Hovorka et al., 2002), simulation (Dalla Man et al., 2007b), and control (Panunzi et al., 2007).

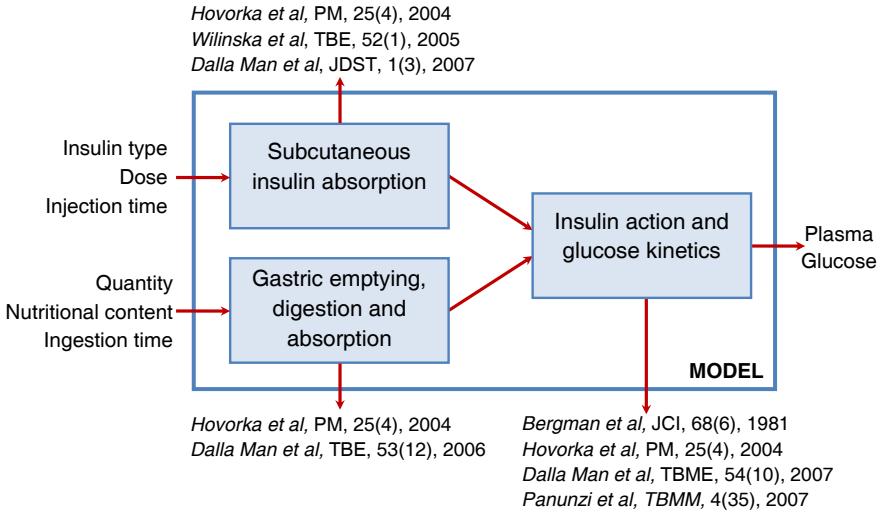

Figure 4.1: Models of the glucose-insulin system in T1DM studied in this work.

4.1.1 Carbohydrate digestion and absorption models

The mathematical models used in this chapter to describe glucose absorption were formulated by Hovorka et al. (2004) and Dalla Man et al. (2006).

Hovorka et. al model

The model formulated by Hovorka et al. (2004), described the carbohydrates catabolism to monosaccharide (mostly glucose) taking place during meal digestion, as well as intestinal absorption. The glucose absorption rate $R_a(t)$ (mg min^{-1}) is represented by:

$$R_{\mathrm{a}}(t) = \frac{D A_G t \exp(-t/t_{\mathrm{max},G})}{t_{\mathrm{max},G}^2} \tag{4.1}$$

being D (mg) the amount of carbohydrates ingested, A_G (dimensionless) is carbohydrate bioavailability and $t_{\mathrm{max},G}$ (min) is the time-of-maximum appearance of glucose in plasma.

Dalla Man et. al model

Dalla Man et al. (2006) proposed a three-compartment nonlinear model (see Figure 4.2), two for the glucose in the stomach solid Q_{sto1} (mg) and liquid Q_{sto2} (mg), and one for the glucose in the intestinal tract Q_{gut} (mg). The meal is digested in the stomach with a grinding coefficient k_{gri} (min^{-1}); then the chyme (partially-digested food) enters the intestine with fractional coefficient of transfer k_{empt} (min^{-1}) and finally glucose is absorbed and enters the bloodstream.

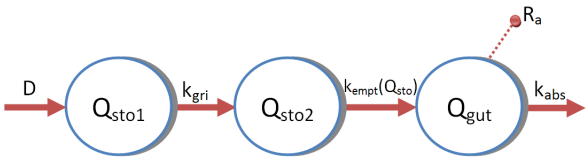

Figure 4.2: Scheme of gastro-intestinal Dalla Man et al. system (adapted from Dalla Man et al. (2007b).

The rate of appearance R_a (mg kg^{-1} min^{-1}) describes glucose transit through the stomach and intestine:

$$\begin{aligned}
Q_{sto}(t) &= Q_{sto1}(t) + Q_{sto2}(t) && Q_{sto}(0) = 0 \\
\frac{\mathrm{d}Q_{sto1}(t)}{dt} &= -k_{gri}\, Q_{sto1}(t) + D\, \delta(t) && Q_{sto1}(0) = 0 \\
\frac{\mathrm{d}Q_{sto2}(t)}{dt} &= -k_{empt}(t, Q_{sto})\, Q_{sto2}(t) + k_{gri}\, Q_{sto1}(t) && Q_{sto2}(0) = 0 \\
\frac{Q_{gut}(t)}{dt} &= -k_{abs}\, Q_{gut}(t) + k_{empt}(t, Q_{sto})\, Q_{sto2}(t) && Q_{gut}(0) = 0 \\
R_a(t) &= \frac{f\, k_{abs}\, Q_{gut}(t)}{BW} && R_a(0) = 0
\end{aligned} \tag{4.2}$$

In order to guarantee model identifiability, k_{gri} is fixed and equal to k_{max} (min^{-1}). Furthermore, f is the fraction of intestinal absorption which actually appears in plasma (90%), k_{abs} (min^{-1}) is the rate constant of intestinal absorption, D (mg) is the amount of carbohydrate to be ingested, $\delta(t)$ is the impulse function, and BW (kg) is the body weight.

The coefficient of gastric emptying k_{empt} is a time-variant nonlinear function of Q_{sto} as shown in Figure 4.3

$$k_{empt}(t, Q_{sto}) = k_{min} + \frac{k_{max} - k_{min}}{2} \{tanh(\alpha(Q_{sto}(t) - b\, D)) - tanh(\beta(Q_{sto}(t) - d\, D)) + 2\} \tag{4.3}$$

The parameters α and β are constraints in order to $k_{empt}(t, Q_{sto}) = k_{max}$ for $Q_{sto}(t) = D$ and $Q_{sto}(t) = 0$, as follows:

$$\alpha = \frac{5}{2\, D\, (1 - b)}, \qquad \beta = \frac{5}{2\, D\, c}$$

where k_{min} and k_{max} are the minimum and maximum rate of gastric emptying respectively, b is the percentage of the dose for which the rate of gastric emptying decreases at k_{mean}, and c is the percentage of the dose for which the rate of gastric emptying is back to k_{mean}.

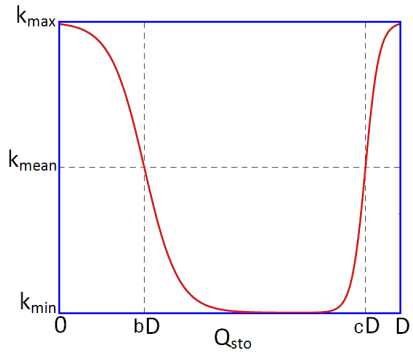

Figure 4.3: $k_{empt}(t, Q_{sto})$ function, where D is the total glucose quantity of the last meal.

4.1.2 Subcutaneous insulin absorption models

Three compartmental models that represent subcutaneous insulin absorption are studied in this work.

Hovorka et al.

An insulin absorption model was developed by Hovorka et al. (2004). This model is described by two-compartments that represents the absorption of subcutaneously administered short-action insulin (see Figure 4.4).

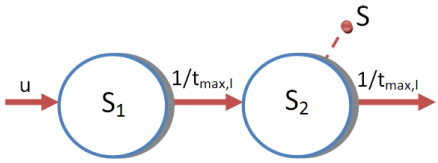

Figure 4.4: Compartment model of subcutaneous insulin absorption proposed by Hovorka et al. (2004).

The model is represented by the following equations:

$$\begin{aligned} \frac{\mathrm{d}S_1(t)}{dt} &= u(t) - \frac{S_1(t)}{t_{max,I}} & S_1(0) &= u(0)\ t_{max,I} \\ \frac{\mathrm{d}S_2(t)}{dt} &= \frac{S_1(t)}{t_{max,I}} - \frac{S_2(t)}{t_{max,I}} & S_2(0) &= S_1(0) \\ S(t) &= \frac{S_2(t)}{t_{max,I}} \end{aligned} \tag{4.4}$$

where S_1 and S_2 (mU) represents insulin masses in the accessible and nonaccessible compartments, u (mU min^{-1}) represents administration (bolus and infusion) of rapid-acting insulin, $t_{max,I}$ (min) is the time-to-maximum of absorption of subcutaneously injected and S (mU min^{-1}) is the appearance rate of insulin in plasma.

Wilinska et al.

Eleven alternative compartment models have been postulated by Wilinska et al. (2005) to represent the insulin kinetics after the administration of a bolus of insulin or the continuous infusion of insulin (lispro). In this work, the model that best fits the experimental data is considered, and is based on the model diagram in Figure 4.5.

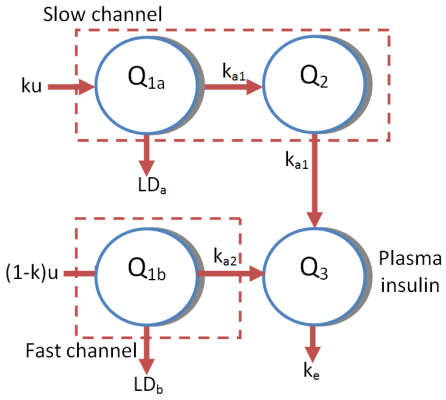

Figure 4.5: Model diagram of subcutaneous insulin absorption proposed by Wilinska et al. (2005).

The model considered two different pathways of insulin absorption, slow and fast. The first consisting of two compartments, Q_{1a} (mU) which represents mass of insulin administered as continuous infusion, and Q_2 (mU) represents insulin mass in the non-accessible subcutaneous compartments. The second is represented by one compartment Q_{1b} (mU) which is mass of insulin given as a bolus. The proportion of insulin channelled through these two pathways was considered to be the same for the two delivery modes, continuous infusion and the bolus. The insulin concentration is now directly calculated from the fourth compartment Q_3 (mU) which represents insulin mass in the plasma compartment. This model was formulated to overcome underestimation of the postprandial plasma insulin peak. The equations of the model are:

$$\begin{aligned}
\frac{\mathrm{d}Q_{1a}(t)}{dt} &= k\ u(t) - k_{a1}Q_{1a}(t) - LD_a(t) && Q_{1a}(0) = 0 \\
\frac{\mathrm{d}Q_{1b}}{dt} &= (1-k)u(t) - k_{a2}Q_{1b}(t) - LD_b(t) && Q_{1b}(0) = 0 \\
\frac{\mathrm{d}Q_2(t)}{dt} &= k_{a1}Q_{1a}(t) - k_{a1}Q_2(t) && Q_2(0) = 0 \\
\frac{\mathrm{d}Q_3(t)}{dt} &= k_{a1}Q_2(t) + k_{a2}Q_{1b}(t) - k_eQ_3(t) && Q_3(0) = 0 \\
I(t) &= \frac{Q_3(t)}{V_i\ BW} && I(0) = 0
\end{aligned} \tag{4.5}$$

being,

$$LD_a(t) = \frac{V_{MAX,LD}\ Q_{1a}(t)}{k_{M,LD} + Q_{1a}(t)}$$

$$LD_b(t) = \frac{V_{MAX,LD}\ Q_{1b}(t)}{k_{M,LD} + Q_{1b}(t)}$$

where u (mU min^{-1}) represents the insulin input; k (unitless) is the proportion of the total input flux passing through the slower, two compartment channel; I (mU L^{-1}) is the insulin concentration; k_{a1}, k_{a2} and k_e are transfer rates (min^{-1}); $V_{MAX,LD}$ (mU min^{-1}) is the saturation level describing Michaelis-Menten dynamics of insulin degradation for continuous infusion and bolus; $k_{M,LD}$ (mU) is the value of insulin mass at which insulin degradation is equal to half of its maximal value for continuous infusion and bolus; LD_a and LD_b (mU min^{-1}) represents local degradation at the injection site for continuous infusion and bolus, respectively; V_i (L kg^{-1}) represents the insulin distribution volume and BW (kg) is the body weight.

Dalla Man et al.

The model formulated by Dalla Man et al. (2007a) to describe the subcutaneous insulin absorption uses two-compartments: S_1 and S_2 (pmol kg^{-1}) to represent the polymeric and the monomeric insulin in the subcutaneous tissue respectively (see Figure 4.6).

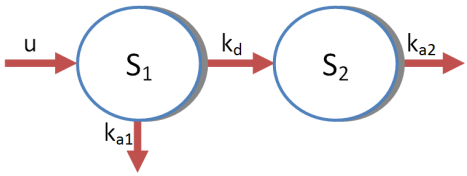

Figure 4.6: Scheme of subcutaneous insulin kinetics proposed by Dalla Man et al. (2007a).

The model is represented by the following equations:

$$\begin{aligned} \frac{\mathrm{d}S_1(t)}{dt} &= u(t) - (k_{a1} + k_d)S_1(t) & S_1(0) &= \frac{u(0)}{k_d + k_{a1}} \\ \frac{\mathrm{d}S_2(t)}{dt} &= k_d\, S_1(t) - k_{a2}S_2(t) & S_2(0) &= \frac{k_d\, S_1(0)}{k_{a2}} \\ S(t) &= k_{a1}\, S_1(t) + k_{a2}\, S_2(t) & S(0) &= S_b \end{aligned} \tag{4.6}$$

where u (pmol kg^{-1} min^{-1}) represents injected insulin flow, k_d (min^{-1}) is called degradation constant, k_{a1} and k_{a2} (min^{-1}) are absorption constants. The quantity S_b (pmol min^{-1}) represents insulin infusion to maintain diabetic patient at basal steady state and S (pmol kg^{-1} min^{-1}) is the rate of appearance of insulin in plasma.

4.1.3 Insulin action and glucose kinetics models

The models used to describe the kinetics of glucose in this work are those presented by Bergman et al. (1981), Hovorka et al. (2002), Dalla Man et al. (2007b), and Panunzi et al. (2007).

Bergman et al.

The model developed by Bergman et al. (1981) has been modified by Roy and Parker (2006) (see Figure 4.7). The modified model is used in this work.

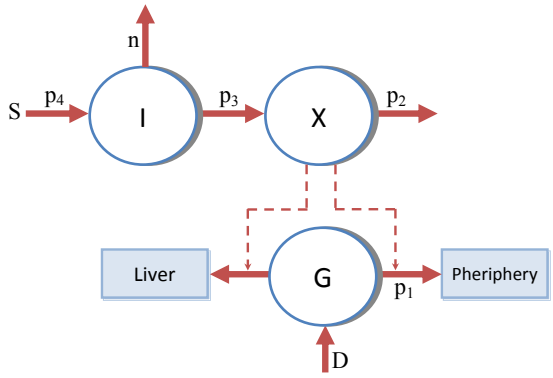

Figure 4.7: Schematic representation of Bergman model.

Bergman *et al.* used a three-compartmental mathematical model to represent the concentrations: plasma insulin I (mU mL^{-1}), remote insulin X (min^{-1}), and plasma glucose G (mg dL^{-1}). Then, the minimal model is given by:

$$\begin{aligned} \frac{\mathrm{d}I(t)}{dt} &= -n\, I(t) + p_4\, S(t) && I(0) = I_b \\ \frac{\mathrm{d}X(t)}{dt} &= -p_2\, X(t) + p_3(I(t) - I_b) && X(0) = 0 \\ \frac{\mathrm{d}G(t)}{dt} &= -p_1\, G(t) - X(t)\, G(t) + p_1\, G_b + \frac{R_a(t)}{V_g} && G(0) = G_b \end{aligned} \tag{4.7}$$

where n (min^{-1}) is the fractional disappearance rate of insulin, p_4 (mL^{-1}) is the insulin distribution model, S (mU min^{-1}) is the exogenous insulin infusion rate obtained of any subcutaneous insulin model, and I_b (mU mL^{-1}) is the basal value of insulin concentration. The remote insulin compartment are governed by the parameters p_2 (min^{-1}), and p_3 (mL mU^{-1}min^{-2}), the first represents the rate constant expressing the spontaneous decrease of tissue glucose uptake ability and the last the insulin-dependent increase in tissue glucose uptake ability per unit of insulin concentration excess over baseline insulin. Parameter p_1 (min^{-1}) represents the rate at which glucose is removed from the plasma space independent of the influence of insulin. Plasma glucose concentration in basal state is denoted by G_b. The glucose absorption rate R_a (mg min^{-1}) is obtained of any digestion and absorption model. Finally, V_g (dL) is the glucose distribution space.

Hovorka et al.

A glucose kinetics and insulin action model was formulated by Hovorka et al. (2002). The model regards separately at each action of insulin on different phenomena with its final effect on blood glucose. The relation between insulin in plasma, every virtual compartment representing insulin actions and the two compartments for glucose are shown in Figure 4.8.

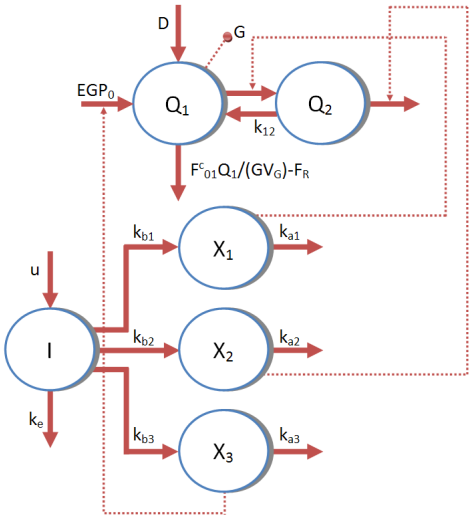

Figure 4.8: Compartment model of glucose-insulin system (adapted from Hovorka et al. (2004)).

Two compartments representing kinetics of native glucose:

$$\begin{aligned}
\frac{\mathrm{d}Q_1(t)}{\mathrm{d}t} &= -X_1(t)Q_1(t) + k_{12}Q_2(t) - F_{01}^c(t) - F_R(t) + R_a(t) \\
&\quad +\mathrm{EGP}_0(1 - X_3(t)) && Q_1(0) = G(0)\ V_g \\
\frac{\mathrm{d}Q_2(t)}{\mathrm{d}t} &= X_1(t)Q_1(t) - (k_{12} + X_2(t))Q_2(t) && Q_2(0) = \frac{Q_1(0)X_1(0)}{k_{12} + X_2(0)} \\
G(t) &= \frac{Q_1(t)}{V_g} && G(0) = G_b
\end{aligned} \tag{4.8}$$

where Q_1 and Q_2 (mmol) represents the masses of glucose in the accessible and non-accessible compartments, k_{12} (min^{-1}) represents the transfer rate constant from the non-accessible to the accessible compartment, V_g (L kg^{-1}) represents the distribution volume of the accessible compartment, G (mmol L^{-1}) is the glucose concentration and EGP_0 (mmol min^{-1}) represents endogenous glucose production extrapolated to the zero insulin concentration. F_{01}^c (mmol min^{-1}) is the total non-insulin-dependent glucose disposal, and F_R is the renal glucose clearance above the glucose threshold of 9 mmol L^{-1}:

$$F_{01}^c(t) = \begin{cases} \dfrac{f_{01}G(t)}{4.5} & \text{if} \quad G(t) < 4.5 \text{ mmol L}^{-1} \\ f_{01} & \text{if} \quad G(t) \geq 4.5 \text{ mmol L}^{-1} \end{cases} \tag{4.9}$$

$$F_R(t) = \begin{cases} 0 & \text{if} \quad G(t) < 9 \text{ mmol L}^{-1} \\ 0.003(G(t) - 9)V_g & \text{if} \quad G(t) \geq 9 \text{ mmol L}^{-1} \end{cases} \tag{4.10}$$

The model adds a new compartment for every action of insulin, and there are three considered events: insulin increases the flow of glucose from blood to the tissues, insulin increases the glucose uptake by muscles and adipose tissue, and insulin inhibits production of glucose of glucose in the liver. These three influences are reflected in the model as virtual compartments (see Figure

4.8). The insulin actions are modelled as first-order processes:

$$\begin{aligned}
\frac{\mathrm{d}X_1(t)}{\mathrm{d}t} &= -k_{a1}X_1(t) + k_{a1}S_{IT}I(t) \qquad X_1(0) = S_{IT}\ I(0) \\
\frac{\mathrm{d}X_2(t)}{\mathrm{d}t} &= -k_{a2}X_2(t) + k_{a2}S_{ID}I(t) \qquad X_2(0) = S_{ID}\ I(0) \\
\frac{\mathrm{d}X_3(t)}{\mathrm{d}t} &= -k_{a3}X_3(t) + k_{a3}S_{IE}I(t) \qquad X_3(0) = S_{IE}\ I(0)
\end{aligned} \tag{4.11}$$

where X_1 (min^{-1}) represents the effects of insulin on glucose distribution/transport, X_2 (min^{-1}) represents the effect on glucose disposal, and X_3 (min^{-1}) the effect on endogenous glucose production; k_{ai}, $i = 1, \ldots, 3$ are deactivation rate constants, and S_{IT}, S_{ID} and S_{IE} (min^{-1} per mU L^{-1}) are insulin sensitivities to transport, disposal, and endogenous glucose production, respectively.

Plasma insulin concentration I (mU L^{-1}) is considered to affect on glucose transport from plasma to the tissues, hepatic glucose production, and peripheral glucose disposal (Hovorka et al., 2004), and thus described as:

$$\frac{\mathrm{d}I(t)}{\mathrm{d}t} = \frac{S(t)}{V_i} - k_e I(t) \qquad I(0) = I_b \tag{4.12}$$

where k_e (min^{-1}) is the fractional elimination rate, V_i (L kg^{-1}) is the insulin distribution volume, and S (mU min^{-1}) is the appearance rate of insulin in plasma.

Dalla Man et al.

The model described here was developed in Cobelli's group in Padova, Italy (Dalla Man et al. (2007b)) and is one of the most important models in diabetes research. Some modifications were presented by Magni et al. (2007) to simulate the specific metabolism of T1DM. This model is composed of one glucose and one insulin subsystem linked by the control of insulin on glucose utilization and endogenous production, as can be seen in Figure 4.9.

Next, the models corresponding to each one of the subsystems are described.

Glucose Subsystem: Dalla Man et al. (2007b) used a two-compartment model to describe glucose kinetics, as can be seen in Figure 4.10.

The model equations are:

$$\begin{aligned}
\frac{\mathrm{d}G_p(t)}{\mathrm{d}t} &= EGP(t) + R_a(t) - U_{ii}(t) - E(t) - k_1 G_p(t) + k_2 G_t(t) \qquad G_p(0) = G_{pb} \\
\frac{\mathrm{d}G_t(t)}{\mathrm{d}t} &= -U_{id}(t) + k_1 G_p(t) - k_2 G_t(t) \qquad G_t(0) = G_{tb} \\
G(t) &= \frac{G_p(t)}{V_g} \qquad G(0) = G_b
\end{aligned} \tag{4.13}$$

where G_p and G_t (mg kg^{-1}) are glucose masses in plasma and rapidly-equilibrating tissues, and in slowly equilibrating tissues, respectively, G (mg dL^{-1}) plasma glucose concentration, with the suffix b denoting the basal state. EGP (mg kg^{-1} min^{-1}) is the endogenous glucose

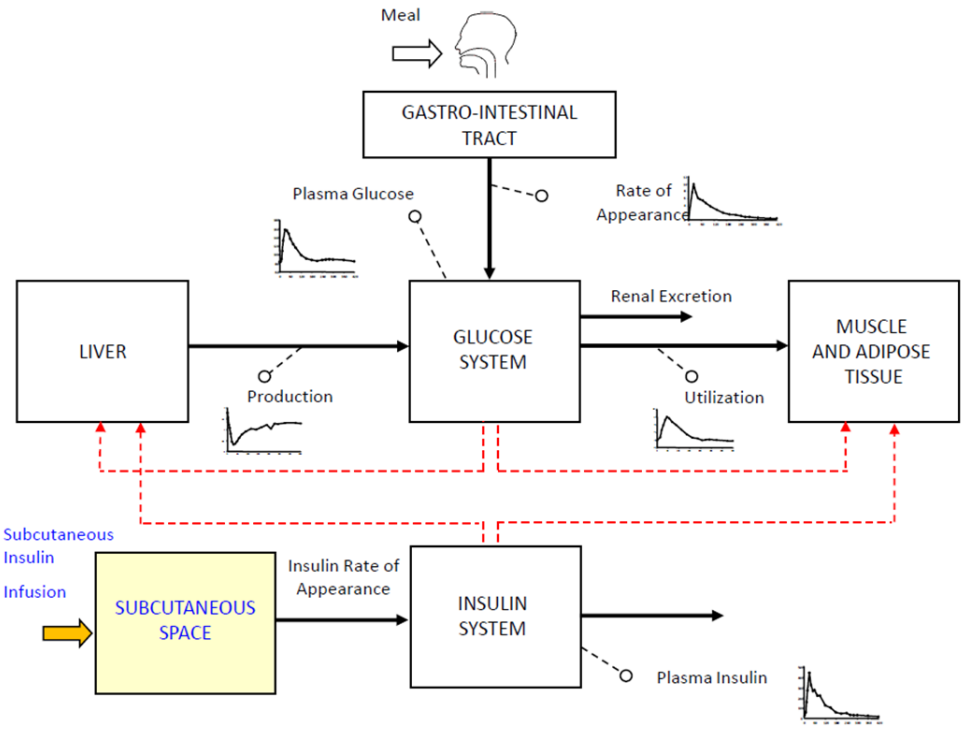

Figure 4.9: Scheme of the glucose-insulin system in T1DM. Solid lines represent glucose and insulin fluxes; dashed lines represent control signals. Physical activity affects insulin-independent glucose utilization (taken from Dalla Man et al. (2009)).

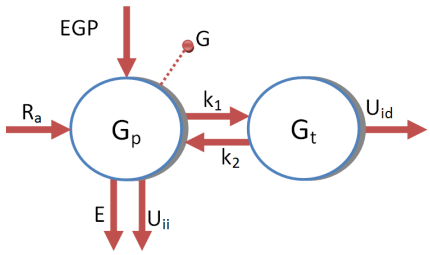

Figure 4.10: Schema of the glucose subsystem (adapted by Dalla Man et al. (2006)).

production, R_a (mg kg^{-1} min^{-1}) is the glucose rate of appearance in plasma, E (mg kg^{-1} min^{-1}) is renal excretion, U_{ii} and U_{id} are the insulin independent and dependent glucose utilizations, respectively. V_g (dL kg^{-1}) is the distribution volume of glucose and k_1 and k_2 (min^{-1}) are the rate parameters.

At basal steady-state endogenous production EGP_b equals glucose disappearance, i.e. the sum of glucose utilization and renal excretion (which is zero in the normal subject), $U_b + E_b$:

$$EGP_b = U_b + E_b \tag{4.14}$$

The glucose renal excretion E is modeled by a linear relationship with plasma glucose

$$E(t) = \begin{cases} k_{e1}\,(G_p(t) - k_{e2}) & \text{if } G_p(t) > k_{e2} \\ 0 & \text{if } G_p(t) \leq k_{e2} \end{cases}$$

where k_{e1} (min^{-1}) is the glomerular filtration rate and k_{e2} (mg kg^{-1}) is the renal threshold of glucose.

Endogenous glucose production EGP: This model incorporates the notion that a portal insulin signal controls the rapid suppression of EGP. Since the portal insulin signal is an anticipated version of plasma insulin, it was approximated with a portal-like derivative of insulin concentration signal.

The endogenous glucose production, is described as:

$$EGP(t) = k_{p1} - k_{p2}G_p(t) - k_{p3}I_d(t) \qquad EGP(0) = EGP_b \tag{4.15}$$

where k_{p1} ($\text{mg kg}^{-1}\ \text{min}^{-1}$) is the extrapolated EGP at zero glucose and insulin, k_{p2} (min^{-1}) liver glucose effectiveness, and k_{p3} ($\text{mg kg}^{-1}\ \text{min}^{-1}$ per pmol L^{-1}) parameter governing amplitude of insulin action on the liver. I_d is a delayed insulin signal realized with a chain of two compartments:

$$\begin{aligned} \frac{\mathrm{d}I_1(t)}{\mathrm{d}t} &= -k_i(I_1(t) - I(t)) \qquad I_1(0) = I_b \\ \frac{\mathrm{d}I_d(t)}{\mathrm{d}t} &= -k_i(I_d(t) - I_1(t)) \qquad I_d(0) = I_b \end{aligned} \tag{4.16}$$

where k_i (min^{-1}) is the rate parameter accounting for delay between insulin signal and insulin action. EGP is also constrained to be non-negative.

At basal steady state, one has,

$$k_{p1} = EGP_b + k_{p2}G_{pb} + k_{p3}I_b$$

so,

$$EGP(t) = EGP_b + k_{p2}(G_{pb} - G_p(t)) + k_{p3}(I_b - I_d(t)) \tag{4.17}$$

Glucose utilization: The model of glucose utilization by body tissues during a meal assumes that glucose utilization is made up of two components: insulin-independent and insulin dependent.

$$U(t) = U_{ii}(t) + U_{id}(t) \tag{4.18}$$

Insulin-independent utilization takes place in the first compartment, is constant, and represents glucose uptake by the brain and erythrocytes (F_{cns}):

$$U_{ii}(t) = F_{cns}$$

Insulin-dependent utilization takes place in the remote compartment and depends nonlinearly (Michaelis Menten) upon glucose in the tissues:

$$U_{id}(t) = \frac{V_m(X(t))\, G_t(t)}{K_m(X(t)) + G_t(t)} \tag{4.19}$$

where $V_m(X(t))$ (mg kg^{-1} min^{-1} per pmol L^{-1}), and $K_m(X(t))$ (mg kg^{-1} per pmol L^{-1}) are assumed to be linearly dependent upon a remote insulin, X (pmol L^{-1}):

$$\begin{aligned} V_m(X(t)) &= V_{m0} + V_{mx}\, X(t) \\ K_m(X(t)) &= K_{m0} \end{aligned} \tag{4.20}$$

which depends from insulinemia in the following way

$$\frac{\mathrm{d}X(t)}{\mathrm{d}t} = -p_{2U}\, X(t) + p_{2U}(I(t) - I_b) \qquad X(0) = 0 \tag{4.21}$$

where I is plasma insulin, and p_{2U} (min^{-1}) is a rate constant defining insulin action on peripheral glucose utilization. V_{m0} (mg kg^{-1} min^{-1}), and K_{m0} (mg kg^{-1}) are the Michaelis-Menten parameter of glucose utilization at zero insulin action, and V_{mx} (mg kg^{-1} min^{-1} per pmol L^{-1}) is the disposal of insulin sensitivity.

In the basal steady state one has:

$$\begin{aligned} G_{tb} &= \frac{F_{cns} - EGP_b + k_1 G_{pb}}{k_2} \\ U_b &= EGP_b = F_{cns} + \frac{V_{m0} G_{tb}}{K_{m0} + G_{tb}} \end{aligned}$$

from which

$$V_{m0} = \frac{(EGP_b - F_{cns})(K_{m0} + G_{tb})}{G_{tb}}$$

Insulin subsystem: Insulin flow S, coming from the subcutaneous compartments, enters the bloodstream and is degraded in the liver and in the periphery. The two-compartment model used to describe insulin kinetics can be seen in Figure 4.11.

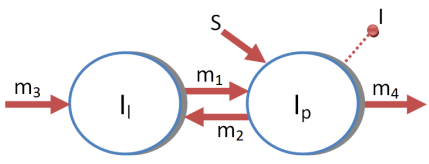

Figure 4.11: Schema of the insulin subsystem (adapted by Dalla Man et al. (2006)).

The model equations are:

$$\begin{aligned}
\frac{\mathrm{d}I_l(t)}{\mathrm{d}t} &= -I_l(t)(m_1+m_3)+m_2\ I_p(t) && I_l(0)=I_{lb}\\
\frac{\mathrm{d}I_p(t)}{\mathrm{d}t} &= -I_p(t)(m_2+m_4)+m_1\ I_l(t)+S(t) && I_p(0)=I_{pb}\\
\frac{\mathrm{d}I(t)}{\mathrm{d}t} &= \frac{I_p(t)}{V_i} && I(0)=I_b
\end{aligned} \tag{4.22}$$

where I_p and I_l (pmol kg^{-1}) are insulin masses in plasma and in liver respectively, I (pmol L^{-1}) is plasma insulin concentration, V_i (L kg^{-1}) is the distribution volume of insulin, m_1, m_2, m_3, and m_4 (min^{-1}) are rate parameters, and m_2, m_3, and m_4 depend on m_1 in the following way:

$$\begin{aligned}
m_2 &= 0.6\frac{CL}{HE_b\ V_i\ BW}\\
m_3 &= m_1\frac{HE_b}{1-HE_b}\\
m_4 &= 0.4\frac{CL}{V_i\ BW}
\end{aligned} \tag{4.23}$$

where HE_b is the basal hepatic insulin extraction and was fixed to 0.6, CL (min^{-1}) is the insulin clearance.

At basal one has

$$I_{lb}=\frac{I_{pb}\ m_2}{m_1+m_3} \qquad I_{pb}=I_b\ V_i \tag{4.24}$$

where I_{lb} and I_{pb} corresponds with to the basal steady state of insulin masses in plasma and in liver respectively.

Panunzi et al.

A discrete single delay model for the IVGTT was proposed by Panunzi et al. (2007). They compared some of the characteristics of the Bergman model and new features for a proposed model of the IVGTT scenario with a delayed insulin secretion rate. The new model surpassed the rest in simulated experiments and in its identifiability properties, but it was only tested in healthy patients. Therefore, in this work, the model was adapted to simulate the specific metabolic parameters of T1DM patients.

This model is described by two-compartments (one for glucose and one for insulin) (see Figure 4.12) which are represented by the following equations:

$$\begin{aligned}
\frac{dG(t)}{dt} &= -K_{xgI}I(t)G(t)+\frac{T_{gh}}{V_g}+\frac{R_a(t)}{V_g} && G(0)=G_b\\
\frac{dI(t)}{dt} &= -K_{xi}I(t)+\frac{T_{igmax}}{V_i}\frac{\left(\frac{G(t-\tau_g)}{G^*}\right)^{\gamma}}{1+\left(\frac{G(t-\tau_g)}{G^*}\right)^{\gamma}}+\frac{S(t)}{Vi} && I(0)=I_b
\end{aligned} \tag{4.25}$$

being,

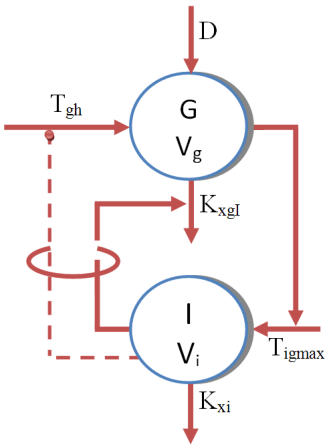

Figure 4.12: Schematic representation of the two-compartments, one-discrete-delay model (adapted by Panunzi et al. (2007)).

$$T_{gh} = K_{xgI}\ I_b\ G_b\ V_g$$
$$T_{igmax} = K_{xi}\ V_i\ \frac{1 + \left(\frac{G_b}{G^*}\right)^{\gamma}}{\left(\frac{G_b}{G^*}\right)^{\gamma}}$$

where G (mmol L^{-1}) represents the glucose plasma concentration at time t, R_a (mmol kg^{-1} min^{-1}) is the glucose absorption rate, and V_g (L kg^{-1}) is the apparent distribution volume for glucose. I (pM) is the insulin plasma concentration, K_{xgI} (min^{-1} pM^{-1}) is the second-order net elimination rate of glucose per unit of insulin concentration, T_{gh} (mmol min^{-1} kg^{-1}) represents the net difference between glucose production and glucose elimination, K_{xi} (min^{-1}) is the first order elimination ratio of insulin, and T_{igmax} (pmol min^{-1} kg^{-1}) is the maximal rate of second-phase insulin release. S (pM min^{-1}) is the exogenous insulin infusion rate, I_b (pM) is the basal value of insulin concentration, V_i (L kg^{-1}) represents the apparent distribution volume for insulin, τ_g (min) is the delay with which the pancreas changes secondary insulin release in response to varying plasma glucose concentrations, γ is the progressivity with which the pancreas reacts to circulating glucose concentrations, and G^* (mM) represents the glycemia at which the insulin secretion rate is half of its maximum.

4.2 Uncertainty and Intra-patient Variability

Dynamic models provide valuable information about postprandial glucose excursions. However, one of the main challenges is in the large intra-individual patient variability that exists, which must be taken into account. The insulin needs of a subject vary throughout the day due to, for example, diurnal changes in insulin sensitivity (intra-subject variability). This variability has been reported by different authors.

A study of intra-patient variation in plasma glucose was presented by Mooy et al. (1996). Intra-subject variability of up to 30% was considered by Chassin et al. (2004) in their implementation of adverse operating conditions to test glucose controllers in a virtual environment. Taking into account the uncertainty in biomedical systems, Kirchsteiger et al. (2009) considered

the uncertainty in the parameters of insulin sensitivity to evaluate the performance of the control system. Other studies about variability on blood glucose prediction were presented in Chapter 2 (Section 2.2.4). In this study, the parameters related to insulin sensitivity are represented by intervals to accommodate intra-patient variability.

There is also an important source of uncertainty in food intake, because in real-life situations, it is impossible to precisely measure the carbohydrate content of a mixed meal. For instance, overestimates of 8.5% and underestimates of 28% have been reported (Graff et al., 2000). Accordingly, most patients tend to underestimate the carbohydrate content of their intake. However, this is usually done in a consistent way, so that their therapy can be adapted to counteract this bias. For this reason, in this work, uncertainty in food intake estimation is considered to represent a deviation relative to this bias-corrected estimation.

Other errors can be included in the estimation of the insulin dose, because this dose is calculated according to intake and blood glucose monitoring, and both may include errors. The variability present in subcutaneous absorption has also been widely studied by Heinemann (2002); Barnett (2003); Heise et al. (2004); Guerci and Sauvanet (2005); Scholtz et al. (2005); Goykhman et al. (2009).

Uncertainty is represented here by an interval model in which the parameters, inputs, and/or initial states take interval values (Calm et al., 2007a, 2011; García-Jaramillo et al., 2011b). The simulation results in the case of a real-valued model are the trajectories of the system variables across time. When the quantities involved in the simulation take values inside the intervals of variation, the set of trajectories determines an envelope, representing the set of all possible responses. In the next section, different models are examined to select an optimal rational computation that takes into account these uncertainties.

4.3 Library of Interval Models of Physiological Subsystems of Glucose Regulation

The prediction of glucose excursions is the key to decision-aid systems for insulin therapy optimization in T1DM (García-Jaramillo et al., 2009a) and glucose control strategies (El Youssef et al., 2009). However, there is great intra- and inter-individual variability in patient behaviour. Food intake (amount of carbohydrates) is another important source of uncertainty because accurate estimates are difficult to make for a mixed meal. Therefore, the development of prediction tools that can accommodate different sources of uncertainty (input, parameters, initial state) is necessary (Calm et al., 2007a).

In this section, the models described in Section 4.1 are evaluated, taking into account the intra-patient variability and the different sources of uncertainty, such as the uncertainty in food intake, insulin dose, preprandial blood glucose and initial states. Then, the parameters and initial states related with these uncertainties were evaluated to obtain an optimal rational computation. To achieve an optimal computation, each interval model is evaluated to avoid multi-incident variables. One of the main problems in interval computations arises from the existence of multiple instances of the same variable in the expression, leading to the overestimation of the result. To avoid this problem, we have used MIA. Therefore, each interval function to be evaluated is analysed and put, if possible, into its optimal form (the expression is rewritten in such a way that the exact range is obtained). Finally, the interval simulation is performed.

The uncertain parameters, which were studied using MIA, that lead to an overestimation of the interval computation were not considered in this work. However, when the optimality cannot be achieved, the f^* algorithm (Herrero et al., 2005) can be launched. This algorithm uses many optimality and coercion theorems from modal interval theory to compute tight approximations of the range by applying branch-and-bound techniques. However, according to the function, the algorithm may require a large computational effort because it is highly complex. A summary of the principal results of MIA was presented in Chapter 3.

Another simulation approach studied in this section to obtain a set of possible postprandial responses is the Monte Carlo simulation (MCS). The output of each interval simulation given by MIA is compared with the outcome produced by MCS. The number of trials for the latter was increased until no significant changes in the upper and lower bounds were observed. Uncertainties in the MCS parameters were represented in terms of uniform probability distributions for comparison with MIA. Multiplicative congruential random generation was used to return successive pseudo-random numbers (Rubinstein and Kroese, 2007). A iterative program was implemented in C/C++ using the function rand(). To guarantee randomness between successive iterations, the seed of the rand() function is initialized at each loop using the srand() function and fixing the seed based on the system's clock. The MIA and MCS simulations were performed using Borland C++ Builder (version 6.0).

The results of the comparison of MIA and MCS show that the latter cannot guarantee that the actual response for a given model is within the set, leading to missed hypo- and hyperglycaemic events. A large computational effort might also be required when the number of uncertain parameters increases (Calm et al., 2011).

The library of interval models proposed in this work has been used in different studies within the projects INSULAID (Bondia and Vehí, 2007) and INSULAID2 (Bondia and Vehí, 2010). Some of these works have been presented by Calm et al. (2007a,b); Bondia et al. (2007); García-Jaramillo et al. (2009a); Bondia et al. (2009); García-Jaramillo et al. (2011a); Calm et al. (2011); Revert et al. (2011); Laguna (2010); García-Jaramillo et al. (2011b).

Currently, an application of the fault detection technique based on the interval model is being developed by the MICELab group in collaboration with the Institute of Biomedical Engineering of Imperial College London. This technique is used to detect erroneous continuous glucose sensor data and insulin infusion faults using retrospective data from a clinical experiment that tested a closed-loop controller.

4.3.1 Carbohydrate digestion and absorption interval models

The glucose absorption model includes uncertainties because patients generally do not know the exact size and composition of their meals, which they must estimate. The absorption time also depends on the patient and the meal composition, so it is also an approximation. Therefore, the amount of carbohydrate ingested, D (mg), is considered an interval.

The models considered here were presented in Section 4.1.1, and were formulated by Hovorka et al. (2004) and Dalla Man et al. (2006) to describe the glucose transit through the stomach and intestine.

Hovorka et al. model

In the model proposed by Hovorka et al. (2004), we consider the input D and the parameter A_G from Equation 4.1 as uncertain. By analysing the monotonic behaviour of Equation 4.1, it can be seen that the function $R_a(t)$ is monotonic increasing with respect to variables D and A_G. An optimal rational computation of the range for the glucose absorption rate, $R_a(t)$, can then be obtained with Equation 4.1:

$$R_{\mathrm{a}}(t) = \frac{D A_G t \exp(-t/t_{\mathrm{max},G})}{t^2_{\mathrm{max},G}}$$

When the parameter $t_{max,G}$ is considered to be uncertain, it is a multi-incident parameter and does not meet the monotonicity conditions of the optimality theorems of MIA. Therefore, an optimal rational computation of the range of the glucose absorption rate, $R_a(t)$, is not possible. Consequently, the f^* algorithm must be used to obtain tight upper and lower bounds for $R_a(t)$. For more information about the f^* algorithm, the reader is referred to Chapter 3.

Dalla Man et al. model

The model considered here is that described by Dalla Man et al. (2006). The Euler discrete time approximation of the glucose rate of appearance model (Equation 4.2) is given by:

$$\begin{aligned}
&Q_{sto}(t) = Q_{sto1}(t) + Q_{sto2}(t)\\
&Q_{sto1}(t+1) = Q_{sto1}(t)(1 - k_{max}\Delta t) + D\Delta t\\
&Q_{sto2}(t+1) = Q_{sto2}(t)(1 - k_{empt}(t, Q_{sto})\Delta t) + k_{max} Q_{sto1}(t)\Delta t\\
&Q_{gut}(t+1) = Q_{gut}(t)(1 - k_{abs}\Delta t) + k_{empt}(t, Q_{sto}) Q_{sto2}(t)\Delta t\\
&R_a(t) = \frac{f k_{abs} Q_{gut}(t)}{BW}
\end{aligned} \tag{4.26}$$

where

$$\begin{aligned}
k_{empt}(t, Q_{sto}) = k_{min} + \frac{k_{max} - k_{min}}{2} \Bigg[tanh\left(\alpha\left(\frac{Q_{sto}(t)}{D} - b\right)\right) -\\
- tanh\left(\beta\left(\frac{Q_{sto}(t)}{D} - c\right)\right) + 2\Bigg]
\end{aligned} \tag{4.27}$$

where α and β are constrained

$$\alpha = \frac{5}{2\,(1-b)}, \qquad \beta = \frac{5}{2\,c}$$

We consider uncertainty only in the input D because only this parameter verifies the monotonicity conditions for optimal computation by the optimality theorems of MIA. The uncertainty of this input causes the result of the interval computation of $Q_{sto1}(t+1)$ and $Q_{sto2}(t+1)$ to be an interval state. The monotonic behaviour of equations (4.26) are then studied with respect to the uncertain variable D to produce the optimal rational computation:

1. Monotony of state function $Q_{sto1}(t+1)$ respect to parameter D

$$\frac{\partial Q_{sto1}(t+1)}{\partial D} = \frac{\partial Q_{sto1}(t)}{\partial D}(1 - k_{max}\Delta t) + \Delta t > 0 \quad \Leftrightarrow \quad \Delta t < \frac{1}{k_{max}}$$

due to,

$$\begin{aligned}
&\frac{\partial Q_{sto1}(0)}{\partial D} = 0\\
&\frac{\partial Q_{sto1}(1)}{\partial D} = \Delta t > 0\\
&\frac{\partial Q_{sto1}(2)}{\partial D} = \Delta t(1-k_{max}) + \Delta t > 0\\
&\frac{\partial Q_{sto1}(3)}{\partial D} = \Delta t(1-k_{max})^2 + \Delta t(1-k_{max}) + \Delta t > 0\\
&\ldots\ldots\ldots\ldots\ldots\ldots\ldots\ldots\ldots\ldots\ldots\ldots\ldots\ldots\ldots\ldots\ldots\ldots\ldots\ldots
\end{aligned}$$

Then $Q_{sto1}(t+1)$ is monotonic increasing respect to D.

2. Monotony of state function $Q_{sto2}(t+1)$ respect to multi-incident parameter D

$$\begin{aligned}
&\frac{\partial Q_{sto2}(t+1)}{\partial D} = \frac{\partial Q_{sto2}(t)}{\partial D}(1-k_{empt}(t,Q_{sto})\Delta t) - Q_{sto2}(t)\left[\frac{k_{max}-k_{min}}{2}\right.\\
&\left.\frac{1}{D^2}\left(D\frac{\partial Q_{sto}(t)}{\partial D} - Q_{sto}(t)\right)\left(\frac{\alpha}{\cosh^2\left(\alpha(\frac{Q_{sto}(t)}{D}-b)\right)} - \frac{\beta}{\cosh^2\left(\beta(\frac{Q_{sto}(t)}{D}-c)\right)}\right)\right]\Delta t +\\
&+k_{max}\frac{\partial Q_{sto1}(t)}{\partial D}\Delta t > 0 \quad\Leftrightarrow\quad \Delta t < \frac{1}{k_{empt}(t,Q_{sto})}
\end{aligned}$$

Then $Q_{sto2}(t+1)$ is globally monotonous respect to D. The monotony of each incidence of every multi-incident component D is:

$$\begin{aligned}
&\frac{\partial Q_{sto2}(t+1)}{\partial D_1} = \left(\frac{k_{max}-k_{min}}{2}\right)\frac{\alpha Q_{sto}(t)}{D^2\cosh^2\left(\alpha(\frac{Q_{sto}(t)}{D}-b)\right)}Q_{sto2}(t)\Delta t > 0\\
&\frac{\partial Q_{sto2}(t+1)}{\partial D_2} = -\left(\frac{k_{max}-k_{min}}{2}\right)\frac{\beta Q_{sto}(t)}{D^2\cosh^2\left(\beta(\frac{Q_{sto}(t)}{D}-c)\right)}Q_{sto2}(t)\Delta t < 0
\end{aligned}$$

Therefore $Q_{sto2}(t+1)$ is totally monotonous respect to D.

3. Monotony of state function $Q_{sto2}(t+1)$ respect to $Q_{sto}(t)$

$$\begin{aligned}
&\frac{\partial Q_{sto2}(t+1)}{\partial Q_{sto}(t)} = 1 - k_{empt}(t,Q_{sto})\Delta t - Q_{sto2}(t)\left[\frac{k_{max}-k_{min}}{2}\right.\\
&\left.\left(\frac{\alpha/D}{\cosh^2\left(\alpha(\frac{Q_{sto}(t)}{D}-b)\right)} - \frac{\beta/D}{\cosh^2\left(\beta(\frac{Q_{sto}(t)}{D}-c)\right)}\right)\right]\Delta t > 0
\end{aligned}$$

Then $Q_{sto2}(t+1)$ is globally monotonous respect to $Q_{sto}(t)$. As in the previous item, the monotony of each incidence of $Q_{sto}(t)$ is studied:

$$\frac{\partial Q_{sto2}(t+1)}{\partial Q_{sto}(t)_1} = \left(\frac{k_{max}-k_{min}}{2}\right)\frac{\alpha/D}{\cosh^2\left(\alpha(\frac{Q_{sto}(t)}{D}-b)\right)}Q_{sto2}(t)\Delta t > 0$$
$$\frac{\partial Q_{sto2}(t+1)}{\partial Q_{sto}(t)_2} = -\left(\frac{k_{max}-k_{min}}{2}\right)\frac{\beta/D}{\cosh^2\left(\beta(\frac{Q_{sto}(t)}{D}-c)\right)}Q_{sto2}(t)\Delta t < 0$$

Thereby, $Q_{sto2}(t+1)$ is totally monotonous respect to $Q_{sto}(t)$.

Then, taking into account the theorem of coercion to optimality an optimal rational computation of R_a (Equation 4.26) is obtained by:

$$\begin{aligned}
&Q_{sto}(t) = Q_{sto1}(t) + Q_{sto2}(t)\\
&Q_{sto1}(t+1) = Q_{sto1}(t)(1-k_{max}\Delta t) + D\Delta t\\
&Q_{sto2}(t+1) = Q_{sto2}(t)(1-k_{empt}(t,Q_{sto})\Delta t) + k_{max}Q_{sto1}(t)\Delta t\\
&Q_{gut}(t+1) = Q_{gut}(t)(1-k_{abs}\Delta t) + k_{empt}(t,Q_{sto})Q_{sto2}(t)\Delta t\\
&R_a(t) = \frac{f k_{abs} Q_{gut}(t)}{BW}
\end{aligned} \tag{4.28}$$

where

$$\begin{aligned}
k_{empt}(t,Q_{sto}) = k_{min} + \frac{k_{max}-k_{min}}{2}\Bigg[&tanh\left(\alpha\left(\frac{\text{Dual}(Q_{sto}(t))}{D}-b\right)\right) -\\
&- tanh\left(\beta\left(\frac{Q_{sto}(t)}{\text{Dual}(D)}-c\right)\right)+2\Bigg]
\end{aligned} \tag{4.29}$$

As an illustration, MIA and MCS were compared when there was a 10% variation in a food intake of 80 g. The model parameters are taken from UVa simulator (patient 1) (Kovatchev et al., 2008). The envelopes obtained for MIA and the simulations obtained for MCS were indistinguishable (see Figure 4.13), because only one parameter was considered uncertain. However, 100 MCS trials were necessary to produce no significant changes in the upper and lower bounds. The number of trials increases in proportion to the number of uncertain parameters. However, MCS cannot guarantee that the actual response for a given model is within the bounds.

The computation time for MIA was 0.078 s, whereas that for MCS was 3.812 s. Thus, MIA took only 2.1% of the time required for MCS (a reduction of 97.9%).

4.3.2 Subcutaneous insulin absorption interval model

An optimality analysis of the three s.c. insulin absorption models described in Section 4.1.2 are examined here.

Hovorka et al.

Because the dose of insulin u is calculated based on meal planning and blood glucose monitoring, an error in the estimate can occur, as mentioned in Section 4.2. The insulin dose will then be

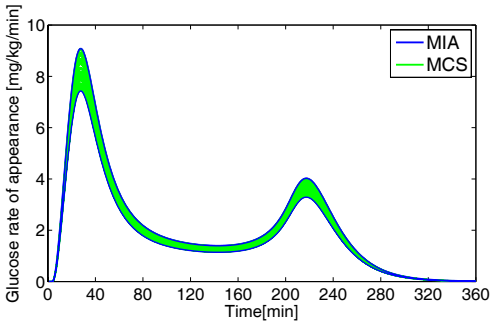

Figure 4.13: Glucose interval rate of appearance with 10% variation in food intake. The green lines indicate each simulation given with the MCS approach and the blue lines show the upper and lower bounds given by the MIA simulation.

uncertain. The Euler discrete time approximation of the subcutaneous insulin absorption model (Equation 4.4) is given by:

$$\begin{aligned} S_1(t+1) &= S_1(t) + \Delta t \left(u(t) - \frac{S_1(t)}{t_{max,I}} \right) \\ S_2(t+1) &= S_2(t) + \frac{\Delta t}{t_{max,I}} (S_1(t) - S_2(t)) \\ S(t) &= \frac{S_2(t)}{t_{max,I}} \end{aligned} \tag{4.30}$$

The only parameter that verifies the monotonicity conditions for optimal rational computation using MIA is the input u. An uncertain input u causes the results of the interval computations of $S_1(t+1)$ and $S_2(t+1)$ to be interval states. Therefore, the monotonic behaviour of Equation 4.30 is studied with respect to this uncertainty to obtain an optimal rational computation using MIA.

1. The function $S_1(t+1)$ is monotonic increasing respect to $u(t)$, since:

$$\frac{\partial S_1(t+1)}{\partial u(t)} = \frac{\partial S_1(t+1)}{\partial u(t)} \left(1 - \frac{\Delta t}{t_{max,I}} \right) + \Delta t > 0 \;\Leftrightarrow\; \Delta t < t_{max,I}$$

2. The function $S_1(t+1)$ is totally monotonous with respect to $S_1(t)$ according with the partial derivatives:

$$\begin{aligned} \frac{\partial S_1(t+1)}{\partial S_1(t)} &= 1 - \frac{\Delta t}{t_{max,I}} > 0 \;\Leftrightarrow\; \Delta t < t_{max,I} \\ \frac{\partial S_1(t+1)}{\partial S_1(t)_1} &= 1 > 0 \\ \frac{\partial S_1(t+1)}{\partial S_1(t)_2} &= -\frac{\Delta t}{t_{max,I}} < 0 \end{aligned}$$

The same study is performed to $S_2(t+1)$, which is totally monotonous with respect to $S_2(t)$.

Applying the theorem of coercion to optimality, the optimal rational computation of equations $S_1(t+1)$ and $S_2(t+1)$ is given by:

$$\begin{aligned} S_1(t+1) &= S_1(t) + \Delta t \left(u(t) - \frac{\text{Dual}(S_1(t))}{t_{max,I}} \right) \\ S_2(t+1) &= S_2(t) + \frac{\Delta t}{t_{max,I}} (S_1(t) - \text{Dual}(S_2(t))) \\ S(t) &= \frac{S_2(t)}{t_{max,I}} \end{aligned} \tag{4.31}$$

with the constraint $\Delta t < t_{max,I}$, so the time step Δt will be defined if this condition is satisfied.

A comparison of MIA and MCS for the bolus administration of 5 IU of insulin with 5% variation showed a reduction in the computation time of 98.33% for MIA with respect to 100 MCS trials (see Figure 4.14).

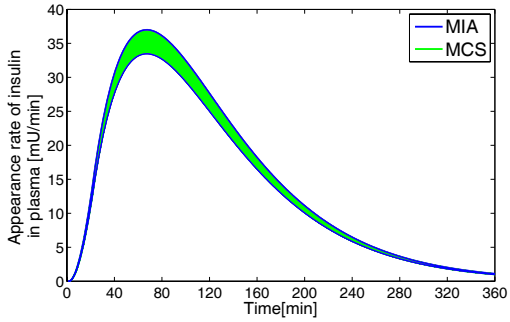

Figure 4.14: Envelopes of s.c. insulin absorption obtained for 5% variations in bolus insulin. The green lines indicate each simulation given with the MCS approach and the blue lines show the upper and lower bounds given by the MIA simulation.

Wilinska et al.

The model developed by Wilinska et al. (2005) is studied here to consider the presence of different sources of uncertainties. The Euler discrete time approximation of the insulin kinetics model (Equation 4.5) is analysed first. The discrete model is given by:

$$\begin{aligned} Q_{1a}(t+1) &= Q_{1a}(t) + \Delta t \left(k\ u(t) - k_{a1}\ Q_{1a}(t) - LD_a(t) \right) \\ Q_{1b}(t+1) &= Q_{1b}(t) + \Delta t \left((1-k)u(t) - k_{a2}\ Q_{1b}(t) - LD_b(t) \right) \\ Q_2(t+1) &= Q_2(t) + \Delta t \left(k_{a1} Q_{1a}(t) - k_{a1}\ Q_2(t) \right) \\ Q_3(t+1) &= Q_3(t) + \Delta t (k_{a1}\ Q_2(t) + k_{a2} Q_{1b}(t) - k_e\ Q_3(t)) \\ I(t) &= \frac{Q_3(t)}{V_i\ BW} \end{aligned} \tag{4.32}$$

Like the model of Hovorka et al., in the model developed by Wilinska et al. (2005), the insulin input u is considered a source of uncertainty. The parameter that represents the transfer rate k_e can also be considered uncertain. This is the only parameter that verifies the monotonicity

conditions for optimal rational computation using MIA.

By analysing the monotonic behaviour of the state functions $Q_{1a}(t+1)$ and $Q_{1b}(t+1)$ with respect to $u(t)$, and $Q_3(t+1)$ with respect to k_e, it can be seen that these state functions are monotonic, increasing with respect to each parameter evaluated.

The uncertainty in the input $u(t)$ and the parameter k_e causes that the results of the interval computation of all state functions will be interval states. For this reason, a study of the monotony of Equation 4.32 with respect to multi-incident variables is performed.

1. Monotony of state function $Q_{1a}(t+1)$ respect to $Q_{1a}(t)$

$$\frac{\partial Q_{1a}(t+1)}{\partial Q_{1a}(t)} = 1 + \Delta t \left(-k_{a1} - \frac{k_{M,LD} V_{MAX,LD}}{(k_{M,LD} + Q_{1a}(t))^2} \right) > 0 \;\Leftrightarrow\; \Delta t < \frac{1}{k_{a1} + \frac{k_{M,LD} V_{MAX,LD}}{(k_{M,LD} + Q_{1a}(t))^2}}$$

$$\frac{\partial Q_{1a}(t+1)}{\partial Q_{1a}(t)_1} = 1 > 0$$

$$\frac{\partial Q_{1a}(t+1)}{\partial Q_{1a}(t)_2} = -k_{a1} < 0$$

$$\frac{\partial Q_{1a}(t+1)}{\partial Q_{1a}(t)_3} = -\frac{V_{MAX,LD}}{k_{M,LD} + Q_{1a}(t)} < 0$$

$$\frac{\partial Q_{1a}(t+1)}{\partial Q_{1a}(t)_4} = \frac{V_{MAX,LD}\; Q_{1a}(t)}{(k_{M,LD} + Q_{1a}(t))^2} > 0$$

Then the function $Q_{1a}(t+1)$ is totally monotonous with respect to $Q_{1a}(t)$.

2. Monotony of state function $Q_{1b}(t+1)$ respect to $Q_{1b}(t)$

$$\frac{\partial Q_{1b}(t+1)}{\partial Q_{1b}(t)} = 1 + \Delta t \left(-k_{a2} - \frac{k_{M,LD} V_{MAX,LD}}{(k_{M,LD} + Q_{1b}(t))^2} \right) > 0 \;\Leftrightarrow\; \Delta t < \frac{1}{k_{a2} + \frac{k_{M,LD} V_{MAX,LD}}{(k_{M,LD} + Q_{1b}(t))^2}}$$

$$\frac{\partial Q_{1b}(t+1)}{\partial Q_{1b}(t)_1} = 1 > 0$$

$$\frac{\partial Q_{1b}(t+1)}{\partial Q_{1b}(t)_2} = -k_{a2} < 0$$

$$\frac{\partial Q_{1b}(t+1)}{\partial Q_{1b}(t)_3} = -\frac{V_{MAX,LD}}{k_{M,LD} + Q_{1b}(t)} < 0$$

$$\frac{\partial Q_{1b}(t+1)}{\partial Q_{1b}(t)_4} = \frac{V_{MAX,LD}\; Q_{1b}(t)}{(k_{M,LD} + Q_{1b}(t))^2} > 0$$

Then the function $Q_{1b}(t+1)$ is totally monotonous with respect to $Q_{1b}(t)$.

3. Monotony of state function $Q_2(t+1)$ respect to $Q_2(t)$

$$\frac{\partial Q_2(t+1)}{\partial Q_2(t)} = 1 - \Delta t\ k_{a1} > 0 \ \Leftrightarrow \quad \Delta t < \frac{1}{k_{a1}}$$
$$\frac{\partial Q_2(t+1)}{\partial Q_2(t)_1} = 1 > 0$$
$$\frac{\partial Q_2(t+1)}{\partial Q_2(t)_2} = -\Delta t\ k_{a1} < 0$$

Then the function $Q_2(t+1)$ is totally monotonous with respect to $Q_2(t)$.

4. Monotony of state function $Q_3(t+1)$ respect to $Q_3(t)$

$$\frac{\partial Q_3(t+1)}{\partial Q_3(t)} = 1 - \Delta t k_e > 0 \ \Leftrightarrow \quad \Delta t < \frac{1}{k_e}$$
$$\frac{\partial Q_3(t+1)}{\partial Q_3(t)_1} = 1 > 0$$
$$\frac{\partial Q_3(t+1)}{\partial Q_3(t)_2} = -\Delta t\ k_e < 0$$

Hence, the function $Q_3(t+1)$ is totally monotonous with respect to $Q_3(t)$.

Applying the theorem of coercion to optimality, the rational computation of the model equations is:

$$\begin{aligned}
Q_{1a}(t+1) &= Q_{1a}(t) + \Delta t \left(k\ u(t) - k_{a1}\ \text{Dual}(Q_{1a}(t)) - \frac{V_{MAX,LD}\ \text{Dual}(Q_{1a}(t))}{k_{M,LD} + Q_{1a}(t)} \right) \\
Q_{1b} &= Q_{1b} + \Delta t \left((1-k)u(t) - k_{a2}\ \text{Dual}(Q_{1b}(t)) - \frac{V_{MAX,LD}\ \text{Dual}(Q_{1b}(t))}{k_{M,LD} + Q_{1b}(t)} \right) \\
Q_2(t+1) &= Q_2(t) + \Delta t(k_{a1}\ Q_{1a}(t) - k_{a1}\text{Dual}(Q_2(t))) \\
Q_3(t+1) &= Q_3(t) + \Delta t(k_{a1}\ Q_2(t) + k_{a2}\ Q_{1b}(t) - k_e\ \text{Dual}(Q_3(t))) \\
I(t) &= \frac{Q_3(t)}{V_i\ BW}
\end{aligned} \tag{4.33}$$

The time step Δt will be defined so that constraint holds.

$$\Delta t < \min \left(\frac{1}{k_{a2} + \frac{k_{M,LD}\ V_{MAX,LD}}{(k_{M,LD} + Q_{1b}(t))^2}}, \frac{1}{k_{a1} + \frac{k_{M,LD}\ V_{MAX,LD}}{(k_{M,LD} + Q_{1a}(t))^2}}, \frac{1}{k_e} \right)$$

The comparison of MIA and MCS for an infusion of 5 IU of insulin for 15 min, with 5% variation in the insulin dose and a transfer rate of k_e, demonstrates a computation time reduction of 99.6% for MIA with respect to 500 MCS trials (see Figure 4.15). The model parameters used were taken from Wilinska et al. (2005).

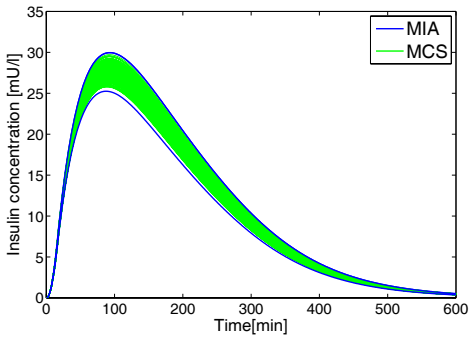

Figure 4.15: Envelopes of s.c. insulin absorption obtained for a 5% variation in bolus insulin and a 5% variation in the transfer rate k_e. The green lines indicate each simulation given with the MCS approach and the blue lines show the upper and lower bounds given by the MIA simulation.

Dalla Man et al.

The third model of subcutaneous insulin absorption studied here was proposed by Dalla Man et al. (2007a). The Euler discrete time approximation model that represents subcutaneous insulin absorption (Equation 4.6) is given by:

$$\begin{aligned} S_1(t+1) &= S_1(t) + \Delta t(u(t) - (k_d + k_{a1})S_1(t)) \\ S_2(t+1) &= S_2(t) + \Delta t(k_d\ S_1(t) - k_{a2}\ S_2(t)) \\ S(t) &= k_{a1}\ S_1(t) + k_{a2}\ S_2(t) \end{aligned} \tag{4.34}$$

Uncertainty in the insulin input u is considered by this model. To obtain an optimal rational computation of Equation 4.34, its monotonic behaviour is studied with respect to this uncertain input.

So, $S_1(t+1)$ is monotonic increasing with respect to the input $u(t)$, since:

$$\frac{\partial S_1(t+1)}{\partial u(t)} = \frac{\partial S_1(t+1)}{\partial u(t)}(1 - \Delta t(k_d + k_{a1})) + \Delta t > 0 \ \Leftrightarrow \ \ \Delta t < \frac{1}{k_{a1} + k_d}$$

Because of the uncertainty in the input $u(t)$, the states $S_1(t+1)$ and $S_2(t+1)$ will be interval states. Therefore, the monotonic behaviour of the state functions $S_1(t+1)$ and $S_2(t+1)$ are studied with respect to $S_1(t)$ and $S_2(t)$, respectively.

The function $S_1(t+1)$ is totally monotonous with respect to $S_1(t)$ if:

$$\Delta t < \left(\frac{1}{k_{a1} + k_d}\right)$$

because the partial derivative with respect to $S_1(t)$ is given by:

$$\frac{\partial S_1(t+1)}{\partial S_1(t)} = 1 + \Delta t(-(k_{a1} + k_d)) > 0 \;\Leftrightarrow\; \Delta t < \frac{1}{k_{a1} + k_d}$$
$$\frac{\partial S_1(t+1)}{\partial S_1(t)_1} = 1 > 0$$
$$\frac{\partial S_1(t+1)}{\partial S_1(t)_2} = -(k_{a1} + k_d) < 0$$

and similar reasoning applies to $S_2(t+1)$, which is totally monotonous with respect to $S_2(t)$:

$$\frac{\partial S_2(t+1)}{\partial S_2(t)} = 1 - \Delta t\, k_{a2} > 0 \;\Leftrightarrow\; \Delta t < \frac{1}{k_{a2}}$$
$$\frac{\partial S_2(t+1)}{\partial S_2(t)_1} = 1 > 0$$
$$\frac{\partial S_2(t+1)}{\partial S_2(t)_2} = -k_{a2} < 0$$

Applying the theorem of coercion to optimality, an optimal rational computation of Equation 4.34, is given by:

$$\begin{aligned} S_1(t+1) &= S_1(t) + \Delta t\ (u(t) - (k_d + k_{a1})\text{Dual}(S_1(t))) \\ S_2(t+1) &= S_2(t) + \Delta t\ (k_d\ S_1(t) - k_{a2}\ \text{Dual}(S_2(t))) \\ S(t) &= k_{a1}\ S_1(t) + k_{a2}\ S_2(t) \end{aligned} \tag{4.35}$$

with the constraint:

$$\Delta t < \min\left(\frac{1}{k_{a1} + k_d}, \frac{1}{k_{a2}}\right) \tag{4.36}$$

To validate the MIA approach, different MCSs were performed for the infusion of 5 IU of insulin in 15 min with 5% variation. Using MIA, a computation time reduction of 98.7% was obtained with respect to 100 MCS trials, as can be seen in Figure 4.16. The model parameters used were taken from Dalla Man et al. (2007a).

4.3.3 Insulin action and glucose kinetics interval model

Because insulin sensitivity exhibits circadian variations in its intensity depending on the patient, the parameters that represent these sensitivities are likely to be uncertain. To examine this, the four insulin action and glucose kinetics models presented in Section 4.1.3 and proposed by Bergman et al. (1981), Hovorka et al. (2004), Dalla Man et al. (2007b), and Panunzi et al. (2007) are studied here, taking into account the uncertainty in the parameter of insulin sensitivity.

Bergman et al.

The model considered here is that described by Bergman et al. (1981) and modified by Roy and Parker (2007). In this model, we consider uncertainty in all the parameters of the model: p_1, p_2, p_3, p_4, and n. The parameters corresponding to insulin sensitivity are p_2 and p_3.

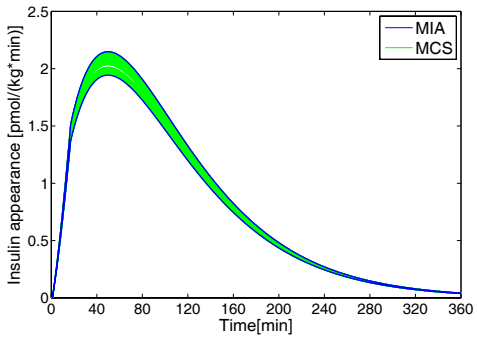

Figure 4.16: Envelopes of s.c. insulin absorption obtained for 5% variation in the insulin infusion. The green lines indicate each simulation given with the MCS approach and the blue lines show the upper and lower bounds given by the MIA simulation.

Taking into account these uncertainties, the monotonic behaviour of the insulin dynamics and insulin action models presented by Roy and Parker (2007) is studied first.

1. Monotony of state function $I(t+1)$ with respect to n:

$$\frac{\partial I(t+1)}{\partial n} = \frac{\partial I(t)}{\partial n}(1 - \Delta t\, n) - \Delta t\, I(t) < 0 \;\Leftrightarrow\quad \Delta t < \frac{1}{n}$$

   Then $I(t+1)$ is monotonic decreasing with respect to n.

2. Monotony of state function $I(t+1)$ with respect to p_4:

$$\frac{\partial I(t+1)}{\partial p_4} = \frac{\partial I(t)}{\partial p_4}(1 - \Delta t\, n) + \Delta t\, S(t) > 0 \;\Leftrightarrow\quad \Delta t < \frac{1}{n}$$

   Hence $I(t+1)$ is monotonic increasing with respect to p_4.

3. Now the monotony of insulin action model is studied. Monotony of state function $X(t+1)$ with respect to parameter p_2:

$$\frac{\partial X(t+1)}{\partial p_2} = \frac{\partial X(t)}{\partial p_2}(1 - \Delta t\, p_2) - \Delta t\, X(t)\, p_2 < 0 \;\Leftrightarrow\quad \Delta t < \frac{1}{n}$$

   Then $X(t+1)$ is monotonic decreasing with respect to p_2.

4. Monotony of state function $X(t+1)$ with respect to p_3:

$$\frac{\partial X(t+1)}{\partial p_3} = \frac{\partial X(t)}{\partial p_3}(1 - \Delta t\, p_2) + \Delta t\, (I(t) - I_b) > 0 \;\Leftrightarrow\quad \Delta t < \frac{1}{p_2}$$

   Then $X(t+1)$ is monotonic increasing with respect to p_3.

According to this study, and taking into account that the insulin dynamics and insulin action models do not have multi-incident variables, a rational calculation can be performed with its Euler discrete model:

$$\begin{aligned} I(t+1) &= I(t)\,(1 - \Delta t\, n) + \Delta t\, p_4\, S(t) \\ X(t+1) &= X(t)\,(1 - \Delta t\, p_2) + \Delta t\, p_3 (I(t) - I_b) \end{aligned} \tag{4.37}$$

Next, the glucose metabolism model (Equation 4.7) is evaluated, considering the uncertainties mentioned above. The Euler discrete time approximation of the glucose metabolism model is given by:

$$G(t+1) = \Delta t\ p_1(G_b - G(t)) + G(t)(1 - \Delta t\ X(t)) + \frac{R_a(t)}{V_g}\Delta t \tag{4.38}$$

In this case, the monotonic behaviour of Equation 4.38 is studied with respect to the uncertain parameter p_1. This uncertainty also causes that the result of the interval computation of state $G(t+1)$ to be an interval state, so the monotonic behaviour of $G(t+1)$ with respect to $G(t)$ is also evaluated.

1. Monotony of state function $G(t+1)$ respect to $G(t)$:

$$\frac{\partial G(t+1)}{\partial p_1} = \Delta t(G_b - G(t)) + \frac{\partial G(t)}{\partial p_1}(1 - \Delta t(p_1 + X(t))) < 0 \ \Leftrightarrow \ \ \Delta t < \frac{1}{p_1 + X(t)}$$

   Then $G(t+1)$ is monotonic increasing respect to p_1.

2. Monotony of state function $G(t+1)$ respect to each incidence of $G(t)$:

$$\frac{\partial G(t+1)}{\partial G(t)} = -\Delta t\ p_1 + (1 - \Delta t\ X(t)) > 0 \quad \Leftrightarrow\ \Delta t < \frac{1}{p_1 + X(t)}$$

$$\frac{\partial G(t+1)}{\partial G(t)_1} = -\Delta t\ p_1 < 0$$
$$\frac{\partial G(t+1)}{\partial G(t)_2} = 1 - \Delta t\ X(t) > 0$$

   The function $G(t+1)$ is totally monotonous with respect to $G(t)$.

Finally, applying the theorem of coercion to optimality to plasma glucose concentration $G(t+1)$ (Equation 4.38) the rational computation is given by:

$$G(t+1) = \Delta t\ p_1(G_b - \text{Dual}(G(t))) + G(t)\ (1 - \Delta t\ X(t)) + \frac{\Delta t\ R_a(t)}{V_g} \tag{4.39}$$

The time step Δt is defined so that $\Delta t < \frac{1}{p_1 + X(t)}$ in order to verify the monotonic conditions.

Different simulations were performed, considering variations in the parameters p_1, p_2, p_3, n, and food intake to validate the model. A general scenario was considered: capillary blood glucose 81 mg/dL, 5 IU of bolus insulin, and 60 g of food intake. The following models were combined to represent the glucoregulatory model:

- For subcutaneous insulin absorption: Tarin et al. model (Tarín et al., 2005)

- For carbohydrate digestion and absorption: Hovorka et al. interval model proposed in Section 4.3.1
- For insulin action and glucose kinetics: Bergman et al. interval model (Section 4.3.3).

Blood glucose was predicted using MIA and MCS, considering variations of 5% in food intake and 10% in the fractional clearance of insulin (n). Figure 4.17 shows the comparison of the two methods.

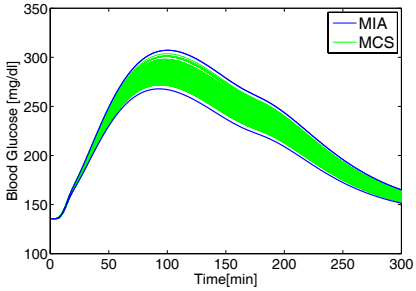

Figure 4.17: Envelopes of blood glucose obtained for 5% variations in food intake and the fractional clearance of insulin and 10% variations in the parameters of the glucose kinetics model. The green lines indicate each simulation given with the MCS approach and the blue lines show the upper and lower bounds given by the MIA simulation.

In Figure 4.18, the MIA and MCS approaches are shown with variations of 5% in D and 10% in p_2 and p_3, with 500 trials performed for MCS. The magenta dashed line illustrates the MCS approach, considering the same uncertainty but taking the lower bound of p_2. In this figure, it can be seen that this case is not included in the MCS obtained beforehand.

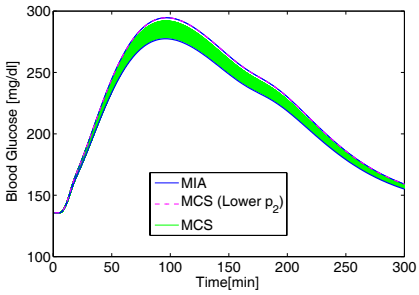

Figure 4.18: Envelopes of blood glucose obtained for 5% variation in food intake and 10% variations in p_2 and p_3. The green lines indicate each simulation given by the MCS approach and the blue lines show the upper and lower bounds given by the MIA simulation. The magenta dashed line indicates the MCS approach considering the lower bound of p_2.

Hovorka et al.

The presence of different sources of uncertainty in the model described by Hovorka et al. (2004) is now examined. First, the monotonic behaviour of the PK model 4.12 is evaluated, considering

uncertainty in k_e. As a result, the function $I(t)$ is monotonic, decreasing with respect to k_e because:

$$\frac{\partial I(t+1)}{\partial k_e} = \frac{\partial I(t)}{\partial k_e}(1 - \Delta t\ k_e) - I(t)\Delta t < 0 \Leftrightarrow \quad \Delta t < \frac{1}{k_e}$$

Therefore, a rational calculation can be performed with its Euler discrete model:

$$I(t+1) = \frac{\Delta t S(t)}{V_i} + (1 - \Delta t k_e) I(t) \tag{4.40}$$

The PD model 4.11 is a more complex interval model because many parameters are uncertain. The initial states of the effects of insulin on glucose, $X_i(0)$, $i = 1, \ldots, 3$, and the sensitivity parameters S_{IT}, S_{ID}, and S_{IE} are uncertain and they are considered as intervals. The Euler discrete time approximation of the insulin PD model is given by:

$$\begin{aligned} X_1(t+1) &= (1 - \Delta t k_{a1}) X_1(t) + \Delta t k_{a1} S_{IT}\ I(t) \\ X_2(t+1) &= (1 - \Delta t k_{a2}) X_2(t) + \Delta t k_{a2} S_{ID}\ I(t) \\ X_3(t+1) &= (1 - \Delta t k_{a3}) X_3(t) + \Delta t k_{a3} S_{IE}\ I(t) \end{aligned} \tag{4.41}$$

According to MIA, this model is optimal because the insulin sensitivities and the initial states appear only once in each equation. Because this is an interval computation, the states $X_1(t+1)$, $X_2(t+1)$, and $X_3(t+1)$ will be interval states (Calm et al., 2007a).

In contrast, the interval output of the carbohydrate digestion and absorption subsystem, as well as the computed interval states from the insulin subsystem, $X_i(t)$, $i = 1, 2, 3$, will be interval inputs in the glucose subsystem. Therefore, even if no uncertainty is considered for the glucose subsystem, it becomes an interval model, and interval methods must be used to compute its evolution.

The Euler discrete time approximation of the glucose metabolism model (Equation 4.8) is given by:

$$\begin{aligned} Q_1(t+1) &= Q_1(t)(1 - \Delta t\ X_1(t)) + \Delta t\ k_{12}\ Q_2(t) - \Delta t(F_{01}^c(t) + F_R(t)) + \\ &\quad + \Delta t(R_a(t) + \mathrm{EGP}_0(1 - X_3(t))) \\ Q_2(t+1) &= \Delta t\ X_1(t) Q_1(t) + Q_2(t)(1 - \Delta t(k_{12} + X_2(t))) \\ G(t) &= \frac{Q_1(t)}{V_g} \end{aligned} \tag{4.42}$$

From total non-insulin-dependent glucose disposal, $F_{01}^c(t)$, and the renal glucose clearance $F_R(t)$, defined by Equations 4.9 and 4.10 respectively, the sum function is considered:

$$F_{01}^c(t) + F_R(t) = \begin{cases} \dfrac{f_{01} Q_1(t)}{4.5 V_g} & \text{if} \quad Q_1(t) < 4.5 V_g \\ f_{01} & \text{if} \quad 4.5 V_g \leq Q_1(t) \leq 9 V_g \\ 0.003\ Q_1(t) - 0.027 V_g + f_{01} & \text{if} \quad Q_1(t) > 9 V_g \end{cases}$$

From the sum function two new constant functions $FC(t)$ and $FR(t)$ are defined as:

$$FC(t) = \begin{cases} \dfrac{f_{01}}{4.5V_g} & \text{if} \quad Q_1(t) < 4.5V_g \\ 0 & \text{if} \quad 4.5V_g \leq Q_1(t) \leq 9V_g \\ 0.003 & \text{if} \quad Q_1(t) > 9V_g \end{cases} \tag{4.43}$$

$$FR(t) = \begin{cases} 0 & \text{if} \quad Q_1(t) < 4.5V_g \\ f_{01} & \text{if} \quad 4.5V_g \leq Q_1(t) \leq 9V_g \\ -0.027V_g + f_{01} & \text{if} \quad Q_1(t) > 9V_g \end{cases} \tag{4.44}$$

so that $F_{01}^c(t) + F_R(t) = FC(t)Q_1(t) + FR(t)$. Then, Equation (4.42) can be rewritten as:

$$\begin{aligned} Q_1(t+1) &= Q_1(t)(1 - \Delta t(X_1(t) + FC(t))) + \Delta t\, k_{12}\, Q_2(t) + \\ &\quad + \Delta t(R_a(t) + \mathrm{EGP}_0(1 - X_3(t)) - FR(t)) \\ Q_2(t+1) &= \Delta t\, X_1(t)\, Q_1(t) + Q_2(t)(1 - \Delta t(k_{12} + X_2(t))) \\ G(t) &= \frac{Q_1(t)}{V_g} \end{aligned} \tag{4.45}$$

Using MIA, the monotonic behaviour of Equation (4.45) is studied with respect to uncertain parameters (S_{ID}, S_{IE}, and S_{IT}) to obtain an optimal rational computation.

The $Q_1(t+1)$ and $Q_2(t+1)$ state functions are monotonic with respect to S_{ID} and S_{IE} if

$$\Delta t < \min\left(\frac{1}{X_1(t) + FC(t)}, \frac{1}{k_{12} + X_2(t)}\right)$$

because the partial derivative with respect to S_{ID} is given by:

$$\begin{aligned} \frac{\partial Q_1(t+1)}{\partial S_{ID}} &= (1 - \Delta t(X_1(t) + FC(t)))\frac{\partial Q_1(t)}{\partial S_{ID}} + \Delta t k_{12}\frac{\partial Q_2(t)}{\partial S_{ID}} < 0 \quad \Leftrightarrow \\ &\Leftrightarrow \quad \Delta t < \frac{1}{X_1(t) + FC(t)} \\ \frac{\partial Q_2(t+1)}{\partial S_{ID}} &= \Delta t X_1(t)\frac{\partial Q_1(t)}{\partial S_{ID}} - \frac{\partial X_2(t)}{\partial S_{ID}}Q_2(t)\Delta t + \\ &\quad + (1 - \Delta t(k_{12} + X_2(t)))\frac{\partial Q_2(t)}{\partial S_{ID}} < 0 \quad \Leftrightarrow \quad \Delta t < \frac{1}{k_{12} + X_2(t)} \end{aligned}$$

and similar reasoning for S_{IE}. But $Q_1(t+1)$ and $Q_2(t+1)$ are not monotonic with respect to the multi-incident variable S_{IT}, because the sign of their partial derivatives are not defined,

$$\begin{aligned} \frac{\partial Q_1(t+1)}{\partial S_{IT}} &= -\Delta t\frac{\partial X_1(t)}{\partial S_{IT}}Q_1(t) + (1 - \Delta t(X_1(t) + FC(t)))\frac{\partial Q_1(t)}{\partial S_{IT}} + \Delta t k_{12}\frac{\partial Q_2(t)}{\partial S_{IT}} \\ \frac{\partial Q_2(t+1)}{\partial S_{IT}} &= \Delta t\frac{\partial X_1(t)}{\partial S_{IT}}Q_1(t) + \Delta t X_1(t)\frac{\partial Q_1(t)}{\partial S_{IT}} + (1 - \Delta t(k_{12} + X_2(t)))\frac{\partial Q_2(t)}{\partial S_{IT}} \end{aligned}$$

A new state function $S(t) = Q_1(t) + Q_2(t)$ is defined to obtain monotonic behaviour with respect to the variable S_{IT}. The model in the new state function is:

$$\begin{aligned} Q_1(t+1) &= (1 - \Delta t(k_{12} + X_1(t) + FC(t)))Q_1(t) + \Delta t k_{12} S(t) + \Delta t A(t) \\ S(t+1) &= \Delta t(X_2(t) - FC(t))Q_1(t) + (1 - \Delta t x_2(t))S(t) + \Delta t A(t) \\ G(t) &= \frac{Q_1(t)}{V_g} \end{aligned} \tag{4.46}$$

where $A(t) := R_a(t) + \mathrm{EGP}_0(1 - X_3(t)) - FR(t)$.

In Equation 4.46 the state function $S(t)$ is monotonic with respect to S_{ID} and S_{IE} because $Q_1(t)$ and $Q_2(t)$ are monotonic. Furthermore, $Q_1(t)$ and $S(t)$ are also monotonic with respect to S_{IT}, if $X_2(t) - FC(t) > 0$ and

$$\Delta t < \min\left(\frac{1}{k_{12} + X_1(t) + FC(t)}, \frac{1}{k_{12} + X_2(t)}\right)$$

because:

$$\begin{aligned} \frac{\partial Q_1(t+1)}{\partial S_{IT}} &= -\Delta t \frac{\partial X_1(t)}{\partial S_{IT}} Q_1(t) + (1 - \Delta t(k_{12} + X_1(t) + FC(t)))\frac{\partial Q_1(t)}{\partial S_{IT}} + \\ &\quad + \Delta t k_{12} \frac{\partial S(t)}{\partial S_{IT}} < 0 \quad \Leftrightarrow \quad \Delta t < \frac{1}{k_{12} + X_1(t) + FC(t)} \end{aligned}$$

$$\begin{aligned} \frac{\partial S(t+1)}{\partial S_{IT}} &= \Delta t(X_2(t) - FC(t))\frac{\partial Q_1(t)}{\partial S_{IT}} + (1 - \Delta t X_2(t))\frac{\partial S(t)}{\partial S_{IT}} < 0 \\ &\quad \Leftrightarrow \quad X_2(t) - FC(t) > 0 \end{aligned}$$

Because of the monotonic behaviour of the model Equations 4.46 with respect to uncertain variables, it is possible to obtain an optimal rational computation. To simplify the computation, the equations 4.46 are rewritten as:

$$\begin{aligned} Q_1(t+1) &= (1 - \Delta t(k_{12} + X_1(t)))Q_1(t) - \Delta t(F_{01}^c(t) + F_R(t)) + \\ &\quad + \Delta t\ k_{12} S(t) + \Delta t B(t) \\ S(t+1) &= \Delta t X_2(t) Q_1(t) - \Delta t(F_{01}^c(t) + F_R(t)) + \\ &\quad + (1 - \Delta t X_2(t))\ S(t) + \Delta t B(t) \\ G(t) &= \frac{Q_1(t)}{V_g} \end{aligned} \tag{4.47}$$

where $B(t) := R_a(t) + \mathrm{EGP}_0(1 - X_3(t))$.

Applying the theorem of coercion to optimality, the optimal rational computation for the equations of the model 4.47 are:

$$\begin{aligned} Q_1(t+1) &= Q_1(t)(1 - \Delta t(k_{12} + X_1(t))) - \Delta t(\mathrm{Dual}(F_{01}^c(t)) + \mathrm{Dual}(F_R(t))) + \\ &\quad + \Delta t k_{12} S(t) + \Delta t\ B(t) \\ S(t+1) &= \Delta t\ \mathrm{Dual}(X_2(t)) Q_1(t) - \Delta t(\mathrm{Dual}(F_{01}^c(t)) + \mathrm{Dual}(F_R(t))) + \\ &\quad + S(t)(1 - \Delta\ t X_2(t)) + \Delta t\ B(t) \\ G(t) &= \frac{Q_1(t)}{V_g} \end{aligned} \tag{4.48}$$

with the constraints:

$$\Delta t < \min\left(\frac{1}{k_{12} + X_1(t) + FC(t)}, \frac{1}{k_{12} + X_2(t)}\right)$$
$$X_2(t) - FC(t) > 0 \tag{4.49}$$

The $F_{01}^c(t)$ and $F_R(t)$ functions are monotonic increasing with respect to $Q_1(t)$, then they can be computed as function of the interval bounds. Therefore,

$$F_{01}^c(t) = \left[\underline{F_{01}^c(t)}, \overline{F_{01}^c(t)}\right]$$
$$F_R(t) = \left[\underline{F_R(t)}, \overline{F_R(t)}\right]$$

where

$$\underline{F_{01}^c(t)} = \begin{cases} \dfrac{f_{01}\underline{Q_1(t)}}{4.5V_g} & \text{if } \underline{Q_1(t)} < 4.5V_g \\ f_{01} & \text{if } \underline{Q_1(t)} \geq 4.5V_g \end{cases}$$

$$\overline{F_{01}^c(t)} = \begin{cases} \dfrac{f_{01}\overline{Q_1(t)}}{4.5V_g} & \text{if } \overline{Q_1(t)} < 4.5V_g \\ f_{01} & \text{if } \overline{Q_1(t)} \geq 4.5V_g \end{cases}$$

and

$$\underline{F_R(t)} = \begin{cases} 0 & \text{if } \underline{Q_1(t)} < 9V_g \\ 0.003\underline{Q_1(t)} - 0.027V_g & \text{if } \underline{Q_1(t)} \geq 9V_g \end{cases}$$

$$\overline{F_R(t)} = \begin{cases} 0 & \text{if } \overline{Q_1(t)} < 9V_g \\ 0.003\overline{Q_1(t)} - 0.027V_g & \text{if } \overline{Q_1(t)} \geq 9V_g \end{cases}$$

The state function $Q_2(t)$ can be obtained from $S(t)$ as:

$$Q_2(t+1) = S(t+1) - \text{Dual}(Q_1(t+1))$$

The time step Δt will be defined so that condition (Equation 4.49) holds. If condition (Equation 4.49) does not hold, the interval model (Equation 4.48) may lead to overestimation.

To run the interval simulation for the whole system, the initial states and inputs must be given. Because not all the states are measurable (in fact, only capillary glucose measurements will be available), the initial state must be estimated. This is done by simulating the past history of the patient in terms of insulin injections and meals. Because there is uncertainty, the initial state will correspond to an interval vector.

In equilibrium state, the initial masses of glucose in the two compartments are:

$$Q_1(0) = G(0)V_g$$
$$Q_2(0) = \frac{\text{Dual}(X_1(0))\ Q_1(0)}{k_{12} + X_2(0)} \tag{4.50}$$

where $G(0)$ represents the (measurable) initial glucose concentration.

A comparison of MIA and MCS in the prediction of postprandial glucose under uncertainty in type 1 diabetes mellitus has been made using this model (Calm et al., 2011). In the present study, the models presented in Tarín et al. (2005) for subcutaneous insulin absorption and the interval model of Hovorka et al. for the other components of the model have been combined to represent the glucoregulatory model. The model parameters used for the components of the last model are taken from Hovorka et al. (2002) (patient 2). The simulations were performed for a 6 h period after a meal, considering the scenarios given in Table 4.1.

Scenario	Capillary blood glucose (mg/dL)	Insulin bolus (IU)	Carbohydrate (g)	Variation in carbohydrate (%)	Variation in insulin sensitivity (%)
scenario 1	80	5.5	60	10	0
scenario 2	250	6.5	60	0	10 (S_{IT}, S_{ID})
scenario 3	150	7.0	70	10	8 (S_{IT}, S_{ID}, S_{IE})
scenario 4	150	7.0	77	0	8 (S_{IT}, S_{ID}, S_{IE})

Table 4.1: Simulation scenarios for the interval model of Hovorka *et al.*.

Figures 4.19–4.22 show the upper and lower bounds for plasma glucose for the different scenarios. The total simulation time for each scenario is reported in Table 4.2. The computation time is drastically reduced by using MIA rather than MCS.

Scenario	Number of trials	MCS time(sec)	MIA time (sec)	Time reduction	Figure
scenario 1	1000	31.32	4.73	84.9%	Figure 4.19
scenario 2	1000	34	4.33	87.3%	Figure 4.20
scenario 3	10000	275	4.58	98.3%	Figure 4.21
scenario 4	10000	268	5	98.1%	Figure 4.22

Table 4.2: Simulation time for a 6-hour period after a meal for different scenarios.

Figure 4.19 shows the results for scenario 1, in which only the uncertainty in the amount of carbohydrate ingested, D, was considered.

The envelopes obtained with MIA and MCS are indistinguishable. However, 1000 MCS trials were required to achieve this result. From a computational perspective, MIA took only 15.1% of the time required for MCS (a reduction of 84.9%). The same conclusion can be drawn from Figure 4.20 for the results for scenario 2, with uncertainty in transport (S_{IT}) and peripheral insulin sensitivity (S_{ID}).

As the number of uncertain parameters increases, a considerable increase in the number of MCS trials is required to obtain good estimates of the envelopes, with a consequent increase in the computational effort. This is not the case for MIA because the computation time does not vary with the number of uncertain parameters. This can be observed in Table 4.2. The MIA computation time was only 1.7% of the MCS time for scenario 3 and only 1.9% for scenario 4. Besides the increase in computational effort, there is no guarantee that the MCS-computed envelope includes all possible trajectories for the uncertainty considered. This can be observed

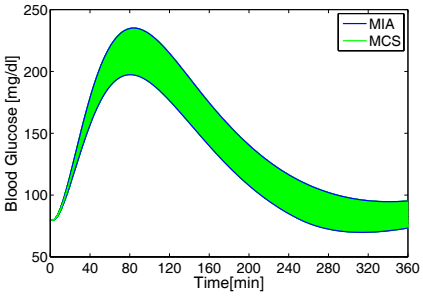

Figure 4.19: Envelopes of blood glucose obtained for 10% variation in $D = 60$ and 0% variation in insulin sensitivity (scenario 1). The green lines indicate each simulation given with the MCS approach and the blue lines show the upper and lower bounds given by the MIA simulation.

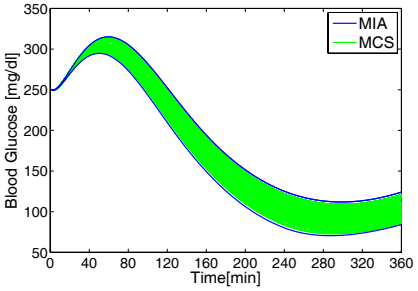

Figure 4.20: Envelopes of blood glucose obtained for $D = 60$ and 10% variation in hepatic and peripheral insulin sensitivity (scenario 2). The green lines indicate each simulation given with the MCS approach and the blue lines show the upper and lower bounds given by the MIA simulation.

in Figures 4.21 and 4.22.

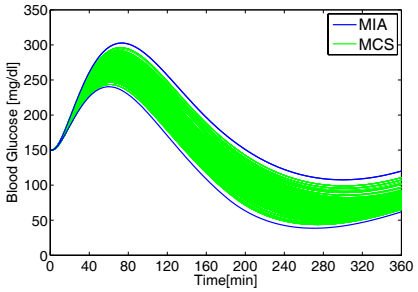

Figure 4.21: Envelopes of blood glucose obtained for 10% variation in $D = 70$ and 8% variation in insulin sensitivity (scenario 3). The green lines indicate each simulation given with the MCS approach and the blue lines show the upper and lower bounds given by the MIA simulation.

The results for MCS with 10,000 trials with a 10% variation in D are shown in Figure 4.21, and Figure 4.22(a) shows the MCS results considering the upper D band, i.e., D=77$\in$[63,77]. It can be seen that this case is not included in the MCS with D=[63,77]. Figure 4.22(b) shows a magnification of the boxed zone in Figure 4.22(a).

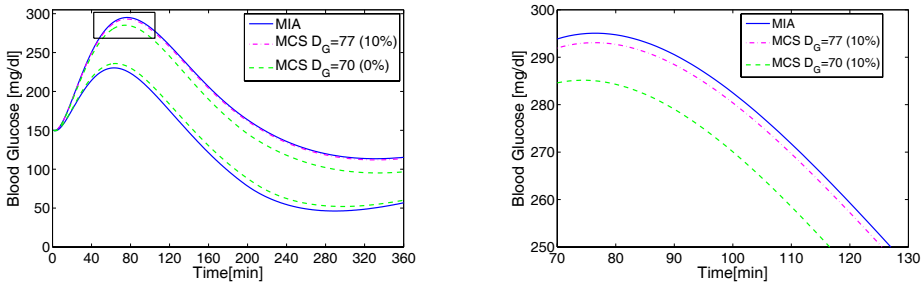

(a) (b)

Figure 4.22: (a) Envelopes obtained for $D = 77$ and 8% variation in insulin sensitivity with scenario 4 compared with those for scenario 3 (b) Magnification of rectangle (Fig. 4.22(a)).

Dalla Man et al.

Each subsystem of the model proposed by Dalla Man et al. (2007b) was studied to obtain optimal interval computations when uncertainty in different parameters was considered. For this model, the parameters related to insulin sensitivity were k_{p3}, V_{mx}, and V_{m0}, which are therefore considered interval parameters. The parameters k_i and p_{2U}, which are related to insulin action, are also considered interval parameters.

Glucose subsystem interval model

The Euler discrete time approximation of the glucose metabolism model (4.13) is given by:

$$\text{If} \quad G_p(t) > k_{e2}$$

$$\begin{aligned} G_p(t+1) = \Delta t[EGP_b + k_{p2}G_{pb} + k_{p3}(I_b - I_d(t)) + R_a(t) - U_{ii}(t) + \\ +k_2 G_t(t) + k_{e1}k_{e2}] + G_p(t)(1 - \Delta t(k_1 + k_{p2} + k_{e1})) \end{aligned} \tag{4.51}$$

else

$$\begin{aligned} G_p(t+1) = \Delta t[EGP_b + k_{p2}G_{pb} + k_{p3}(I_b - I_d(t)) + R_a(t) - U_{ii}(t) + \\ +k_2 G_t(t)] + G_p(t)(1 - \Delta t(k_1 + k_{p2})) \end{aligned} \tag{4.52}$$

$$G_t(t+1) = \Delta t \left(k_1 G_p(t) - \frac{V_m(X(t))G_t(t)}{K_{m0} + G_t(t)} \right) + G_t(t)(1 - \Delta t k_2) \tag{4.53}$$

$$G(t) = \frac{G_p(t)}{V_g} \tag{4.54}$$

Because of the uncertainty in the insulin sensitivity parameters, G_t and G_p (mg/kg) are also interval states. The uncertain parameters are uni-incident and do not produce computational problems because verifies the monotonicity conditions. $G_t(t)$ is multi-incident in Equation 4.53, so monotony is studied with respect to this multi-incidence.

$$\frac{\partial G_t(t+1)}{\partial G_t(t)} = \Delta t \left(-\frac{V_m(X(t))K_{m0}}{(K_{m0}+G_t(t))^2} + (1-k_2\Delta t) \right) > 0 \quad \Leftrightarrow$$

$$\Leftrightarrow \quad \Delta t < \frac{1}{\frac{V_m(X(t))K_{m0}}{(K_{m0}+G_t(t))^2} + k_2}$$

$$\frac{\partial G_t(t+1)}{\partial G_t(t)_1} = \Delta t \left(-\frac{V_m(X(t))}{K_{m0}+G_t(t)} \right) < 0$$

$$\frac{\partial G_t(t+1)}{\partial G_t(t)_2} = \Delta t \left(\frac{V_m(X(t))G_t(t)}{(K_{m0}+G_t(t))^2} \right) > 0$$

$$\frac{\partial G_t(t+1)}{\partial G_t(t)_3} = 1 - k_2\Delta t > 0 \quad \Leftrightarrow \quad \Delta t < \frac{1}{k_2}$$

Applying the theorem of coercion to optimality, the optimal rational computation for the equations of the model are:

$$\begin{aligned}
&\text{If } \ G_p(t) > k_{e2} \\
&G_p(t+1) = \Delta t[EGP_b + k_{p2}G_{pb} + k_{p3}(I_b - I_d(t)) + R_a(t) - U_{ii}(t) + \\
&\qquad +k_2G_t(t) + k_{e1}k_{e2}] + G_p(t)(1 - \Delta t(k_1 + k_{p2} + k_{e1})) \\
&\text{else} \\
&G_p(t+1) = \Delta t[EGP_b + k_{p2}G_{pb} + k_{p3}(I_b - I_d(t)) + R_a(t) - U_{ii}(t) + \\
&\qquad +k_2G_t(t)] + G_p(t)(1 - \Delta t(k_1 + k_{p2})) \\
&G_t(t+1) = \Delta t \left(k_1G_p(t) - \frac{V_m(X(t))\text{Dual}(G_t(t))}{K_{m0}+G_t(t)} \right) + G_t(t)(1 - k_2\ \Delta t) \\
&G(t) = \frac{G_p(t)}{V_g}
\end{aligned} \tag{4.55}$$

The time step Δt is defined so that

$$\Delta t < \min \left(\frac{1}{k_2}, \frac{1}{\frac{V_m(X(t))\ K_{m0}}{(K_{m0}+G_t(t))^2} + k_2} \right) = \frac{1}{\frac{V_m(X(t))\ K_{m0}}{(K_{m0}+G_t(t))^2} + k_2}$$

Endogenous glucose production interval model

For this subsystem, uncertainty is considered in the parameter k_i (the rate parameter accounting for the delay between the insulin signal and insulin action). The Euler discrete time approximation of the model for the delayed insulin signal (Equation 4.16) is given by:

$$\begin{aligned}
I_1(t+1) &= I_1(t) + k_i\Delta t(I(t) - I_1(t)) \\
I_d(t+1) &= I_d(t) + k_i\Delta t(I_1(t) - I_d(t))
\end{aligned} \tag{4.56}$$

By analysing the monotonic behaviour of state functions $I_1(t+1)$ and $I_d(t+1)$ with respect to parameter k_i, it can be seen that these state functions are monotonic with respect to k_i.

The uncertainty in the parameter k_i causes that the results of the interval computations of $I_1(t+1)$ and $I_d(t+1)$ will be interval states. For this reason, a study of the monotony of Equation 4.56 with respect to multi-incident variables is performed.

1. Monotony of state function $I_1(t+1)$ respect to $I_1(t)$

$$\frac{\partial I_1(t+1)}{\partial I_1(t)} = 1 - \Delta t\ k_i < 0 \quad \Leftrightarrow \quad \Delta t < \frac{1}{k_i}$$
$$\frac{\partial I_1(t+1)}{\partial I_1(t)_1} = 1 > 0$$
$$\frac{\partial I_1(t+1)}{\partial I_1(t)_2} = -\Delta t\ k_i < 0$$

   Then the function $I_1(t+1)$ is totally monotonous with respect to $I_1(t)$.

2. Monotony of state function $I_d(t+1)$ respect to $I_d(t)$

$$\frac{\partial I_d(t+1)}{\partial I_d(t)} = 1 - \Delta t\ k_i < 0 \quad \Leftrightarrow \quad \Delta t < \frac{1}{k_i}$$
$$\frac{\partial I_d(t+1)}{\partial I_d(t)_1} = 1 > 0$$
$$\frac{\partial I_d(t+1)}{\partial I_d(t)_2} = -\Delta t\ k_i < 0$$

   Then the function $I_d(t+1)$ is totally monotonous with respect to $I_d(t)$.

Therefore, the optimal rational computation of the delayed insulin signal 4.56 is given by:

$$\begin{aligned} I_1(t+1) &= I_1(t) + \Delta t\ k_i\ (I(t) - \text{Dual}(I_1(t))) \\ I_d(t+1) &= I_d(t) + \Delta t\ k_i\ (I_1(t) - \text{Dual}(I_d(t))) \end{aligned} \tag{4.57}$$

with the constrain: $\Delta t < \dfrac{1}{k_i}$.

Glucose utilization interval model

For this subsystem, uncertainty is considered in the parameter corresponding to the rate constant for insulin action on peripheral glucose utilization p_{2U}. The Euler discrete model that represents the insulin in the interstitial fluid (Equation4.21) is given by:

$$X(t+1) = \Delta t\ p_{2U}(-X(t) + I(t) - I_b) + X(t) \tag{4.58}$$

When the monotony of this equation is analysed with respect to parameter p_{2U}, it can be seen that the state function $X(t+1)$ is monotonic with respect to p_{2U}. Furthermore, the uncertainty of this parameter means that the results of the interval computation of $X(t+1)$ will be

interval states. Therefore, a study of the monotonic behaviour of Equation 4.21 is performed.

Therefore, the function $X(t+1)$ is totally monotonous with respect to $X(t)$ according to the partial derivatives:

$$\frac{\partial X(t+1)}{\partial X(t)} = -\Delta t\ p_{2U} + 1 > 0 \quad \Leftrightarrow \quad \Delta t < \frac{1}{p_{2U}}$$
$$\frac{\partial X(t+1)}{\partial X(t)_1} = -\Delta t\ p_{2U} < 0$$
$$\frac{\partial X(t+1)}{\partial X(t)_2} = 1 > 0$$

Applying the theorem of coercion to optimality, the optimal rational computation for the equations of the model 4.58 is:

$$X(t+1) = \Delta t\ p_{2U}(-\text{Dual}(X(t)) + I(t) - I_b) + X(t) \tag{4.59}$$

Different simulations were performed, considering uncertainties in the parameters k_i, k_{p3}, V_{mx}, and V_{m0} to validate the model. A general scenario was considered: capillary blood glucose 150 mg/dL, 5 IU of bolus insulin, and 70 g of food intake. To represent the interval glucoregulatory model, the following interval models were combined:

- For subcutaneous insulin absorption: Dalla Man et al. interval model
- For carbohydrate digestion and absorption: Dalla Man et al. interval model
- For insulin action and glucose kinetics: Dalla Man et al. interval model.

As in the previous models studied, MCS and MIA were compared, considering in this case 5% variations in the uncertain parameters corresponding to the glucose subsystem. Figure 4.23 shows the results of this comparison.

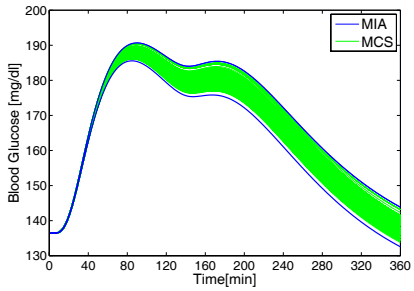

Figure 4.23: Envelopes of blood glucose obtained for 5% variations in the parameters of the glucose kinetics model (k_i, k_{p3}, V_{mx}, and V_{m0}). The green lines indicate each simulation given with the MCS approach and the blue lines show the upper and lower bounds given by the MIA simulation.

Panunzi et al.

In this model, the parameter corresponding to insulin sensitivity, K_{xgI}, is considered uncertain. The Euler discrete time approximation of the model 4.25 is given by:

$$\begin{aligned} I(t+1) &= I(t)(1 - K_{xi}\Delta t) + \Delta t \, \frac{T_{igmax}}{V_i} \frac{1}{\left(\frac{G^*}{G(t-\tau_g)}\right)^{\gamma} + 1} + \frac{S(t)}{V_i}\Delta t \\ T_{igmax} &= K_{xi} I_b \left[\left(\frac{G^*}{G_b}\right)^{\gamma} + 1\right] \end{aligned} \tag{4.60}$$

When t is greater than τ_g, the optimal rational computation for insulin plasma concentration is given by:

$$I(t+1) = I(t)(1 - K_{xi}\Delta t) + \Delta t \; T_{igmax} \; \frac{1}{\left(\frac{G^*}{\text{Dual}(G(t-\tau_g))}\right)^{\gamma} + 1} + \frac{S(t)}{V_i}\Delta t \tag{4.61}$$

The Euler discrete time approximation of the glucose metabolism model (Equation 4.25), is given by:

$$G(t+1) = G(t)(1 - K_{xgI} \; I(t)\Delta t) + K_{xgI} \; I_b \; G_b \Delta t + \frac{R_a(t)}{V_g}\Delta t. \tag{4.62}$$

The function $G(t+1)$ is totally monotonous with respect to multi-incident parameter K_{xgI}, because:

$$\begin{aligned} \frac{\partial G(t+1)}{\partial K_{xgI}} &= \frac{\partial G(t)}{\partial K_{xgI}}(1 - K_{xgI} I(t)\Delta t) - G(t)I(t)\Delta t + I_b G_b \Delta t < 0 \quad \Leftrightarrow \quad \Delta t < \frac{1}{K_{xgI} I(t)} \\ \frac{\partial G(t+1)}{\partial K_{xgI_1}} &= -G(t)I(t)\Delta t < 0 \\ \frac{\partial G(t+1)}{\partial K_{xgI_2}} &= I_b \; G_b \Delta t > 0 \end{aligned}$$

Applying the theorem of coercion to optimality, the optimal rational computation for the plasma glucose concentration $G(t)$ (Equation 4.62) is:

$$G(t+1) = G(t)(1 - K_{xgI} \; I(t)\Delta t) + \text{Dual}(K_{xgI}) I_b \; G_b \Delta t + \frac{R_a(t)}{V_g}\Delta t. \tag{4.63}$$

The results for MCS with 500 trials that considered a variation of 10% in D are shown in Figure 4.24. A general scenario was considered: capillary blood glucose 81 mg/dL, 5 IU of bolus insulin, and 70 g of food intake. A time reduction of 99.68% was obtained with MIA with respect to the time required for MCS.

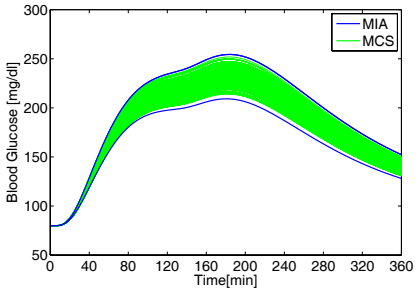

Figure 4.24: Envelopes of blood glucose obtained for a 10% variation in D and a 10% variation in insulin sensitivity K_{xgI}. The green lines indicate each simulation given with the MCS approach and the blue lines show the upper and lower bounds given by the MIA simulation.

4.4 Comparative Study of Three Interval Models

Different simulation models of glucose regulation in T1DM patients have been reviewed (Wilinska and Hovorka, 2008; Cobelli et al., 2009), but no comparative study is available, in contrast to the situation for ICU glucose models (Van Herpe et al., 2009). Here, we focus on models that predict postprandial glucose.

There is no consensus about the degree of complexity a glucoregulatory model should use to describe physiological phenomena, considering the large intra-patient variability observed, which can jeopardize any attempt to obtain accurate model predictions after a few hours. Here, we compare three postprandial insulin action and glucose kinetics models in the presence of intra-patient variability (insulin sensitivity) and uncertainty in food intake estimates (García-Jaramillo et al., 2011c). These models are combined with shared insulin pharmacokinetic and glucose intestinal absorption sub-models. The influence of the complexity of the insulin action and glucose kinetics sub-models on postprandial glucose excursions under uncertainty is then analysed. The kinetic parameters for the comparison of each model are adjusted based on data for 10 adults from the educational version of the University of Virginia (UVa) simulator (Kovatchev et al., 2009).

As described in detail in the previous section, MIA (Gardeñes et al., 2001) is used to predict the plasma glucose for each model, taking into account the different sources of uncertainty. This yields upper and lower bounds that define an envelope for all possible glucose excursions experienced by the patient predicted by each model.

To compare the three insulin action and glucose kinetics models, some interval models that were rewritten and presented in this chapter (Section 4.3) to consider uncertainty are used here to represent the glucose–insulin system:

- For intestinal glucose absorption: Dalla Man et al. interval model
- For subcutaneous insulin absorption: Dalla Man et al. interval model
- For insulin action and glucose kinetics: Bergman et al., Dalla Man et al. and Hovorka et al. interval models.

Subcutaneous insulin absorption was used with no consideration of uncertainty. Therefore, to predict postprandial glycaemia, we combined the model for gastric emptying, digestion, and

absorption and the model for subcutaneous insulin absorption with each of the models for insulin action and glucose kinetics. The relationships among the different models used are shown in Figure 4.25.

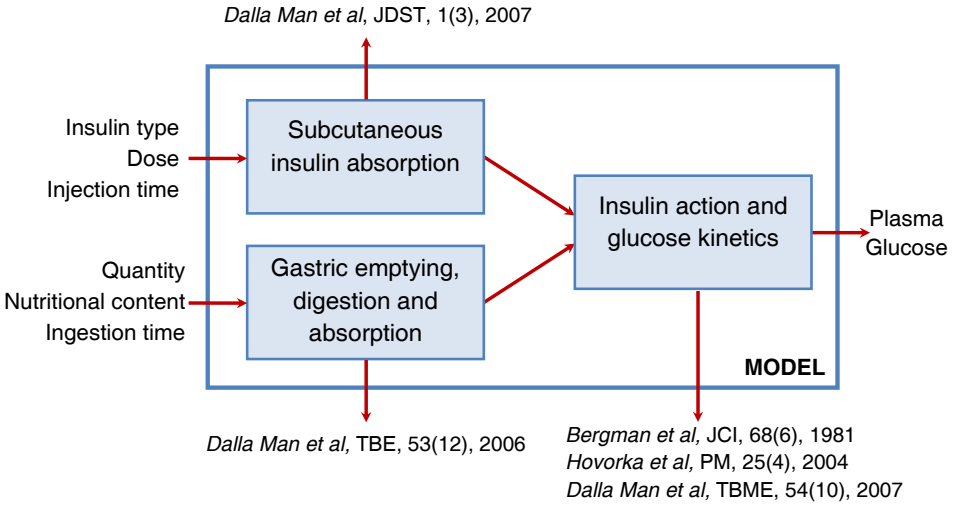

Figure 4.25: Glucose-insulin system in T1DM.

4.4.1 Parameter adjustment

The main objective of this study was to compare the plasma glucose dynamics of three models, Bergman et al. (1981) (model 1), Hovorka et al. (2004) (model 2), and Dalla Man et al. (2007b) (model 3), in the insulin therapy for a specific patient. This requires that the parameters of each model be adjusted, considering intra-patient variability, to reflect the "same" patient.

The glucose kinetics parameters of model 1 and model 2 were adjusted for a suite of virtual patients from the UVa simulator using model 3. The UVa simulator (Kovatchev et al., 2009) is an in silico model of T1DM accepted by the US FDA as a substitute for animal trials in the pre-clinical testing of closed-loop control strategies. The simulator provides a set of virtual subjects based on real individual data, a simulated sensor that replicates typical errors in continuous glucose monitoring, and a simulated insulin pump. In the educational version of the simulator, 30 virtual subjects are available, including 10 children, 10 adolescents, and 10 adults.

The parameters related to insulin sensitivity in model 1 and model 2 were adjusted because these physiological parameters display huge variations between patients and they are critical to the patient's treatment. The parameters considered to be oscillatory, according to Wilinska et al. (Wilinska and Hovorka, 2008) for model 2, were also adjusted. The parameters of each model were then adjusted numerically with the non-linear least-squares method, using simulation analysis and modelling (SAAM II) (Barrett et al., 1998). SAAM II is a software tool for simulation and data fitting, returning optimal parameter estimates and the associated statistics.

SAAM II has a flexible graphical user interface for the easy implementation of compartmental models using drag-and-drop icons. Figure 4.26 shows the implementation of compartmental model 1 (see Figure 4.26(a)) and model 2 (see Figure 4.26(b)) in SAAM II. For each model, the number of compartments is specified and then connected by transfer coefficients, and the input data are associated by forcing functions. A type is established for each parameter, fixed or adjustable, and the latter has upper and lower limits. Finally, when the model is built, the system of equations is automatically generated from the model structure.

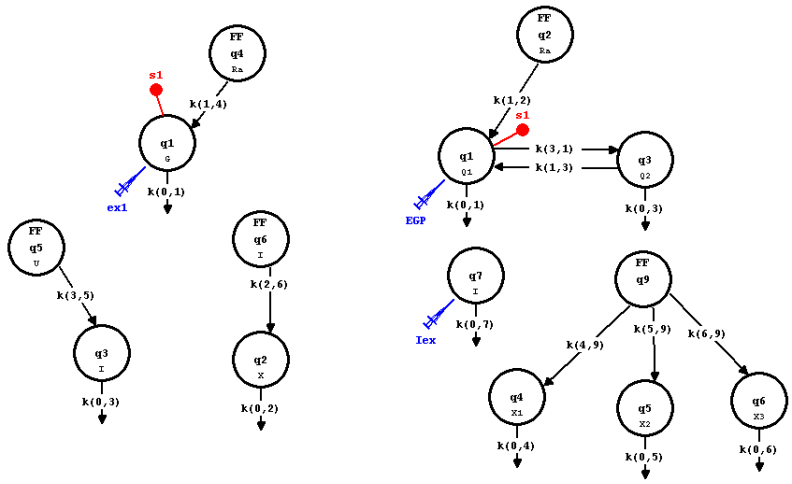

(a) (b)

Figure 4.26: Visual representation of model 1 (a) and model 2 (b) constructed using SAAM II.

Profiles of the glucose rate of appearance in the plasma, the rate of appearance of insulin in the plasma, and the plasma glucose concentration were obtained with the UVa simulator. These experimental data for each patient were then used to adjust the parameters of model 1 and model 2 (see Figure 4.27).

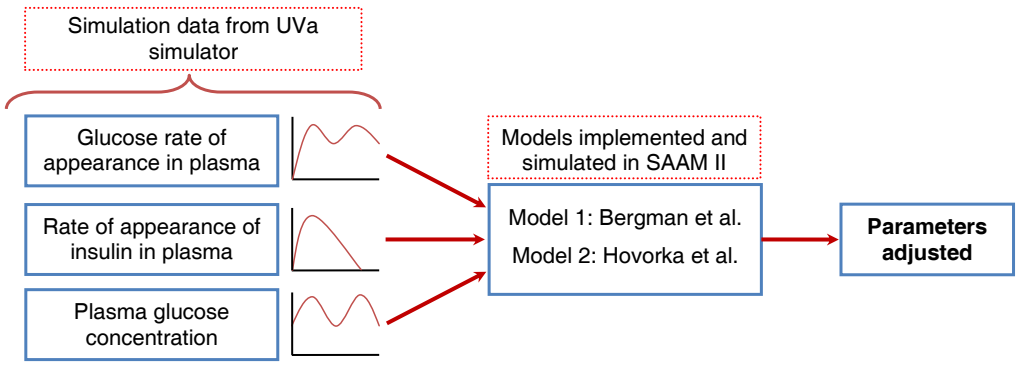

Figure 4.27: Methodology for parameter adjustment using SAAM II.

The adjustable parameters have upper and lower limits. These limits are established for

each model according to the inter- and intra-patient variability, taking into account that the limits are not widely divergent from the initial value. SAAM II uses information on these limits as part of the fitting procedure. The limits are established by considering the inter- and intra-patient variability in the parameters for model 1 (Dua et al., 2006; Roy and Parker, 2007) and the inter-patient variability in the parameters for model 2, based on the six patients reported by Hovorka et al. (Hovorka et al., 2002). The limits of these parameters and the values for the fixed parameters are shown in Table 4.3.

Model	Parameter	Fixed	Lower limit	Upper limit
Model 1	p_1	–	0.0035	0.0665
	p_2	–	0.0050	0.0950
	p_3	–	2.68e-6	5.32e-5
	n	–	0.0142	0.2698
	p_4	0.0980	–	–
	V_g	*	–	–
Model 2	f_{01}	–	0.0071	0.0121
	k_{12}	–	0.0390	0.0968
	k_{a1}	–	0.0007	0.0157
	k_{a2}	–	0.0231	0.1630
	k_{a3}	–	0.0114	0.0691
	k_{b1}	–	3.25e-6	7.58e-5
	k_{b2}	–	6.77e-6	2.50e-4
	k_{b3}	–	2.31e-4	3.99e-3
	k_e	–	0.0138	0.2622
	V_g	*	–	–
	V_i	*	–	–

Table 4.3: Limit values for the adjustment parameters and values for the fixed parameters. * Values are taken from UVa simulator patients.

When the model has been fully specified and the initial parameter estimates have been entered, the model can be fitted to the data. For some patients, SAAM II does not yield successful identification and therefore report statistics, which provide information on the identification accuracy, are not obtained.

Once the parameters of each model are adjusted for a specific therapy, the next step is to compare the behaviours of the three interval models when considering the uncertainties in insulin sensitivity and food intake. The percentage variations in the parameters related to insulin sensitivity were set to achieve similar upper and lower bounds in the steady state.

4.4.2 Adjustment results

The glucose concentrations for 10 adults from the UVa simulator were simulated in an open loop over a period of 1000 min. For each patient, the following typical scenario was assumed:

- Food intake: 80 g
- Bolus insulin: 5 IU

- Insulin rate to achieve basal glucose of 100 mg/dL.

The glucose kinetics parameters for models 1 and 2 were adjusted according to the methodology presented above. The results of the adjustment study are shown in Table 4.4, and Figure 4.28 shows a representative fit of the models for a set of glucose data for adult patient 3 from the UVa simulator.

Parameter	Nominal	1	2	3	4	5	6	7	8	9	10
p_1	0.0350	0.0096	0.0096	0.0082	0.0349	0.0112	0.0035	0.0287	0.0200	0.0083	0.0122
p_2	0.0500	0.0349	0.0294	0.0126	0.0050	0.0231	0.0875	0.0050	0.0779	0.0712	0.0950
p_3	2.80e-5	2.68e-6	7.33e-6	5.68e-6	5.72e-6	2.68e-6	5.32e-5	8.89e-6	2.68e-6	2.68e-6	5.39e-6
n	0.1420	0.0585	0.1064	0.1063	0.1000	0.1221	0.1230	0.1106	0.0142	0.0496	0.0886
f_{01}	0.0075	0.0071	0.0071	0.0071	0.0071	0.0071	0.0071	0.0071	0.0074	0.0071	0.0071
k_{12}	0.0871	0.0968	0.0968	0.0968	0.0625	0.0390	0.0390	0.0414	0.0390	0.0968	0.0390
k_{a1}	0.0157	0.0022	9.31e-4	0.0073	0.0081	0.0155	0.0030	0.0157	0.0056	0.0157	0.0157
k_{a2}	0.0231	0.0231	0.0231	0.0231	0.1630	0.0231	0.0962	0.0893	0.0231	0.0231	0.0253
k_{a3}	0.0143	0.0691	0.0691	0.0114	0.0160	0.0691	0.0691	0.0114	0.0691	0.0691	0.0691
k_{b1}	2.49e-5	4.72e-6	3.25e-6	1.02e-5	1.95e-5	3.61e-6	7.64e-6	2.44e-5	3.25e-6	3.25e-6	3.25e-6
k_{b2}	1.41e-5	1.46e-5	8.00e-6	2.20e-5	1.05e-4	2.50e-4	6.77e-6	3.26e-5	9.23e-5	6.39e-5	1.08e-4
k_{b3}	5.42e-4	2.31e-4	2.31e-4	4.00e-3	3.13e-4	2.31e-4	2.31e-4	2.95e-4	2.31e-4	2.31e-4	2.31e-4
k_e	0.1380	0.2191	0.2622	0.2622	0.2144	0.2622	0.2622	0.1936	0.1452	0.2622	0.2622

Table 4.4: Adjustment parameters for 10 patients of model 1 (first four parameters) and model 2 (last nine parameters).

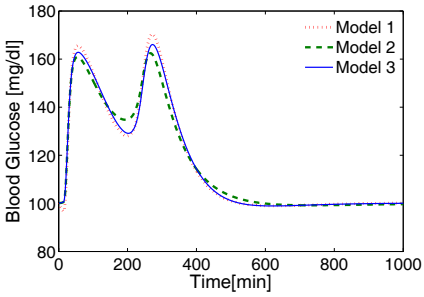

Figure 4.28: Representative adjustments of the models to a set of glucose data. The blue solid line represents the glucose concentration for a virtual patient (model 3); the red dotted line shows the glucose concentration estimated by adjusted model 1; and the green dashed line shows that estimated by adjusted model 2.

Model fitting was assessed with the method of least-squares. The fitting was classified as very good (<20,000), good (20,000–60,000), or fair (>60,000) according to the indices obtained for adjusted model 1 and model 2 for each patient. Figure 4.29 shows that very good fitting was achieved for 70% of the UVa simulator patients (2, 3, 4, 5, 7, 9, and 10) for model 1, but for only 40% of the patients (1, 3, 4, and 7) for model 2. Fitting was good for 30% (patients 1, 6, and 8) and 40% of the patients (2, 5, 8, and 10) for model 1 and model 2, respectively, because the adjustment in the transient state was not fully achieved for some patients. Finally, fitting was fair for 20% of the patients (6 and 9) for model 2. The parameters of model 1 were easily adjusted from experimental data because it is a low-order model.

The models were compared with the parameters adjusted. For this comparison, we considered only the eight patients for whom the adjustments in model 1 and model 2 were very

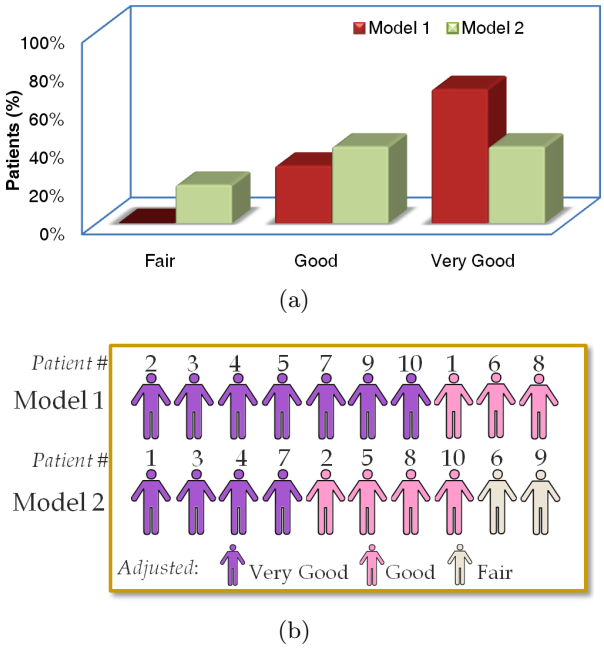

Figure 4.29: Assessment of the model adjustments (a) by model, and (b) by associated patient.

good or good, and excluded two patients for whom the adjustments were only fair in model 2. The interval simulation for each model was performed taking into account the uncertainty in the parameters related to insulin sensitivity and the uncertainty in the amount of carbohydrate ingested. The percentage variation for each insulin sensitivity parameter was established based on the standard errors presented by Hovorka et al. (2002) for model 2. Thus, the uncertain parameters of model 1 and model 3 were varied to achieve a range bound similar to that of model 2 at steady state. The percentages assigned are shown in Table 4.5.

Model	Parameter uncertainty		
Model 1	p_1 (min^{-1}): 8%	p_2 (min^{-1}): 10%	p_3 ($\text{mL mU}^{-1}\ \text{min}^{-2}$): 10%
Model 2	S_{IT} (mU L min^{-1}): 4%	S_{ID} (mU L min^{-1}): 6%	S_{IE} (mU L min^{-1}): 3%
Model 3	V_{m0} ($\text{mg kg}^{-1}\text{min}^{-1}$): 7%	V_{mx} ($\text{mg kg}^{-1}\text{min}^{-1}$ per pmol L^{-1}): 5%	k_{p3} ($\text{mg kg}^{-1}\text{min}^{-1}$ per pmol L^{-1}): 4%

Table 4.5: Uncertain parameters.

A variation of 7% in the basal glucose concentration in the initial state of model 1 was also considered, to establish a relationship with the V_{m0} parameter, which affects the steady state of model 3. A 7.5% uncertainty for meal ingestion was considered in all models as the corrected carbohydrate estimation to counteract deviations from the average bias.

The interval simulations for each model and each patient were performed considering the uncertainties described above. When the three envelopes generated by the models for each patient were compared, it was clear that the simplest insulin model assessed (model 1) included the responses of the other two models when a good fit of the model parameters was achieved. To evaluate how much of the response of model 2 (Y_{M2}) or model 3 (Y_{M3}) was included in the model 1 response (Y_{M1}), the absolute error was then calculated for each sample time. The maximum absolute error is a measure of the inclusion accuracy. The absolute error for each step

is given by:

$$\begin{aligned} Absolute\ error(k) = &\max(Inf\ (Y_{M1}(k)) - \min(Inf\ (Y_{M1}(k)), Inf\ (Y_{Mj}(k))), \\ &\max(Sup\ (Y_{M1}(k)), Sup\ (Y_{Mj}(k))) - Sup\ (Y_{M1}(k))) \\ &j = 2, 3;\ k = 0, \ldots, T, \end{aligned} \tag{4.64}$$

where T is the total simulation time. Then,

$$Maximum\ absolute\ error = \max_{k}(Absolute\ error(k)). \tag{4.65}$$

The mean absolute error for model 2 was 8.2, with a standard deviation of 3.58, whereas the mean value for model 3 was 6.94, with a standard deviation of 6.52 (see Table 4.6). This difference is the result of the parameter adjustment, because better adjustment leads to a lower absolute error. Considering the maximum absolute error between model 2 and model 3, the mean $\pm$ SD value was 9.36 ± 5.19. These mean values correspond to differences between the sensor and reference values reported in the literature on blood glucose monitoring (Wentholt et al., 2008).

Patient	Model 2	Model 3
1	9.77	14.77
2	6.09	1.96
3	3.75	2.89
4	14.12	18.39
5	4.30	4.25
7	11.61	9.37
8	8.68	1.64
10	7.26	2.20
Mean	8.20	6.94
SD	3.58	6.52

Table 4.6: Maximum absolute errors (mg/dL) for the envelopes of model 2 and model 3 with respect to model 1.

As an illustration, a comparison of the three glucose kinetics models for adult patient 3, considering the uncertainties discussed above, is shown in Figure 4.30(a). This patient belongs to the set of 30% of adults for whom a very good fit was observed for models 1 and 2. The envelope for model 1 contains all possible glucose concentration responses of model 2 and model 3. The same effect was observed for postprandial glucose in 50% of the patients for whom very good adjustment was achieved (for example patient 5), as evident in Figure 4.30(b). For the remaining 20% of patients, the absolute error was greater because the envelopes differed more widely.

According to the results obtained here, the consideration of model 1, which has low complexity together with uncertainty, may be enough to tightly embed the responses of the other models in most cases.

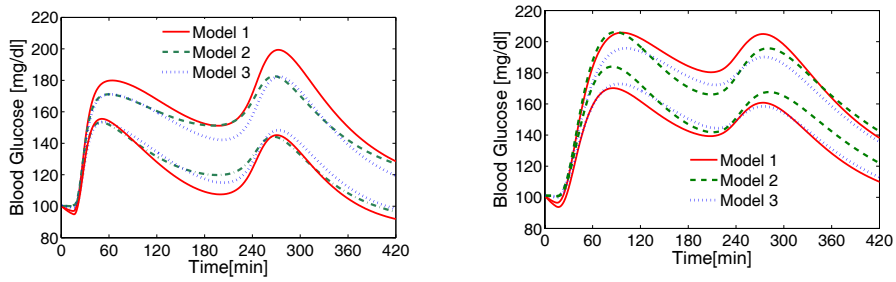

Figure 4.30: Comparison of the glucose concentrations for adult patients 3 (a) and 5 (b), for whom a good fit was observed. The red solid line indicates the blood glucose response envelope given by model 1; the green dashed line shows that given by adjusted model 2; and the blue dotted line that given by model 3.

To validate the previous statement and the parameter adjustment, additional tests were carried out using the same adjusted parameters for each model and each patient, but with a different therapy. The example of a therapy consisting of 4 IU of bolus insulin and a food intake of 60 g given to patient 3 is shown in Figure 4.31(a). The envelope for model 1 contains the model 2 and model 3 envelopes, corresponding to the glucose concentration responses for approximately the first 7 h. The same can be seen in Figure 4.31(b) for patient 5.

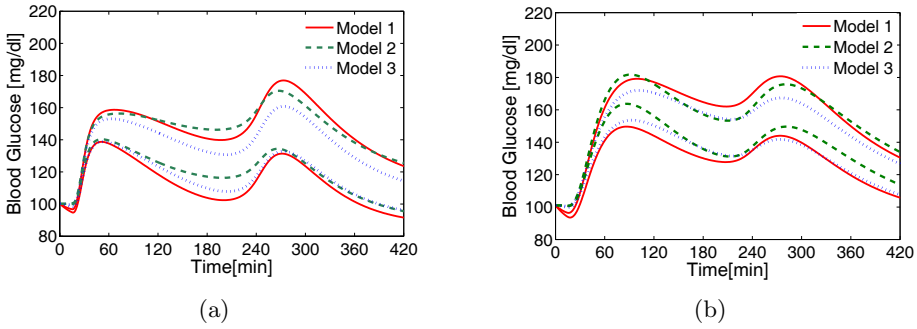

Figure 4.31: Validation of the proposed methodology by varying the food intake and bolus insulin for patients 3 (a) and 5 (b). The red solid lines indicates the blood glucose response envelope given by model 1; the green dashed line shows that given by adjusted model 2; and the blue dotted line that given by model 3.

Finally, the responses obtained with the therapy used in the adjustment were compared with those obtained with the therapy used in the validation. For this purpose, the absolute error was calculated using Equation 4.64 for each patient used in the validation and then compared with the absolute error obtained for the adjusted patients (see Figure 4.32).

This comparison shows that the absolute error obtained for the validation and the absolute error obtained for the adjusted patients are strongly related (the Pearson correlation coefficients for the absolute errors with respect to model 1 were 0.83 and 0.98 for model 2 and model

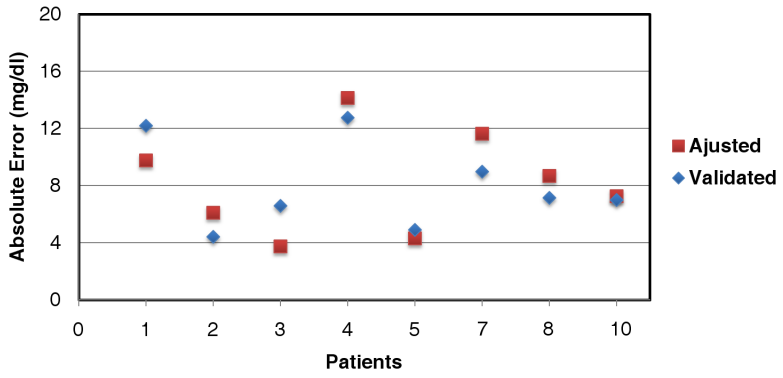

(a)

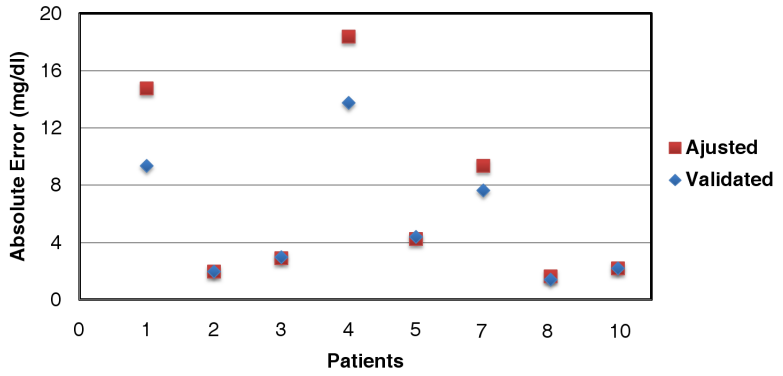

(b)

Figure 4.32: Adjusted absolute errors vs validation absolute errors for model 2 (a) and model 3 (b), with respect to model 1.

3, respectively). Therefore, we can conclude that when a good fit of parameters is achieved, these can be used in other therapies and different meals. Similarly, the conclusion that model 1 includes the responses of models 2 and 3 was verified.

4.5 Summary

In this chapter, different carbohydrate digestion and absorption models, subcutaneous insulin absorption models, and insulin action and glucose kinetics models were studied using MIA to consider different sources of uncertainty. Equations that allows an optimal interval computation of the postprandial glucose in patients with T1DM for each model were obtained.

MIA has been presented as a tool to predict glucose excursions in type 1 diabetes with uncertain parameters, initial conditions, and meal intake. In contrast to probabilistic methods, such as MCS, sharp envelopes containing all possible patient responses can be computed using MIA (guaranteed simulation). Its computational efficiency has been compared with that of MCS. In contrast to the latter, the computation time of MIA is independent of the number of uncertain parameters, yielding time reductions of up to 98%. Therefore, a worst-case analysis can be performed efficiently, which is extremely important in the context of diabetes. The prediction of possible hyper- and hypoglycaemic episodes considering patient variability may yield safer and

more robust insulin infusion algorithms.

A comparison of three insulin action and glucose kinetics models was presented. The behaviours of the models proposed by Bergman et al. (1981), Hovorka et al. (2004), and Dalla Man et al. (2007b) for insulin therapy were analysed in detail. The plasma glucose dynamics were compared by adjusting the model parameters to accommodate intra-patient variability when the "same" patient was used for each model. As a result, the glucose response envelope for a simple model (Bergman et al. (1981)) included the responses of the other two models (Hovorka et al. (2004) and Dalla Man et al. (2007b)) when a very good fit of the simple model parameters was achieved. Therefore, with variability, simple glucose–insulin models may be sufficient to describe patient dynamics in most situations.

The proposed methodology was validated for each model by varying the therapy tested, and high correlation coefficients were obtained.

Chapter 5

Postprandial Hypo- and Hyperglycaemia Risk Index

In intensive insulin therapy, the patient calculates the adjusted insulin dose according to his/her preprandial blood glucose level and food intake, but if the dose is too high, there is a risk of severe hypoglycaemia, with all its consequences. High glycaemic variability is another risk factor for hypoglycaemia.

So far, no gold standard method has been devised to analyse the risk of suffering hypoglycaemic or hyperglycaemic events in the postprandial state. The possible methods can be classified as:

- Glycemic variability measures: M-value was formulated by Schlichtkrull et al. (1965) to encapsulate a glycemic profile in a single quantitative value. Later, mean amplitude of glycemia excursions (MAGE) (Service et al., 1970) was proposed to quantify major swings of glycemia and to exclude minor ones. Subsequently, the mean of daily differences (MODD) based on day-to-day variability was designed by Molnar et al. (1972). Mean absolute difference (MAD) (Moberg et al., 1993) is other glucose variability measure which is calculated by adding the absolute differences of all blood glucose values and dividing them by the number of values minus one. More recently continuous overall net glycemic action (CONGA_n) was formulated by McDonnell et al. (2005) to assess intra-day glycemic variation. CONGA_n has been defined as the standard deviation of the differences in glucose concentration using varying time differences of n hours.

- Extreme values risk measures: low blood glucose index (LBGI) (Kovatchev et al., 1998) and high blood glucose index (HBGI) (Kovatchev et al., 2002) were proposed as a measure of the risk of severe hypoglycaemia and hyperglycaemia respectively, based on self monitoring blood glucose (SMBG). Lability index (LI) (Ryan et al., 2004) was presented as a measure of hypoglycaemia and glycaemic lability for islet transplantation. Average daily risk range (ADRR) (Kovatchev et al., 2006) which is a variability measure computed from routine SMBG combining the LBGI and HBGI. On the other hand, glycaemic penalty index was proposed by Van Herpe et al. (2008) as a tool for assessing the overall glycemic control behavior in ICU patients.

- A probabilistic model for predicting hypoglycaemia was presented by Murata et al. (2004).

A review of the advantages, limitations, and inter-relationships of the available methods for evaluating the quality of glycaemic control and assessing glycaemic variability has been pub-

lished by Rodbard (2009), and measures with which to evaluate glycaemic control have been classified by de Adana et al. (2008).

Any attempt to predict the risk of postprandial hypo- or hyperglycaemia should consider the different sources of uncertainty and patient variability, so that the method is reliable enough to be used in any insulin dosage advisory system. However, none of the aforementioned methods deals with this problem.

As mentioned throughout this work, the interval simulation of glucose prediction models can provide valuable information about postprandial glucose responses in the presence of, for instance, intra-individual variability and uncertain food intake. Therefore, one of the goals of this research is to develop a method to quantify the risk of developing different grades of hypo- and hyperglycaemic episodes using interval prediction.

In this chapter, a method for computing the risk of postprandial hypo- or hyperglycaemia in T1DM patients, considering intra-patient variability and other sources of uncertainty, is presented. Similarly, the relationship between the risk index (RI) and the probability of a hypo- or hyperglycaemic event is evaluated with the Monte Carlo simulation (MCS). A model-based prediction of the worst-case glucose excursion is then made, considering intra-patient variability, an uncertain initial state, and uncertain food intake.

5.1 Hyper- and Hypoglycaemia Risk Index

Calculating RI requires the evaluation of the impact of bolus insulin and food intake on postprandial glucose, thus allowing the sufficiently accurate prediction of short-term postprandial glycaemia, taking into account the large intra-individual variability of the patients. For this reason, a worst-case approach is introduced to calculate RI (García-Jaramillo et al., 2008, 2009a,b).

The RI is computed from a quantification of the excursions, provided by the glucoregulatory model with uncertainty, in the mild and severe hypo- and hyperglycaemia ranges and their relative importance. A library of the interval glucoregulatory models for this purpose was presented in Chapter 4. To compute RI, the following considerations are taken into account:

1. Glucose ranges corresponding to severe (H_s) and mild (H_m) hyperglycaemia and to severe (h_s) and mild (h_m) hypoglycaemia are those depicted in Figure 5.1 with thresholds h_s=36, h_m=70, H_m=150, and H_s=250 mg/dL.

2. A weighting function $\gamma(t)$ is defined for the time occurrence of hyperglycaemia (mild and severe). Major relevancy is given to zones far from meal time to take into account long-term hyperglycaemia (see Figure 5.1).

$$\gamma(t) = \begin{cases} 0.5 & 0 \leq t < 60 \\ 0.75 & 60 \leq t < 120 \\ 1 & 120 \leq t < 180 \\ 1.25 & 180 \leq t < 240 \\ 1.5 & 240 \leq t < 300. \end{cases}$$

   This weight is assigned only in cases of hyperglycaemia, because glucose levels commonly increase after intake. So the more time has elapsed after the intake, greater weight is

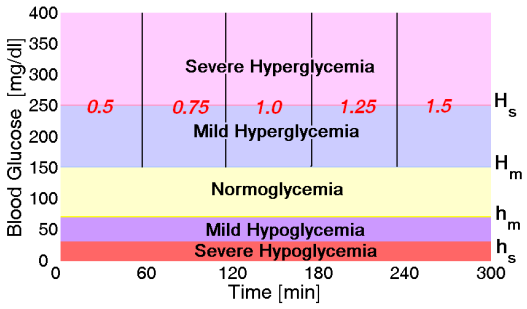

Figure 5.1: Grid for glucose ranges and hyperglycaemia time weights (cursive numbers) used for risk index computation.

assigned. In the case of hypoglycaemia, the relevancy of risk is independent of the time after intake.

3. Weights are defined to quantify the relative importance of mild and severe hypo- and hyperglycaemic events (α_{hs}, α_{hm}, α_{Hm}, and α_{Hs}). They are adjusted using a quadratic function in the following way: α_{hs}=α_{hm} = 1; for mild hyperglycaemia, α_{Hm}=1/16; and for severe hyperglycaemia, α_{Hs}=1/4 (see Figure 5.2).

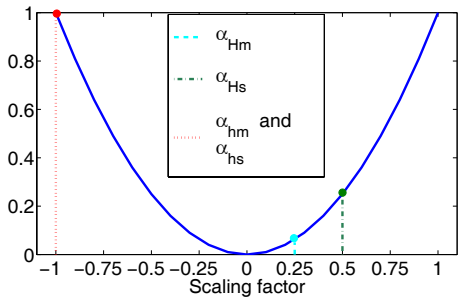

Figure 5.2: Quadratic function to quantify the relative importance of severe and mild hypoglycaemia (red dotted line), mild hyperglycaemia (cyan dashed line), and severe hyperglycaemia (green dash-dotted line).

These values, obtained heuristically with clinical judgements, can be modified by the physician according to patient's specific needs.

The greatest weight is assigned to the risk of hypoglycaemia, because it can cause serious complications in the short and long terms. Hypoglycaemia affects the brain or central nervous system, which derives almost all of its energy from glucose. Severe hyperglycaemia presents a greater risk than moderate hyperglycaemia, and is therefore assigned a greater weight.

We define $G_{\max}(t)$ and $G_{\min}(t)$ as the upper and lower bounds of the predicted manifold glucose trajectories. The RI is then computed as a weighted sum of the risk of each event (mild

or severe hypo- or hyperglycaemia), given by a normalized measure of the area under the curve in each glucose range:

$$
\begin{aligned}
J_{Hs} &= \frac{\int_{T_{Hs}} \gamma(t)\ (G_{\max}(t) - H_m)\ dt}{H_s - H_m} && T_{Hs} = \{t \ / \ G_{max}(t) \geq H_s\} \\
J_{Hm} &= \frac{\int_{T_{Hm}} \gamma(t)\ (G_{\max}(t) - H_m)\ dt}{H_s - H_m} && T_{Hm} = \{t \ / \ H_m \leq G_{max}(t) < H_s\} \\
J_{hs} &= \frac{\int_{T_{hs}} (h_m - G_{\min}(t))\ dt}{h_m - h_s} && T_{hs} = \{t \ / \ G_{min}(t) \leq h_s\} \\
J_{hm} &= \frac{\int_{T_{hm}} (h_m - G_{\min}(t))\ dt}{h_m - h_s} && T_{hm} = \{t \ / \ h_s < G_{min}(t) \leq h_m\}
\end{aligned} \tag{5.1}
$$

where H_s, H_m, h_s, and h_m are the threshold values described in item 1 and $\gamma(t)$ is the weighting assigned to the time of occurrence of hyperglycaemia.

The RI is finally calculated as the weighted sum:

$$J := \alpha_{Hs}\ J_{Hs} + \alpha_{Hm}\ J_{Hm} + \alpha_{hs}\ J_{hs} + \alpha_{hm}\ J_{hm}. \tag{5.2}$$

Example 5.1 An example of RI calculation for one predicted manifold, defined by its upper and lower bounds, is shown in Figure 5.3. The area under the curve (AUC) in each glucose range for the different episodes is represented by $m_i\ i = 1, .., 3$ for mild hyperglycaemia and by $s_i\ i = 1, .., 3$ for severe hyperglycaemia. The components of RI corresponding to hyperglycaemia are then calculated according to Equation 5.1 as:

$$
\begin{aligned}
J_{Hm} &= \frac{0.5\ m_1 + 0.75\ m_2 + 1.5\ m_3}{H_s - H_m} \\
J_{Hs} &= \frac{0.75\ s_1 + 1\ s_2 + 1.25\ s_3}{H_s - H_m}.
\end{aligned} \tag{5.3}
$$

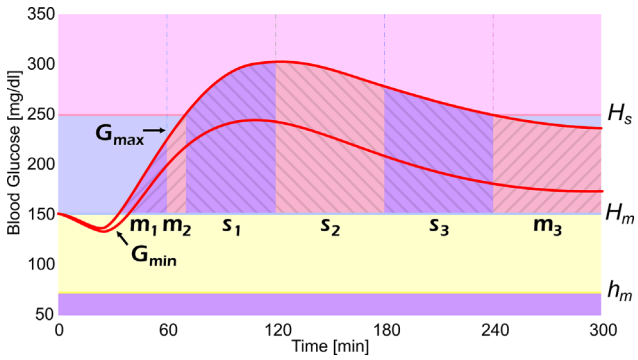

Figure 5.3: Example of an RI computation for hyperglycaemic events.

In this example, episodes of hypoglycaemia (J_{hm} and J_{hs}) are not induced. Therefore, to obtain the final RI, Equation 5.2 is applied to the risk obtained in Equation 5.3.

$$J = \frac{1}{4}\left(\frac{0.75\ s_1 + 1\ s_2 + 1.25\ s_3}{H_s - H_m}\right) + \frac{1}{16}\left(\frac{0.5\ m_1 + 0.75\ m_2 + 1.5\ m_3}{H_s - H_m}\right). \tag{5.4}$$

Example 5.2 We present another example to illustrate the risk of hypoglycaemia and hyperglycaemia. In this case, three AUCs present the risk of mild hyperglycaemia (m_1, m_2, and m_3), two AUCs the risk of severe hyperglycaemia (s_1, s_2), one AUC the risk of mild hypoglycaemia (m_4), and one AUC the risk of severe hypoglycaemia (s_3), as shown in Figure 5.4.

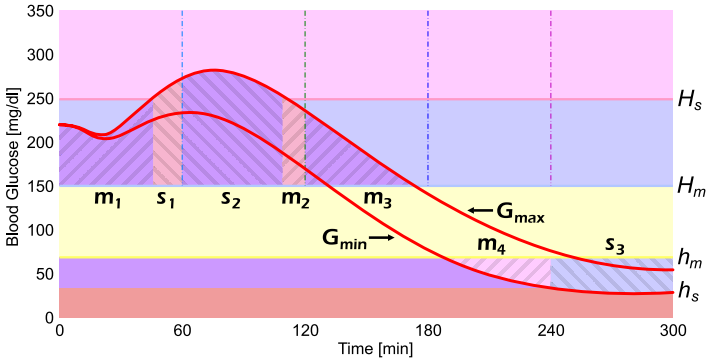

Figure 5.4: Example of RI computation for hypo- and hyperglycaemic events.

Then, the components of RI corresponding to hypo- and hyperglycaemia are:

$$J_{Hm} = \frac{0.5\ m_1 + 0.75\ m_2 + 1\ m_3}{H_s - H_m}$$

$$J_{Hs} = \frac{0.5\ s_1 + 0.75\ s_2}{H_s - H_m}$$

$$J_{hm} = \frac{m_4}{h_m - h_s}$$

$$J_{hs} = \frac{s_3}{h_m - h_s}.$$

With the normalized measure of the AUC for each glucose range (mild and severe hypoglycaemia and hyperglycaemia), RI is calculated, taking into account the relative importance of the risk of each event by:

$$\begin{aligned} J = \frac{1}{4}\left(\frac{0.5\ s_1 + 0.75\ s_2}{H_s - H_m}\right) + \frac{1}{16}\left(\frac{0.5\ m_1 + 0.75\ m_2 + 1\ m_3}{H_s - H_m}\right) + \\ + 1\left(\frac{s_3}{h_m - h_s}\right) + 1\left(\frac{m_4}{h_m - h_s}\right). \end{aligned} \tag{5.5}$$

5.2 Risk Index Validation

To validate the feasibility of RI, different scenarios were analysed. First, an interval simulation of each scenario was performed, considering different sources of uncertainty, and then RI was calculated. Next, the set of RIs was analysed globally and, as a result, similar behaviours for

different ranges of indices and preprandial glucose values were encountered. An MCS was used to verify these behaviours. Throughout this section, each phase of the validation of RI is discussed in detail.

5.2.1 Scenarios

A virtual patient with nominal parameters taken from Hovorka et al. (2002) (patient 2) was used in the validation of RI. A total of 3315 different scenarios were established for this patient:

- Preprandial glucose: 80–240 mg/dL in increments of 10 mg/dL
- Food intake: 40, 60, and 80 g
- Bolus insulin: thirteen insulin doses in increments of 0.5 IU selected within the range of 2–10 IU
- Mealtimes: 0, 15, 30, 45, and 60 min (after bolus insulin).

The uncertainty in the patient's hepatic and peripheral insulin sensitivities was considered: S_{IT} (distribution/transport) with 11% variation, S_{ID} (disposal) with 8% variation, and S_{IE} (endogenous glucose production) with 2% variation, according to the standard deviation presented by Hovorka et al. (2002).

An uncertainty of 5% in the carbohydrate content of the planned meal was also considered. In this context, it is well known that diabetic patients tend to consistently underestimate the carbohydrate content of their meals. When RI is applied to a specific patient, this deviation is taken into account in the process of adjusting the model by correcting for the bias in the patient's carbohydrate estimate. Therefore, the 5% uncertainty considered here represents the deviation with respect to this bias-corrected estimate.

5.2.2 Interval simulation

In this study, the insulin action and glucose kinetic, and carbohydrate digestion and absorption model from Hovorka et al. (2004) and insulin absorption model from Tarín et al. (2005) were used to represent the glucoregulatory model. However, this index can also be used with other glucoregulatory models representing the patient's behaviour. The interval model of Hovorka et al., presented in Section 4.3.3, was used to compute the tight enclosure of the envelope that includes all possible behaviours of the system. This model has been combined with the model proposed by Tarín et al. (2005) for subcutaneous insulin absorption. Interval simulations of the model were performed during the 5 h period after a meal.

To run the interval simulation of the whole system, the initial states and inputs must be given. In this study, three days were simulated for the given therapy. Starting from a real initial state, the interval values for the states at the beginning of the third day will be considered to represent the set of possible initial states the patient may experience.

5.2.3 Study of RI

Based on the interval simulation, RI was calculated for each scenario. Next, the behaviour of RI in the set of 3315 scenarios was studied with respect to the risk of mild or severe hypoglycaemia or mild or severe hyperglycaemia. In this way, it was possible to establish similar behaviours for some risk groups. Consequently, RI was classified into one of the following four types:

- Low risk: index lower than 10
- Intermediate risk: index between 10 and 60
- High risk: index between 60 and 120
- Very high risk: index higher than 120.

In the same way, it was also possible to establish similar behaviours for indices in three ranges of preprandial glucose: 80–120 mg/dL (range 1), 130–190 mg/dL (range 2), and 200–240 mg/dL (range 3).

To validate the relationships referred to above, a MCS study was then carried out. MCS was used to calculate the probability of the different hypo- and hyperglycaemic events for each preprandial glucose range. To reduce the number of MCS trials required, a reference model for the preprandial glucose ranges was proposed. This model corresponded to the value for preprandial glucose with least variation in each range. To establish the reference model for each preprandial glucose range, the χ^2 test was used as:

$$\chi^2 = \sum_{i=1}^{n} \frac{(O_i - E_i)^2}{E_i}, \tag{5.6}$$

where O_i is the observed frequency of the preprandial glucose value, E_i is the reference model, and n is the number of cells in the table. In our case, the number of cells was 12, which was determined by the three ranges of preprandial glucose and the four types of risk. The χ^2 statistic can then be used to calculate a p value by comparing the value of the statistic to a χ^2 distribution. Because there were two independent variables (preprandial glucose range and type of risk), six degrees of freedom were established for the χ^2 test. The reference model was chosen as the preprandial glucose that presented the lowest p value with respect to the different preprandial glucose values in each range.

Based on the result of the χ^2 test, the reference models selected for each preprandial glucose range were: 100, 160, and 220 mg/dL, as indicated by each ellipse in Figure 5.5. The null hypothesis formulated was that $p > \alpha$. The significance level α was set as 0.05. The resulting p value for 97% of the preprandial glucose was greater than α, so the null hypothesis was accepted. This indicates that the distribution of RI values for the reference model and a high percentage of preprandial glucose in the same range do not show variation.

5.2.4 Results of RI validation

Once a reference model was proposed for each preprandial glucose value corresponding to the reference model, 19,500 MCSs were performed for the variation in food intake and bolus insulin described in Section 5.2.1. In the MCSs, parameter uncertainty was represented in terms of normal probability distributions. The occurrence of hypo- or hyperglycaemic events was then computed for each MCS. An event of severe hyperglycaemia was considered to occur when the maximum glucose value was greater than 250 mg/dL and mild hyperglycaemia when it was between 150–250 mg/dL. Severe hypoglycaemia was considered to occur when the minimum glucose value was lower than 36 mg/dL and mild hypoglycaemia when it was 36–70 mg/dL.

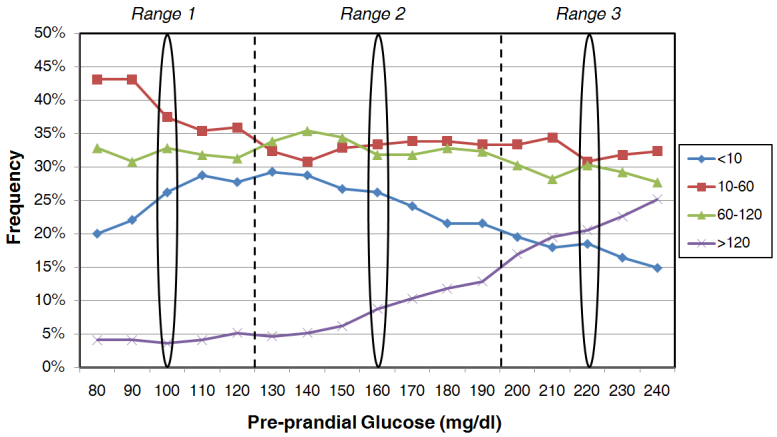

Figure 5.5: RI value distribution versus preprandial glucose. Preprandial glucose with least variation in each range is indicated by an ellipse.

The percentage of scenarios in which hypo- or hyperglycaemic events occurred in the MCSs was calculated for each preprandial glucose reference model. An analysis of each event according to the value of RI was then performed, considering the ranges of RI previously described (<10, 10–60, 60–120, and >120). These results are shown in Figure 5.6, classified according to preprandial glucose (euglycaemia, mild and severe hyperglycaemia).

When these results are analysed, the information contained in RI is clearly dependent on the preprandial glucose. For preprandial euglycaemia (Figure 5.6(a)), there is risk of mild hypoglycaemia and a significant risk of mild hyperglycaemia. An important risk of mild hypoglycaemia occurs for RI values between 10 and 60. For RI values between 60 and 120, the risk will translate into severe hyperglycaemia. Values greater than 120 reflect the occurrence of severe hypoglycaemia in 100% of cases. Mild hyperglycaemic events may occur for RI values in the lower and upper ranges, whereas a significant risk of severe hyperglycaemia will be reflected in the intermediate ranges. Therefore, if an insulin therapy yields RI values below 10, there will be no risk of severe hyperglycaemia or severe hypoglycaemia. Values between 10 and 60 will indicate a risk of mild hypoglycaemia or severe hyperglycaemia. Values between 60 and 120 will predict a significant risk of severe hyperglycaemia. Finally, with RI values greater than 120, severe hypoglycaemia will occur.

In the case of preprandial values in mild hyperglycaemia (Figure 5.6(b)), there is a risk of severe hyperglycaemia for RI values between 10 and 60. For RI values greater than 60, this risk increase rapidly, reaching a probability of about 90%. A risk of mild hypoglycaemia can occur at RI values lower than 60, but when values greater than 60 are reached, there is a risk of severe hypoglycaemia. Similar behaviour is observed for preprandial values in the severe hyperglycaemia range (Figure 5.6(c)), except that the risk of severe hypoglycaemia is lower.

5.3 Interpretation of RI

Based on the results obtained in the validation of RI, a summary of the probability of mild or severe hypoglycaemic events and mild or severe hyperglycaemic events is depicted as a grid in Table 5.1. To construct this grid, a descriptive statistic, specifically a frequency analysis, was

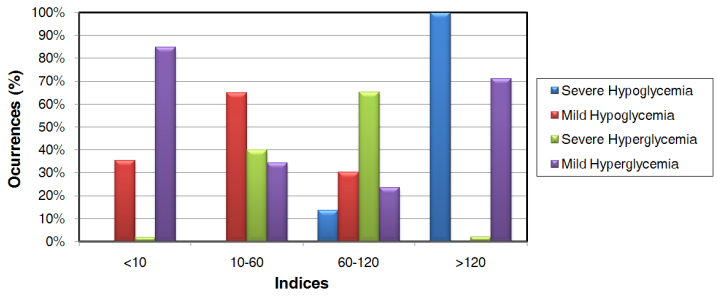

(a)

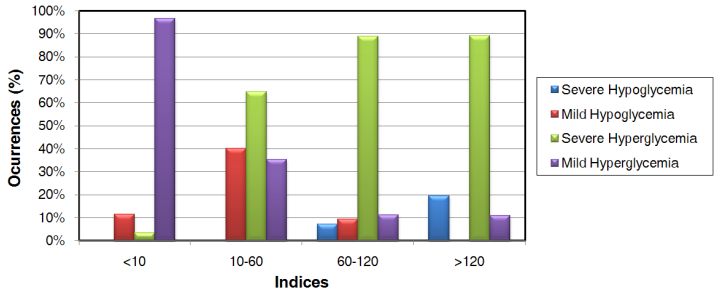

(b)

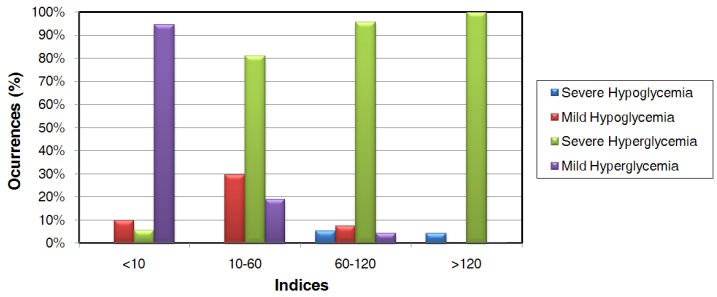

(c)

Figure 5.6: Percentage of scenarios in which hypo- and hyperglycaemic events can occur: (a) preprandial euglycaemia 100 mg/dL; (b) preprandial mild hyperglycaemia 160 mg/dL; (c) preprandial severe hyperglycaemia 220 mg/dL.

used to calculate the number of occurrences. For each one of the 19,500 MCS trials performed in each range of preprandial glucose, the percentage occurrence of each RI value (mild or severe hypoglycaemia and mild or severe hyperglycaemia) was calculated. These percentages were analysed and classified according to the probability of occurrence:

- Very low: less than 10%
- Low: between 10% and 30%
- Moderate: between 30% and 50%
- High: between 50% and 80%
- Very high: higher than 80%.

A percentage of risk occurrences lower than 10% indicates a very low risk probability, and is represented on the grid by cyan boxes. Percentages between 10% and 30% represent a low risk probability (lavender blue boxes); a moderate risk probability is indicated for percentages between 30% and 50% (medium purple boxes). A high risk probability occurs when the percentage is between 50% and 80% (azure boxes). Finally, a percentage higher than 80% represents a very high risk probability (dark azure boxes). White boxes in the Table 5.1 indicate no risk.

Pre-prandial Glucose	Risk Index	Hypoglycemia		Hyperglycemia	
		Mild	Severe	Mild	Severe
Euglycemia	<10				
	10-60				
	60-120				
	>120				
Mild Hyperglycemia	<10				
	10-60				
	60-120				
	>120				
Severe Hyperglycemia	<10				
	10-60				
	60-120				
	>120				

Probability: Very Low — Low — Moderate — High — Very High

Table 5.1: Probability of hypo- and hyperglycaemia classified according to preprandial capillary glucose and the RI.

To check whether the probabilities shown in Table 5.1 represent the risk probabilities for different therapies, RIs for different scenarios were calculated. Table 5.2 shows RIs for different bolus insulin–meal time pairs for each preprandial glucose range, classified by severe and mild hypoglycaemia, and severe and mild hyperglycaemia risk indices. The time column indicated in the table corresponds to the meal time after the bolus insulin is administered. The total index is shown in the last column.

Examples of the blood glucose responses for selected bolus insulin–meal time pairs, indicated in the colours used in Table 5.2, are shown in Figure 5.7. This figure illustrates different scenarios for preprandial glucose values in euglycaemia, mild hyperglycaemia, and severe hyperglycaemia. The red solid line corresponds to a scenario with RI values <10; the blue dashed line corresponds to a scenario with RI values in the 10–60 range; the green dotted line shows RI values in the 60–120 range; and the magenta dash-dotted line corresponds to RI values >120 (see Table 5.2).

With euglycaemic preprandial glucose, an RI value <10 corresponds to a bolus insulin–meal time pair producing the envelope closest to euglycaemia (red solid line in Figure 5.7(a)). When severe and mild hyperglycaemic episodes and/or mild hypoglycaemic episodes occurred during the simulation, an intermediate RI value (10<RI<60) was generated (blue dashed line, Figure 5.7(a)). A high risk (60<RI value<120) appears when sustained hyperglycaemia is present and/or mild hypoglycaemia is produced (green dotted line, Figure 5.7(a)). Finally, an RI value >120 arises when there is severe hypoglycaemia for a long time (magenta dashed-dotted line, Figure 5.7(a)). These risks relate to the probabilities listed in Table 5.1.

Preprandial Glucose (mg/dL)	Bolus (IU)	Meal (g)	Meal (min)	Hypoglycaemia Severe (Index)	Hypoglycaemia Mild (Index)	Hyperglycaemia Severe (Index)	Hyperglycaemia Mild (Index)	Total Index
100	4.5	40	45	0.00	0.15	0.00	0.23	**0.38**
	2.5	40	60	0.00	0.32	0.00	6.85	7.17
	4.5	60	15	0.00	0.00	3.96	6.49	10.45
	7.5	80	0	0.00	35.16	14.66	1.78	**51.60**
	3.5	60	60	0.00	2.32	63.29	1.07	**66.68**
	4.0	60	15	0.00	3.36	101.96	0.46	105.78
	9.0	80	0	85.44	29.44	6.79	1.59	123.26
	7.0	60	0	119.40	35.52	0.00	0.15	**152.07**
160	7.0	60	45	0.00	0.31	0.00	1.51	**1.83**
	3.0	40	30	0.00	0.00	0.00	8.59	8.59
	6.5	80	60	0.00	0.00	22.41	4.12	**26.53**
	7.0	60	0	0.00	50.00	8.00	1.93	59.93
	2.5	40	30	0.00	0.00	59.23	1.33	**60.56**
	9.0	80	15	27.54	49.19	6.72	2.00	85.45
	4.0	80	45	0.00	0.00	120.44	0.45	**120.89**
	10	80	0	138.52	21.24	11.83	1.24	172.83
220	9.0	80	60	0.00	1.50	0.00	2.62	**4.12**
	6.5	60	30	0.00	0.00	2.64	4.55	7.19
	5.5	40	0	0.00	3.42	9.92	2.08	15.42
	7.5	80	0	0.00	17.80	36.22	1.62	**55.64**
	4.5	60	15	0.00	0.00	57.35	4.62	**61.97**
	8.0	60	0	27.54	36.70	15.64	1.34	117.38
	9.5	80	15	0.00	29.11	13.88	1.75	**120.10**
	2.0	60	30	138.52	0.00	171.97	0.75	172.72

Table 5.2: Examples of risk indices for each preprandial glucose value with different bolus insulin doses and meal time combinations.

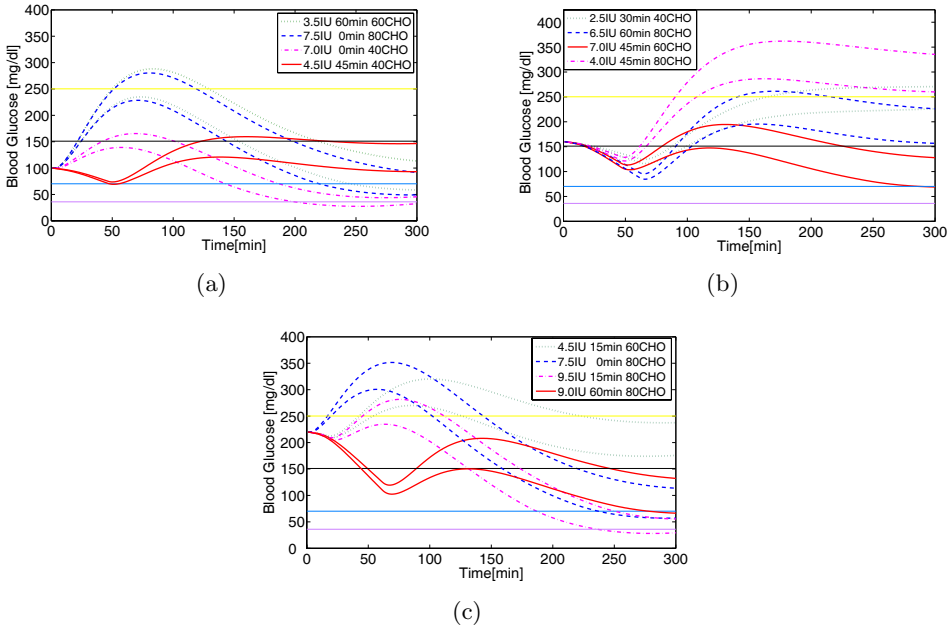

Figure 5.7: Blood glucose response for 5 h considering preprandial glucose: (a) euglycaemia, (b) mild hyperglycaemia, and (c) severe hyperglycaemia. The red solid line indicates RI values less than 10, the blue dashed line represents RI values between 10 and 60, the green dotted line represents RI values between 60 and 120, and the magenta dashed−dotted line represents RI values greater than 120.

Similarly, Figure 5.7(b) illustrates scenarios with preprandial glucose values of 160 mg/dL. As observed, RI value is proportional to the presence of sustained hyperglycaemia. Figure 5.7(c) illustrates the scenarios for a preprandial glucose value of 220 mg/dL. Similar conclusions are drawn. The lowest index indicates that the glucose trajectory will converge on euglycaemia, with the lowest exposure to a hyperglycaemic state. On the contrary, the greatest risk occurs when there is an excess (magenta dashed-dotted line) or lack (green dotted line) of insulin.

These results show that there are some risks according to the probabilities shown in Table 5.1.

5.4 Worst-case Prediction of Hypo- and Hyperglycaemic Events

A methodology has been developed to evaluate postprandial hypo- and hyperglycaemic events based on the worst-case glucose excursions (García-Jaramillo et al., 2009b). In Chapter 4, different models representing the glucose–insulin system have been described that consider intra-patient variability and other sources of uncertainty. The worst case is obtained from the prediction of glucose excursions derived from several interval models. For this purpose, it is necessary to adjust the parameters of each model to reflect the "same" patient. For more information about parameter adjustment, a comparative study of three interval models was performed in Chapter 4 (Section 4.4), for which the parameters of each model were adjusted to accommodate intra-patient variability.

To apply this methodology, the postprandial glucose excursions are first predicted for each glucose–insulin interval model (Model_i, $i = 1, \ldots, n$) for which intra-patient variability and uncertainty in the initial state, food intake, and insulin dose can be considered. The worst case is obtained by considering the envelope that includes all the predicted glucose excursions of each model (Model_i, $i = 1, \ldots, n$) (see Figure 5.8). The worst case allows the estimation of the probability of experiencing a postprandial hypo- or hyperglycaemic event independently of the model used.

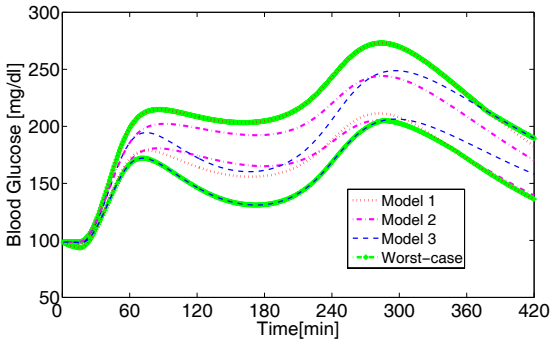

Figure 5.8: The worst case is indicated by thicker green line, for model 1 (red dotted line), model 2 (magenta dashed-dotted line), and model 3 (blue dashed line).

Finally, the risk of a hypo- or hyperglycaemic event can be predicted for the worst case using RI, according to the metrics previously established by the physician. For the different examples

of the methodology presented in this section, hyperglycaemia is considered relevant only 2 h after a meal. A measurement of plasma glucose 2 h after the start of a meal is practical, generally approximates the peak value in patients with diabetes, and provides a reasonable assessment of postprandial hyperglycaemia (American Diabetes Association, 2001).

Therefore, in this case the weighting function $\gamma(t)$ used to calculate RI is:

$$\gamma(t) = \begin{cases} 0 & 0 \leq t < 60 \\ 0 & 60 \leq t < 120 \\ 1 & 120 \leq t < 180 \\ 1.25 & 180 \leq t < 240 \\ 1.5 & 240 \leq t < 300. \end{cases}$$

A scheme for the prediction of hypo- and hyperglycaemic events is shown in Figure 5.9.

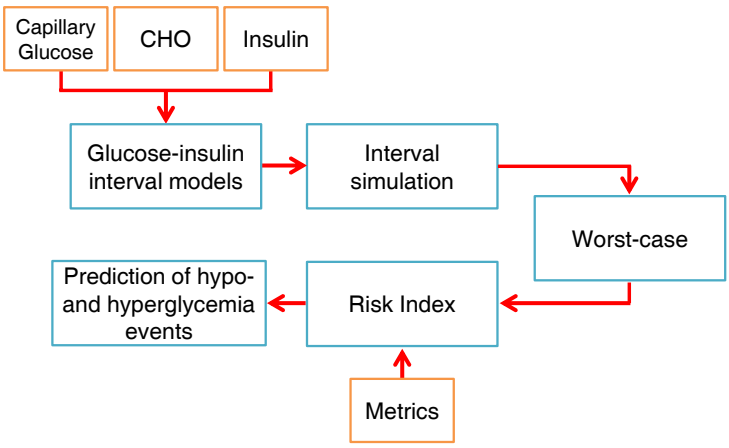

Figure 5.9: Methodology used to evaluate postprandial hypo- and hyperglycaemic events considering the worst case.

By analysing the example presented in Figure 5.8, it can be clearly seen that the probability of experiencing severe hyperglycaemia is between 245 and 340 min and that of experiencing mild hyperglycaemia is between 121 and 244 min and between 341 to 420 min (see Figure 5.10).

An example of this methodology applied to postprandial glucose excursions predicted with two insulin action and glucose kinetics interval models (Hovorka et al. (2004) and Dalla Man et al. (2007b)) for a 5 h period after a meal is presented. A virtual patient from a validated glucoregulatory model reported in the literature (patient 2) (Hovorka et al., 2002) is considered. The degrees of uncertainty in the patient's insulin sensitivity and the carbohydrate contents of the planned meal were established. The worst-case envelope are used to evaluate severe and mild hypo- and hyperglycaemic events.

For this patient, 65 different scenarios were evaluated, considering:

- Preprandial glucose: 150 mg/dL

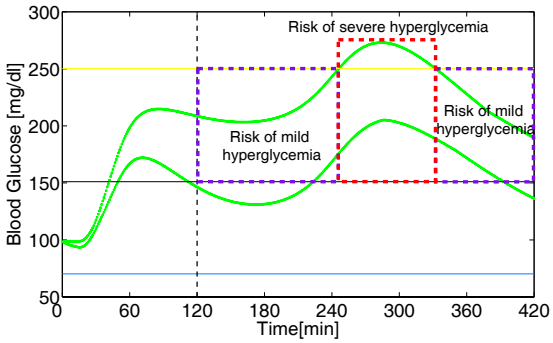

Figure 5.10: Example of risk prediction considering the worst case. Severe and mild hyperglycaemic events are indicated by red and purple rectangles, respectively. The vertical dashed line indicates the relevance of hyperglycaemia 2 h after a meal.

- Food intake: 60 g with 5% variation
- Bolus insulin: thirteen insulin doses in increments of 0.5 IU selected within the range of 2–10 IU
- Mealtimes: 0, 15, 30, 45, and 60 min (after bolus insulin)
- Insulin sensitivity parameters: S_{IT} with 11% variation, S_{ID} 8% variation and S_{IE} 2% variation.

The severe and mild hypo- and hyperglycaemic events were calculated according to RI for the worst-case prediction (see Figure 5.11). The RI value varies in the range 1.54–142.7, performing well in all cases according to clinical judgments.

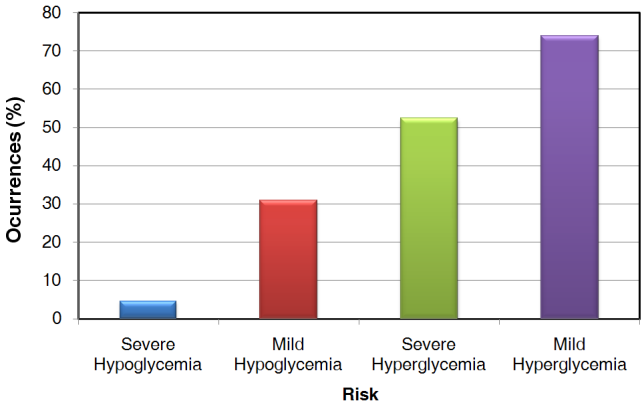

Figure 5.11: Percentage of scenarios in which hypo- and hyperglycaemic events can occur.

Of the scenarios, 52.31% presented a risk of severe hyperglycaemia for a long time, 73.85% mild hyperglycaemia, 4.62% severe hypoglycaemia, and 30.77% mild hypoglycaemia. The RI values for some scenarios are shown in Table 5.3.

Bolus (IU)	Meal (min)	Hypoglycaemia				Hyperglycaemia				Total Index
		Severe		Mild		Severe		Mild		
		Index	Duration	Index	Duration	Index	Duration	Index	Duration	
6.5	45	0.00	0	0.00	0	0.00	0	2.28	143	2.28
5.5	30	0.00	0	0.00	0	0.00	0	5.47	180	5.47
6.0	15	0.00	0	2.43	31	0.00	0	3.92	113	6.35
5.0	30	0.00	0	0.00	0	4.67	14	6.71	164	11.38
8.0	45	0.00	0	54.55	100	0.00	0	0.30	44	54.85
7.5	15	26.35	26	55.41	86	0.00	0	1.85	55	83.61
3.5	30	0.00	0	0.00	0	86.50	180	0.00	0	86.50
7.5	0	73.78	64	35.29	59	0.00	0	2.09	44	111.16
2.5	30	0.00	0	0.00	0	20.68	180	0.00	0	120.68
2.0	45	0.00	0	0.00	0	135.88	180	0.00	0	135.88
8.0	0	113.70	87	26.77	47	0.00	0	2.23	34	142.70

Table 5.3: Examples of RI values considering the worst-case.

The risk was lowest when the bolus insulin–meal time pair produced an envelope closer to euglycaemia, i.e., when a low risk of hypo- and hyperglycaemia was produced. The RI value increases when severe hyperglycaemia and/or mild hypoglycaemia occur. The risk is high when some cases of severe hypoglycaemia and/or severe hyperglycaemia appear. Finally, severe hypoglycaemia and/or severe hyperglycaemia for a long time generated a very high risk, as shown in the duration column (Table 5.3). In the latter case, the hyperglycaemia that occurred 2 h after intake produced the highest RI values, especially those generated at great distances from the intake point. The influence of the weighting factor $\gamma(t)$ is apparent in these situations.

5.5 Summary

In this chapter, the objective was to develop a methodology to quantify the risk of suffering different grades of hypo- and hyperglycaemic episodes in the postprandial state. When intra-patient variability and uncertainty in the carbohydrate content are considered, a safer prediction can be made of possible hyper- and hypoglycaemic episodes induced by the insulin therapy tested.

The RI proposed in this work is based on metrics that have been established according to the clinical relevance of each episode of hypo- and hyperglycaemia. The relevance of these metrics can be clearly appreciated in risk interpretation. Moreover, an intensive study analysed the relationship between different ranges for the value of RI and the occurrence of mild and severe hypoglycaemic and hyperglycaemic events. These events were also calculated in terms of the worst-case predictions for the models of Hovorka et al. and Dalla Man et al. However, the methodology developed here can be applied to any interval model.

Chapter 6

Insulin Dosage Optimization

The calculation of an insulin dose is a complex process in which numerous factors must be taken into account, such as the preprandial glucose level, meal composition, insulin sensitivity, active insulin, and intra-patient variability. The inappropriate calculation of these factors can lead to either under- or overdosing of prandial insulin (Toussi et al., 2008), resulting in undesired glucose fluctuations.

Because of the difficulty of selecting the correct insulin dose and the problem of hyper- and hypoglycaemic episodes in T1DM patients, dosage-aid systems are very useful for these patients. In this chapter, a novel method is presented for estimating the doses and injection times relative to meal times required for low-risk intensive insulin therapy. The algorithm is based on the interval simulation of an individual patient's glucoregulatory model. For this purpose, a library of interval models of the physiological subsystems of glucose regulation was presented in Chapter 4. The predicted envelopes of glucose excursions are used to calculate RI values for severe and mild hyper- and hypoglycaemic episodes (García-Jaramillo et al., 2009a; Calm et al., 2009). This information is integrated into a dosage-aid system to calculate the optimum insulin dose and injection-to-meal time with the lowest risk according to the model (García-Jaramillo et al., 2011a).

The system presented is constructed in a modular way and can be used with other glucoregulatory models, as well as in a feed-forward action in closed-loop glucose control.

6.1 Background on Insulin Dosage

T1DM patients are often advised to use dose adjustment guidelines to calculate their doses of insulin for each self-administration event. However, they may follow their guidelines totally, partially, or not at all. Therefore, blood glucose levels can be affected by the adherence of patients to these guidelines (Toussi et al., 2008).

The bolus calculator is one of the most common methods used to calculate insulin doses for continuous subcutaneous insulin infusions (CSII). It uses rules based on the amount of carbohydrate to be ingested, insulin sensitivity expressed as an insulin-to-carbohydrate ratio, and the active insulin (Walsh et al., 2010). Another calculator based on a nutrition database indicates to the patient the type of boluses needed to deliver an extended bolus for meals (Pankowska and Blazik, 2010). However, many patients might not estimate their carbohydrates accurately, so an under- or overdose of prandial insulin can be calculated.

Precise carbohydrate counting was associated with lower HbA1c in one study of children with diabetes (Mehta et al., 2009), and inaccurate carbohydrate counting has been identified as one of the two major sources of error in predicting blood glucose levels, together with blood glucose monitor inaccuracy (Kildegaard et al., 2007). A novel tool used to achieve greater accuracy in estimating the insulin bolus ("bolus guide") was presented by Shapira et al. (2010), and this system is based on ranges of carbohydrate load.

A brief chronological summary of the different methods used to support patients in the insulin dosage process is presented here for educational purposes and decision support. The first advisory algorithms for intensive insulin therapy were presented in the early 1980s. Skyler et al. (1981) developed an algorithm in which heuristic rules and preprandial glucose measurements were used to tune the insulin dose. Similarly, the use of a pocket computer to help to determine the proper insulin dose for people with diabetes was formulated by Chanoch et al. (1985) based on the algorithm proposed by Jovanovic and Peterson (1982). To optimize the insulin dose, the algorithm takes into account patient-specific parameters, such as weight, sex, and physical activity, together with the carbohydrate content of meals and blood glucose measurements.

Schiffrin et al. (1985) also explored the use of a computer to adjust short- and intermediate-acting insulin doses. Their algorithm used preprandial blood glucose measurements and was based on a two injections per day strategy. However, it also used a linear dose calculation and variable maximal value. The same team later presented an advanced algorithm with complete linear regulation (Albisser et al., 1986). An algorithm for dose adjustment combined with an evaluation program for a personal computer that contains a control matrix structured according to Skyler's algorithm was published by Pernick and Rodbard (1986).

Schrezenmeir and colleagues developed algorithms for different therapies using a pocket computer: the computer-assisted meal-related insulin therapy (CAMIT) (Schrezenmeir et al., 1985, 1990) for CSII (Schrezenmeir et al., 1987), and the computer-assisted conventional insulin therapy (CACIT) (Beyer et al., 1990).

The use of a computer algorithm in children was investigated by Chiarelli et al. (1990), who compared insulin doses adjusted with computer algorithms with those adjusted with manual methods in two matched groups of a priori well-controlled diabetic children. Their results showed fewer episodes of hypoglycaemia in the computer-assisted group. However, the same comparison was made by Peters et al. (1991), and their conclusion was that the metabolic control and safety of the two techniques were similar. Several algorithms that have been developed to assist in the processes of diabetes self-management for better blood glucose control have been presented by Albisser (2003).

Many systems have also been developed to educate and support the patient in the process of insulin dose estimation (Lehmann and Deutsch, 1995). The majority of these systems are intended for educational purposes, as listed below. The computer program DIABLOG was developed by Biermann and Mehnert (1990) to graphically represent glucose and insulin profiles for a 24 h period for a patient-specific insulin-pump therapy. In 1992, Lehmann and Deutsch (1992a) designed one of the most popular educational systems for diabetics based on a simple model of the interaction between glucose and insulin in the human body (Lehmann and Deutsch, 1992b; Lehmann, 1999, 2001) called the Automated Insulin Dosage Advisor (AIDA). This tool helps the user (patients or health-care workers) to understand the glucoregulatory system in

patients with T1DM.

Another educational tool that allows the patient to predict his/her daily profiles of glycaemia and insulinaemia based on a mathematical model is the Karlsburg Diabetes Management System (KADIS) (Rutscher et al., 1994). The models developed by Puckett and Lightfoot (1995) for glucose kinetics and the model of glucose absorption developed by Hovorka et al. (2002) are used to predict glucose profiles for GlucoSim (Agar et al., 2005), a Web-based educational simulation package that computes the dynamics of glucose–insulin levels in the human body.

The Särimner diabetes simulator was created during the late 1980s and was validated by patients and professionals in the early 1990s (Hedbrant et al., 1991). Its purpose is to create a learning situation to teach and communicate intuitive thinking in relation to insulin dose decisions. Another educational tool called EduDIABNET, which is based on a physiological model represented by a quantitative causal probabilistic network, was proposed by Hernando et al. (2001). Later, Hedbrant et al. (2007) presented the experiences from previous work with teenagers using the Särimner diabetes simulator. More recently, a novel educational tool, the Glucose–Insulin and Glycemic Index Web Simulator (GIGISim) (Bulka et al., 2009), has been proposed, based on artificial intelligence. The postprandial glucose profiles of T1DM patients are simulated according to a human carbohydrate metabolism model.

Decision-support systems for people with diabetes have also been devised, such as the Diabetes Advisory System (DIAS) (Cavan et al., 1996, 1998; Hejlesen et al., 1997), which incorporates a model of human carbohydrate metabolism implemented in a Bayesian network, whereas two feed-forward neural networks were used by Mougiakakou and Nikita (2000): the first neural network provides the insulin regime, which is applied as the input into the second neural network, which estimates the appropriate insulin dose for a short-term period. The Intelligent Dosing System (IDS) (Cook et al., 2005) is an intelligent dosing strategy that suggests the average daily insulin dose to patients with predominantly type 2 diabetes between clinic visits. This approach is somewhat related to run-to-run control, but leaves decisions about how to distribute the insulin dose throughout the day to the clinician.

Insulin dosage advisory systems have also been incorporated into insulin pumps (Takahashi et al., 2008; Zisser et al., 2008) based on proportionality rules that consider the insulin/carbohydrate ratio, insulin sensitivity, and the insulin remaining from previous injections (insulin on board).

In the area of telemedicine, several platforms have been proposed for diabetes monitoring and management (Bellazzi, 2008). The Vie-diab system (Popow et al., 2003) creates a daily colour-coded graph plot of the patient's data that allows the physician to easily track the patient's management of his/her diabetes. SMARDIAB was recently developed by Mougiakakou et al. (2010) and is designed to support the monitoring, management, and treatment of patients with T1DM. This platform allows the optimization of diabetes treatments with computational tools for the real-time personalized estimation of the infusion rate, for which the patient has a user-friendly Web and mobile-phone interface.

In recent years, different advisory/control systems have been developed that take into account the repetitive nature of an intensive glucose control therapy regimen, because patients must perform the same tasks each day to adjust their insulin therapies. Some of these systems, based on a run-to-run strategy, have been presented by Zisser et al. (2005), Owens et al. (2006),

and Palerm et al. (2007a,b). They considered a proportional correction term for the reference error. Therefore, after each day, the insulin doses are updated, looking for an eventual reference value. An extension of previous approaches was proposed by Campos-Delgado et al. (2008) that follows the run-to-run philosophy using a Proportional Integrative (PI) correction strategy and combining rapid- and slow-acting insulins.

In summary, most insulin dosage systems are intended for educational purposes, and only a few decision-support systems have been developed. Most of these support systems do not take into account intra-patient variability or different sources of uncertainty. The main contribution of the tool proposed in this chapter is to integrate these uncertainties into a dosage-aid system.

6.2 Bolus Insulin Dose and Injection-to-Meal Time Optimization

Patient-specific bolus insulin optimization unavoidably requires the evaluation of its impact on postprandial glucose, so sufficiently accurate short-term postprandial glycaemia predictions are necessary. As mentioned in Chapter 4, a glucose prediction tool that considers different sources of uncertainty has been developed in this work, so a worst-case approach is introduced to optimize the insulin dose and injection-to-meal time. With this worst-case approach, the prediction of possible hyper- and hypoglycaemic episodes induced by insulin therapy, based on an individual patient's parameters, is more robust. Finally, this information is integrated into a dosage-aid system, where the optimal insulin dose and injection-to-meal time can be calculated.

To accommodate the uncertainty in glucose prediction, it is necessary to consider the dynamic model $\mathbf{\Sigma}(\mathbf{x}, \mathbf{u}; \mathbf{p}, \mathbf{x_0})$, where $\mathbf{x}$ is the state vector, $\mathbf{u}$ is the input vector, $\mathbf{p}$ is the parameter vector, and $\mathbf{x_0}$ is the initial state vector. The input vector $\mathbf{u}$ contains information about the meal, insulin injection, and the respective times. If uncertainty is introduced into model $\mathbf{\Sigma}$, considering the uncertain parameters, inputs, and initial states (these correspond to the interval vectors denoted $\mathbf{P}$, $\mathbf{U}$, and $\mathbf{X_0}$, respectively), an interval extension of model $\mathbf{\Sigma}$ is obtained. Then, using MIA, the glucose excursions are calculated taking into account all sources of uncertainty.

The safety of the predicted manifold postprandial glucose excursions is quantified using a cost function J, which represents the risk index (RI). RI comprises metrics that classify hyper- and hypoglycaemic episodes of the glucose prediction provided by the dynamic model with uncertainties (García-Jaramillo et al., 2009a) (see Chapter 5 for more information). The cost function should be easily tunable because the therapeutic goal is patient-specific.

Therefore, given the interval extension of the model, denoted as $\mathbf{\Sigma}(\mathbf{X}, \mathbf{U}; \mathbf{P}, \mathbf{X_0})$, the optimal insulin dose and timing are formulated as the following optimization problem:

$$(t_{im}, d_i) = argmin_{t_{im}, d_i} J(\mathbf{\Sigma}(\mathbf{X}, \mathbf{U}; \mathbf{P}, \mathbf{X_0})),$$

where d_i is the bolus insulin dose and t_{im} denotes the relative time between the insulin injection and meal ingestion.

To calculate the dose and injection-to-meal time that minimize the cost function, an initial dose and injection-to-meal time are estimated and taken as the starting point of a two-dimensional grid search (see Section 6.2.1). The initial dose is calculated according to rules for

the carb factor and correction factor, and the initial injection-to-meal time is established according to the preprandial blood glucose. The RI value is then computed for each pair of bolus insulin and injection-to-meal time on the grid. Finally, the optimization algorithm selects the solution that generates the lowest risk of hyper- and hypoglycaemia. Other useful information can be extracted from this analysis, such as the dose that allows greater injection time flexibility, i.e., the insulin dose that produces a similar risk with different injection times.

Next, the optimization strategy used is presented.

6.2.1 Grid search method

To calculate the optimum insulin dose and injection-to-meal time, a two-dimensional grid search can be performed because the input space is discrete. The grid is built from a starting point composed of an initial insulin dose and an initial injection-to-meal time (start time for the meal after the insulin dose). The steps used to build the grid search are detailed below.

First, the starting point is calculated to be the centre of the exploratory grid. The initial insulin dose (II) is computed based on heuristic rules and the injection-to-meal time (IM) is established according to the preprandial blood glucose. II is calculated using the carb factor and correction factor rules. These rules are based on the patient's total daily dose (TDD) and the factor value associated with each rule (i.e., 450 or 500 for the carb factor and 1500 or 2000 for the correction factor). To determine the carb factor (the number of grams of carbohydrate that will be metabolized by one unit of insulin), the "500 Rule" is used for rapid-acting insulin and the "450 Rule" for short-acting insulin (Walsh and Roberts, 1994).

In contrast, the "1500 Rule" for regular short-acting insulin and the "2000 Rule" for rapid-acting insulin are used to determine the correction factor, which estimates how far the blood glucose level is likely to drop per unit of insulin (Hanas, 2004). The correction factor is only calculated when the patient has high levels of glucose and requires a bolus of insulin to bring it down.

The carb factor and correction factor are then given by factor/TDD.

Example 6.1 .

1. Carb factor using the 450 Rule: for a TDD=25 IU.

   carb factor=$\frac{450}{25}$ = 18 g of carb metabolized by 1 unit of insulin.

2. Correction factor using the 2000 Rule: for a TDD=25 IU.

   correction factor=$\frac{2000}{25}$ = 80 mg/dL per unit of insulin.

An analysis of the different formulae proposed to derive the pump doses from the TDD has been presented by Walsh et al. (2010). The formulae were initially empirical, but were later based on research conducted by single clinics.

Using the planned carbohydrate (grams) intake, the carb factor, and the correction factor, II is calculated based on the preprandial glucose measurement GC (mg/dL) as:

$$II = \begin{cases} \dfrac{\text{CHO}}{\text{carb factor}} + \dfrac{GC - G_{objmin}}{\text{correction factor}} & \text{if } GC < G_{objmin} \\ \dfrac{\text{CHO}}{\text{carb factor}} + \dfrac{GC - G_{objmax}}{\text{correction factor}} & \text{if } GC > G_{objmax} \\ \dfrac{CHO}{\text{carb factor}} & \text{if } G_{objmin} \leq GC \leq G_{objmax} \end{cases} \tag{6.1}$$

where G_{objmin} and G_{objmax} are the minimum and maximum glucose objectives, respectively, defined to regulate blood glucose to around the normal level (target). Therefore, subtracting the glucose objective from the preprandial glucose level will determine the reduction (mg/dL) in insulin required. To calculate II in this work, the minimum glucose objective was established as 70 mg/dL and the maximum as 150 mg/dL.

The other component from the centre of the grid search is set. In accordance with preprandial glucose, different values for IM (Hanas, 2004), which indicates the start time for the meal after the regular insulin dose, were established as shown in Table 6.1.

Blood Glucose (mg/dL)	IM (min)
< 70	0
$70 - 140$	30
$140 - 180$	45
> 180	60

Table 6.1: Initial meal time (IM) during regular insulin therapy according to preprandial glucose.

The blood glucose reading before a meal will indicate when it is appropriate to administer the injection. For instance, when the blood glucose is high, the patient can wait 45–60 min before eating. However, if the blood glucose is low, the patient should leave the injection until it is time to eat. For a normal glucose level, the patient should administer the insulin at least 30 min before eating. In this work, II was established for a regular short-acting insulin, but it can be modified for other types of insulin, based on clinical judgements.

Once the initial estimate is calculated, the exploratory grid is defined as the Cartesian product $(II + n_i \Delta I) \times (M_1 + n_t \Delta M)$, where $n_i = -k_i, \ldots, k_i$ (with one step size) indicates the range of the insulin grid size, k_i, that allows the lower and upper limits of the insulin grid to be established, and ΔI is the increase in bolus insulin. With respect to the injection-to-meal time, the lower limit of the grid is denoted by M_1, the range of the grid size is established by $n_t = 0, \ldots, k_t$ (with one step size), k_t, which allows the upper limit of the grid to be set, and finally, ΔM indicates the granularity of the injection-to-meal time. The values considered in this study are: $\Delta I = 0.5$, $k_i = 6$, $M_1 = 0$, $k_t = 4$, and $\Delta M = 15$. The element of the grid with the lowest RI value is finally chosen.

Example 6.2 A general scenario is considered to build the two-dimensional grid search.

- Preprandial glucose measurement: 180 mg/dL
- Food intake: 60 g
- TDD: 45 IU
- Insulin injection: regular short-acting insulin.

First, taking into account the type of insulin injection, the rule for the carb and correction factors is chosen and the centre of the exploratory grid is calculated as:

$$\text{carb factor} = \frac{450}{45} = 10 \text{ g} \qquad \text{correction factor} = \frac{1500}{45} = 33 \text{ mg/dL}.$$

Then, considering these factors, the food intake, and the preprandial glucose measurement, II is given by:

$$II = \frac{60}{10} + \frac{180 - 150}{33} = 7 \; IU,$$

and according to Table 6.1, IM is 45 min.

Next, the two-dimensional exploratory grid is defined as the following Cartesian product:

$$(4, 4.5, 5, 5.5, 6, 6.5, \mathbf{7}, 7.5, 8, 8.5, 9, 9.5, 10) \times (0, 15, 30, 45, 60)$$

Hence, the maximum grid size is ±3 IU and 0-60 min for the injection-to-meal time, as shown in Figure 6.1.

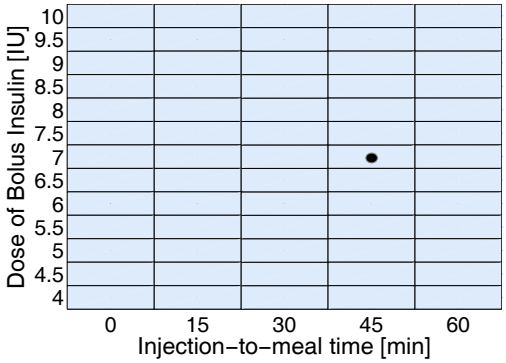

Figure 6.1: Example of a two-dimensional grid search. The point corresponds to the initial insulin dose and the initial injection-to-meal time.

6.2.2 Dose and injection-to-meal time optimization algorithm

Once the grid search is performed, an optimization algorithm is developed to obtain the insulin dose and injection-to-meal time that minimizes the risk of postprandial hyper- and hypoglycaemia. Algorithm 1 summarizes the main steps of this algorithm in a pseudocode form.

To simplify the presentation of the algorithm, the following notation and concepts are introduced.

- The metrics used in the computation of RI to quantify the clinical relevance of each episode of hypo- and hyperglycaemia.
  - h_s and h_m: Glucose ranges corresponding to severe and mild hypoglycaemia respectively
  - H_s and H_m: Glucose ranges corresponding to severe and mild hyperglycaemia respectively
  - αh_s, αh_m: Weights defined to quantify the relative importance of severe and mild hypoglycaemic events
  - αH_s, αH_m: Weights defined to quantify the relative importance of severe and mild hyperglycaemic events
  - $\gamma(t)$: weighting function to quantify the time occurrence of hyperglycaemia.
- The grid search is performed using the following steps:
  1. The initial bolus insulin dose II is obtained from the heuristic rules and the initial injection-to-meal time, IM, according to the values specified in Table 6.1 (Section 6.2.1).
  2. The grid size is calculated according to the step size established from the bolus insulin, ΔI, and the injection-to-meal time, ΔM, as well as the search range of the insulin dose n and the search range of the injection-to-meal time (initial=$M1$, final=$M2$).
  3. IM and II are used to initialize the list where the results for RI are stored.
- According to the established metrics, RI is calculated with the cost function, J, for each insulin dose and injection-to-meal time of the grid search. This RI is computed as a weighted sum of the risk for each severe (J_{hs}) and mild hypoglycaemic event (J_{hm}) and severe (J_{Hs}) and mild hyperglycaemic event (J_{Hm}). Finally, the results for J are stored for each insulin dose and injection-to-meal time pair and then sorted from lowest to highest. For more information about the RI, the reader is referred to Chapter 5.

Algorithm 1. Dose and meal time optimization.

Input:

Dynamical model with uncertainty $\mathbf{\Sigma}(\mathbf{X}, \mathbf{U}; \mathbf{P}, \mathbf{X_0})$

Meal size (grams CH)

Capillary Glucose (GC)

Metrics (h_s, h_m, H_s, H_m, α_{hs}, α_{hm}, α_{Hs}, α_{Hm}, $\gamma(t)$)

Output:

Sorted list $\pounds$ of mealtime, bolus insulin and associated risk index

1. Build grid search:

   Calculate initial estimate for bolus insulin dose (II) by means of heuristic rules

   Calculate initial mealtime (IM)

   $I1 := II - n\Delta I$, $I2 := II + n\Delta I$, ΔI:=granularity considered for the insulin dose.

   $M1 := 0$, $M2 := 60$, ΔM:=granularity considered for the mealtime.

   $\pounds := (IM, II, J(IM, II))$;

2. **for** $(Bolus\ insulin = I1 : \Delta I : I2)$
3. **for** $(Mealtime = M1 : \Delta M : M2)$
4. Compute glucose prediction envelopes (interval simulation)
5. Obtain hyperglycaemia and hypoglycaemia episodes and calculate J_{Hs}, J_{Hm}, J_{hs}, J_{hm}
6. Calculate risk index J
7. $\pounds := \pounds \cup (Mealtime, Bolus\ insulin, J)$
8. **end for**
9. **end for**
10. **return** sort_by_risk_index ($\pounds$)

6.3 Methodology Assessment

To demonstrate the feasibility of the proposed methodology, three different scenarios were considered for a virtual patient with nominal parameters, and predictions of the patient's postprandial glucose at 5 h intervals were used to predict the risk associated with a given therapy. The insulin dose and injection-to-meal time with the lowest risk were then calculated.

6.3.1 Scenarios

The following daily situation was evaluated for a virtual patient taken from Hovorka et al. (2002) (patient 2):

- Meal ingestion: 60 g of carbohydrate with 5% variation
- Insulin injection: regular insulin
- Insulin sensitivity parameters: S_{IT} with 11% variation, S_{ID} with 8% variation and S_{IE} with 2% variation according to the standard deviation presented in (Hovorka et al., 2002).

Three scenarios were considered, corresponding to preprandial glucose levels:

i) Initial euglycemia: 100 mg/dL

ii) Initial mild hyperglycaemia: 180 mg/dL

iii) Initial severe hyperglycaemia: 250 mg/dL.

For this example, the models presented in (Tarín et al., 2005) for subcutaneous insulin absorption and the Hovorka et al. insulin action and glucose kinetics interval model were combined to illustrate the glucoregulatory model. The Hovorka interval model is presented in Chapter 4 (Section 4.3.3).

6.3.2 Initial states

To run an interval simulation of the whole system, the initial states and inputs must be given. Because not all the states are measurable (in fact, only preprandial glucose measurements will be available), the initial state must be estimated. This is done by simulating the past history of the patient in terms of his/her insulin injections and meals. Because it is uncertain, the initial state will correspond to an interval vector.

In this study, three days were simulated for a given therapy, assuming that the patient followed the same regime every day. Starting from the real initial state, the interval values for the states at the beginning of the third day will be considered to represent the set of possible initial states the patient may experience.

6.3.3 Results

The algorithm was initialized using the insulin bolus calculated with Equation 6.1 and the injection-to-meal time (Table 6.1) as described in item 6.2.1. The search grid is built with increments of 0.5 IU and 15 min. The maximum grid size in this study was established as ± 3 IU and 0–60 min for the injection-to-meal time. A total of 65 grid points were then examined. However, the grid size can be modified according to the desired search area.

An example of RI calculation, in this case for scenario i), is shown in Table 6.2, which summarizes the results for low risk (index value <10), intermediate risk (index value of 10–60), high risk (index value of 60–120), and very high risk (index value >120). The initialization value obtained with the heuristic rules is an insulin dose of 5 IU injected 30 min before eating, which has an RI value of 5.36. The minimum RI value for hyper- and hypoglycaemia is 2.10, corresponding to an insulin dose of 6 IU administered 30 min before eating.

The metrics proposed in this work (see Chapter 5) were established according to the clinical relevance of every hyper- and hypoglycaemic episode. Therefore, these metrics can be modified by the physician according to the patient's medical history. The relevance of these metrics can be clearly appreciated in the results shown in Table 6.2.

Very high RI values occur when the insulin bolus–meal time pair produces severe hypoglycaemia for a long time and/or mild hyperglycaemia (index value of 125.15 in Table 6.2). There is also a high risk when the combinations produce the highest blood glucose level for a long time

Bolus (IU)	Meal (min)	Severe Hypoglycaemia Index	Mild Hypoglycaemia Index	Severe Hyperglycaemia Index	Mild Hyperglycaemia Index	Total Index
6.0	30	0.00	0.00	0.00	2.10	2.10
6.5	45	0.00	2.31	0.00	1.12	3.43
5.0	30	0.00	0.00	0.00	5.36	5.36
4.5	30	0.00	0.00	0.00	7.25	7.25
7.0	45	0.00	8.79	0.00	0.54	9.34
5.0	0	0.00	0.00	7.21	3.86	11.07
7.0	60	0.00	17.30	0.00	0.45	17.75
4.0	45	0.00	0.00	23.92	5.39	29.31
6.5	0	0.00	36.50	0.00	2.28	38.78
3.5	15	0.00	0.00	43.57	4.40	47.97
8.0	45	0.00	51.03	0.00	0.02	51.05
3.5	45	0.00	0.00	64.50	0.97	65.47
3.0	60	0.00	1.06	77.19	0.84	79.09
3.0	15	0.00	0.00	82.58	0.54	83.12
7.5	0	31.40	62.22	0.00	1.55	95.17
2.0	60	0.00	0.00	105.78	0.57	106.35
2.0	0	0.00	0.00	116.27	0.30	116.57
8.0	0	91.10	32.76	0.00	1.29	125.15

Table 6.2: Risk in scenario (i) is classified as: low risk (<10), intermediate risk (10-60), high risk (60-120), and very high risk (>120).

and/or mild hypoglycaemia (index values of 65.47–116.57).

When severe and mild hyperglycaemic episodes and/or mild hypoglycaemic episodes occur during the simulation, an intermediate RI value is generated (index values of 11.07–51.05). The lowest RI values (<10) all indicate mild hyperglycaemic episodes, and a few reflect mild hypoglycaemia (lasting for <20 min and with values close to those for euglycaemia). Hyperglycaemic episodes occurring within 2 h after ingestion generated a low level of risk. In contrast, hyperglycaemia occurring for long periods after food intake generated the highest RI values.

The previous results are also shown in Figure 6.2, where Figure 6.2(a), (c) and (e) show a two-dimensional grid with RI evaluation for each scenario. The area demarcated by the rectangle corresponds to the four lowest values for RI, and the points correspond to the initial insulin dose and the injection-to-meal time calculated with heuristic rules.

Another graphical interpretation can be drawn from these data that reflects the influence of the injection-to-meal time with respect to the insulin dose. For each injection-to-meal time, RI value associated with each insulin dose is placed in a continuous line, where RI values are expressed in logarithmic form to minimize the influence of their variability. In this way, the insulin dose and injection-to-meal time pair with the lowest risk is more easily detected. Similarly, it is possible to find the insulin dose that generates a similar risk for different injection-to-meal times in order to identify the insulin dose that allows more flexibility in the injection time. These interpretations can be seen in Figure 6.2, where (b), (d) and (f) show the influence of the meal time with respect to the bolus insulin dose.

For scenario i), the lowest RI values occur between 5.5 and 6.0 IU of insulin and between 15 and 30 min for the injection-to-meal time, with an RI value of <3.60 (see Figure 6.2(a). In this case, the combinations of bolus insulin doses and injection-to-meal times that produce fewer episodes of hyper- and hypoglycaemia are in the centre of the grid. The greatest risk occurs at the borders, corresponding to excess or insufficient insulin. This greatest risk with respect to

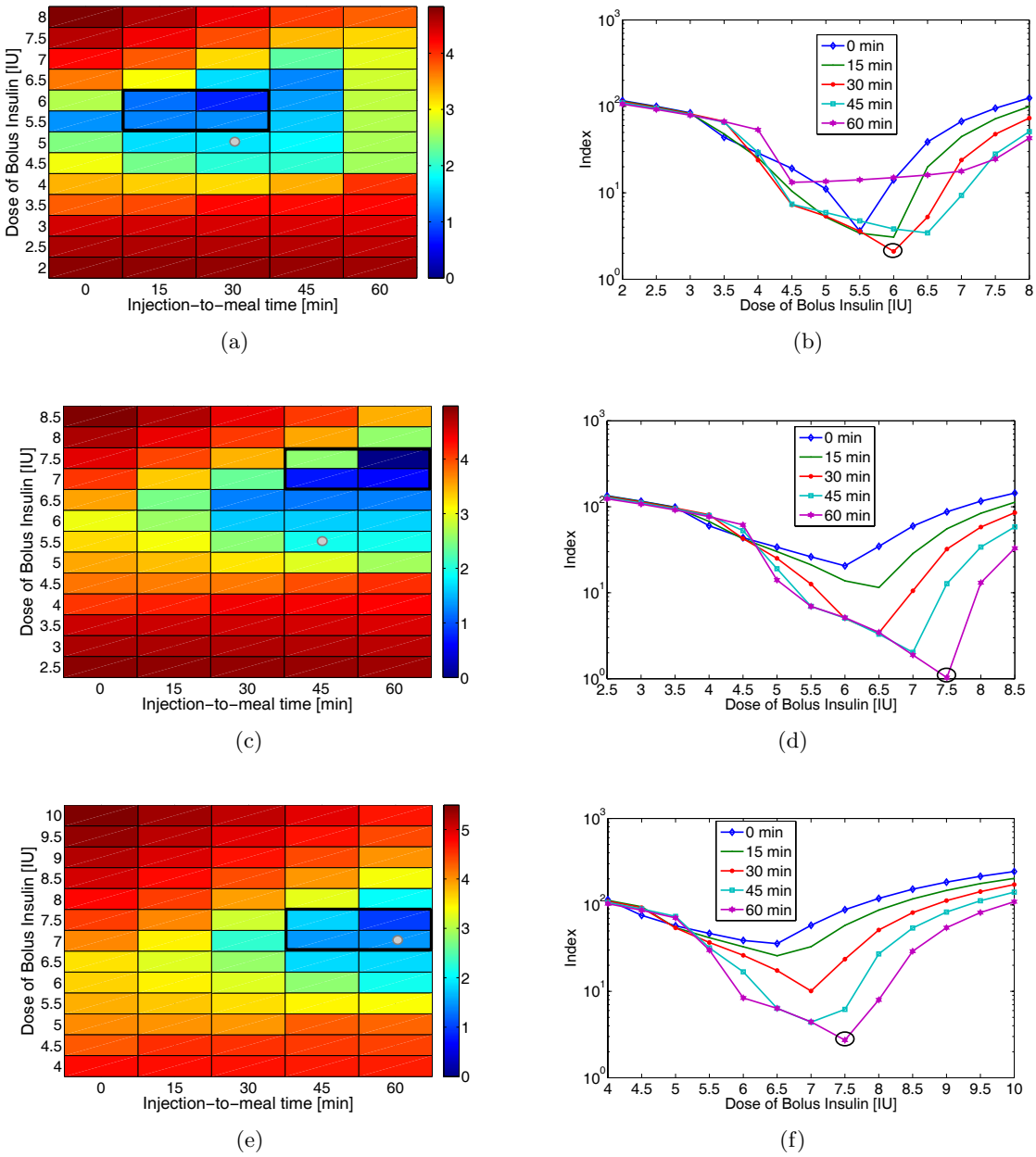

Figure 6.2: Grid-based optimization for scenarios i (a), ii (c), and iii (e). The points correspond to currently used heuristic rules. Relationship between insulin bolus and injection-to-meal time, with the optimal RI indicated by a circle for scenarios i (b), ii (d), and iii (f). The RI value is represented on a logarithmic scale.

the insulin dose is also evident in Figures 6.2(c) and (e), but in these cases, the corresponding injection-to-meal times are longer because of the preprandial glucose level.

For scenario ii), RI value is <3.42 when the insulin dose is between 7.0 and 7.5 IU and the injection-to-meal time is between 45 and 60 min (see Figure 6.2(c)). In this case, the dose that generates the lowest index is greatly influenced by the meal time. This means that the selection

of 6 IU may be too risky if the patient does not adhere exactly to the recommended meal time. For this reason, a safer bolus insulin dose would be 5.5 IU, which is less dependent on the meal time.

Finally, for scenario iii), the area demarcated is the same as that for scenario ii), but RI value is <6.20 (see Figure 6.2(e)). For scenarios ii) and iii), the risk is directly related to the injection-to-meal time.

The previous results are summarized in Table 6.3, where a comparison is presented of the initial estimate versus the optimal insulin performance calculated with the proposed methodology.

Scenario	Initial estimate			Optimal estimate		
	II (IU)	IM (min)	RI	di (IU)	t_{im} (min)	RI
(i)	5.0	30	5.36	6.0	30	2.10
(ii)	5.5	45	6.95	7.5	60	1.03
(iii)	7.0	60	4.44	7.5	60	2.72

Table 6.3: Comparison of RI values for the initial estimate (II) versus the optimal insulin performance for each scenario.

In Figure 6.3, the glucose excursions for the optimal therapy are compared with the initial estimate therapy. The optimum bolus dose d_i and the injection-to-meal time t_{im} for the three preprandial scenarios considered were calculated with the optimization algorithm. The initial insulin dose II and the initial injection-to-meal time IM were also calculated for the same scenarios using heuristic rules.

With regard to the initial meal times versus the optimal meal times, the minimum RI value in scenario i) was obtained for an injection given 30 min before eating. However, the optimization suggests a higher bolus insulin dose, which reduces RI value by 61% (see Figure 6.3(a)).

To reduce the risk for scenario ii) (Figure 6.3(b)), it is necessary to increase the injection-to-meal time and the bolus insulin dose compared with those determined with heuristic rules. This yields a reduction of 85% in the mild hyperglycaemia risk. Finally, for scenario iii), the optimum bolus dose is 7.5 IU injected 1 h before eating (Figure 6.3(c)). This reduces by 39% the risk of mild hyperglycaemia given by the initial estimation.

6.4 Summary

In this chapter, RI presented in Chapter 5 has been integrated into a dosage-aid system of bolus insulin doses and injection-to-meal times that minimizes the risk of postprandial hyper- and hypoglycaemia in patients with T1DM. A summary of the different methods used to support the patient in the insulin dosage process were presented.

Three scenarios were evaluated for a virtual patient, and the Hovorka et al. model was used to illustrate the prediction of glucose excursions. In each scenario, the bolus insulin and injection time computed by the insulin dosage proposed in this work achieved a reduction in RI values

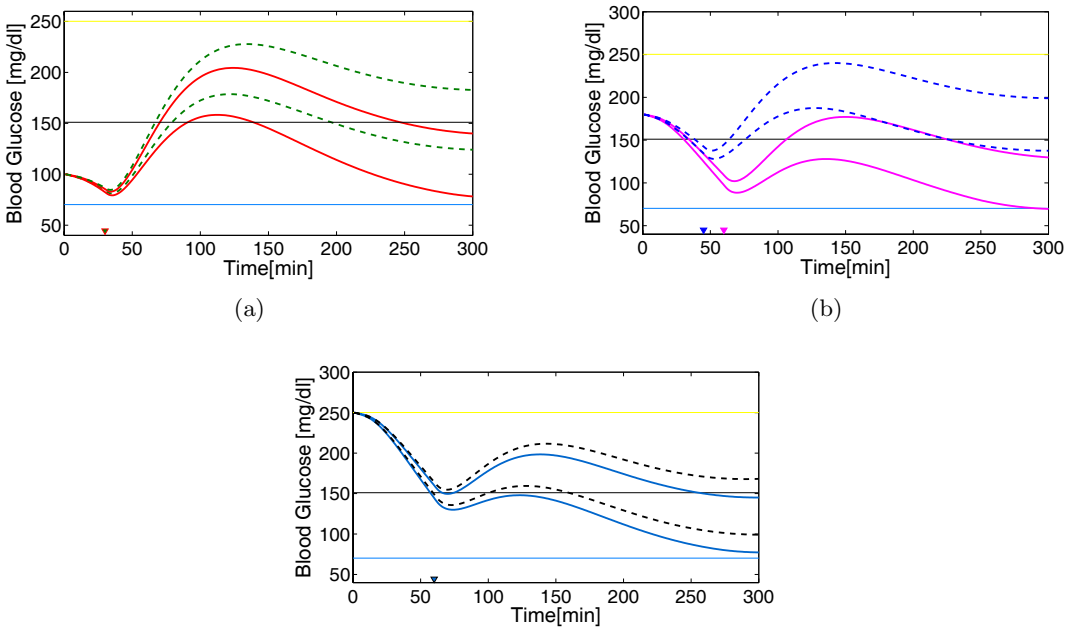

Figure 6.3: Blood glucose response over 5 h for scenarios i (a), ii (b), and iii (c). Triangles indicate the start time of the meals. The solid line indicates the blood glucose for the correct bolus dose of insulin (minimal index) and the dotted line is the blood glucose response to the initial insulin bolus and meal.

with respect to RI values obtained with heuristic rules.

To apply the methodology presented here in a patient-specific scenario, it is necessary to adjust the model to that patient. The model parameters would be estimated from measurements made for several days with a continuous glucose monitor.

Chapter 7

Conclusions and Future Work

I conclude this thesis by noting the contributions presented in the previous chapters. Some directions for possible future work on the subject of this thesis are also discussed.

7.1 Contributions

The main contribution of this thesis is the integration of intra-patient variability and other sources of uncertainty into the design of strategies for insulin dosage adjustment. Specifically, the contributions of the thesis can be summarized as follows:

- A library of interval models of the physiological subsystems of glucose regulation was built. Different mathematical models of the glucose–insulin system were studied that took into account the large intra-patient variability and different sources of uncertainty. This variability and uncertainty were represented by an interval model in which the parameters, inputs, and/or initial states took interval values. Each model was studied to determine the parameters that reflect intra-patient variability and the inputs and parameters that are sources of uncertainty. The parameters related to insulin sensitivity were then represented by intervals to accommodate patient variability. Similarly, food intake and insulin dose inputs were considered as interval values. The interval simulation was performed using MIA, in contrast to probabilistic methods such as MCS, to demonstrate its superior performance, which allows the worst-case analysis to be addressed in a mathematically guaranteed way with little computational effort. Therefore, the worst-case analysis can be performed efficiently, which is extremely important in the context of diabetes.

- A comparative study was performed to assess the behaviour of three postprandial insulin action and glucose kinetics models for a specific insulin therapy regime in the presence of intra-patient variability and uncertainty in food intake estimation. The results of that study showed that a low-complexity model that can be easily identified for a single patient and that includes uncertainty may be enough to tightly embed the patient dynamics response of the complex models.

- A cost function was proposed to compute the risk of postprandial hypo- and hyperglycaemic episodes in T1DM patients that considers intra-patient variability and other sources of uncertainty. The RI is based on the interval simulation of an individual patient's glucoregulatory model. To quantify the relevance of RI to each hypo- and hyperglycaemic episode, different metrics were established based on clinical judgments. Therefore, these metrics can be modified by the physician according to the patient's medical history. The

predicted envelopes of the glucose excursions and the established metrics were used in the cost function to calculate RI values for severe and mild hyper- and hypoglycaemic episodes. By considering the intra-patient variability and uncertainty in food intake, a safer prediction of the possible hyper- and hypoglycaemic episodes induced by insulin therapy can be calculated, reducing the number of false negative predictions.

- A dosage-aid system that minimizes the risk of postprandial hyper- and hypoglycaemia in T1DM patients is proposed. For this purpose, RI was integrated into an optimization algorithm. This algorithm calculates RI value for each bolus insulin dose and injection-to-meal time pair in a two-dimensional grid search and then selects the optimum insulin dose and injection-to-meal time that generate the lowest risk according to the model. Other useful information can also be extracted from the dosage-aid system, such as the dose that allows the greatest flexibility in the injection time, i.e., the insulin dose that produces a similar risk with different injection times. The system proposed is modular and can be used with other glucoregulatory models, and in a feed-forward action for closed-loop glucose control. The resulting optimum bolus dose is apparently consistent with clinical judgments. However, formal clinical validation is required. The author is currently working on the clinical validation of this decision-support system.

7.2 Future Work

Besides the contributions presented, several open improvements should be undertaken.

The first is aimed to the development of a software application of the library of glucorregulatory interval models.

The second is related to the adjusted models using data from real patients. In this thesis, an in silico simulation was performed using virtual patient profiles, but another simulation must be performed using the profiles of real patients.

The third is oriented toward the clinical validation of the dosage-aid system. The resulting bolus dose presented in this research is apparently consistent with clinical judgments, but a formal clinical validation is required. This should involve a survey of different specialists in the field of T1DM to analyse different glucose excursions and evaluate the possible risk of hypo- and hyperglycaemia in each of them. The results will be compared with those obtained with the cost function proposed in this thesis.

Finally, a novel tool to help physicians administer safe therapies to their patients will be developed based on RI. The performance of the therapy could be evaluated from measurements made for several days with a continuous glucose monitor.

7.3 Publications

During the research work leading to this thesis, the following conference and journal papers have been published:

7.3.1 Journal papers

García-Jaramillo, M., Calm, R., Bondia, J., Tarín, C., and Vehí, J. (2009a). Computing the risk of postprandial hypo- and hyperglycemia in type 1 diabetes mellitus considering intrapatient variability and other sources of uncertainty. Journal of Diabetes Science and Technology, 3(4):895-902.

García-Jaramillo, M., Calm, R., Bondia, J., Tarín, C., and Vehí, J. (2011a). Insulin dosage optimization based on prediction of postprandial glucose excursions under uncertain parameters and food intake. Computer Methods and Programs in Biomedicine, *In press*, doi:10.1016/j.cmpb.2010.08.007.

Calm, R., **García-Jaramillo, M.**, Bondia, J., Sainz, M., and Vehí, J. (2011). Comparison of interval and monte carlo simulation for the prediction of postprandial glucose under uncertainty in type 1 diabetes mellitus. Computer Methods and Program in Biomedicine, *In press*, doi:10.1016/j.cmpb.2010.08.008.

García-Jaramillo, M., Calm, R., Bondia, J., and Vehí, J. (2011c). Prediction of postprandial blood glucose under uncertainty and intra-patient variability in type 1 diabetes: a comparative study of three interval models. Computer Methods and Programs in Biomedicine, *Submitted*.

7.3.2 Conference papers

Calm, R., **García-Jaramillo, M.**, Vehí, J., Bondia, J., Tarín, C., and García-Gabín, W. (2007a). Prediction of glucose excursions under uncertain parameters and food intake in intensive insulin therapy for type 1 diabetes mellitus. In *29th Annual International Conference of the IEEE Engineering in Medicine and Biology Society*, pages 1770-1773, 22-26 August, Lyon, France.

Calm, R., **García-Jaramillo, M.**, Vehí, J., Bondia, J., Tarín, C., and García-Gabín, W. (2007b). Simulación intervalar del metabolismo de la glucosa en pacientes con diabetes mellitus tipo 1. In *IX Jornadas de ARCA*. Sistemas Cualitativos y Diagnosis, Lloret de Mar, Spain.

Bondia, J., Calm, R., **García-Jaramillo, M.**, Vehí, J., Tarín, C., and García-Gabín, W. (2007). Predicción de glucemia en pacientes con diabetes tipo 1 ante incertidumbre. In *I Simposio de Modelado y Simulación de sistemas dinámicos (SIMOSI)*, Congreso Español de Informática (CEDI), Zaragoza, Spain.

Calm, R., **García-Jaramillo, M.**, Bondia, J., and Vehí, J. (2009). Insulin dosage based on risk index of postprandial hypo- and hyperglycemia in type 1 diabetes mellitus with uncertain parameters and food intake. In *Small Workshop on Interval Methods (SWIM)*, Lausanne, Switzerland.

García-Jaramillo, M., Calm, R., Bondia, J., and Vehí, J. (2011b). Interval simulation of glucose prediction models in presence of intra-individual variability and uncertain food intake. In *Workshop on Control, Dynamics, Monitoring and Applications*, Caldes de Montbui, Spain.

7.3.3 Poster

García-Jaramillo, M., Calm, R., Bondia, J., Tarín, C., and Vehí, J. (2008). Risk index of Postprandial Hypo- and Hyperglycemia in Type 1 Diabetes Mellitus with consideration of intra-patient variability and other sources of uncertainty. Poster, In *Eighth Annual Diabetes Technology Meeting*, Bethesda, Maryland, USA.

García-Jaramillo, M., Calm, R., Bondia, J., Tarín, C., and Vehí, J. (2009b). Prediction of postprandial hypo- and hyperglycemia events by means of interval models with uncertain parameters and food intake. Poster, In *2nd International Conference on Advanced Technologies & Treatments For Diabetes*, Athens, Greece.

Bibliography

Acikgoz, S. U. and Diwekar, U. M. (2010). Blood glucose regulation with stochastic optimal control for insulin-dependent diabetic patients. *Chemical Engineering Science*, 65:1227–1236.

Ackerman, E., Rosevear, J. W., and McGuckin, W. F. (1964). A mathematical model of the glucose tolerance test. *Physics in Medicine and Biology*, 9(2):203–213.

Agar, B. U., Eren, M., and Cinar, A. (2005). Glucosim: Educational software for virtual experiments with patients with type 1 diabetes. In *IEEE Engineering in Medicine and Biology 27th Annual Conference*, pages 845–848.

Albisser, A. M. (2003). Analysis: toward algorithms in diabetes self-management. *Diabetes Technology and Therapeutics*, 5(3):371–373.

Albisser, A. M., Schiffrin, A., Schulz, M., Tiran, J., and Leibel, B. S. (1986). Insulin dosage adjustment using manual methods and computer algorithms: A comparative study. *Medical and Biological Engineering and Computing*, 24(6):577–584.

American Diabetes Association (2001). Postprandial blood glucose. *Diabetes Care*, 24(4):775–778.

American Diabetes Association (2004). Tests of glycemia in diabetes. *Diabetes Care*, 27 (suppl 1):S91–S93.

American Diabetes Association (2010). Diagnosis and classification of diabetes mellitus. *Diabetes Care*, 33 (suppl 1):S62–S69.

Arleth, T., Andreassen, S., Federici, M. O., and Benedetti, M. M. (2000). A model of the endogenous glucose balance incorporating the characteristics of glucose transporters. *Computer Methods and Programs in Biomedicine*, 62:219–234.

Armengol, J. (1999). *Application of modal interval analysis to the simulation of the behaviour of dynamic systems with uncertain parameters.* PhD thesis, Universitat de Girona.

Armengol, J., Travé-Massuyès, L., Vehí, J., and de la Rosa, J. (2000). A survey on interval model simulators and their properties related to fault detection. *Annual Reviews in Control*, 24:31–39.

Barnett, A. H. (2003). A review of basal insulins. *Diabetic Medicine*, 20:873–885.

Barrett, P. H., Bell, B. M., Cobelli, C., Golde, H., Schumitzky, A., Vicini, P., and Foster, D. (1998). Saam ii: Simulation, analysis, and modeling software for tracer and pharmacokinetic studies. *Metabolism*, 47:484–492.

Beers, M. and Jones, T. (2004). *Merck Manual of Health and Aging*. Merck Research Laboratories.

Bellazzi, R. (2008). Telemedicine and diabetes management: Current challenges and future research directions. *Journal of Diabetes Science and Technology*, 2(1):98–104.

Bendtsen, C. and Stauning, O. (1996). Fadbad, a flexible c++ package for automatic differentiation. Technical report, Department of mathematical modelling, Technical University of Denmark.

Berger, M. and Rodbard, D. (1989). Computer simulation of plasma insulin and glucose dynamics after subcutaneous insulin injection. *Diabetes Care*, 12:725–736.

Bergman, R. (1997). *The Minimal Model Approach and Determinants of Glucose Tolerance*, volume 7, chapter The minimal model: yesterday, today, and tomorrow., pages 3–50. Pennington Center Nutrition Series.

Bergman, R., Phillips, L., and Cobelli, C. (1981). Physiologic evaluation of factors controlling glucose tolerance in man: measurement of insulin sensitivity and beta-cell glucose sensitivity from the response to intravenous glucose. *The Journal of Clinical Investigation*, 68(6):1456–1467.

Berleant, D. and Kuipers, B. (1993). *Recent advances in qualitative physics*, chapter Qualitative-numeric simulation with Q3, pages 3–16. Mit Press.

Beyer, J., Schrezenmeir, J., Schulz, G., Strack, T. H., Küstner, E., and Schulz, G. (1990). The influence of different generations of computer algorithms on diabetes control. *Computer Methods and Program in Biomedicine*, 32:225–232.

Biermann, E. and Mehnert, H. (1990). Diablog: a simulation program of insulin-glucose dynamics for education of diabetics. *Computer Methods and Programs in Biomedicine*, 32:311–318.

Bondia, J., Calm, R., García-Jaramillo, M., Vehí, J., Tarín, C., and García-Gabín, W. (2007). Predicción de glucemia en pacientes con diabetes tipo 1 ante incertidumbre. In *I Simposio de Modelado y Simulación de sistemas dinámicos*.

Bondia, J., Dassau, E., Zisser, H., Calm, R., Vehí, J., Jovanovic, L., and Doyle III, F. (2009). Coordinated basal-bolus for tighter postprandial glucose control in insulin pump therapy. *Journal of Diabetes Science and Technology*, 3(1):8–97.

Bondia, J. and Vehí, J. (2005-2007). Insulaid: Glucose prediction and insulin dosage-aid system for patients with type 1 diabetes mellitus. DPI2004-07167-C02.

Bondia, J. and Vehí, J. (2008-2010). Insulaid2: closed-loop glucose control in diabetes mellitus 1 and critically-ill patients. http://www.insulaid2.org/. DPI2007-66728-C02-01 and DPI2007-66728-C02-02.

Bondia, J., Vehí, J., Palerm, C. C., and Herrero, P. (2010). El páncreas artificial: control automático de infusión de insulina en diabetes mellitus tipo 1. *Revista Iberoamericana de Automática e Informática Industrial*, 7(2):5–20.

Boutayeb, A. and Chetouani, A. (2006). A critical review of mathematical models and data used in diabetology. *BioMedical Engineering OnLine*, 5:–.

Bremer, T. and Gough, D. A. (1999). Is blood glucose predictable from previous values? a solicitation for data. *Diabetes*, 48:445–451.

Brönnimann, H., Melquiond, G., and Pion, S. (2003). The boost interval arithmetic library. In *Real Numbers and Computers*.

Bulka, J., Izworski, A., Koleszynska, J., Lis, J., and Wochlik, I. (2009). Automatic meal planning using artificial intelligence algorithms in computer aided diabetes therapy. In *4th International Conference on Autonomous Robots and Agents*, pages 393–397.

Calderón-Espinoza, G., Armengol, J., Vehí, J., and Gelso, E. R. (2007). Dynamic diagnosis based on interval analytical redundancy relations and signs of the symptoms. *Artificial Intelligence Communications*, 20:39–47.

Calm, R. (2005). *Análisis intervalar modal: su construcción teórica, implementación y posibilidades de aplicación a la simulación y al control*. PhD thesis, Universitad Politècnica de Catalunya.

Calm, R., García-Jaramillo, M., Bondia, J., Sainz, M. A., and Vehí, J. (2011). Comparison of interval and monte carlo simulation for the prediction of postprandial glucose under uncertainty in type 1 diabetes mellitus. *Computer Methods and Program in Biomedicine*, In press.

Calm, R., García-Jaramillo, M., Bondia, J., and Vehí, J. (2009). Insulin dosage based on risk index of postprandial hypo- and hyperglycemia in type 1 diabetes mellitus with uncertain parameters and food intake. In *Small Workshop on Interval Methods*.

Calm, R., García-Jaramillo, M., Vehí, J., Bondia, J., Tarín, C., and García-Gabín, W. (2007a). Prediction of glucose excursions under uncertain parameters and food intake in intensive insulin therapy for type 1 diabetes mellitus. In *29th Annual International Conference of the IEEE Engineering in Medicine and Biology Society*, pages 1770–1773.

Calm, R., García-Jaramillo, M., Vehí, J., Bondia, J., Tarín, C., and García-Gabín, W. (2007b). Simulación intervalar del metabolismo de la glucosa en pacientes con diabetes mellitus tipo i. In *IX Jornadas de ARCA. Sistemas Cualitativos y Diagnosis*.

Campos-Delgado, D. U., Campos-Cornejo, F., and Hernández-Ordoñez, M. (2008). Extension of the run-to-run control to multi-boluses schemes. In *17th IEEE International Conference on Control Applications Part of 2008 IEEE Multi-conference on Systems and Control*, pages 678–683.

Campos-Delgado, D. U., Ruiz-Velazquez, R. F. E., and Gordillo-Moscoso, A. (2003). Knowledge-based controllers for blood glucose regulation in type i diabetic patients by subcutaneous route. In *IEEE International Symposium on Intelligent Control*, pages 592–597.

Candas, B. and Radziuk, J. (1994). An adaptive plasma glucose controller based on a nonlinear insulin/glucose model. *IEEE Transactions on Biomedical Engineering*, 41(2):116–124.

Carson, E. and Cobelli, C. (2001). *Modelling methodology for physiology and medicine*. Elsevier.

Caumo, A. and Cobelli, C. (1993). Hepatic glucose production during the labeled ivgtt: Estimation by deconvolution with a new minimal model. *The American Journal of Physiology*, 264:E829–E841.

Cavan, D. A., Hejlesesn, O. K., Hovorka, R., Evans, J., Metcalfe, J. A., Cavan, M. L., Halim, M., Andreassen, S., Carson, E. R., and Sonksen, P. H. (1998). Preliminary experience of the dias computer model in providing insulin dose advice to patients with insulin dependent diabetes. *Computer Methods and Programs in Biomedicine*, 56:157–164.

Cavan, D. A., Hovorka, R., Hejlesesn, O. K., Andreassen, S., and Sonksen, P. H. (1996). Use of the dias model to predict unrecognised hypoglycemia in patients with insulin-dependent diabetes. *Computer Methods and Programs in Biomedicine*, 50:241–246.

Cerasi, E., Fick, G., and Rudemo, M. (1974). A mathematical model for the glucose induced insulin release in man. *European Journal of Clinical Investigation*, 4:269–278.

Chanoch, L. H., Jovanovic, L., and Peterson, C. M. (1985). The evaluation of a pocket computer as an aid to insulin dose determination by patients. *Diabetes Care*, 8(2):172–176.

Chassin, L. J., Wilinska, M. E., and Hovorka, R. (2004). Evaluation of glucose controllers in virtual environment: methodology and sample application. *Artificial Intelligence in Medicine*, 32:171–181.

Chee, F. and Fernando, T. (2007). *Closed-Loop Control of Blood Glucose*, volume 368 of *Lecture Notes in Control and Information Sciences*. Springer.

Chiarelli, F., Tumini, S., Morgese, G., and Albisser, A. M. (1990). Controlled study in diabetic children comparing insulin-dosage adjustment by manual and computer algorithms. *Diabetes Care*, 13(10):1080–1084.

Cobelli, C., Dalla Man, C., Sparacino, G., Magni, L., Nicolao, G. D., and Kovatchev, B. (2009). Diabetes: Models, signals, and control. *IEEE Reviews in Biomedical Engineering*, 2:54–96.

Cobelli, C., Pacini, G., Toffolo, G., and Sacca, L. (1986). Estimation of insulin sensitivity and glucose clearance from minimal model: new insights from labeled ivgtt. *American Journal of Physiology*, 250:E591–E598.

Coghill, G. (1996). *Mycroft: a framework for constraint based fuzzy qualitative reasoning*. PhD thesis, Heriot-Watt University.

Cook, C., Mcmichael, J., Lieberman, R., Mann, L., King, E., New, K., Vaughn, P., Dunbar, V., and Caudle, J. (2005). The intelligent dosing system: Application for insulin therapy and diabetes management. *Diabetes Technology and Therapeutics*, 7:58–71.

Dalla Man, C., Breton, M., and Cobelli, C. (2009). Physical activity into the meal glucose-insulin model of type 1 diabetes: In silico studies. *Journal of Diabetes Science and Technology*, 3(1):56–67.

Dalla Man, C., Camilleri, M., and Cobelli, C. (2006). A system model of oral glucose absorption: Validation on gold standard data. *IEEE Transactions on Biomedical Engineering*, 53:2472–2478.

Dalla Man, C., Raimondo, D., Rizza, R., and Cobelli, C. (2007a). Gim, simulation software of meal glucose-insulin model. *Journal of Diabetes Science and Technology*, 1(3):323–330.

Dalla Man, C., Rizza, R., and Cobelli, C. (2007b). Meal simulation model of the glucose-insulin system. *IEEE Transactions on Biomedical Engineering*, 54:1740–1749.

DCCT (1993). The effect of intensive treatment of diabetes on the development and progression of long-term complications in insulin-dependent diabetes mellitus. *The New England Journal of Medicine*, 329 (14):977–986.

de Adana, M. S. R., Dominguez-López, M., Tapia, M. J., de la Higuera, M., González, S., and Soriguer, F. (2008). How to evaluate the glycemic variability? *Avances en Diabetología*, 24:77–81.

De Gaetano, A. and Arino, O. (2000). Mathematical modelling of the intravenous glucose tolerance test. *Journal of Mathematical Biology*, 40:136–168.

Derouich, M. and Boutayeb, A. T. (2002). The effect of physical exercise on the dynamics of glucose and insulin. *Journal of Biomechanics*, 35:911–917.

Dua, P., Doyle III, F. J., and Pistikopoulos, E. N. (2006). Model-based blood glucose control for type 1 diabetes via parametric programming. *IEEE Transactions on Biomedical Engineering*, 53:1478–1491.

Efrat, S. (2003). Beta-cell expansion for therapeutic compensation of insulin resistance in type 2 diabetes. *International Journal of Experimental Diabesity Research*, 4(1):1–5.

Elashoff, J. D., Reedy, T. J., and Meyer, J. H. (1982). Analysis of gastric emptying data. *Gastroenterology*, 83:1306–1312.

El Youssef, J., Castle, J., and Kenneth Ward, W. (2009). A review of closed-loop algorithms for glycemic control in the treatment of type 1 diabetes. *Algorithms*, 2(1):518–532.

Fabietti, P. G., Calabrese, G., Iorio, M., Bistoni, S., Brunetti, P., Sarti, E., and Benedetti, M. M. (2001). A mathematical model describing the glycemic response of diabetic patients to meal and i.v. infusion of insulin. *The International Journal of Artificial Organs*, 24:736–742.

Fernandez, M., Villasana, M., and Streja, D. (2007). Glucose dynamics in type i diabetes: insights from the classic and linear minimal models. *Computer Methods and Program in Biomedicine*, 37 (5):611–627.

Fisher, M. E. (1991). A semiclosed-loop algorithm for the control of blood glucose levels in diabetics. *IEEE Transactions on Biomedical Engineering*, 38(1):57–61.

Fishman, G. (1996). *Monte Carlo: Concepts, Algorithms and Applications*. Springer.

Flórez-Díaz, J. (2008). *Improvements in the Ray Tracing of Implicit Surfaces based on Interval Arithmetic*. PhD thesis, Universitat de Girona.

Fowler, M. J. (2007). Diabetes treatment, part 1: Diet and exercise. *Clinical Diabetes*, 25(3):105–109.

Galvanin, F., Barolo, M., Macchietto, S., and Bezzo, F. (2009). On the optimal design of clinical tests for the identification of physiological models of type 1 diabetes mellitus. *Computer Aided Chemical Engineering*, 27:183–188.

García, O., Vehí, J., e Matos, J. C., Henriques, A. A., and Casas, J. R. (2008). Structural assessment under uncertain parameters via interval analysis. *Journal of Computational and Applied Mathematics*, 218(1):43–52.

García-Jaramillo, M., Calm, R., Bondia, J., Tarín, C., and Vehí, J. (2009a). Computing the risk of postprandial hypo- and hyperglycemia in type 1 diabetes mellitus considering intrapatient variability and other sources of uncertainty. *Journal of Diabetes Science and Technology*, 3(4):895–902.

García-Jaramillo, M., Calm, R., Bondia, J., Tarín, C., and Vehí, J. (2008). Risk index of postprandial hypo- and hyperglycemia in type 1 diabetes mellitus with consideration of intra-patient variability and other sources of uncertainty. In *Eighth Annual Diabetes Technology Meeting*.

García-Jaramillo, M., Calm, R., Bondia, J., Tarín, C., and Vehí, J. (2009b). Prediction of postprandial hypo- and hyperglycemia events by means of interval models with uncertain parameters and food intake. In *2nd International Conference on Advanced Technologies & Treatments For Diabetes*.

García-Jaramillo, M., Calm, R., Bondia, J., Tarín, C., and Vehí, J. (2011a). Insulin dosage optimization based on prediction of postprandial glucose excursions under uncertain parameters and food intake. *Computer Methods and Programs in Biomedicine*, In press.

García-Jaramillo, M., Calm, R., Bondia, J., and Vehí, J. (2011b). Interval simulation of glucose prediction models in presence of intra-individual variability and uncertain food intake. In *Workshop on Control, Dynamics, Monitoring and Applications*, Caldes de Montbui, Spain.

García-Jaramillo, M., Calm, R., Bondia, J., and Vehí, J. (2011c). Prediction of postprandial blood glucose under uncertainty and intra-patient variability in type 1 diabetes: a comparative study of three interval models. *Computer Methods and Programs in Biomedicine*, Submitted.

García Reyero, S. and Martínez, J. L. (1999). Modal intervalar arithmetic implementation using floating point emulation. In *Workshop on Applications of Interval Analysis to Systems and Control with special emphasis on recent advances in Modal Interval Analysis (MISC 99)*, pages 211–223, Girona.

Gardeñes, E., Sainz, M. A., Jorba, L., Calm, R., Estela, R., Mielgo, H., and Trepat, A. (2001). Modal intervals. *Reliable Computing*, 7(2):77–111.

Gasca, R. M., Ortega, J. A., and Toro, M. (2002). A framework for semiqualitative reasoning in engineering applications. *Applied Artificial Intelligence*, 16(3):173–197.

Gelso, E. R. (2009). *A proposal for the diagnosis of uncertain dynamic systems based on interval models*. PhD thesis, Universitat de Girona.

Gossain, V. (2003). Insulin analogs and intensive insulin therapy in type 1 diabetes. *International Journal of Diabetes in Developing Countries*, 23(2):26–36.

Goualard, F. (2002). Gaol, not just another interval library. http://www.sourceforge.net/projects/gaol/.

Goykhman, S., Drincic, A., Desmangles, J. C., and Rendel, M. (2009). Insulin glargine: a review 8 years after its introduction. *Expert Opinion on Pharmacotherapy*, 10(4):705–718.

Graff, M. R., Gross, T. M., Juth, S. E., and Charlson, J. (2000). How well are individuals on intensive insulin therapy counting carbohydrates? *Diabetes Research and Clinical Practice*, 50:S238.

Granvilliers, L. and Benhamou, F. (2006). Algorithm 852: Realpaver: An interval solver using constraint satisfaction techniques. *ACM Transactions on Mathematical Software*, 32(1):138–156.

Guerci, B. and Sauvanet, J. P. (2005). Subcutaneous insulin: pharmacokinetic variability and glycemic variability. *Diabetes and Metabolism*, 31(4):S7–S24.

Guilhem, I., Leguerrier, A., Lecordier, F., Poirier, J. Y., and Maugendre, D. (2006). Technical risks with subcutaneous insulin infusion. *Diabetes and Metabolism*, 32(3):279–284.

Guyton, J. R., Foster, R. O., Soeldner, J. S., Tan, M. H., Kahn, C. B., Koncz, L., and Gleason, R. E. (1978). A model of glucose-insulin homeostasis in man that incorporates the heterogeneous fast pool theory of pancreatic insulin release. *Diabetes*, 27(10):1027–42.

Hanas, R. (2004). *Type 1 Diabetes in children, adolescents and young adults*. Class publishing.

Harvey, R. A., Wang, Y., Percival, B. G. M. W., Bevier, W., Finan, D. A., Zisser, H., Seborg, D. E., Jovanovic, L., Doyle III, F. J., and Dassau, E. (2010). Quest for the artificial pancreas: combining technology with treatment. *IEEE Engineering in Medicine and Biology Magazine*, 29(2):53–62.

Hedbrant, J., Ludvigsson, J., and Nordenskjold, K. (1991). Sarimner: a computer model of diabetes physiology for education of physicians and patients. *Diabetes Research and Clinical Practice*, 14:113–122.

Hedbrant, J., Nordfeldt, S., and Ludvigsson, J. (2007). The särimner diabetes simulator - a look in the rear view mirror. *Diabetes Technology and Therapeutics*, 9:10–16.

Heinemann, L. (2002). Variability of insulin absorption and insulin action. *Diabetes Technology and Therapeutics*, 4(5):673–682.

Heise, T., Nosek, L., Ronn, B. B., Endahl, L., Heinemann, L., Kapitza, C., and Draeger, E. (2004). Lower within-subject variability of insulin detemir in comparison to nph insulin and insulin glargine in people with type 1 diabetes. *Diabetes*, 53(6):1614–1620.

Hejlesen, O. K., Plougmann, S., and Cavan, D. A. (2000). Diasnet–an internet tool for communication and education in diabetes. *Studies in Health Technology and Informatics*, 77:563–567.

Hejlesen, O. K., S.Andreassen, Hovorka, R., and Cavan, D. A. (1997). Dias: the diabetes advisory system: an outline of the system and the evaluation results obtained so far. *Computer Methods and Programs in Biomedicine*, 54:49–58.

Hernando, M. E., Gomez, E. J., and Pozo, F. D. (2001). Educational tool for diabetic patients based on causal probabilistic networks. In Quaglini, S., Barahona, P., and Andreassen, S., editors, *Proceedings of Artificial Intelligence in Medicine in Europe, LNAI 2101*, pages 203–206. Springer-Verlag.

Herrero, P. (2006a). Miso. http://sites.google.com/site/pauherrero/software.

Herrero, P. (2006b). *Quantified real constraint solving using modal intervals with applications to control*. PhD thesis, Universitat de Girona.

Herrero, P., Sainz, M. A., Vehí, J., and Jaulin, L. (2005). Quantified set inversion algorithm with applications to control. *Reliable Computing*, 11(5):369–382.

Hoshino, M., Haraguchi, Y., Mizushima, I., and Sakai, M. (2009). Recent progress in mechanical artificial pancreas. *Journal of Artificial Organs*, 12(3):141–149.

Hovorka, R. (2006). Continuous glucose monitoring and closed-loop systems. *Diabetic Medicine*, 23(1):1–12.

Hovorka, R., Canonico, V., Chassin, L. J., Haueter, U., Massi-Benedetti, M., Federici, M. O., Pieber, T. R., Schaller, H., Schaupp, L., Vering, T., and Wilinska, M. E. (2004). Nonlinear model predictive control of glucose concentration in subjects with type 1 diabetes. *Physiological Measurement*, 25:905–920.

Hovorka, R., Kremen, J., Blaha, J., Matias, M., Anderlova, K., Bosanska, L., Roubicek, T., Wilinska, M., Chassin, L. J., and Svacina, S. (2007). Blood glucose control by a model predictive control algorithm with variable sampling rate versus a routine glucose management protocol in cardiac surgery patients: a randomized controlled trial. *The Journal of Clinical Endocrinology Metabolism*, 92(8):2960–2964.

Hovorka, R., Shojaee-Moradie, F., Carroll, P., Chassin, L., Gowrie, I., Jackson, N., Tudor, R., Umpleby, A., and Jones, R. (2002). Partitioning glucose distribution/transport, disposal, and endogenous production during ivgtt. *American Journal of Physiology Endocrinology and Metabolism*, 282:992–1007.

International Diabetes Federation (2009). *IDF Diabetes Atlas 4th edition.*

Interval Computations (2010). Interval and related software. http://www.cs.utep.edu/interval-comp/intsoft.html.

Jeitler, K., Horvath, K., Berghold, A., Gratzer, T. W., Neeser, K., Pieber, T. R., and Siebenhofer, A. (2008). Continuous subcutaneous insulin infusion versus multiple daily insulin injections in patients with diabetes mellitus: systematic review and meta-analysis. *Diabetologia*, 51:941–951.

Jovanovic, L. and Peterson, C. M. (1982). Home blood glucose monitoring. *Comprehensive Therapy*, 8(1):10–20.

Kaucher, E. W. (1980). Interval analysis in the extended interval space ir. *Computing (Suppl.)*, 2:33–49.

Kay, H. (1996). *Refining imprecise models and their behaviours.* PhD thesis, University of Texas at Austin.

Kay, H. and Kuipers, B. (1992). Numerical behavior envelopes for qualitative models. In *6th International Workshop on Qualitatiave Reasoning about Physical Systems QR 92*, pages 252–267.

Kildegaard, J., Randlov, J., Poulsen, J. U., and Hejlesen, O. K. (2007). The impact of non-model-related variability on blood glucose prediction. *Diabetes Technology and Therapeutics*, 9(4):363–371.

Kirchsteiger, H., del Re, L., Renard, E., and Mayrhofer, M. (2009). Robustness properties of optimal insulin bolus administrations for type 1 diabetes. In *2009 American Control Conference*, pages 2284–2289.

Knüppel, O. (1994). Profil/bias - a fast interval library. *Computing*, 53:277–287.

Kobayashi, T., Sawano, S., Itoh, T., Kosaka, K., Hirayama, H., and Kasuya, Y. (1983). The pharmacokinetics of insulin after continuous subcutaneous infusion or bolus subcutaneous injection in diabetic patients. *Diabetes*, 32:331–336.

Kovatchev, B., Breton, M., Dalla Man, C., and Cobelli, C. (2009). In silico preclinical trials: A proof of concept in closed-loop control of type 1 diabetes. *Journal of Diabetes Science and Technology*, 3(1):44–55.

Kovatchev, B., Breton, M. D., Cobelli, C., and Dalla Man, D. (2008). Method, system and computer simulation environment for testing ap systems, in particular the monitoring and control strategies in diabetes. US2008/067725.

Kovatchev, B. P., Cox, D. J., Gonder-Frederick, L. A., and Clarke, W. L. (2002). Methods for quantifying self-monitoring blood glucose profiles exemplified by an examination of blood glucose patterns in patients with type 1 and type 2 diabetes. *Diabetes Technology and Therapeutics*, 4:295–303.

Kovatchev, B. P., Cox, D. J., Gonder-Frederick, L. A., Young-Hyman, D., Schlundt, D., and Clarke, W. L. (1998). Assessment of risk for severe hypoglycemia among adults with iddm: validation of the low blood glucose index. *Diabetes Care*, 21:1870–1875.

Kovatchev, B. P., Otto, E., Cox, D., Gonder-Frederick, L., and Clarke, W. (2006). Evaluation of a new measure of blood glucose variability in diabetes. *Diabetes Care*, 29:2433–2438.

Kowalski, A. and Lum, J. W. (2009). Juvenile diabetes research foundation artificial pancreas consortium update. *Journal of Diabetes Science and Technology*, 3(5):1224–1226.

Kraegen, E. W. and Chisholm, D. J. (1984). Insulin responses to varying profiles of subcutaneous insulin infusion: kinetic modelling studies. *Diabetologia*, 26:208–213.

Kuipers, B. (1994). *Qualitative reasoning. Modeling and simulation with incomplete knowledge.* MIT Press.

Kuipers, B. and Berleant, D. I. (1988). Using incomplete quantitative knowledge in qualitative reasoning. In *Sixth National Conference on Artificial Intelligence.*

Kumareswaran, K., Evans, M. L., and Hovorka, R. (2009). Artificial pancreas: an emerging approach to treat type 1 diabetes. *Expert Review of Medical Devices*, 6(4):401–410.

Laguna, A. (2010). Model identification from ambulatory data for post-prandial glucose control in type 1 diabetes. Master's thesis, University of Valencia.

Lehmann, E. and Deutsch, T. (1992a). Aida: an automated insulin dosage advisor. In *Annual Symposium on Computer Application in Medical Care*, pages 818–819.

Lehmann, E. and Deutsch, T. (1992b). A physiological model of glucose-insulin interaction in type 1 diabetes mellitus. *Journal of Biomedical Engineering*, 14:235–242.

Lehmann, E., Tarín, C., Bondia, J., Teufel, E., and Deutsch, T. (2009). Incorporating a generic model of subcutaneous insulin absorption into the aida v4 diabetes simulator: (3) early plasma insulin determinations. *Journal of Diabetes Science and Technology*, 3(1):190–201.

Lehmann, E. D. (1999). Experience with the internet release of aida v4.0 - http://www.diabetic.org.uk/aida.htm - an interactive educational diabetes simulator. *Diabetes Technology and Therapeutics*, 1:41–54.

Lehmann, E. D. (2001). The freeware aida interactive educational diabetes simulator - http://www.2aida.org-(1)adownload survey for aida v4.0. *Diagnostics an Medical Technology*, 7:504–515.

Lehmann, E. D. and Deutsch, T. (1995). Application of computers in diabetes care a review i. computers for data collection and interpretation. *Medical Informatics*, 20:281–302.

Levy, M., Ferrand, P., and Chirat, V. (1989). Sesam-diabete, an expert system for insulin-requiring diabetic patient education. *Computers and Biomedical Research*, 22:442–453.

Lin, Y. and Stadtherr, M. A. (2006). Validated solution of odes with parametric uncertainties. *Computer-Aided Chemical Engineering*, 21:167–172.

Magni, L., Raimondo, D., Bossi, L., Dalla Man, C., Nicolao, G. D., Kovatchev, B., and Cobelli, C. (2007). Model predictive control of type 1 diabetes: an insilico trial. *Journal of Diabetes Science and Technology*, 1(6):804–812.

Makino, K. and Berz, M. (2006). Cosy infinity version 9. *Nuclear Instruments and Methods in Physics Research*, 558:346–350.

Makroglou, A., Li, J., and Kuang, Y. (2006). Mathematical models and software tools for the glucose-insulin regulatory system and diabetes: an overview. *Applied Numerical Mathematics*, 56:559–573.

Mari, A. (2002). Mathematical modeling in glucose metabolism and insulin secretion. *Current Opinion in Clinical Nutrition and Metabolic Care*, 5(5):495–501.

Mazze, R. S., Strock, E., Borgman, S., Wesley, D., Stout, P., and Racchini, J. (2009). Evaluating the accuracy, reliability, and clinical applicability of continuous glucose monitoring (cgm): is cgm ready for real time? *Diabetes Technology and Therapeutics*, 11(1):11–18.

McDonnell, C. M., Donath, S. M., Vidmar, S. I., Werther, G. A., and Cameron, F. J. (2005). A novel approach to continuous glucose analysis utilizing glycemic variation. *Diabetes Technology and Therapeutics*, 7(2):253–263.

Mehta, S. N., Quinn, N., Volkening, L. K., and Laffel, L. M. (2009). Impact of carbohydrate counting on glycemic control in children with type 1 diabetes. *Diabetes Care*, 32(6):1014–1016.

Metropolis, N. (1987). The beginning of the monte carlo method. *Los Alamos Science*, 15:12.

Moberg, E., Kollind, M., Lins, P. E., and Adamson, U. (1993). Estimation of blood-glucose variability in patients with insulin-dependent diabetes mellitus. *Scandinavian Journal of Clinical ad Laboratory Investigation*, 53(5):507–514.

Mokdad, A. H., Ford, E. S., Bowman, B. A., Dietz, W. H., Vinicor, F., Bales, V. S., and Marks, J. S. (2003). Prevalence of obesity, diabetes, and obesity-related health risk factors. *Journal of the American Medical Association*, 289(1):76–79.

Molnar, G. D., Taylor, W. F., and Ho, M. M. (1972). Day-to-day variation of continuously monitored glycaemia: a further measure of diabetic instability. *Diabetologia*, 8(5):342–348.

Moore, R. (1979). *Methods and Applications of Interval Analysis*. SIAM.

Mooy, J. M., Grootenhuis, P. A., de Vries, H., Kostense, P. J., Popp-Snijders, C., Bouter, L. M., and Heine, R. J. (1996). Intra-individual variation of glucose, specific insulin and proinsulin concentrations measured by two oral glucose tolerance tests in a general caucasian population: the hoorn study. *Diabetologia*, 39(3):298–305.

Mosekilde, E., Jensen, K. S., Binder, C., Pramming, S., and Thorsteinsson, B. (1989). Modeling absorption kinetics of subcutaneous injected soluble inslulin. *Journal of Pharmacokinetics and Biopharmaceutics*, 17:67–87.

Mougiakakou, S. and Nikita, K. (2000). A neural network approach for insulin regime and dose adjustment in type 1 diabetes. *Diabetes Technology and Therapeutics*, 2:381–389.

Mougiakakou, S. G., Bartsocas, C. S., Bozas, E., Chaniotakis, N., Iliopoulou, D., Kouris, I., Pavlopoulos, S., Prountzou, A., Skevofilakas, M., Tsoukalis, A., Varotsis, K., Vazeou, A., Zarkogianni, K., and Nikita, K. S. (2010). Smartdiab: A communication and information technology approach for the intelligent monitoring, management and follow-up of type 1 diabetes patients. *IEEE Transactions on Information Technology in Biomedicine*, 14(3):622–633.

Mukhopadhyay, A., De Gaetano, A., and Arino, O. (2004). Modeling the intra-venous glucose tolerance test: A global study for a single-distributed-delay model. *Discrete and continuous dynamical systems*, 4:407–417.

Murata, G., Hoffman, R., Shah, J., Wendel, C., and Duckworth, W. (2004). A probabilistic model for predicting hypoglycemia in type 2 diabetes mellitus: The diabetes outcomes in veterans study (doves). *Archives of Internal Medicine*, 164(13):1445–1450.

National Institutes of Health (2006). *Regenerative Medicine*, chapter Are Stem Cells the Next Frontier for Diabetes Treatment?, page 69.

Nedialkov, N. S. (2002). The design and implementation of an object-oriented validated ode solver. Technical report, Kluwer Academic Publishers.

Nucci, G. and Cobelli, C. (2000). Models of subcutaneous insulin kinetics. a critical review. *Computer Methods and Programs in Biomedicine*, 62:249–257.

Owens, C., Zisser, H., Jovanovic, L., Srinivasan, B., Bonvin, D., and Doyle III, F. J. (2006). Run-to-run control of blood glucose concentrations for people with type 1 diabetes mellitus. *IEEE Transactions on Biomedical Engineering*, 53(6):996–1005.

Palerm, C. C. (2003). *Drug Infusion control: an extended direct model reference adaptative control strategy.* PhD thesis, Rensselaer Polytechnic Institute.

Palerm, C. C., Zisser, H., Bevier, W. C., Jovanovic, L., and Doyle III, F. J. (2007a). Prandial insulin dosing using run-to-run control: application of clinical data and medical expertise to define a suitable performance metric. *Diabetes Care*, 30(5):1131–1136.

Palerm, C. C., Zisser, H., Jovanovic, L., and Doyle III, F. J. (2007b). A run-to-run framework for prandial insulin dosing: handling real-life uncertainty. *Int. Journal of Robust and Nonlinear Control*, 17:1194–1213.

Pankowska, E. and Blazik, M. (2010). Bolus calculator with nutrition database software, a new concept of prandial insulin programming for pump users. *Journal of Diabetes Science and Technology*, 4(3):571–576.

Panunzi, S., Palumbo, P., and De Gaetano, A. (2007). A discrete single delay model for the intra-venous glucose tolerance test. *Theoretical Biology and Medical Modelling*, 4:35. doi:10.1186/1742-4682-4-35.

Parker, R. S., Doyle III, F. J., and Peppas, N. A. (1999). A model-based algorithm for blood glucose control in type i diabetic patients. *IEEE Transactions on Biomedical Engineering*, 46:148–157.

Pernick, N. L. and Rodbard, D. (1986). Personal computer programs to assist with self-monitoring of blood glucose and selfadjustment of insulin dosage. *Diabetes Care*, 9:61–69.

Peters, A., Rübsamen, M., Jacob, U., Look, D., and Scriba, P. (1991). Clinical evaluation of decision support system for insulin-dose adjustment in iddm. *Diabetes Care*, 14(10):875–880.

Popow, C., Horn, W., Rami, B., and Schober, E. (2003). Vie-diab: a support program for telemedical glycaemic control. In Springer, editor, *Proceedings of the 9th Conference on Artificial Intelligence in Medicine in Europe*, pages 350–354.

Puckett, W. R. and Lightfoot, E. N. (1995). A model for multiple subcutaneous insulin injections developed from individual diabetic patient data. *American Journal of Physiological Endocrinology and Metabolism*, 269:E1115–E1124.

Rabasa-Lhoret, R., Garon, J., Langelier, H., Poisson, D., and Chiasson, J. L. (1999). Effects of meal carbohydrate content on insulin requirements in type 1 diabetic patients treated intensively with the basal-bolus (ultralente-regular) insulin regimen. *Diabetes Care*, 22:667–673.

Ratschan, S. and She, Z. (2004). Hsolver. http://hsolver.sourceforge.net/. Software package.

Rauh, A., Auer, E., and Hofer, E. P. (2005). A novel interval method for validating state enclosures of the solution of initial value problems. Technical report, Institute of Measurement, Control, and Microtechnology University of Ulm.

Revert, A., Calm, R., Vehí, J., and Bondia, J. (2011). Calculation of the best basal-bolus combination for postprandial glucose control in insulin pump therapy. *IEEE Transactions on Biomedical Engineering*, 58(2):274–281.

Rodbard, D. (2009). Interpretation of continuous glucose monitoring data: Glycemic variability and quality of glycemic control. *Diabetes Technology and Therapeutics*, 11 (Supp. 1):S–55–S–67.

Roy, A. and Parker, R. (2006). Mixed meal modeling and disturbance rejection in type 1 diabetic patients. In *IEEE EMBS Annual Internationa Conference*.

Roy, A. and Parker, R. S. (2007). Dynamic modeling of exercise effects on plasma glucose and insulin levels. *Journal of Diabetes Science and Technology*, 1(3):338–347.

Rubinstein, R. and Kroese, D. P. (2007). *Simulation and the Monte Carlo Method (2nd ed.)*. New York: John Wiley & Sons.

Rump, S. M. (1999). Intlab - interval laboratory. *Developments in Reliable Computing*, pages 77–104.

Rutscher, A., Salzsieder, E., and Fischera, U. (1994). Kadis: model-aided education in type i diabetes. *Computer Methods and Programs in Biomedicine*, 41:205–215.

Ryan, E. A., Shandro, T., Green, K., Paty, B. W., Senior, P. A., Bigam, D., Shapiro, A. M. J., and Vantyghem, M. C. (2004). Assessment of the severity of hypoglycemia and glycemic lability in type 1 diabetic subjects undergoing islet transplantation. *Diabetes*, 53:955–962.

Sainz, M. A., Armengol, J., and Vehí, J. (2002). Fault diagnosis of the three tanks system using the modal interval analysis. *Journal Process Control*, 12 (2):325–330.

Sainz, M. A., Herrero, P., Armengol, J., and Vehí, J. (2008). Continuous minimax optimization using modal intervals. *Journal of Mathematical Analysis and Applications*, 339:18–30.

Salzsieder, E., Albrecht, G., Fischer, U., and Freyse, E.-J. (1985). Kinetic modeling of glucoregulatory system to improve insulin therapy. *IEEE Transactions on biomedical engineering*, 32(10):846–855.

Schiffrin, A., Mihic, M., Leibel, B. S., and Albisser, A. M. (1985). Computer-assisted insulin dosage adjustment. *Diabetes Care*, 8(6):545–552.

Schlichtkrull, J., Munck, O., and Jersild, M. (1965). The m-value, an index for blood sugar control in diabetics. *Archives Medical Scandinavian*, 177:95–102.

Scholtz, H. E., Pretorius, S. G., Wessels, D. H., and Becker, R. H. A. (2005). Pharmacokinetic and glucodynamic variability: assessment of insulin glargine, nph insulin and insulin ultralente in healthy volunteers using a euglycaemic clamp technique. *Diabetologia*, 48(10):1988–1995.

Schrezenmeir, J., Achterberg, H., Bergeler, J., Küstner, E., Stürmer, W., Hutten, H., and Beyer, J. (1985). Computer-assisted meal related insulin therapy (camit). In Beyer, J., Albisser, A., Schrezenmeir, J., and Lehmann, L., editors, *1st International Symposium on Computer Systems for Insulin Adjustment in Diabetes Mellitus*, pages 133–144.

Schrezenmeir, J., Müller-Haberstock, S., Achterberg, H., Dahlke, U., Dirting, K., Küstner, E., Hogan, M., and Beyer, J. (1990). Computer-assisted insulin dosage adjustment-perspectives for diabetes control. *Hormone and Metabolic Research*, Suppl. 24:116–123.

Schrezenmeir, J., Tato, F., Tato, S., Müller-Haberstock, S., Achterberg, H., Stürmer, W., Hogan, M., and Beyer, J. (1987). Algorithms for csii-quantified approach to basal rate and meal induced insulin-dependent diabetes. In Brunetti, P. and Waldhaüsl, W., editors, *Serono Symposium Publication*, volume 37, pages 191–197.

Service, F. J., Molnar, G. D., Rosevear, J. W., Ackerman, E., Gatewood, L. C., and Taylor, W. F. (1970). Mean amplitude of glycemic excursions, a measure of diabetic instability. *Diabetes*, 19:644–655.

Shapira, G., Yodfat, O., HaCohen, A., Feigin, P., and Rubin, R. (2010). Bolus guide: a novel insulin bolus dosing decision support tool based on selection of carbohydrate ranges. *Journal of Diabetes Science and Technology*, 4(4):893–902.

Shaw, J. E., Sicreea, R. A., and Zimmeta, P. Z. (2010). Global estimates of the prevalence of diabetes for 2010 and 2030. *Diabetes Research and Clinical Practice*, 87(1):4–14.

Shimoda, S., Nishida, K., Sakakida, M., Konno, Y., Ichinose, K., Uehara, M., Nowak, T., and Shichiri, M. (1997). Closed-loop subcutaneous insulin infusion algorithm with a short-acting insulin analog for long-term clinical application of a wearable artificial endocrine pancreas. *Frontiers of Medical and Biological Engineering*, 8:197–211.

SIGLA/X Group (1999). Modal intervals, basic tutorial. In *Proceedings of MISC99*, pages 157–227. University of Girona (Spain).

Simon, G., Brandenberger, G., and Follenius, M. (1987). Ultradianoscillations of plasmaglucose,insulinandc-peptideinmanduringcontinuous enteral nutrition. *Journal of Clinical Endocrinology & Metabolism*, 64:669–674.

Skyler, J. S., Skyler, D. L., Seigler, D. E., and O'Sullivan, M. J. (1981). Algorithms for adjustment of insulin dosage by patients who monitor blood glucose. *Diabetes Care*, 4(2):311–318.

Sorensen, J. T. (1985). *A physiological model of glucose metabolism in man and its use to design and assess improved insulin therapies for diabetes*. PhD thesis, Massachusetts Institute of Technology.

Takahashi, D., Xiao, Y., Hu, F., and Lewis, M. (2008). A survey of insulin-dependent diabetes - part i: Therapies and devices. *International Journal of Telemedicine and Applications*.

Tarín, C., Teufel, E., Picó, J., Bondia, J., and Pfleiderer, H. J. (2005). Comprehensive pharmacokinetic model of insulin glargine and other insulin formulations. *IEEE Transactions on Biomedical Engineering*, 52:1994–2005.

Toffolo, G., Grandi, F. D., and Cobelli, C. (1995). Estimation of beta cell sensitivity from ivgtt c-peptide data: Knowledge of the kinetics avoids errors in modeling the secretion. *Diabetes*, 44:845–854.

Toussi, M., Choleau, C., Reach, G., Cahané, M., Bar-Hen, A., and Venot, A. (2008). A novel method for measuring patients' adherence to insulin dosing guidelines: introducing indicators of adherence. *BMC Medical Informatics and Decision Making*, 8:55.

Trajanoski, Z., Wach, P., Kotanko, P., Ott, A., and Skraba, F. (1993). Pharmacokinetic model for the absorption of subcutaneously injected soluble insulin and monomeric insulin analogues. *Biomedical Engineering*, 38:224–231.

Van Herpe, T., Brabanter, J., Beullens, M., Moor, B., and den Berghe, G. V. (2008). Glycemic penalty index for adequately assessing and comparing different blood glucose control algorithms. *Critical Care*, 12(1):R24.

Van Herpe, T., Haverbeke, N., den Berghe, G. V., and Moor, B. D. (2009). Prediction performance prediction performance comparison between three intensive care unit glucose models. In *7th IFAC Symposium on Modelling and Control in Biomedical Systems*, pages 7–12, Aalborg.

Van Herpe, T., Pluymers, B., Espinoza, M., den Berghe, G. V., and Moor, B. D. (2006). A minimal model for glycemia control in critically ill patients. In *Conf Proc IEEE Eng Med Biol Soc*, pages 5432–5435.

Vehí, J. (1998). *Análisi i Disseny de Controladors Robustos Mitjançant Intervals Modals*. PhD thesis.

Vescovi, M., Farquhar, A., and Iwasaki, Y. (1995). Numerical interval simulation: combined qualitative and quantitative simulation to bound behaviors of non-monotonic systems. In *14 th International Joint Conference On Artificial Intelligence*, volume 2.

Vicini, P., Caumo, A., and Cobelli, C. (1997). The hot ivgtt twocompartment minimal model: indexes of glucose effectiveness and insulin sensitivity. *The American Journal of Physiology*, 273:E1024–E1032.

Vicini, P., Caumo, A., and Cobelli, C. (1999). Glucose effectiveness and insulin sensitivity from the minimal models: Consequences of undermodeling assessed by monte carlo simulation. *IEEE Transactions on Biomedical Engineering*, 46:130–137.

Walsh, J. and Roberts, R. (1994). *The Pocket pancreas: your diabetes guide for improved blood sugars*. Diabetes Services Inc.

Walsh, J., Roberts, R., and Bailey, T. (2010). Guidelines for insulin dosing in continuous subcutaneous insulin infusion using new formulas from a retrospective study of individuals with optimal glucose levels. *Journal of Diabetes Science and Technology*, 4(5):1174–1181.

Wan, J. (2007). *Computationally reliable approaches of contractive MPC for discrete-time systems*. PhD thesis, Universitat de Girona.

Wentholt, I. M., Hart, A. A., Hoekstra, J. B., and Devries, J. H. (2008). How to assess and compare the accuracy of continuous glucose monitors? *Diabetes Technology and Therapeutics*, 10(2):57–68.

Wiegand, M. E. (1991). *Constructive qualitative simulation of continous dynamic systems*. PhD thesis, Heriot-Watt University.

Wilinska, M. E., Chassin, L. J., Acerini, C. L., Allen, J. M., Dunger, D. B., and R.Hovorka (2010). Simulation environment to evaluate closed-loop insulin delivery systems in type 1 diabetes. *Journal of Diabetes Science and Technology*, 4(1):132–144.

Wilinska, M. E., Chassin, L. J., Schaller, H. C., Schaupp, L., Pieber, T. R., and Hovorka, R. (2005). Insulin kinetics in type-1 diabetes: Continuous and bolus delivery of rapid acting insulin. *IEEE Transactions on Biomedical Engineering*, 52:3–12.

Wilinska, M. E. and Hovorka, R. (2008). Simulation models for in silico testing of closed-loop glucose controllers in type 1 diabetes. *Drug Discovery Today: Disease Models*, 5(4):289–298.

Wong, X. (2008). *Model-Based Therapeutics for Type 1 Diabetes Mellitus*. PhD thesis, University of Canterbury.

Worthington, D. R. (1997). Minimal model of food absorption in the gut. *Medical Informatics*, 22:35–45.

Zhang, P., Zhang, X., Brown, J., Vistisen, D., Sicree, R., Shaw, J., and Nichols, G. (2010). Global healthcare expenditure on diabetes for 2010 and 2030. *Diabetes Research and Clinical Practice*, 87(3):293–301.

Zisser, H., Jovanovic, L., Doyle III, F. J., Ospina, P., and Owens, C. (2005). Run-to-run control of meal-related insulin dosing. *Diabetes Technology and Therapeutics*, 7(1):48–57.

Zisser, H., Robinson, L., Bevier, W., Dassau, E., Ellingsen, C., Doyle III, F. J., and Jovanovic, L. (2008). Bolus calculator: A review of four "smart" insulin pumps. *Diabetes Technology and Therapeutics*, 10(6):441–444.